



**The University of Sheffield**  
**Chemical and Biological Engineering**

**Application of Microbubbles Generated by  
Fluidic Oscillation in the Anaerobic  
Digestion Process**

**A PhD thesis submitted**

**by**

**Mahmood Khazzal Hummadi Al-Mashhadani**

**February 2013**

## *Dedication*

*I would like to dedicate my dissertation to my father, my mother, my brothers, and my sisters. As well as I like to dedicate my dissertation to my wife with her family and my daughter.*

*Mahmood*

## **Acknowledgements**

I would like to express sincere gratitude to my supervisors Prof. William B. Zimmerman and Dr. Stephen J. Wilkinson for their invaluable academic guidance and support during this project. Thanks and appreciation to Dr. Hemaka Bandulasena for his great support. I also like to thank my mother and my family for their support and encouragement. I express my heartfelt gratitude to my wife for her support and encouragement during study the doctorate. I would like to acknowledge support from the staff and technicians of the department of chemical and biological engineering in the University of Sheffield who have contributed towards this project. I want to show appreciation to my brother Asst. Prof. Khalid Khazzal Hummadi for his support. I like to thank Valentina O. Igenegbai and Hanlin Li for their help. I express my gratitude to Iraqi ministry of higher education and scientific research for a doctoral scholarship. I would like to thank the staff of Iraqi Cultural Attaché in London, UK, for their support and help. Finally, Many thanks also to staff of Chemical Engineering Department in Baghdad University.

## Abstract

Recently significant attention has been paid globally to renewable energy as an alternative to fossil fuels, which are responsible for climate change and economic crises. Although various sources of clean energy exist, the amount generated from these sources has not reached levels capable of meeting the world's energy needs. Biogas produced from the digestion of organic material in the absence of oxygen is one of the most promising possible alternatives for use in generating electrical and heat energy or fuel for vehicles. In addition, it is considered a cheap alternative compared with biofuels produced from other biological processes. However, anaerobic digestion (means of producing biogas) faces many challenges, including low production levels and operational problems.

The current research is a serious attempt to address these problems through the exploitation of possible ways to increase production of methane and reduce the operation and maintenance costs. The study suggests the use of a sparging system in anaerobic digesters to convert unspontaneous reactions to spontaneous reactions by reducing the partial pressure of intermediate gases; thus, the reactions become thermodynamically favourable and provide impetus for a higher level of production. In order to increase the momentum, mass and heat transfer rates, microbubbles generated by fluidic oscillation was used in a gaslift bioreactor. The application of microbubbles in airlift bioreactors has been experimented with studying the kinetics of carbon dioxide transfer mechanisms. The efficiency of CO<sub>2</sub> removal from the liquid as a step toward upgrading biogas has been increased up to 29% by microbubble sparging (550 $\mu$ m) compared with fine bubble sparging (1300 $\mu$ m). The design and simulation of a gaslift bioreactor with microbubbles generated by fluidic oscillation is discussed in the present research. The simulation study was carried out by using computational fluidic dynamics. The effect of bubble size, location of the diffuser, and dead zone on the efficiency of the bioreactor has also been investigated. The simulation results show that the use of microbubbles not only increased the surface area to volume ratio, but also increased mixing efficiency through increasing the velocity of the circulation liquid around the draft tube. Moreover, the simulation data demonstrated that when the diameter of the microbubbles exceeded 200  $\mu$ m, the “downcomer” region, which is equivalent to more than half of the overall volume of the airlift bioreactor, is free from gas bubbles. The designed gaslift bioreactor was also used for processing the digested sludge from acidic gases (carbon dioxide and hydrogen sulphide), which have a

pejorative effect on the environment when they are eventually released, as well as causing operational difficulties through creating cavitation phenomena and the accompanying pump load. The results obtained from the experiments show that the removal of acidic gases in an airlift digester is significantly greater with microbubble technology than with a conventional digester.

Application of a sparging system in anaerobic digestion to break down the organic matter under mesophilic conditions was investigated in the present thesis. The study involved the use of different gases: nitrogen, nitrogen with carbon dioxide, undiluted biogas, diluted biogas by carbon dioxide, and finally pure carbon dioxide. The experiments were carried out with and without fluidic oscillation in three identical lab-scale gaslift anaerobic digesters fed by kitchen waste under different operational conditions. The results show that using pure nitrogen as a sparged gas in anaerobic digestion, with or without microbubble technology, leads to a reduction in methane production. The study concluded that the nitrogen sparging system causes the stripping of all intermediate gases, such as carbon dioxide and hydrogen, which are necessary for other bacteria to produce acetate and methane. Although the carbon dioxide was compensated for the second part of experiments, this action did not lead to an increase in methane production. Enhancement in methane production was observed when the undiluted and diluted biogas was recycled in the anaerobic digestion. The results show that 10-14% more methane was produced from the gaslift digester than was observed in the conventional anaerobic digester. In the final part the gaslift digester was sparged with pure carbon dioxide. The results show that using pure carbon dioxide led to the production of double the amount of methane than was produced by the conventional digester.

The sparging system used in the study also incorporated a new heating system for anaerobic digestion that used direct-contact evaporation process. The study used Central Composite Rotatable Design to create an equation based on three parameters (liquid level, flow rate and heating time). This equation was obtained by taking the five values for the individual parameters in each experiment while the percentage of evaporation, water temperature and humidity were measured as objective variables. The results show that liquid level has a significant effect on the liquid temperature due to the existence of competition between the latent heat transferred and the sensible heat in the direct contact system. The conversion of heat supplied to sensible heat was observed

with an increase in liquid level, which can be converted to latent heat when the liquid level is decreased.

Finally, and according to the above results, the present thesis proposes the integration of anaerobic digestion unit, combined heat and power (CHP unit), removal of acid gases unit and upgrading of biogas unit. This integration, along with microbubbles generated by a fluidic oscillator, represents an effective way to increase the efficiency of biogas production and reduce the operational difficulties.

## Table of contents

<b>Dedication</b> .....	(I)
<b>Acknowledgments</b> .....	(II)
<b>Abstract</b> .....	(III)
<b>Table of contents</b> .....	(VI)
<b>Nomenclature</b> .....	(XII)
<b>Abbreviations</b> .....	(XV)
<b>List of figures</b> .....	(XVI)
<b>List of Tables</b> .....	(XXVI)
<b>Chapter One (Introduction)</b> .....	(1)
Introduction.....	(2)
<b>Chapter Two (Literature Review)</b> .....	(8)
2.1 Literature Review.....	(9)
2.2 Microbiology of the Digestion Process.....	(13)
2.2.1 Hydrolysis Stage.....	(14)
2.2.2 Fermentation Stage.....	(15)
2.2.3 Methanogenesis Stage.....	(15)
2.3 Effect of the Parameters on the Anaerobic Digestion Process.....	(16)
2.3.1 Temperature .....	(16)
2.3.2 pH.....	(17)
2.3.3 Hydraulic Retention Time.....	(19)
2.3.4 Tolerance of Oxygen.....	(19)
2.4 Characteristics of Biogas.....	(19)
2.4.1 Removal of Carbon Dioxide.....	(21)
2.4.2 Removal of Water.....	(22)
2.4.3 Removal of Hydrogen Sulphide.....	(22)
2.5 Challenges in the Anaerobic Digestion Process.....	(22)

2.5.1 Mixing System in Anaerobic Digestion.....	(22)
2.5.2 Heating Systems in Anaerobic Digestion.....	(27)
2.6 Using the Airlift Bioreactor.....	(31)
2.7 Biochemical Reactions During Anaerobic Digestion.....	(33)
2.8 Effect of Partial Pressure on the Production of Biogas.....	(35)
2.9 Microbubble Technology.....	(38)
2.10 Summary.....	(43)
2.11 Hypothesis and Objectives of Current Research.....	(43)
<b>Chapter Three (Materials and Methods).....</b>	<b>(47)</b>
3.1 Introduction .....	(48)
3.2 Materials and Methods for (Carbon Dioxide Mass Transfer Induced Through an Airlift Loop) (Chapter Four).....	(48)
3.3 Anaerobic Digestion for Laboratory Purposes.....	(50)
3.3.1 Collection of Biogas for Laboratory Purpose.....	(50)
3.3.1.1 Introduction.....	(50)
3.3.1.2 Description of Suggested Biogas Collection.....	(53)
3.3.1.3 Water Used in Biogas Collection.....	(59)
3.3.1.4 Other Benefits of this Method.....	(59)
3.3.2 Synthesis of the Sludge for Laboratory Purpose.....	(60)
3.3.2.1 Introduction.....	(60)
3.3.2.2 Materials and Methods.....	(61)
3.3.2.3 Results and Discussion.....	(65)
3.4 Materials and Methods for (Removal of Acid-gases from Digested Sludge using Periodic Sparging in an Airlift Bioreactor with Microbubble Generated by Fluidic Oscillation) (Chapter Six).....	(72)
3.5 Materials and Methods for (Investigation of the Effects of Sparging in Anaerobic Digestion using Various Gases and Microbubbles Generated by Fluidic Oscillation) (Chapter Seven).....	(74)
3.5.1 Using Pure Nitrogen.....	(74)
3.5.2 Using Nitrogen and Carbon Dioxide.....	(76)
3.5.3 Recycling of the Biogas in Anaerobic Digestion.....	(78)
3.5.3.1 The Procedure for Recycling the Undiluted Biogas .....	(79)
3.5.3.2 The Procedure for Recycling the Diluted Biogas.....	(79)
3.5.4 Using pure Carbon Dioxide.....	(82)
3.6 Materials and Methods for (Direct-contact Evaporation to Direct-contact Heating as a step to improve heating in a Biological Application) (Chapter Eight).....	(83)

---

3.6.1. Setup of the Experiments.....	(83)
3.6.2 Experimental Design Used in Chapter Eight.....	(85)
3.6.2.1 Central Composite Rotatable Design (CCRD).....	(85)
3.6.2.2 Experimental Error in CCRD.....	(86)
<b>Chapter Four (Carbon Dioxide Mass Transfer Induced Through an Airlift Loop).....</b>	<b>(87)</b>
4.1 Introduction.....	(88)
4.2 Experiments for Mass Transfer of Carbon Dioxide with Microbubbles....	(91)
4.2.1. Physical Chemistry of Carbon Dioxide Gas Exchange.....	(91)
4.2.2. Absorption of Carbon Dioxide in the Water.....	(92)
4.2.3. Relationship between pH and Dissolved Carbon Dioxide.....	(93)
4.2.4. Thin Film Theory of Mass Transfer Coefficients.....	(94)
4.2.5 Bubble Analysis.....	(96)
4.2.6 Results and Discussion.....	(97)
4.3 Computational Modeling of Carbon Dioxide Dissolution in a Batch Airlift Loop Mixer.....	(101)
4.3.1. Chemical Kinetics Model.....	(102)
4.3.2. Dilute Species Chemical Transport Model.....	(104)
4.3.3. Laminar Bubbly Flow Model.....	(105)
4.3.4 Results and Discussion: Computational Study.....	(108)
4.4 Summary.....	(114)
<b>Chapter Five (Gaslift bioreactor for biological applications with microbubble mediated transport processes).....</b>	<b>(115)</b>
5.1 Introduction.....	(116)
5.2 Airlift Bioreactor Design and Simulation.....	(119)
5.3 Flow Modelling of the Airlift Bioreactor.....	(121)
5.4 Results and Discussion of Simulation Study.....	(123)
5.5 Liquid and Gas Velocity Profile.....	(128)
5.6 Penetration of the Microbubbles.....	(132)
5.7 Dead Zones in Gaslift Bioreactor.....	(135)
5.8 Effect of Draft Tube Diameter.....	(136)
5.9 Summary.....	(141)

<b>Chapter Six (Removal of acid-gases from Digested Sludge using Periodic Sparging in an Airlift Bioreactor with Microbubble Generated by Fluidic Oscillation)</b> .....	(142)
6.1 Introduction.....	(143)
6.2 Results and Discussion of Using Airlift Digester.....	(145)
6.3 Results and Discussion of Using Microbubbles Technology.....	(150)
6.4 Summary.....	(152)
<b>Chapter Seven (Investigation of the Effects of Sparging in Anaerobic Digestion using Various Gases and Microbubbles Generated by Fluidic Oscillation)</b> .....	(154)
7.1 Introduction.....	(155)
7.2 Sparging Using Nitrogen: Part I.....	(156)
7.2.1 Results and Discussion.....	(157)
7.2.2 Effect of Microbubbles Generated by a Fluidic Oscillator.....	(165)
7.2.3 Conclusion Part I.....	(165)
7.3 Sparging Using Nitrogen and Carbon Dioxide: Part II.....	(166)
7.3.1 Results and Discussion.....	(166)
7.3.2 Application of Microbubbles Technology.....	(176)
7.3.3 Conclusion Part II.....	(177)
7.4 Recycling the Undiluted Biogas in Anaerobic Digestion and Diluted Biogas with Carbon Dioxide: Part III.....	(178)
7.4.1 Results and Discussion.....	(179)
7.4.1.1 Recycling the Undiluted Biogas.....	(179)
7.4.1.2 Recycling the Diluted Biogas.....	(180)
7.4.2 Conclusion to Part III.....	(182)
7.5 Sparging Using Pure Carbon Dioxide: Part IV.....	(183)
7.5.1 Results and Discussion.....	(183)
7.5.2 Conclusion Part IV.....	(185)
7.6 Summary.....	(186)
<b>Chapter Eight (Direct-Contact Evaporation to Direct-Contact Heating as a Step to Improve Heating in a Biological Application)</b> .....	(187)

8.1 Introduction.....	(188)
8.2 Objective of the Proposed Heating System.....	(189)
8.3 Results and Discussion.....	(190)
8.4 Model Development and Analysis.....	(195)
8.4.1 Percentage of Evaporation.....	(195)
8.4.1.1 Effect of Liquid Level and Air Flow Rate on Percentage of Evaporation.....	(200)
8.4.1.2 Effect of Liquid Level and Evaporation Time on Percentage of Evaporation.....	(201)
8.4.1.3 Effect of Evaporation Time and Flow Rate on the Percentage of Evaporation.....	(203)
8.4.2 Liquid Temperature.....	(205)
8.4.2.1 Effect of Liquid Level and Flow Rate on Liquid Temperature.....	(208)
8.4.2.2 Effect of Heating Time and Flow Rate on Liquid Temperature.....	(209)
8.4.2.3 Effect of Liquid Level and Heating Time on Liquid Temperature.....	(210)
8.5 Summary.....	(211)
<b>Chapter Nine (Conclusions and Future Work).....</b>	<b>(212)</b>
9.1 Conclusion.....	(213)
9.1.1 Anaerobic Digestion for Laboratory Purpose.....	(213)
9.1.2 Carbon Dioxide Mass Transfer Induced Through an Airlift Loop .....	(214)
9.1.3 Gaslift Bioreactor for Biological Applications with Microbubble Mediated Transport Processes (Design and Simulation).....	(215)
9.1.4 Removal of Acid-gases From Digested Sludge.....	(216)
9.1.5 Investigation of the Effects of Sparging in Anaerobic Digestion Using Various Gases and Microbubbles Generated by Fluidic Oscillation.....	(217)
9.1.6 Improvement Heating System in Anaerobic Digester.....	(219)
9.2. Integration of Biological Processes in a Wastewater Treatment Plant Using Microbubble Generated by Fluidic Oscillator.....	(219)
9.3 Future Work.....	(223)
9.3.1 Mass Transfer Study.....	(223)
9.3.2 Simulation Study.....	(223)
9.3.3 Removal of Acid Gases.....	(223)

9.3.4 Anaerobic Digestion.....	(223)
9.3.5. Heating System.....	(224)
<b>References</b> .....	(225)
<b>Appendix</b> .....	(245)
A.1 Chemical Oxygen Demand (COD).....	(246)
A.2 Volatile Acids.....	(246)

## Nomenclature

$A_s$	Total interfacial surface area	( $m^2$ )
$A$	Area of bubble	( $m^2$ )
$C^*$	Equilibrium concentration	(mole $m^{-3}$ )
$C_1, C_2$	Concentration of Carbone dioxide	(mole $m^{-3}$ )
$C_E$	Equilibrium concentration of dissolved carbon dioxide in water	(mole $m^{-3}$ )
$C_L$	Concentration of dissolved carbon dioxide in water	(mole $m^{-3}$ )
$C_g$	Molar concentration in the gas phase	(mole $m^{-3}$ )
$C_L$	Molar concentration in liquid phase	(mole $m^{-3}$ )
$C_d$	Viscous drag coefficient	(dimensionless)
$D_c$	Diameter of collector	(m)
$D_i$	Diffusion coefficient	( $m^2 s^{-1}$ )
$d_b$	Bubble diameter	(m)
$G$	Gravitational acceleration	( $m s^{-2}$ )
$H_1$	Level acidic aqueous solution in balance tank	(m)
$H_2$	Level of acidic aqueous solution in collector tank	(m)
$H_3$	Length of tube dispersed in collector tank	(m)
$H_{hs}$	Height of collected biogas	(m)
$K_{La}$	Overall mass transfer coefficient	( $min^{-1}$ )
$M$	Molecular weight of species transferred across the interface	( $g mole^{-1}$ )
$N_b$	Number of fine bubble	(dimensionless)
$NA$	Mass transfer fluxes	(mole $s^{-1}$ )
$P$	Hydrostatic pressure	(mbar)
$P_c$	Pressure of collector biogas	(mbar)
$P_{tube}$	Pressure inside tube dispersed in the collector tank	(mbar)

$R$	Universal gas constant	(J mole <sup>-1</sup> K <sup>-1</sup> )
$R_b$	Fine bubble radius	(m)
$Re_b$	Reynolds number	(dimensionless)
$r_b$	Microbubble radius	(m)
$V_{bg}$	Volume of collected biogas	(m <sup>3</sup> )
$V_f$	Volumetric flow rate of fine bubbles	(m <sup>3</sup> s <sup>-1</sup> )
$V_i$	Inlet gas volume to digester	(m <sup>3</sup> )
$V_m$	Volumetric flow rate of microbubbles	(m <sup>3</sup> s <sup>-1</sup> )
$V_o$	Outlet gas volume to digester	(m <sup>3</sup> )
$V_{stokes}$	Terminal velocity of the gas bubbles	(m s <sup>-1</sup> )
$X_{iCH_4}$	Inlet fraction of methane to digester	(dimensionless)
$X_{iCO_2}$	Inlet fraction of Carbon dioxide to digester	(dimensionless)
$X_{oCH_4}$	Outlet fraction of methane from digester	(dimensionless)
$X_{oCO_2}$	Outlet fraction of Carbon dioxide from digester	(dimensionless)
$n_b$	Number microbubble	(dimensionless)
$u_g$	Gas velocity	(m s <sup>-1</sup> )
$u_l$	Velocity field for the liquid phase	(m s <sup>-1</sup> )
$u_l$	Velocity of liquid phase	(m s <sup>-1</sup> )
$\eta_l$	Dynamic viscosity of liquid phase	(Pa.s)
$\mu_l$	Viscosity of liquid	(kg m <sup>-1</sup> s <sup>-1</sup> )
$\rho_g$	Density of gas	(kg m <sup>-3</sup> )
$\rho_l$	Density of liquid	(kg m <sup>-3</sup> )
$\varphi_l$	Liquid volumetric phase fraction	(m <sup>3</sup> m <sup>-3</sup> )
$\Delta G_o$	Gibbs free energy at standard conditions	(kJ mole <sup>-1</sup> )
$\Delta G$	Gibbs free energy	(kJ mole <sup>-1</sup> )

$\Delta H$	Different height between the two tanks	(m)
$\Delta P$	Different Pressure	(bar)
$\Delta\rho$	Density difference between gas and liquid	(kg m <sup>-3</sup> )
$t$	Time	(sec)
$\rho$	Density of the fluid	(kg m <sup>-3</sup> )
$\dot{m}_{lg}$	Mass transfer rate in gas-liquid system	(kg m <sup>-3</sup> s <sup>-1</sup> )
$\phi_l$	Liquid volume fraction	(m <sup>3</sup> m <sup>-3</sup> )

## Abbreviations

BCs	Boundary conditions
CCD	Central composite design
CCRD	Central Composite Rotatable Design
CCS	Carbone capture and storage
CFD	Computational Fluid Dynamics
CHP	Combined heat and power
COD	Chemical engineering demined (g/l)
DCE	Direct contact evaporation
DCH	Direct contact heating
MEA	Monoethanolamine
PIV	Particle image velocimetry
VFA	Volatile fatty acid (mg/l)

## List of Figures

### Chapter One

Figure 1.1: Integration of biological processes using sparging system and microbubbles generated by fluidic oscillation.....(5)

### Chapter Two

Figure 2.1: Closed cycle to generate quasi zero-waste .....(12)

Figure 2.2: Schematic of flow chart of sludge from primary and secondary clarifiers in anaerobic digestion.....(13)

Figure 2.3: Mesophilic anaerobic digesters located in Woodhouse wastewater treatment plant in Sheffield, UK.....(14)

Figure 2.4: Schematic of degradation steps in anaerobic digestion.....(16)

Figure 2.5: Utilisation of biogas produced from anaerobic digestion and upgrading step required.....(21)

Figure 2.6: Some types of mixing systems used in anaerobic digester.....(25)

Figure 2.7: Submersible mixer is lifted out from the digester for cleaning.....(26)

Figure 2.8: Arrhenius plot for different types of bacteria.....(28)

Figure 2.9: Mutually beneficial relationship between anaerobic digestion and CHP in WWTP.....(29)

Figure 2.10: Snapshot of accumulation of solids on the heating tube in lab-scale experiments.....(30)

Figure 2.11: Schematic of airlift bioreactor with (a) external recirculation and (b) internal recirculation.....(32)

Figure 2.12: Biological reactions in anaerobic digestion. Standard Gibbs free-energy changes are estimated at standard conditions (25°C).....(34)

Figure 2.13: Division of a volume into smaller, equally sized objects produces additional surface area that is in scale with the cube root of the dividing number.....(38)

Figure 2.14: Bubbles generated by fluidic oscillation, and without fluidic oscillation.....(41)

Figure 2.15: Fluidic oscillator system for microbubble generation (reproduced from Zimmerman et al. 2009. (a) Oscillator block containing no moving mechanical parts, with single input and two outputs. (b) Illustration of feedback loop connecting the two

control terminals that causes gas pulses to be alternately emitted from each output. (c) Flow rate time history for the fluidic oscillator connected to a parallel percolation nozzle bank with apertures of  $600\mu\text{m}$  diameter.....(42)

Figure 2.16: Fluidic oscillator system for microbubble generation. Each oscillating output is 803 connected to a diffuser and the rapid interruptions in gas flow in each result in bubble 804 diameters of the order of the aperture diameter.....(43)

### Chapter Three

Figure 3.1: Image of experimental work.....(48)

Figure 3.2: Process flow schematic for Carbon dioxide dosing and stripping experiments.....(49)

Figure 3.3: Communicating vessels..... (53)

Figure 3.4: Schematic diagram of biogas collector by vacuum pressure as first stage.....(54)

Figure 3.5: Hydrostatic pressure in the headspace of collector tube..... (55)

Figure 3.6: Vacuum and gage pressure at different level of water.....(56)

Figure 3.7: Schematic of collector of biogas.....(57)

Figure 3.8: Pressures created in collection system.....(58)

Figure 3.9: Process flow schematic for synthesis of the sludge for laboratory purpose.....(64)

Figure 3.10: Methane production from anaerobic digester from the both digester.....(66)

Figure 3.11: Cumulative methane production from anaerobic digester with and without kitchen waste.....(66)

Figure 3.12: Percentage of methane ( $\text{CH}_4$ ) and carbon dioxide ( $\text{CO}_2$ ) in biogas produced from anaerobic digester contains digested sludge and fed by kitchen waste.....(67)

Figure 3.13: Variations in volatile fatty acids concentration in the digester fed with kitchen waste and the digester contains only digested sludge.....(68)

Figure 3.14: pH values in the anaerobic digester that contains simulated sludge. The pH value remained stable at optimum conditions.....(69)

Figure 3.15: Methane production from anaerobic digester fed with digested sludge and kitchen waste.....(69)

- Figure 3.16: Values of carbon dioxide produced from anaerobic digester fed with simulated sludge.....(70)
- Figure 3.17: Percentage of methane and carbon dioxide in the biogas produced from anaerobic digester fed with simulated sludge.....(70)
- Figure 3.18: Hydrogen sulphide produced from anaerobic digester fed with simulated sludge.....(71)
- Figure 3.19: pH value in the anaerobic digester that contains simulated sludge.....(71)
- Figure 3.20: Process flow schematic removal of acid-gases from digested sludge using pure nitrogen. Two digesters were used; the digester in right side operates without fluidic oscillator, and the digester in left side operates without sparging system.....(73)
- Figure 3.21: Process flow schematic for sparging the digester with pure nitrogen. Three digesters were used; the digester in right side operates with fluidic oscillator, the digester in the middle operates without fluidic oscillator, and the digester in left side operates without sparging system.....(76)
- Figure 3.22: Process flow schematic for sparging the digester with nitrogen and carbon dioxide. Three digesters were used; the digester in right side operates with fluidic oscillator, the digester in the middle operates without fluidic oscillator, and the digester in left side operates without sparging system.....(77)
- Figure 3.23: Process flow schematic for sparging the digester with recycling the biogas. Two digesters were used; the digester in right side operates with recycling the biogas but without fluidic oscillator, and the digester in left side operates without sparging system.....(81)
- Figure 3.24: Process flow schematic for sparging the digester with recycling the diluted biogas by carbon dioxide. Two digesters were used; the digester in right side operates with recycling the diluted biogas but without fluidic oscillator, and the digester in left side operates without sparging system.....(81)
- Figure 3.25: Snapshot of the digesters in the experiments showing the dilution in the unsparged digester (light colour on left picture), while the sludge in the other digesters (middle and right) is thicker (dark colour).....(82)

Figure 3.26: Process flow schematic for sparging the digester with pure carbon dioxide. Two digesters were used; the digester in right side operates with fluidic oscillator, and the digester in left side operates without sparging system.....(83)

Figure 3.27: Schematic diagram of the experimental set up.....(84)

## Chapter Four

Figure 4.1: Use of energy efficient microbubbles to generate airlift loop effect, suspension of algae by flotation, and gas exchange-CO<sub>2</sub> dosing and O<sub>2</sub> stripping. The operating region of the flow structure induced by the microbubble rise and liquid released by the bursting of the bubbles causes the downcomer flow. The fluidic oscillator is external to the device. The “draft tube” effect produces mixing because the microbubble cloud drags a significant amount of liquid with it—due to all the surface area- and as the bubbles spread out across the top surface, the liquid is released when the bubbles burst. In the downcomer region, there are practically no bubbles, so it is solely a liquid flow.....(90)

Figure 4.2: Interfacial dynamics of mass transfer for gas exchange.....(94)

Figure 4.3: Microbubble cloud generated from a two-chamber microporous ceramic diffuser with fluidic oscillation leading to a more uniform bubble size distribution and spatially regular bubble separation.....(95)

Figure 4.4: Bubble size distribution using nickel diffuser.....(96)

Figure 4.5: Bubble size distribution using ceramic diffuser.....(97)

Figure 4.6: Response of pH during bubbling of carbon dioxide into water with fine bubbles (1.3 mm diameter).....(98)

Figure 4.7: Response of pH with time during stripping of carbon dioxide by sparging with pure N<sub>2</sub> with fine bubbles (1.3 mm diameter).....(98)

Figure 4.8: Concentration time profile of carbon dioxide in both dissolution and removal processes for fine bubbles and microbubbles.....(99)

Figure 4.9: Response of pH with time during stripping of CO<sub>2</sub> by sparging with pure N<sub>2</sub> for both microbubbles (c. 550 μm) and fine bubbles (1.3 mm diameter).....(99)

Figure 4.10: Canonical thin film theory semilog plot for determining K<sub>L</sub>a by the slope of the supposed line.....(100)

Figure 4.11: Mole fraction of ionic and dissolved species inferred from pH measurements for dissolution of carbon dioxide with fine bubbles.....(104)

Figure 4.12: Velocity profiles in the reactor predicted by the CFD model. Velocity magnitude of the liquid phase is shown by the greyscale, while streamlines depict fluid

structure. Simulation times are 50, 60, 70, 80, 90, 100, 110, and 120 s from top left. The flow structure is apparently transient, from observation of the animation, with the first and last frame practically periodically reproduced.....(108)

Figure 4.13: Horizontal profile of velocity across the reactor 12 cm below the water level is shown.....(109)

Figure 4.14 Mass flux of liquid rising in the riser region of the reactor for microbubble and fine bubble aeration.....(110)

Figure 4.15: Dissolved carbon dioxide concentration in the liquid phase predicted by the CFD model. Concentration is shown by greyscale and streamlines depict flow currents. Simulation times are 50, 60, 70, 80, 90, 100, 110, and 120 s from top left.....(111)

Figure 4.16: Dissolved carbon dioxide concentration in the reactor during nitrogen bubbling predicted by the computational model. Initial concentration of carbon dioxide was taken as  $8 \text{ mole/m}^3$ .....(112)

Figure 4.17: Dissolved carbon dioxide concentration in the reactor during nitrogen bubbling predicted by the computational model. Initial concentration of  $\text{CO}_2$  was taken as  $2 \text{ mole/m}^3$ . .....(113)

## Chapter Five

Figure 5.1: Schematic of airlift bioreactor with internal recirculation.....(117)

Figure 5.2: Dimensions of airlift bioreactor used in this study.....(120)

Figure 5.3: Snapshots of gas concentration at different bubble diameter after 120 sec a) bubble diameter  $20 \mu\text{m}$ , (b) bubble diameter  $40 \mu\text{m}$ , (c) bubble diameter  $100 \mu\text{m}$ , (d) bubble diameter  $200 \mu\text{m}$ , (e) bubble diameter  $400 \mu\text{m}$ , (f) bubble diameter  $600 \mu\text{m}$ , (g) bubble diameter  $800 \mu\text{m}$ , (h) bubble diameter  $1000 \mu\text{m}$ .....(127)

Figure 5.4: Volume gas fraction in cross section downcomer at different bubble diameter ( $20, 40, 100\mu\text{m}$ ) after steady state.....(128)

Figure 5.5: Velocity gas profile in cross-section riser zone after steady state at different gas bubble diameter ( $40, 100, 200, 400, 600, 800, 1000 \mu\text{m}$ ) after steady state.....(130)

Figure 5.6: Velocity profile in certain point riser zone after steady state.....(130)

Figure 5.7: Velocity liquid profile in cross-section riser zone after steady state at different gas bubble diameter ( $40, 100, 140, 200, 400, 600, 800, 1000 \mu\text{m}$ ) after steady state.....(131)

Figure 5.8: Velocity profile in certain point in riser zone after steady state. ....(131)

Figure 5.9: Velocity of liquid phase in riser region and gas volume fraction in downcomer region for  $40 \mu\text{m}$  and  $100 \mu\text{m}$  bubble diameter after steady state. It can be

- seen that the velocity of liquid in left side of chart, while gas velocity in right side of the chart.....(132)
- Figure 5.10: Gas volume fraction versus height above bottom of reactor in the downcomer for (40, 70, 85, 100, 140  $\mu\text{m}$ ) after steady state. Note that the diffuser position for these simulations is 0.05 m above the bottom of the reactor.....(133)
- Figure 5.11: A steady state distribution of gas concentration in the reactor for different bubbles sizes (40, 70, 85, 100 and 140 $\mu\text{m}$ ).....(133)
- Figure 5.12: Volume gas fraction with height of airlift digester at different diffuser position (5,6.5, 8,9.5,11 cm) at 40  $\mu\text{m}$  and after steady state.....(134)
- Figure 5.13: Height of diffuser and height of reactor ratio ( $h_d / H$ ) with height of penetration and height of reactor ratio ( $P_b/H$ ) at micro-bubble diameter of 40  $\mu\text{m}$ ... (134)
- Figure 5.14: Snapshots of gas concentration after steady state condition different diffuser position (0.05, 0.065, 0.08, 0.095, 0.11 m).....(135)
- Figure 5.15: Percentage of dead zone after 120 sec, microbubble diameter 20  $\mu\text{m}$ , and at different diffuser position (0.05, 0.065, 0.08, 0.095, 0.11 m).....(136)
- Figure 5.16: Snapshots of gas concentration at different  $d/D$  ( $d/D = 0.6, 0.7, 0.8,$  and 0.9) when microbubble diameter is 400  $\mu\text{m}$  and after 120 sec.....(137)
- Figure 5.17: Velocity liquid profile in cross-section after 120 sec.....(138)
- Figure 5.18: Velocity liquid in cross-section riser region at different draft tube diameter after steady state.....(138)
- Figure 5.19: Snapshots of gas concentration at different  $d/D$  ( $d/D = 0.6, 0.7, 0.8,$  and 0.9) when microbubble diameter is 400  $\mu\text{m}$  and after 900 sec.....(139)
- Figure 5.20: Velocity liquid profile in cross-section after 120 sec.....(139)
- Figure 5.21: Actual airlift bioreactor modelled in this study and used in the current experiments.....(140)

## Chapter Six

- Figure 6.1: Cumulative methane production in the airlift digester vs. the unsparged digester. ....(145)
- Figure 6.2: Comparison of methane production in the airlift digester during the daily one hour sparging period versus that in the preceding 23 hours unsparged operation.....(146)
- Figure 6.3: pH values of both Airlift digester and the conventional digester.....(148)

- Figure 6.4: Cumulative carbon dioxide production from the airlift digester with periodic nitrogen bubbling compared to the conventional unsparged digester.....(148)
- Figure 6.5: Cumulative hydrogen sulphide production from the airlift digester with periodic nitrogen bubbling compared to the conventional unsparged digester.....(149)
- Figure 6.6: Cumulative carbon dioxide production from airlift digester with and without nitrogen bubbling.....(151)
- Figure 6.7: Cumulative hydrogen sulphide production from anaerobic digestion with and without nitrogen sparging.....(152)

## Chapter Seven

- Figure 7.1: Cumulative methane production from the sparged digesters and unsparged digester in the first stage.....(158)
- Figure 7.2: Methane produced from the sparged digesters and unsparged digester in the first stage.....(158)
- Figure 7.3: Cumulative carbon dioxide production from the sparged digesters and unsparged digester in the first stage.....(159)
- Figure 7.4: Carbon dioxide produced from the sparged digesters and unsparged digester in the first stage.....(159)
- Figure 7.5: Methane produced from the sparged digesters and unsparged digester in the second stage.....(160)
- Figure 7.6: Efficiency of cumulative methane produced from the sparged digesters and unsparged digesters in the second stage.....(160)
- Figure 7.7: Methane produced from the sparged digesters and unsparged digester in the third, fourth, and fifth stages.....(161)
- Figure 7.8: Efficiency of cumulative methane production from sparged digesters and unsparged digester third, fourth, and fifth stage.....(161)
- Figure 7.9: Methane produced from the sparged digesters and unsparged digester in the sixth stage.....(162)
- Figure 7.10: Efficiency of cumulative methane production from the sparged digesters and unsparged digester during the sixth stage.....(162)

---

Figure 7.11: Methane produced from the sparged digesters and unsparged digester .....	(163)
Figure 7.12: Methane produced from the sparged digester (before and after sparging the process) and in the unsparged digester.....	(164)
Figure 7.13: Methane to carbon dioxide ratio throughout the experiments.....	(164)
Figure 7.14: Cumulative carbon dioxide produced from the sparged digester and unsparged digester in the first stage.....	(167)
Figure 7.15: Methane produced from the sparged digester (before and after the sparging process).....	(167)
Figure 7.16: Methane produced from sparged digester and unsparged digester in the first stage.....	(168)
Figure 7.17: Methane produced from sparged digester and unsparged digester in the second stage.....	(168)
Figure 7.18: Efficiency of cumulative methane production from sparged digester and unsparged digester in second stage.....	(169)
Figure 7.19: Cumulative carbon dioxide production from the sparged digester and unsparged digester up to the second stage.....	(170)
Figure 7.20: Cumulative carbon dioxide production from the sparged digester and unsparged digester up to the third stage.....	(170)
Figure 7.21: Efficiency of cumulative methane production from the sparged digester and unsparged digester up to the third stage.....	(171)
Figure 7.22: Cumulative carbon dioxide production from the sparged digester and unsparged digester up to fourth stage.....	(172)
Figure 7.23: Cumulative carbon dioxide production from the sparged digester and unsparged digester up to fourth stage.....	(172)
Figure 7.24: Average methane production from sparged digester.....	(173)
Figure 7.25: Schematic of experimental work used in the separated tests.....	(174)
Figure 7.26: Methane and carbon dioxide produced from anaerobic digestion.....	(175)
Figure 7.27: Percentage of methane and carbon dioxide in the biogas.....	(175)

Figure 7.28: Percentage of methane produced in the sparged digester and unsparged digester.....	(176)
Figure 7.29: Cumulative methane production from the gaslift digester using microbubbles generated by a fluidic oscillator, gaslift digester without fluidic oscillator, and unsparged digester.....	(177)
Figure 7.30: Efficiency of methane production from a gaslift digester using microbubbles generated by a fluidic oscillator and in a unsparged digester.....	(177)
Figure 7.31: Methane produced from sparged and unsparged digesters.....	(179)
Figure 7.32: Cumulative methane production from sparged digester and unsparged digester.....	(181)
Figure 7.33: pH values in the sparged digester (before and after bubbling process).....	(182)
Figure 7.34: Methane produced from the gaslift digester and unsparged digestion over 19 days of operation.....	(184)
Figure 7.35: pH value in the gaslift digester sparged by pure carbon dioxide for 5 min.....	(185)
Figure 7.36: Cumulative methane production from the gaslift digester and unsparged digester when the pure carbon dioxide is sparged.....	(185)
<b>Chapter Eight</b>	
Figure 8.1: Integration between anaerobic digestion and combined heat and power.....	(189)
Figure 8.2: Relative humidity of outlet air.....	(191)
Figure 8.3: The variation of outlet air temperature at different heights of water above the ceramic diffuser (2, 4, 8, and 12cm).....	(191)
Figure 8.4: Plot of outlet air humidity versus time for different liquid levels.....	(192)
Figure 8.5: Water temperature at different water levels in tank.....	(193)
Figure 8.6: Percentage of evaporation at different water levels in tank.....	(193)
Figure 8.7: Liquid temperature at different liquid level.....	(194)
Figure 8.8: Efficiency of liquid temperature at different water levels in column.....	(194)
Figure 8.9: Observed values and predicted values resulted from developed equation.....	(198)

Figure 8.10: Variation of percentage of evaporation with different code levels.....	(198)
Figure 8.11: Effect of liquid level, flow rate and heating time on percentage of evaporation.....	(199)
Figure 8.12: Response surface predicting percentage of evaporation from the model equation: effect of flow rate and liquid level .....	(201)
Figure 8.13: Response surface predicting percentage of evaporation from the model equation: effect of liquid level and evaporation time.....	(202)
Figure 8.14: Effect of evaporation time on the percentage of evaporation at different liquid level.....	(203)
Figure 8.15: Response surface predicting percentage of evaporation from the model equation: effect of evaporation time and flow rate.....	(204)
Figure 8.16: Effect of flow rate on the percentage of evaporation at different evaporation time.....	(204)
Figure 8.17: Observed values and predicted values resulted from developed equation.....	(207)
Figure 8.18: Variation of liquid temperature with different code levels.....	(207)
Figure 8.19: Response surface predicting liquid temperature from the model equation: effect of flow rate and liquid level.....	(208)
Figure 8.20: Response surface predicting liquid temperature from the model equation: effect of flow rate and heating time.....	(209)
Figure 8.21: Response surface predicting liquid temperature from the model equation: effect of liquid level and heating time.....	(210)

## **Chapter nine**

Figure 9.1: Integration of biological processes in wastewater treatment plant using microbubble generated by fluidic oscillator.....	(221)
Figure 9.2: Benefits of the integration process.....	(222)

## List of tables

Table 2.1: Optimum PH for some types of methanogenesis bacteria.....	(18)
Table 2.2: General characteristics of biogas according to its sources.....	(20)
Table 2.3: Composition of biogas and natural gas.....	(20)
Table 3.1: Experimental Conditions.....	(49)
Table 3.2: Type of organic matters in kitchen waste.....	(62)
Table 3.3: Details of materials which used in synthetic the sludge.....	(62)
Table 3.4 Operational conditions for conducting the experiments.....	(75)
Table 3.5 Operational conditions applied in present study.....	(78)
Table 4.1: Reactions modelled in dissolution, dissociation, and association reactions for CO <sub>2</sub> aqueous chemistry, at room temperature and atmospheric pressure.....	(103)
Table 4.2: Initial species conditions for the kinetics only (CSTR) and distributed system model.....	(105)
Table 4.3: Diffusion coefficients for the six species treated in the computational model.....	(105)
Table 5.1: The properties of flow modelling.....	(121)
Table 7.1: The temperature of the sludge before and after adjusting the setting of the controller.....	(180)
Table 7.2: Effect the sparging system on methane produced from anaerobic digester.....	(186)
Table 8.1: Real and coded levels of operating variables.....	(195)
Table 8.2: Coded and real levels of x-variables used in present study.....	(196)
Table 8.3: Regression coefficients of model equation.....	(196)
Table 8.4: Predicted data and experimental data of percentage of evaporation.....	(197)
Table 8.5: Re-arrangement of percentage of evaporation with codes.....	(199)
Table 8.6: Re-arrangement of average of evaporation with codes.....	(199)
Table 8.7: Regression coefficients of model equation.....	(205)
Table 8.8: Predicted data and experimental data of liquid temperature.....	(206)
Table A.1: Reagents used in measuring the volatile acid.....	(246)
Table A.2 Equipments and tools required for measuring.....	(247)



CHEMICAL & BIOLOGICAL ENGINEERING

# Chapter One

## Introduction

# **Application of microbubbles generated by fluidic oscillation in the anaerobic digestion process**

## **1.1 Introduction**

Economic crises resulting from fluctuations in fossil fuel prices and the negative effects on the environment caused by emissions of greenhouse gases have become major global problems. The search for renewable fuels has become the main focus for many researchers and those interested in the production of renewable energy. Alternative clean sources of energy are available, for instance, solar, hydroelectric and wind; however, these have not so far been able to produce sufficient energy to substitute for fossil fuels.

Production of bio-fuels from agricultural crops is regarded as a major potential alternative and has engendered a sense of optimism with regard to addressing the economic and environmental problems associated with fossil fuels. However, it has not emerged as a viable replacement for traditional fuels. The fact is that the amount of biofuel produced from agricultural crops has been relatively small compared with the large areas of fertile land used for agriculture; and inevitably, the use of such land for biofuel production would create the conditions for a global food crisis.

This scenario could be averted by using microalgae to produce biodiesel, instead of oil crops, due to their high oil content, which in some species reaches almost 50%. Photosynthesis of microalgae requires sunlight, water, nutrients and carbon dioxide as a source of carbon. According to previous studies, the percentage of carbon in the biomass of algae is 40-50%. This means that the production of 1 kg of biomass needs 1.5 to 2 kg of carbon dioxide. This quantity of carbon dioxide is relatively large; therefore, supplying carbon dioxide to the cultivation of microalgae is one of the fundamental difficulties that must be resolved to reduce the cost of producing bio-fuels.

In addition, the provision of pure carbon dioxide and transferring it to the culture is one of the major costs for the production of bio-fuels from microalgae. According to previous studies, there are alternatives that can be used for providing carbon dioxide, but gases and impurities that accompany the carbon dioxide production have a negative impact on the cultivation of microalgae. In addition, the technical and economic obstacles to the achievement of the required level of biofuel production from microalgae remain.

Anaerobic digestion represents a renewable energy source. It is commonly used for nutrient and energy recovery from biomass and also to stabilise the sludge produced in wastewater treatment. Organic matter is broken down through four biodegradation stages into methane ( $\text{CH}_4$ ), carbon dioxide ( $\text{CO}_2$ ), varying amounts of hydrogen sulphide ( $\text{H}_2\text{S}$ ), and the digested sludge, which can be used as a soil fertilizer. Bio-methane can be used for generation of electricity or used as biofuel for vehicles after upgrading processes. The production and upgrading costs of biogas are lower than the costs of production and upgrading of bio-fuel produced from agriculture crop or from microalgae. However the challenges facing the anaerobic digestion process have become a major obstacle to this source becoming a leading renewable energy source. Among these challenges are the low level of biogas production and operational difficulties.

The present study is a serious attempt to address these problems through intensive study and numerous experiments in which several recently developed techniques are used in an attempt to improve production and overcome operational problems.

The current research suggests the use of a sparging system in anaerobic digestion to reduce the partial pressure of the product gases with a negative value change in Gibbs free energy; hence the reaction becomes thermodynamically favourable and provides impetus for the formation of more products. The present study offers the use of a gaslift bioreactor as an alternative to a conventional digester for reduction of the partial pressure of carbon dioxide, hydrogen and methane. The airlift (gaslift) reactors (ALRs), which have been used in several industrial applications requiring gas-liquid contacting, have many advantages over stirred tanks. For instance, the fact that there are no moving parts inside the reactor can potentially lower costs of installation and maintenance as well as energy consumption. In addition to good mixing, ALRs maintain long periods of gas-liquid contacting and do not cause shear damage to cells. This has led to their widespread use in various biological processes. However, these bio-reactors still need

further technical development in order to increase the efficiency of the mass and heat transfer rate in gas-liquid processes.

There have been many attempts to develop reactors for biological applications. These attempts have been targeted at increasing the contact time and interfacial area between gas and liquid phases and improving heat transfer and mass transfer between the two phases (gas and liquid).

Use of traditional methods, such as stirred tanks with high speeds, can contribute to achieving the desired goals; however, the economic costs and operational problems have hampered the development of these reactors. This scenario could be changed if microbubbles technology could be applied to chemical and biochemical processes. These systems could achieve significant improvements in mass flux by increasing the surface area to volume ratios of the bubbles. In spite of successive developments in microbubble generation systems, the energy requirements are still fairly high and these systems are not yet economically viable.

The current study suggests the use of a modern technology (microbubble technology) in anaerobic digestion to enhance the mass transfer and mixing system. This technology generates bubbles with micron size by fluidic oscillation but with lower energy requirements. The idea of this technology is to limit the time required to grow the bubbles generated from the pores and prevent them from growing any bigger than micron size.

In the present study, the hypothesis says that the use of microbubbles generated by fluidic oscillation in anaerobic digestion increases methane production through reduction of the partial pressure of methane, enhancing the mixing efficiency and reduces production costs through enhancement of momentum and mass transfer rate.

In addition this technology can be used for processing the digested sludge by removal of acid-gases, which cause damage to pipelines and storage equipment. Furthermore, the study also hypothesises that the development of a heating system in anaerobic digestion can be achieved by conversion of direct-contact evaporation to direct-contact heating. These ideas represent the first attempt to use this technology in anaerobic digestion processes.

In the present study, sparging system and microbubbles generated by fluidic oscillation were applied in:

1. Upgrading process of biogas generated from anaerobic digestion.
2. Anaerobic digestion process.
3. Re-processing the digested sludge.
4. Development of heating system in anaerobic digestion.



In addition, this chapter includes the materials and methods for all experiments that carried out in the present thesis.

**Chapter Four** discusses mass transfer in gas-liquid contact systems and is titled **CO<sub>2</sub> Mass Transfer Induced through an Airlift Loop**. In this chapter the enhancement of the mass transfer rate using fine bubbles and microbubbles generated by fluidic oscillation is investigated as well as the dynamics of producing microbubble clouds through fluidic oscillation to enhance CO<sub>2</sub> gas transfer for either scrubbing or stripping operations in aqueous solutions. The kinetics of carbon dioxide transfer mechanisms are studied in relation to sparging with conventional fine bubbles and microbubbles.

**Chapter Five** deals with the design of a gaslift bioreactor for anaerobic fermentation (**Gaslift bioreactor for biological applications with microbubble mediated transport processes: design and simulation**). This chapter considers utilization of microbubbles generated by fluidic oscillation with gaslift in bioprocessing applications. Design and simulation of a gaslift bioreactor with microbubbles was facilitated by using Comsol multiphysics software. The effects of bubble size, draft tube diameter and position of diffuser on the fluidic dynamic are investigated.

**Chapter Six** recommends the use of a gaslift bioreactor, which the design and simulation were discussed in the previous chapter, in enhancement of the amount of biogas produced from the digested sludge. This chapter proposes further processing of already digested sludge by using an airlift bioreactor and, in particular, considers the effects of periodic sparging through the use of nitrogen gas in anaerobic digestion. This chapter focuses on the application of the suggested design for **removal of acid gases from the digested sludge using microbubbles generated by fluidic oscillation**. The present section addresses the mechanism of post anaerobic digestion of digested sludge for removal of acid gases (CO<sub>2</sub> and H<sub>2</sub>S) using microbubbles generated by fluidic oscillator.

**Chapter Seven** addresses application of microbubbles generated in anaerobic digestion using different gases and is titled **Investigation of sparging systems in anaerobic digestion using different gases and microbubbles generated by fluidic oscillation**. Effects of the sparging system caused by using different gas types, such as pure nitrogen, nitrogen and carbon dioxide, undiluted biogas, diluted biogas by carbon dioxide, and finally pure carbon dioxide on the efficiency of biogas yield are investigated in this chapter.

The chapter presents and discusses the results obtained from the experiments using different concentrations of different gases and their effects on the production of biogas from anaerobic digestion.

**Chapter Eight** suggests the use of direct contact evaporation to improve the heating system in anaerobic digestion and is titled **Direct-contact evaporation to direct-contact heating as a step to improve heating in a biological application**. This study addresses the utilization of direct-contact evaporation for process heating through the conversion of direct-contact evaporation into direct-contact heating. Conversion of the latent heat into sensible heat in direct contact evaporation is discussed based on the three parameters used in this study: liquid level, flow rate of hot gas and heating time.

**Chapter Nine** addresses conclusions and recommendations of the current study



CHEMICAL & BIOLOGICAL ENGINEERING

# Chapter Two

## Literature Review

## **Chapter Two**

### **Literature Review**

#### **2.1 Literature Review**

Increasing global demand for energy and the economic crises resulting from fluctuations in fossil fuel prices have been major problems facing the world for many decades (Dryzek, 2011). In addition, gas emissions have now reached critical and dangerous levels that have resulted in climate change and global warming. Hence many researchers have sought solutions to these problems. Renewable energy sources are considered to offer one such solution by reducing the incidence of such crises and the environmental effects. Recently, researchers have focused their attention on one of the most daunting challenges currently facing the world in terms of preserving global stability, economic prosperity and quality of life on this earth, namely, finding ways of providing adequate supplies of clean energy.

Fossil fuels represent around three-quarters of total global energy requirements, supplying transportation, industries and household needs. Electricity only accounts at present for around one-third of global energy consumption (Gouveia et al. 2009). The excessive use of fossil fuels will lead eventually to the depletion of resources. Emissions of greenhouse gases are causing climate change; carbon dioxide emissions, in particular, have exceeded dangerous levels and account for 450 parts per million of the total greenhouse gases (Schenk et al., 2008).

Although there are clean alternatives to fossil fuel, for example, hydroelectric, solar, wind, tidal, and geothermal power, the production of energy from these alternatives at present supplies a very low percentage of the world's energy needs.

For the above reasons, researchers have begun to focus on the production of bio-fuels, which not only offer an alternative to fossil fuels, but also can reduce emission of greenhouse gases (Chisti, 2007).

The production of bio-fuel (bio-diesel and bio-ethanol) from agricultural crops is one of the most promising alternative sources of fuel and would reduce damage to the environment (Schenk et al., 2008; Scott et al., 2010; Singh, 2012). Research has focused on reducing the cost of the extraction of oil from plants and animal fats or the use of food waste as a second source for bio-fuel production (Chisti, 2007; Vasudevan and Briggs; 2008, Hettinga et al. 2009; De wit, 2010). However, the biggest problem is that the extraction of bio-fuel from agricultural crops could have severe consequences for global food supplies, especially in poor countries because it requires large areas of arable land (Rosgaard et al., 2012). In addition, current supplies from these sources account for only approximately 0.3% of the current demand for transport fuel and there is no possibility of such fuel replacing petroleum derived liquid fuels in the foreseeable future (Chisti, 2005; Schenk et al., 2008; Eriksen, 2008).

The production of biofuel from microalgae (algae) has already been commercialized and has greater potential to change the current scenario (Scott et al., 2010). Banerjee et al. (2002) stated that the oil content in certain types of microalgae represents 50-80% by weight of dry biomass, while the oil content in agricultural crops is no more than 5% (W/W<sub>DW</sub>) (Amaro et al. 2011). In addition, productivity of biomass of some types of microalgae is as much as 7.3 g/l/d (Suali and Sarbatly, 2012). Phototrophic microalgal growth requires solar energy, nutrients, water, and also carbon dioxide gas as a carbon source (Xiong et al., 2010) as well as control of the pH in the culture (Sobczuk et al., 2000; Wang et al., 2008).

According to previous studies, chemical analysis has shown that the content of biomass includes around 40-50% carbon, which suggest that the production of 1 kg of algal biomass requires 1.5 to 2.0 kg of carbon dioxide. This quantity is relatively large, and represents 33% of the cost of full scale production; therefore, the supply of carbon dioxide to microalgae culture is one of the fundamental difficulties that must be

resolved to reduce the cost of producing biofuels (Sobczuk et al., 2000). These estimates emphasise the need to find sources of carbon dioxide which are cheap and readily available.

In the current literature, many scholars tend to highlight capturing carbon dioxide from power plants and cement industries (Benemann, 1997; Worrel and Price, 2001; Feng, 2008; Barker et al., 2009; Bosoaga et al., 2009). However, Negoro et al. (1991;1993); Zeiler et al., (1995) and Brown et al., (1996), have confirmed that there are some gases and impurities associated with carbon dioxide, which affect the growth of micro-algae, with only a few being able to tolerate them. The separation of these gases and impurities from the carbon dioxide significantly adds to the cost of the production of biofuel from micro-algae. Kadam (1997) studied the economics of supplying carbon dioxide to microalgae cultivation by developing an economic model for the recovery of carbon dioxide from a power plant, and found that the extraction, compression, hydration and transport costs amounted to about \$40 per ton.

In spite of many attempts to improve the production of biofuel from micro-algae, many technical and economic obstacles remain to the achievement of the required level of production (Scott et al., 2010). Economic costs range the production costs to the cost of treatment and upgrading of the biofuel produced.

Biogas produced from fermentation processes of organic matter represents another clean alternative (Wang, 1999). The production and upgrading costs of biogas are lower than the costs of production and upgrading of bio-fuel produced from microalgae.

Biogas qualifies as a renewable energy source (Budzianowski, 2012), since the carbon dioxide that is taken from the atmosphere is returned to the atmosphere again but without any excess. In other words, in the photosynthesis process, the plant consumes carbon dioxide found in the atmosphere as a source of carbon. The plants are eaten by animals that then produce waste, which is converted to bio-methane by biodegradation processes. The methane is burnt to produce energy and carbon dioxide, thus the net of greenhouse gas (carbon dioxide) is absent as shown in the Figure 2.1 (Poeschl et al., 2010). This zero-net can be also converted into “negative-net” if the carbon dioxide produced from the anaerobic digester is captured by waste liquid alkaline, or the carbon-rich digested sludge is used as fertilizer for arable soil.

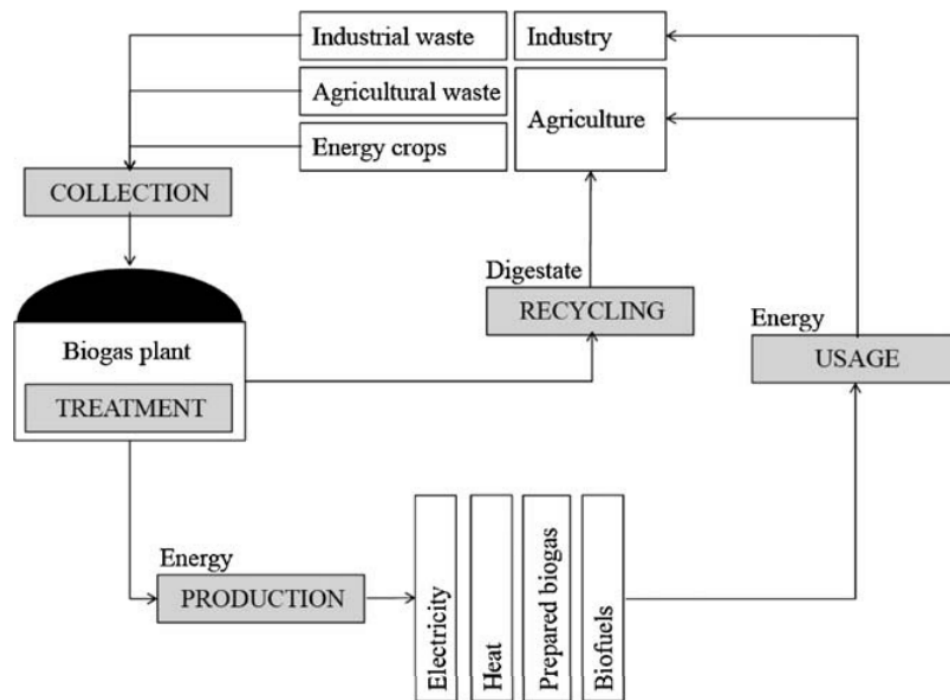


Figure 2.1: Closed cycle to generate quasi zero-waste (Poeschl et al. 2010)

Biogas can be produced from different resources; sewage, livestock, manure landfill, energy crops, organic waste and waste biomass (Budzianowski, 2012) as well as mixtures of industrial waste with energy crops (Nges et al. 2012). The methane production and stability of the digestion process are affected significantly by changes in the substrate composition. For instance, the lipid found in the feedstock can increase the methane productivity (Hwu et al 1998). However, Luostarinen et al. (2009) reported that an increase in the lipids in the feedstock produces LOCF (Long-chain fatty acids), which have a negative effect on the performance of methanogenic bacteria. Similarly Hansen et al. (1998) mentioned that the ammonia produced from fermentation of the proteins inhibits methane production.

The difference between bio-methane produced from anaerobic fermentation and natural gas is that natural gas contains a mixture of hydrocarbons for example, propane, ethane and butane (Lusk, 1998). Therefore, more greenhouse gas is produced from burning natural gas than is that produced from burning bio-methane.

Production of biogas can be achieved by using anaerobic microorganisms found in an environment that is devoid of oxygen in wastewater plants via the anaerobic digestion

process. The latter, originally, was used for processing and stabilization of the raw sewage discharged from the primary and secondary clarifier units in wastewater treatment plants (Tiehm et al., 2003) as illustrated in Figure 2.2. Thus, anaerobic digestion is an important economic and biological process. It includes four stages (hydrolysis, acidogenesis, acetogenesis, and methanogenesis) in the absence of oxygen. The main benefits of this process are sludge stabilisation, reduction of pathogens, reduction of odour and solids content in the sludge, conversion of organic matter into energy (biogas) for use as a renewable energy source, while the effluents can be used as fertilizer for agriculture (Appels, et al. 2008; Sahlstrom, 2003; Birgitte, 2003; Metcalf and Eddy, 2003).

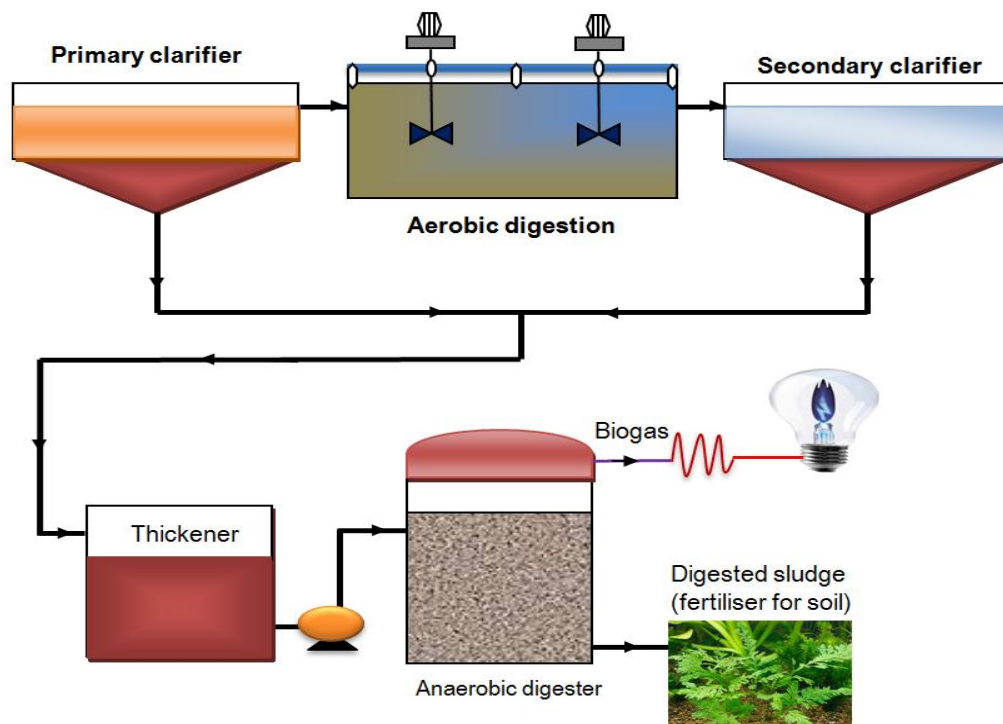


Figure 2.2: Schematic of flow chart of sludge from primary and secondary clarifiers in anaerobic digestion

## 2.2 Microbiology of the Digestion Process

The anaerobic digestion process, which uses different types of bacteria, is divided into four stages; hydrolysis, acidogenesis, acetogenesis, and methanogenesis. High efficiency can be achieved in anaerobic digestion when the biodegradation rate in all

these stages is equal. If any of the bacteria used in these stages, are inhibited, this leads to the other bacteria in this process being inhibited; thus, the production of methane decreases. The anaerobic bacteria work in sequence, thus, the materials that are produced from the first stage, for example, are utilized in the second stage as substrate. Figure 2.3 shows the full-scale mesophilic anaerobic digestion system at Woodhouse wastewater treatment plant in the city of Sheffield in the United Kingdom.



Figure 2.3: Mesophilic anaerobic digesters located in Woodhouse wastewater treatment plant in Sheffield, UK

### 2.2.1 Hydrolysis Stage

In this stage, insoluble and high molecular weight compounds (colloidal and particulate waste) are hydrolyzed into soluble compounds by enzymes released by hydrolysis bacteria. Fats (lipids), carbohydrate, proteins and nucleic acids, which are colloidal and particulate waste present in primary and secondary sludge, are converted into fatty acids, monosaccharides, amino acids, purines and pyrimidines respectively (Vavilin, 2008). These are small molecules that are soluble in water; however, the chemical bonds have the ability to convert them into insoluble molecules. The hydrolysis process breaks these chemical bonds, joining the small molecules together to produce large molecules. For example the glucose is soluble in water, but by chemical bonding is converted into insoluble cellulose. Therefore, the hydrolysis bacteria releases enzyme

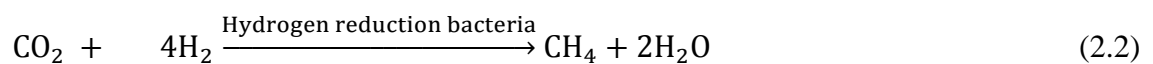
cellulose to break these bonds into soluble compounds (glucose) (Appels, et al. 2008, Metcalf & Eddy, 2003).

### 2.2.2 Fermentation Stage

In this stage, two processes occur spontaneously: acidogenesis and acetogenesis. The soluble materials produced from the hydrolysis stage are disintegrated by facultative anaerobic bacteria. The degradation process produces propionate, butyrate, succinate, lactate, and ethanol as a first step, while acetate, carbon dioxide, and hydrogen are produced as a second step due to fermentation of the propionate and butyrate. All bioprocesses in this stage occur under low pressure of hydrogen ( $10^{-4}$ ). Also, organic-nitrogen and organic-sulfur are produced through degradation of proteins and amino acid. The acetate as a main organic compound is fermented further as a substrate by methane-forming bacteria in the final stage (Metcalf & Eddy, 2003).

### 2.2.3 Methanogenesis Stage

The methanogenesis stage or methane-production stage is the final stage in the anaerobic digestion process and is carried out by methanogenic bacteria. The compounds produced from the fermentation stage are broken-down into methane and carbon dioxide by two means. First, the acetate is converted into methane and carbon dioxide by acetate reduction bacteria, while, second, methane and water can be produced through the reaction of hydrogen and carbon dioxide via hydrogen reduction bacteria (Appels, et al. 2008; Sahlstrom 2003; Birgitte, 2003; Metcalf & Eddy, 2003).



These three stages of anaerobic digestion are illustrated in Figure 2.4.

The methanogenic stage represents a rate-limited stage in the digestion process according to Gujer and Zehnder (1983). Nevertheless, Miron et al. (2000) demonstrated from their experiments that the types of organic matter in raw sludge can play an important role in determining the rate-limited stage in anaerobic digestion. The authors indicated that the hydrolysis stage is considered a rate-limited stage if carbohydrate

(Cellulose, hemicellulose and lignin fractions) is used as a substrate in anaerobic digestion, since the hydrolysis rate of cellulose is very low (Nicles et al., 1983).

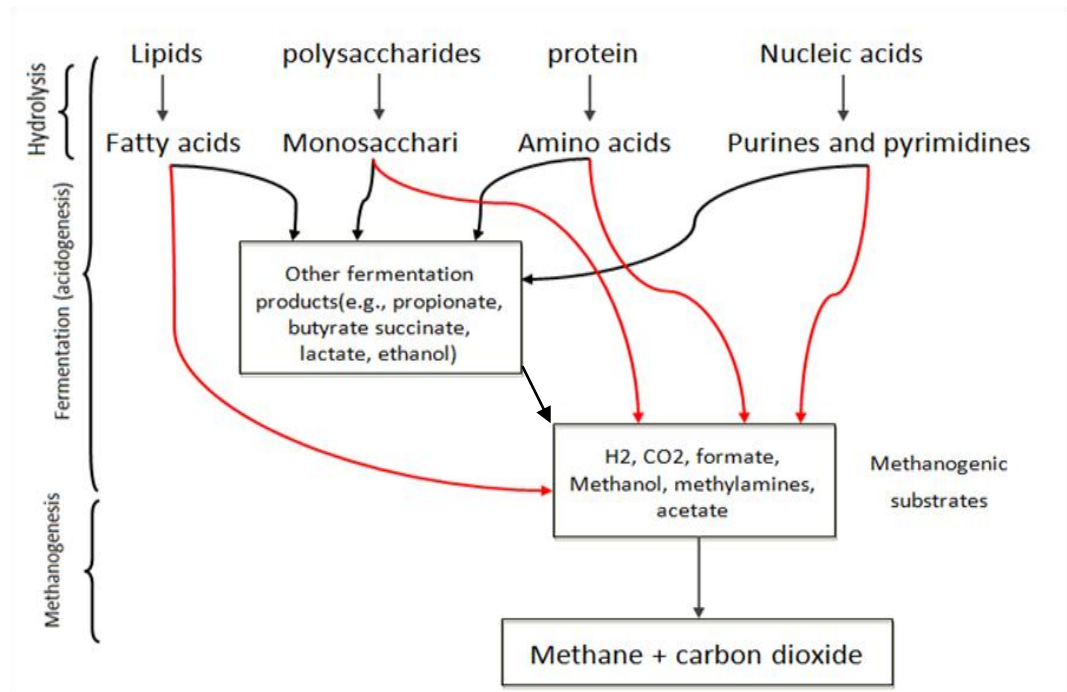


Figure 2.4: Schematic of degradation steps in anaerobic digestion

## 2.3 Effect of the Parameters on the Anaerobic Digestion Process.

There are many parameters that affect the performance of anaerobic digestion, some of them including the following:

### 2.3.1 Temperature

Temperature is one of the main variables that affect the activity and performance of the microorganisms, conversion, stability, effluent and amount of production of biogas (Ahring et al. 2001, Sanchez et al, 2001). In general, microorganisms in anaerobic digestion can be classified into three thermal group according to their ability to live within a particular temperature range (Bartlett, 1971; Van et al, 1997). In the case of

psychrophiles, the temperature is below than 20 °C; with mesophiles, temperatures are between 25 and 40°C; and for thermophiles; temperatures are higher than 40°C. In each stage of the anaerobic digestion (hydrolysis, acidogenesis and methanogenesis), temperature change has a different impact. Donoso, et al. (2009) and Bouallagui et al. (2003) studied the influence of temperature on each stage of anaerobic digestion. They found that minimum effectiveness of microorganisms occurs in the Psychrophiles process, while a significant increase was observed with temperatures higher than 30 °C. Increasing the digester temperature has a significant effect on the degradation rate of organic matter, improving dewatering for solid-liquid separation and increasing efficiency (Varel et al. 1980; Metcalf & Eddy, 2003). However, increasing the temperature does not lead necessarily to increased methane production, especially if the temperature increases to higher than 55°C, which causes increase in inhibition by the free NH<sub>3</sub>, resulting in the process being uneconomic (Varel et al., 1980; Hashimoto et al., 1981; Angelidaki and Ahring, 1995; Ahring, 1995; Ahring et al., 2001; Kim et al., 2006).

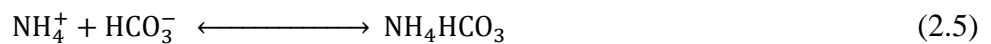
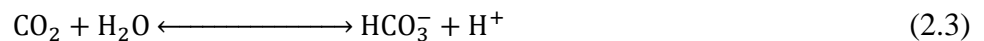
### 2.3.2 pH

Anaerobic bacteria, especially methanogenic bacteria, are very sensitive to changes in pH. The activity of methanogenic bacteria is inhibited if the pH falls below 6.2 and methane production will stop with the accumulation of volatile fatty acids (Cheremisiuff, 1996; Metcalf & Eddy, 2003). There are a few species, for instance *Methanlobus taylorii* GS-16 and *Methanobacterium subterraneum*, capable of living and growing with a pH of up to 9 (Barber and Ferry, 2001). Perto et al. (1988) defined the optimum conditions for hydrolytic bacteria as pH equal to 6.8. Leitao et al. (2006) indicated that the best conditions for the activity of methanogenesis bacteria are pH between 6.5 and 7.5, while Leitao et al. (2006) suggested that acidogenic bacteria are less affected by variation of pH value in anaerobic digestion. Gerardi 2003, summarised the optimum pH for some types of methanogenesis bacteria as illustrated in Table 2.1. The anaerobic digestion process tends to lower pH, therefore the control of pH is achieved by adding buffer solution.

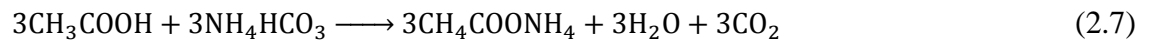
Table 2.1: Optimum PH for some types of methanogenesis bacteria (Gerardi 2003)

Genus	pH
Methanosphaera	6.8
Methanothermus	6.5
Methanogenium	7.0
Methanolacina	6.6-7.2
Methanomicrobium	6.1-6.9
Methanospirillum	7.0-7.5
Methanococcoides	7.0-7.5
Methanohalobium	6.5-7.5
Methanolobus	6.5-6.8
Methanotherix	7.1-7.8

Enhancement of digestion stability can be achieved through the presence of alkalinity in the sludge. A decline in alkalinity in anaerobic digestion represents an indicator of process failure. Accumulation of organic acids, which results from the failure of methanogenic bacteria to convert these acids to methane, is one of main causes of decreases in alkalinity below the desired level. The biodegradation of proteinaceous substances and production of ammonia due to the release of amino group (-NH<sub>2</sub>) is the main source of alkalinity in the digestion process. On the other hand, degradation of amino acids also produces carbon dioxide. Therefore natural equilibrium in the digestion process can be obtained through a reaction of carbon dioxide and ammonia to produce ammonium bicarbonate as illustrated in the following equation.



This equilibrium is continuous in the digestion process unless there are external causes that influence the pH or alkalinity of digester. For example, the presence of organic acids or wastes in sludge fed to anaerobic digester affects the activity of methanogenic bacteria. However, the degradation of other compounds, for instance glucose, can also play a role in this equilibrium. For example, the acetate formed from degradation of glucose reacts with ammonium bicarbonate, thus, the alkalinity is destroyed until formation of biomethane is brought about by methanogenic bacteria.



### 2.3.3 Hydraulic Retention Time

Retention time (Hydraulic retention time and solid retention time): is the average time of retention of liquids or solids inside a bioreactor (anaerobic digestion), which is one of the factors affecting the performance of the anaerobic digestion, and is usually measured in days (Metcalf and Eddy, 2003). The temperature increase corresponds to a decrease of retention time; therefore, in the thermophilic digestion process the retention time is between 10-15 days, while mesophilic digestion takes between 20-30 days.

### 2.3.4 Tolerance of Oxygen

Anaerobic processes take place in the absence of oxygen, which is a toxic gas for all anaerobic bacteria; however, the degree of sensitivity of these bacteria to oxygen varies (Rolfe et al. 1977). In the anaerobic digestion process, oxygen is toxic to methanogenesis bacteria. Scott et al. (1983) used mass spectrometry to determine the level of sensitivity of methanogenic bacteria to oxygen in an anaerobic digester. It was found that the methane production decreases by 48% when the process is exposed to 10% oxygen for 6 min and 34% when it is exposed to 20% oxygen for 5 min. Optimal conditions for the methane bacteria are found to occur when the solubility of oxygen is lower than 0.003 mg/ L. However, some strains are viable in environmental conditions more exposed to oxygen (Kato et al., 1993; Zahnder and Wuhmann, 1997).

## 2.4 Characteristics of Biogas

The composition of biogas depends on the chemical and physical properties of feedstock. For example, raw sewage has a high protein content that leads to production of a biogas with high concentrations of ammonia (Hansen et al., 1998); however, this is an extreme situation. In general, industrial waste (organic waste), domestic waste, and animal waste produce a biogas that has a general composition as illustrated in Tables 2.2 and 2.3.

Table 2.2: General characteristics of biogas according to its sources (B.R.E. 2012)

Components	Household waste	Wastewater treatment plants sludge	Agricultural wastes	Waste of agrifood industry
Methane(% vol)	50-60	60-75	60-75	68
Carbone dioxide (% vol)	34-38	19-33	19-33	26
Water (% vol)	6 (@ 40°C)	6 (@ 40°C)	6 (@ 40°C)	6 (@ 40°C)
Nitrogen (% vol)	5-0	1-0	1-0	-
Oxygen (% vol)	1-0	<0.5	<0.5	-
Hydrogen sulphide (mg/m <sup>3</sup> )	100-900	1000-4000	3000-10000	400
Ammonia(mg/m <sup>3</sup> )	-	-	50-100	-
Aromatic (mg/m <sup>3</sup> )	0-200	-	-	-

Table 2.3: Composition of biogas and natural gas (B.R.E. 2012)

Types of gas	Biogas produced from Household waste	Biogas produced from Agrifood industry	Natural gas
Composition	60% CH <sub>4</sub>	68% CH <sub>4</sub>	97.0% CH <sub>4</sub>
	33 % CO <sub>2</sub>	26 % CO <sub>2</sub>	2.2% C <sub>2</sub>
	1% N <sub>2</sub>	1% N <sub>2</sub>	0.3% C <sub>3</sub>
	0% O <sub>2</sub>	0% O <sub>2</sub>	0.1% C <sub>4+</sub>
	6% H <sub>2</sub> O	5 % H <sub>2</sub> O	0.4% N <sub>2</sub>
PCS kWh/m <sup>3</sup>	6.6	7.5	11.3
PCI kWh/m <sup>3</sup>	6	6.8	10.3
Density	0.93	0.85	0.57
Indiex of Wobbe	6.9	8.1	14.9

Utilization of the biogas depends mainly on these characteristics of its composition as well as the level of impurities as can be seen in Figure 2.5. For instance, biogas produced from the digester is used by the combined heat and power to generate electricity and heat energy, but cannot be used as vehicle fuel unless purified of carbon dioxide, hydrogen sulphide and water vapour. These materials, which occur in biogas, not only reduce its thermal value but also can cause serious damage to combustion engines. The purification of biogas involves multiple stages and the use of advanced technology.

Upgrading of the biogas produced from anaerobic digestion is required to enhance its heating value. The presence of impurities and gases in the content of the biogas causes operational damage and environmental problems.

Purification of biogas can be achieved by the removal of carbon dioxide, water, and H<sub>2</sub>S.

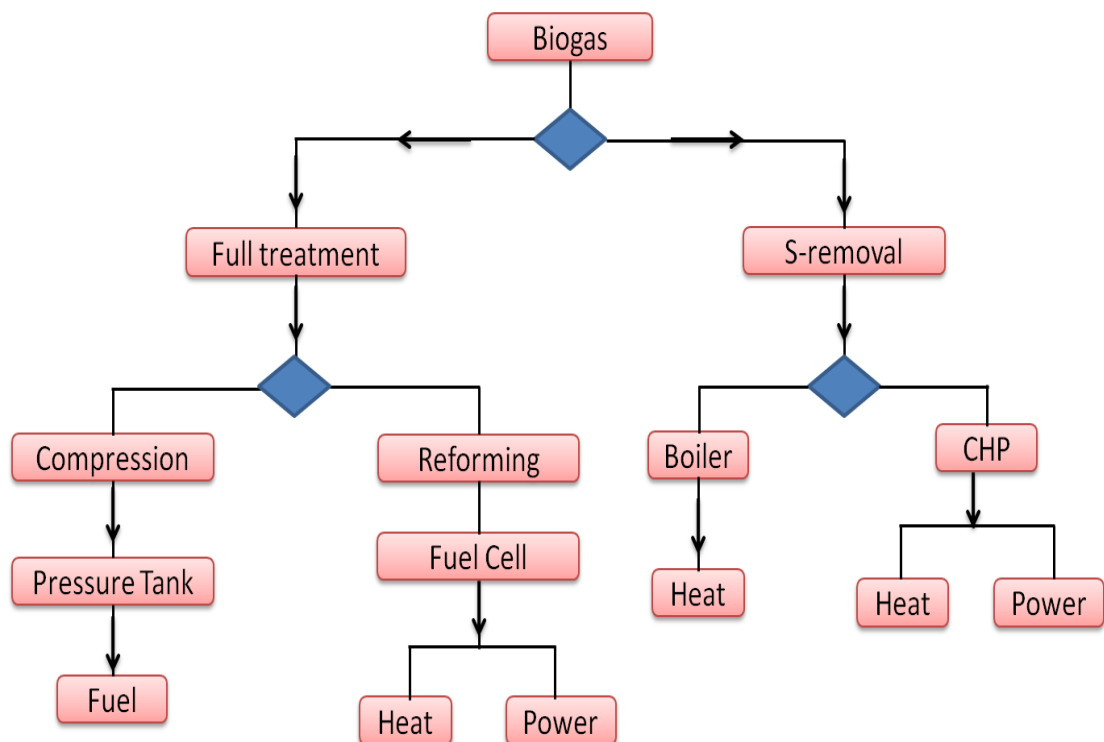


Figure 2.5: Utilisation of biogas produced from anaerobic digestion and upgrading step required

### 2.4.1 Removal of Carbon Dioxide.

Carbon dioxide reacts with water to produce carbonic acid causing corrosion in pipelines and combustion equipment. In addition, high carbon dioxide content in biogas leads to reduction of the heating value to less than 600 BTU.

Removal of carbon dioxide is carried out by various methods, including physical, chemical and biological methods (Degre`ve et al., 2001). These methods include absorption processes, pressure scrubbing, Organic solvents (Appels et al. 2008),

pressure swing adsorption (Pande and Fabian, 1989), Cryogenic separation (Deublein and Steinhauser, 2008), Membrane separation (Harasimowicz et al. 2007; Lastella et al. 2002; Stern et al. 1998; Li and Teo 1993), and chemical conversion [Appels et al. 2008].

### **2.4.2 Removal of Water**

The water content in biogas reaches a saturation state. Removal of water reduces its potential conversion to acidic water by H<sub>2</sub>S and CO<sub>2</sub>. Silica gel and hygroscopic salts are materials commonly used in the removal process (Deublein and Steinhauser, 2008).

### **2.4.3 Removal of Hydrogen Sulphide**

Although hydrogen sulphide is one of the trace gases in biogas, this gas has environmental effects as well as causing corrosion in pipelines and combustion equipment. Removal can be achieved by added iron to the sludge to produce insoluble sulphides or by biological treatment through utilisation of the Thiobacillus family in oxidation of sulphides to elementary sulphur (Horikawa, 2004, Abatzoglou and Boivin, 2009, Appels et al. 2008).

## **2.5 Challenges in the Anaerobic Digestion Process**

Anaerobic digestion, like any biological process, has benefits and problems. Advantages include lower energy consumption, lower biomass production, less pollution in the wastewater, and as sources of nitrogen and phosphate for fertilizing the soil (Appels, et al. 2008; Sahlstrom 2003; Birgitte, 2003; Metcalf & Eddy, 2003). Moreover, the process can convert the energy stored in organic material to methane to generate electrical and heat energy, whilst less bioreactor volume is required with high volumetric organic matter loads. However, anaerobic digestion has potential disadvantages that present obstacles to its development as a major source of clean energy (Salomoni, & Petazzoni, 2006). These problems include low production, high energy required for the mixing system, poor heating system as well as generation of acid gases that cause potential problems for subsequent processes (Metcalf and Eddy, 2003).

### **2.5.1 Mixing System in Anaerobic Digestion**

The mixing process in bioreactors is a critical factor in determining the efficiency of fermentation and the nature of the design. It plays an active role in providing a suitable

environment for micro-organisms, helping to maintain uniformity of temperature, pH and added chemicals throughout all parts of the reactor. It is important in providing the bacteria with substrate, dissolved gases and (if necessary) heat and also prevents the formation of a scum layer in the top of the reactor (Bellow-Mendoza and Sharratt, 1998; Monteith et al., (1981).

Hence, many researchers have studied the crucial role of mixing in terms of its effects on the performance of anaerobic digestion and biogas production (Borole et al., 2006).

Stroort et al., (2001) studied the effects of mixing on the performance of anaerobic digestion, and compared continuous mixing with non-continuous mixing. The authors found that reducing the level of mixing in the process helps to improve the performance of anaerobic digestion and concluded that constant mixing is not necessary for good performance of the process, and may lead to inhibition at high loading rates. Similarly Stafford (1982) found that high-speed mixing in the anaerobic digestion process leads to reduced production of biogas, due to shear forces which separate the microorganisms from their substrates. Also, McMahon et al. (2001) claimed that a high level of mixing causes the accumulation of propionate, acetate, and volatile fatty acid. In addition, it leads to inhibition of the mutually beneficial interaction which occurs between different species of bacteria in anaerobic digestion. Reduction of the level of mixing, on the other hand, leads to degradation of propionate and an increase in the stability of the anaerobic digester. Therefore, the level of mixing determines the stability of the anaerobic digestion process.

There is a proportional relation between the level of the mixing required and the concentration of total solids which enter the bioreactor. Karim et al. (2005), demonstrated that the effect of mixing on anaerobic digestion is related to the amount of manure slurry in the feed. They found that mixing is not critical (i.e. it does not affect the production of bio-gas) if the amount of manure slurry is only 5%, because this concentration of solids needs only natural mixing to provide a suitable environment for the bacteria. The effect of forced mixing on anaerobic digestion appears when the level of the solids is increased, and at a solids concentration of 10% it leads to an increase in bio-gas production of 29%.

Bello-Mendoza and Sharratt (1998) created a dynamic model for the diagnosis of the impact of mixing on the amount of methane production and efficiency of the process.

The authors found that non-efficient mixing leads to a decrease in both efficiency of anaerobic digestion and amount of methane produced. More importantly, results indicated that mixing efficiently helps to reduce the hydraulic retention time as long as the same level of efficiency of treatment required is maintained throughout.

It is possible to conclude that the efficiency of the mixing helps to reduce the size of the reactor and increase the amount of sludge treated and the amount of methane produced. In the same context, Monteith et al., (1981) indicated that uniformity in mixing in the anaerobic digestion process will result in the reduction of hydraulic retention time. The authors suggested that an inefficient mixing system leads to instability in the process and affects the performance of anaerobic digestion.

Previous investigations have highlighted the mixing factor effect and its importance on digestion, and the amount of biogas produced, and indeed plays a critical role in the success or failure of the entire process. Also confirmed is the fact that, for several reasons, high velocity in the process of mixing is detrimental for digestion and the production of methane, and may lead to low efficiency of digestion and lack of methane output. In addition, high velocity of mixing involves a higher level of energy input, which affects the resulting energy balance; therefore the process is less efficient due to the higher input of energy required for mixing.

Therefore, it is possible to conclude, that the efficient mixing of sludge at low or moderate speeds is a more efficient mode of operation, and research into this process will form the main focus of this investigation. Anaerobic digestion already utilizes a natural mixing system, since biogases are produced, such as methane and carbon dioxide and due to the natural mixing capacity of its high buoyancy force. However, although the process is able to mix the sludge in the digester, it is not able to break the scum and prevent the formation of a thermal layer.

The main types of mixing system in anaerobic digestion can be classified in to external pumped recirculation, internal pumped recirculation and gas injection as illustrated in Figure 2.6.

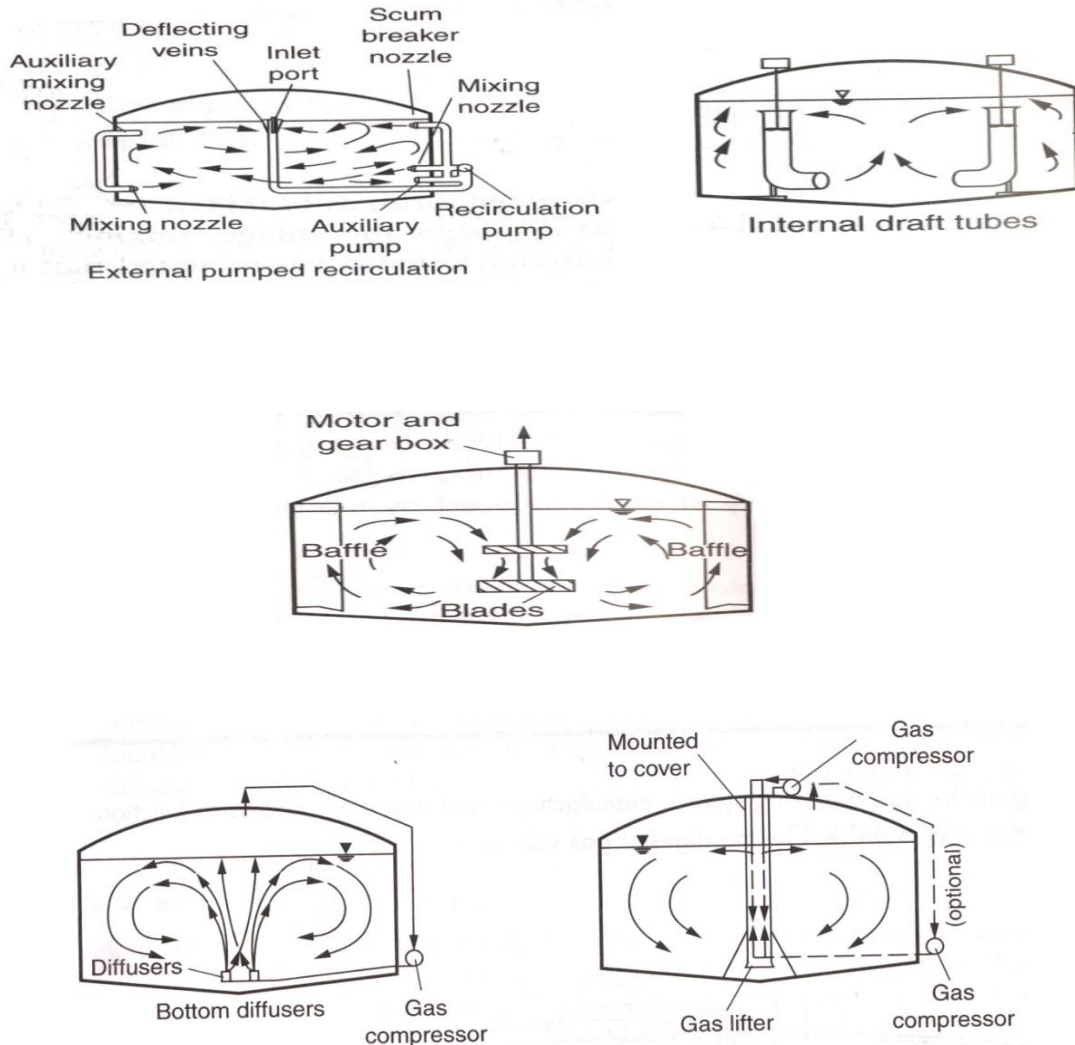


Figure 2.6: Some types of mixing systems used in anaerobic digester (Metcalf & Eddy, 2003)

External pumped recirculation includes recycling the sludge using an external pump specialized for this purpose. The active sludge and raw sewage are mixed and are recycled by this method of mixing at a high flow rate to ensure the efficient mixing of all the sludge in the digester. However, this method requires high energy, depending on the characteristics of the sludge and geometry of the digester. In addition, the friction caused by the deposition of some solids and rags on the inner walls of the pipelines in effect increases the energy required for this type of mixing. The operational problems

inherent in this system are many and varied, and include damage to the pump and pipes (Appels et al., 2008).

The machinery for internal mechanical mixing consists of three main parts. The first is the pump, which is placed at the top of the digester; the second is the pipeline for transmission of the movement generated by the engine to the third part (impellers) that are submerged in the sludge. The amount of electrical energy required for this type of mixing is less than for external pumped recirculation; however, the cost of maintenance and installation is high, especially in the third part of this system, due to accumulation of solids in the impeller as shown in the Figure 2.7 (Metcalf &Eddy, 2003).



Figure 2.7: Submersible mixer is lifted out from the digester for cleaning

Gas injection processes consist of two types. First, there is the unconfined gas system, whereby the gas is collected from the top of the digester, and then discharged by a diffuser at the bottom. The second type is the confined gas system, whereby the gas is collected from the top of digester, and then discharged via confined tubes (Metcalf &Eddy, 2003).

The most common problems associated with these types are:

1. Corrosion of impellers, shifts, gas piping, and other equipment.

2. Scaling and wear of the equipment by solids (grits).
3. High manufacturing cost and high level maintenance needed of the oversized gear-box for mechanical stirring and mechanical pumping.
4. Mechanical pumping is sensitive to sludge levels.
5. Pumps become plugged by rags and other debris.

### 2.5.2 Heating Systems in Anaerobic Digestion

The overall performance of a biological process is assessed by the biological reaction rate constants, which depend on the temperature of the medium. The temperature not only affects the metabolic activity of the bacteria but also the gas-liquid transfer rate and the characteristics of the biological medium (Metcalf & Eddy 1991; Stannard et al 1985; Davey, 1994).

Predictive modelling can be used to study the response of the bacteria when the chemical and physical conditions of the environment are changed. Although there are many parameters that affect the activity of microorganisms, temperature is the factor that affects with the strongest effect growth rate (Zwietering et al., 1991, 1994).

Basically, the effect of the temperature on chemical reactions can be expressed by an Arrhenius equation, which indicates that the chemical reaction constant exponentially increases with temperature as shown in the following equation.

$$\frac{dK}{dT} = \frac{E}{RT^2} \quad (2.9)$$

Where  $K$  is the chemical reaction constant,  $T$  is temperature,  $R$  is the universal gas constant, and  $E$  is activation energy.

Arrhenius law has been modified for biological applications through the creation of an Arrhenius plot which shows clearly that the temperature represents a cardinal factor in the bioprocess. The plot demonstrates that increasing the temperature leads to increase in the growth rate constant depending on the type of bacteria as shown in Figure 2.8 (Ratkowsky et al., 1982, 1983).

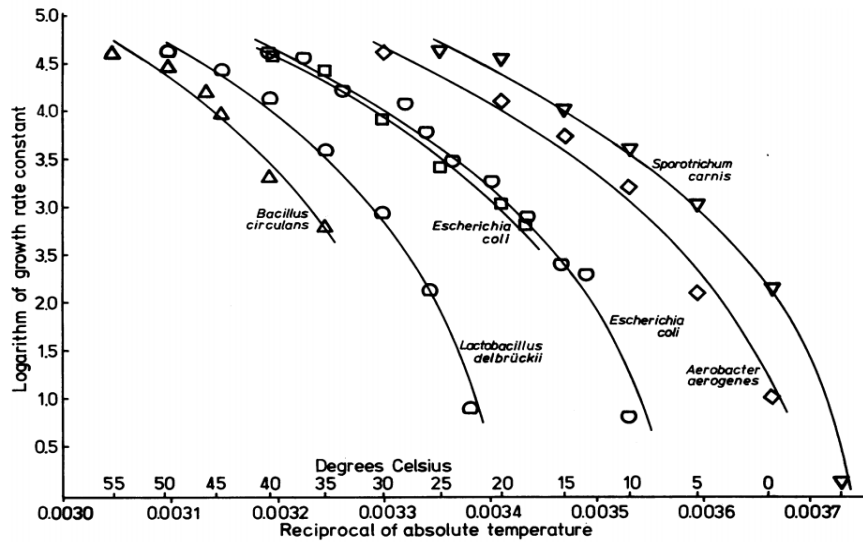


Figure 2.8: Arrhenius plot for different types of bacteria

Anaerobic digestion (AD) is one of the biological processes that need heating systems. It can be classified into three potential operating points; Psychrophiles (15-20 °C), Mesophiles (25-40 °C) and Thermophiles (45-60 °C) (Bartlett, 1971; Van et al, 1997; Maly and Fadrus, 1971). The minimum effectiveness of microorganisms occurs in the Psychrophilic process, while a significant increase is observed when the temperature rises above 30 °C (Donoso, et al., 2009; and Bouallagui et al., 2003). Higher the degradation rate, lower retention time and high methane production can be achieved in thermophilic anaerobic process. However, mesophilic anaerobic process is widely used in order to ensure the stability of the digestion process and reduce energy requirements (Zupancić and Ros, 2003).

The biogas produced from anaerobic digestion is used as a fuel in combined heat and power (CHP) systems to generate electricity, while the heat energy can be recovered and used to heat other endothermic bioprocesses. In wastewater treatment plants, the heating system in the anaerobic digester is usually run by heat energy produced from CHP, (Appels et al., 2008). The CHP process and anaerobic digester can be integrated, because the CHP process needs a cooling system, while anaerobic digestion needs a heating system, thus, these units are mutually beneficial. In other words, the hot water produced from CHP can be used directly to heat the sludge in a heat exchange while the cold water is returned to CHP by a closed loop system as shown in the Figure 2.9.

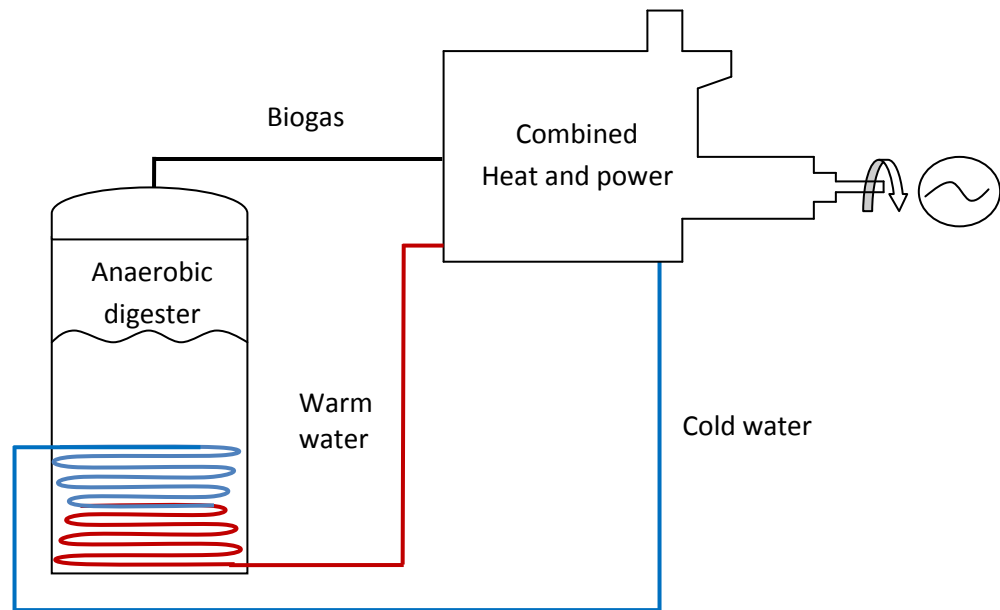


Figure 2.9: Mutually beneficial relationship between anaerobic digestion and CHP in WWTP.

Heating the sludge can be achieved by an external or internal heat exchanger. In fact, the form of heating system traditionally used in anaerobic digesters is very problematic. For example, during the process of heating the sludge, the suspended solids accumulate in the heating tubes, causing an increase in the thickness of the tube walls. Consequently, heating efficiency is reduced (Vinton, 1944). Moreover, the dissolved gases such as  $\text{CO}_2$  and  $\text{H}_2\text{S}$ , may cause corrosion of the heating pipes. If this happens, the sludge will penetrate inside the heat exchanger tubes leading to damage of the CHP system. In addition, there is an increase in energy usage due to loading of the pump generated by an increased fall in pressure as well as several problems associated with temperature control. For instance, a lag time is created between sludge entry and discharge. Moreover, the hot water used for heating conventional anaerobic digesters creates hot spots which cause burning and a build-up of sludge on the heat exchanger tubes. Consequently, this causes an increase in mass transfer resistance and maintenance costs.

Figure 2.10 shows an example of the accumulation of the suspended solids on the heater tubes that occurred during our previous experiments which led to failure of the anaerobic digestion process.

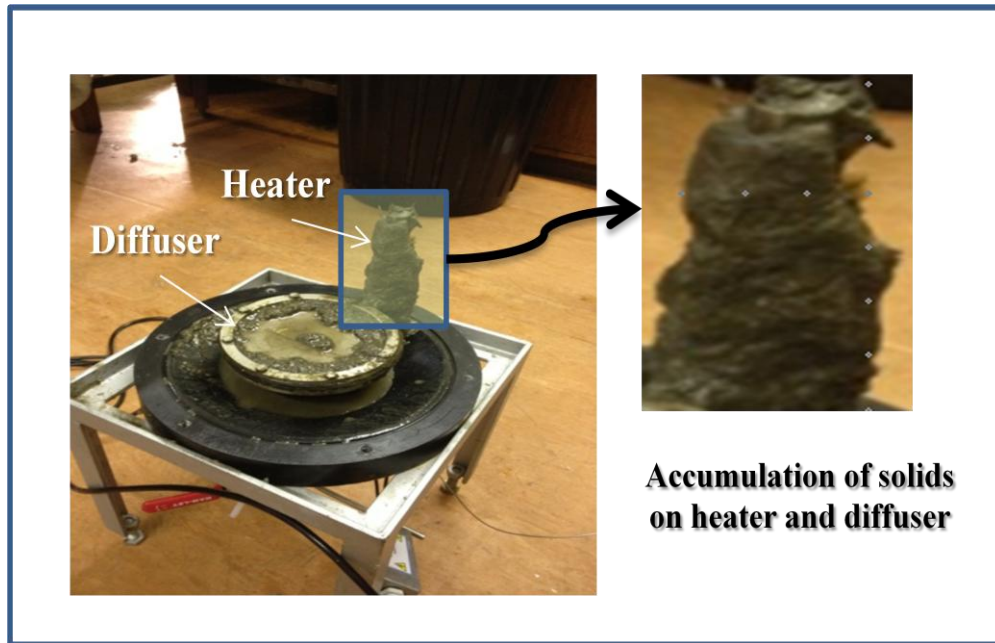


Figure 2.10: Snapshot of accumulation of solids on the heating tube in lab-scale experiments.

Therefore, the current study suggests *the utilization of direct-contact evaporation for process heating through the conversion of direct-contact evaporation into direct-contact heating.*

Direct contact evaporation (DCE) is a process that is employed industrially for concentrated mixtures such as fruit juices and aqueous solutions (Switzer et al., 1963; Cronan, 1956; Williams, 1965; Zaida et al., 1987). In DCE, a gas is normally bubbled through a sparger present at the bottom of a column containing some liquid at a different temperature. Most DCE units operate using a superheated gas bubbled through a relatively cold liquid in such a way that energy from the superheated gas within the bubbles is transferred either as sensible heat: leading to a liquid temperature rise, or as latent heat of vaporisation, resulting in evaporation of the liquid into the interior of the bubbles (Ribeiro and Lage, 2004; Ribeiro and Lage, 2005; Ribeiro et al, 2005).

The performance of a DCE unit depends on the amount of evaporation that can be achieved in a given time, therefore it is beneficial to develop methods to maximise the evaporation rate. Various operating variables can affect the evaporation rate in DCE. Such parameters include hot gas flow rate, bubble size, level of liquid and time for evaporation. Ribeiro & Lage (2004) studied the effect of changing gas flow rate on the

operation of a DCE unit and found the rate of evaporation to increase with increasing gas flow rate. Iyer and Chu (1971) observed the same effect in submerged combustion experiments.

Utilization of direct contact evaporation in the present study is aimed at addressing some problems that occur in traditional heating systems for the anaerobic digester as will explained in chapter eight.

In the present study, the development of the mixing system and heating system in the anaerobic digestion process study involved the use of an airlift bioreactor.

## **2.6 Using the Airlift Bioreactor**

In spite of the accelerated development of bioreactors due to their widespread use, there are still difficulties in maintaining stability and efficiency of bioprocesses. It is believed that the most important causes of failure have been poor construction and design, leading to inadequate mixing, which may jeopardize the stability and performance of the process (Karim et al 2003(a), Karim et al. 2005(b), Monteith et al. 1981, Lay 2000 and 2001).

The mixing process in bioreactors is critical factor in determining the efficiency of the fermentation process and the nature of design that will provide a suitable environment for microorganisms.

The traditional mixing method (i.e. stirred tanks) may yield better performance in the degradation process, yet when the energy requirements of the process are weighed against the energy obtained from the biogas produced, the process becomes economically unviable. Therefore, the reduction of the energy required for mixing is one the most challenging targets faced in the development of bioprocess applications.

The present study proposes the use of an airlift bioreactor for application to bioprocessing. The airlift reactor (ALR) has been used in several industrial applications, and it has become the most appealing option for any process involving gas-liquid contact. Compared to stirred tanks, the airlift reactor has been shown to perform mixing more efficiently. According to their structure, airlift reactors (gaslift reactors) can be classified into two main types: the external loop airlift reactor, in which the circulation takes place in separate conduits, and the internal loop airlift reactor, which is provided

with a tube or a plate to create the conduit (channel) inside a single reactor for circulating the liquid inside the reactor (Majizat et al. 1997) (Figure 2.11).

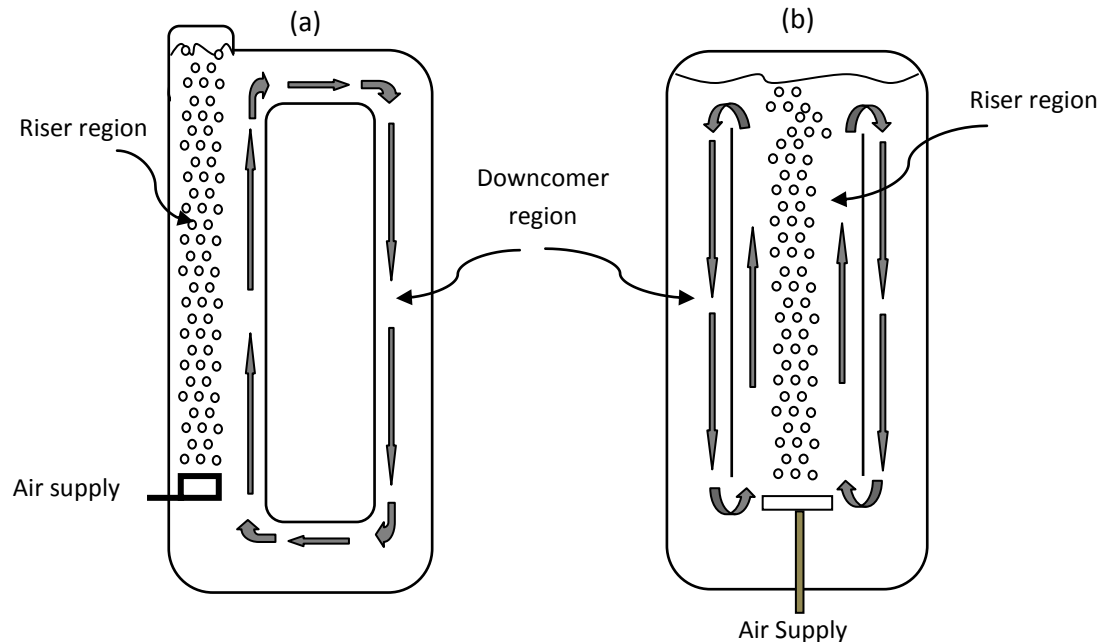


Figure 2.11: Schematic of airlift bioreactor with (a) external recirculation and (b) internal recirculation

Although airlift bioreactors have many advantages over continuous stirred tank reactors for example; lower consumed energy and lower installation and maintenance costs, these reactors still needs further technical development to increase the interfacial area between the gas phase and liquid phase.

According to our knowledge, the use of airlift bioreactors in the anaerobic digestion process using different gases has not yet been investigated. Since this process is very sensitive to oxygen. In order to investigate the possibility of using the airlift bioreactor in anaerobic digestion, it is necessary to study bio-reactions that occur during the anaerobic digestion process. However, some researchers studied design of airlift if circulation of biogas is chose as a mixing method in the anaerobic digestion (Wu and Chen (2008); Karim et al. (2007)).

## 2.7 Biochemical Reactions during Anaerobic Digestion

The anaerobic digestion process consists of a group of reactions that are occurred biologically by bacteria and lead to the formation of methane and carbon dioxide through disintegration of organic matter. Each reaction has a specific value of Gibbs free energy that determines the direction of reaction as shown in Figure 2.12. As can be seen, some of these reactions have standard Gibbs free energy with a negative sign; this signifies that the reactions are spontaneous and favourable energetically, while others have a positive sign, which means these reactions are unfavourable energetically and prevent spontaneous production of methane causing the failure of the digestion process as a whole (Metcalf and Eddy, 2003; Schmidt and Ahring, 1993).

However, there is a relationship between the methanogenic and acidogenic bacteria that is termed “mutually beneficial”. This relationship helps to convert unfavourable reactions into favourable reactions by maintaining low partial pressure of hydrogen. The partial pressure should be lower than  $10^{-4}$  (Ahring and Westermann, 1988), to allow the necessary equilibrium shift in the right direction and formation of more formate and acetate. The production of hydrogen by acidogenesis and its utilization by methanogenesis is achieved by interspecies-hydrogen-transfer.

In fact, the methanogenic bacteria play an important role in the process. Therefore, the failure to provide a suitable environment for these bacteria prevent hydrogen from being consumed in sufficient quantity and thus will inevitably lead to accumulation of VFAs and low pH, and ultimately the failure of the digestion process (Eddy, 2003; McCarty and Smith, 1986; Schmidt 1993).



## 2.8 Effect of Partial Pressure on the Production of Biogas

The mathematical relationship between Gibbs free energy and vapour pressure is as follows:

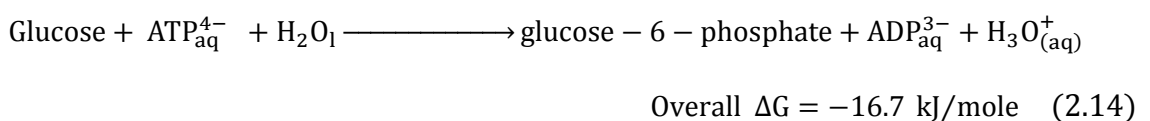
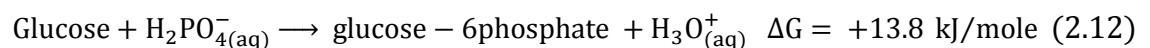


$$\Delta G = \Delta G^\circ + RT \ln \frac{[pC]^c [pD]^d}{[pA]^a [pB]^b} \quad (2.11)$$

Where  $\Delta G$  is Gibbs free energy change,  $\Delta G^\circ$  is standard Gibbs free energy,  $R$  is universal gas constant,  $T$  is temperature of reaction,  $pA$ ,  $pB$ ,  $pC$ , and  $pD$  are partial pressure of reactants and products, and  $a, b, c$ , and  $d$  are the coefficients in the balanced chemical equation.

From the above equation, it is possible to note that the low partial pressure of the products contributes to Gibbs free energy with a negative sign, hence the reaction becomes thermodynamically favourable towards the formation of more products, and vice versa (Gary 2004).

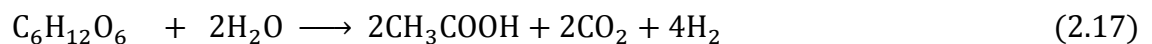
In the biological processes, some of bio-reactions are unspontaneous reactions and thermodynamically not favourable ( $+\Delta G$ ). Typically, these reactions can be treated by two methods. The first method includes providing enough energy to endergonic reactions to convert them to spontaneous reactions. For instance; conversion of glucose to glucose-6-phosphate, which occurs in our body, is not spontaneous reactions ( $+\Delta G$ ). To force this reaction to proceed, it should be coupled by another exergonic reaction, such as hydrolysis of ATP (Adenosine triphosphate) to ADP (Adenosine diphosphate) to provide enough energy. Therefore, the overall Gibbs free energy for both reactions has a negative value ( $\Delta G = -16.7$ ) kJ/mole as can be shown in the following reactions:



Reducing the partial pressure of products represents another method can be used to convert unspontaneous reactions to spontaneous reactions that occur in bioprocesses, which they share intermediates. For example, fermentation of propionate in anaerobic digestion has a negative value Gibbs free energy, thus, this reaction is thermodynamically not favourable. Forcing this reaction to spontaneous reaction can be occurred if the partial pressure of hydrogen reduces to  $10^{-4}$  by methanogenesis bacteria as explained earlier. Thus, the overall Gibbs free energy will be negative value as can be seen in the following reactions:



There has been much research based on the mathematical relationship between partial pressure and Gibbs free energy with widespread applications. But the major results of these applications emerged from biological processes, particularly the production process for bio-hydrogen. This process has caused debate among researchers about how to control the partial pressure of hydrogen or carbon dioxide and its effects on the production of hydrogen. Many researchers have noted that an increase in hydrogen production could be achieved by reducing the partial pressure of hydrogen or carbon dioxide or both depending on the following equation:



Tanisho et al. (1998); Park et al., (2005); Alshiyab et al., (2008) studied the effects of the reduction of the partial pressure of carbon dioxide on hydrogen production. Tanisho et al., (1998), found that hydrogen production increased when the partial pressure of carbon dioxide decreased. Park et al. (2005) demonstrated that reducing the concentration of carbon dioxide from 24.5% to 5.3% in the headspace caused an increase in the hydrogen yield of 43%. Alshiyab et al. (2008) indicated that there was an increase in the hydrogen yield when partial pressure of carbon dioxide was decreased.

Liang et al. (2002); Mizuno et al., (2000); Kim et al. (2006), Kraemer and Bagley (2008) studied the effect of reduction in the partial pressure of hydrogen on hydrogen production. Liang et al. (2002) reported that the reduction of partial pressure of hydrogen by using silicone rubber membrane, to remove the dissolved gases, caused an increase in hydrogen yield of 15%. Mizuno et al. (2000) found that the hydrogen yield reached 68% when the partial pressure decreased, which caused an increase in its activity (Kim et al. 2006; Kraemer and Bagley, 2008).

The satisfactory results of these investigations have shown the importance of the removal of gases from biological processes and the effect this has on increasing production of hydrogen.

The behaviour of bacteria in biological operations produces similar responses to those achieved by removing some of the gases. Therefore, in hydrogen production, the removal of some gases during anaerobic digestion is necessary for the production of methane.

Hansson (1979) demonstrated that the production of methane will increase if the partial pressure of carbon dioxide is decreased. The author noted that high CH<sub>4</sub> production occurs if the partial pressure of CO<sub>2</sub> is 0.2 atm., while low CH<sub>4</sub> production occurs if the partial pressure of CO<sub>2</sub> is 1.0 atm.

In a similar study, Cort et al. (1988) used two methods to remove the product gases. The first method (phototrophic *Rhodospirillum rubrum* culture) and the second method (sulfate-reducing bacteria growth) were used to remove the hydrogen. Both methods, led to an increase in methane production and the removal of more VFA from the sludge.

Therefore, it is possible to summarize that the reduction of the partial pressure of gases which are produced from biological operations leads to improvement the performance of bacteria, increased production of these gases, and allows the reactions to proceed due to thermodynamic favourability.

The current study also utilized a new technology in the aeration system for anaerobic digestion. Microbubbles generated by a fluidic oscillator were used to develop the operation of the airlift process and increase the performance of the digestion process.

## 2.9 Microbubble Technology

In gas-liquid systems, enhancement of the mass transfer rate depends, traditionally, on increasing the surface area between the two phases. The desired interfacial area can be obtained by increasing the agitation speed. This approach has now become economically unviable due to the large amount of energy required and the prohibitive cost (Worden and Marshall, 1995). Bubble columns have many advantages over the stirred bioreactor; for example, there are no moving parts inside the bioreactor, installation and maintenance costs are lower and energy requirements are lower. Also, the use of bubble columns offers the potential for improvement in the mass and heat transfer rate by increasing the interfacial area between the two phases (gas and liquid) through the injection of gas in the bottom zone of the reactor. However, the low residence time, poor mixing and high turbulence of the flow has limited the use of the bubble column in bioprocessing (Chisti, 2007).

Because of the advantages mentioned earlier: good mixing, long period of gas-liquid contact, and avoidance of shear damage to cells, the airlift reactor has been widely used in various biological processes. However, technical development of the bio-reactor is still needed in order to increase the mass and heat transfer rates in the gas-liquid interface. This challenge can be addressed by equipping the airlift bioreactor with microbubbles (Figure 2.13).

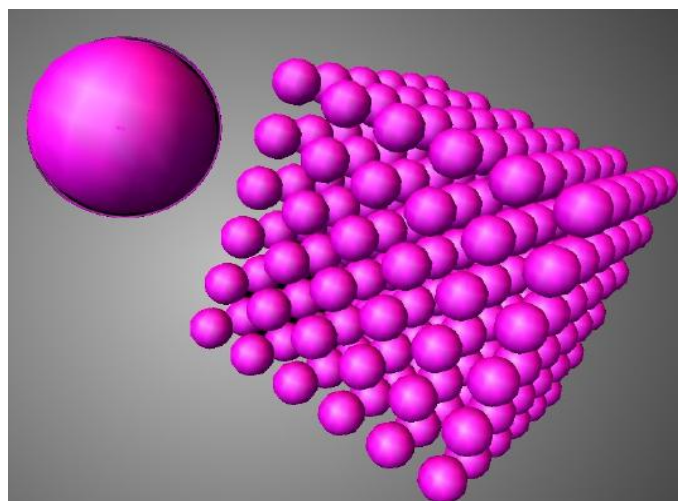


Figure 2.13: Division of a volume into smaller, equally sized objects produces additional surface area that is in scale with the cube root of the dividing number

Mass transfer, heat transfer and momentum transfer rate are basic phenomenological in the chemical engineering processes and significantly increase with an increase in the total interfacial surface area between gas-liquid systems according to the following equation:

$$NA = K_L A_s (C_g - C_L) \quad (2.18)$$

Where NA represents mass transfer fluxes (Mole/ sec),  $K_L$  is the mass transfer coefficient (m/s),  $A_s$  is the total interfacial surface area ( $m^2$ ),  $C_g$  is equilibrium molar concentration in the gas phase ( $mole/m^3$ ),  $C_L$  is molar concentration in liquid phase ( $mole/m^3$ ).

The benefits of microbubble technology in terms of the above phenomenological processes can be illustrated by simple algebraic equations in the cases of a) fine bubble and b) microbubbles:

**a) For fine bubble:**

$$V_f = N_b \left( \frac{4}{3} \pi R_b^3 \right) \quad (2.19)$$

**b) For microbubble:**

$$V_m = n_b \left( \frac{4}{3} \pi r_b^3 \right) \quad (2.20)$$

Where  $V_f$  and  $V_m$  represent a volumetric flow rate for fine bubbles and microbubbles respectively,  $N_b$  and  $n_b$  represent the number of fine bubble and microbubble sized gas bubbles, while  $R_b$  and  $r_b$  represent the fine bubble diameter and micro bubble diameter respectively.

Using the same volumetric flow rate for each case and dividing the volumetric flow rate of the fine bubble by the volumetric flow rate of the microbubble, the equations can be re-arranged as follows:

$$\frac{N_b}{n_b} = \frac{r_b^3}{R_b^3} \quad (2.21)$$

On the other hand, the surface area for each case is written as follows:

$$\frac{A_{s2}}{A_{s1}} = \frac{n_b \pi r_b^2}{N_b \pi R_b^2} \quad (2.22)$$

Equation 2.21 and equation 2.22 together describe the relationship between the surface area and bubble diameter:

$$\frac{A_{s2}}{A_{s1}} = \frac{R_b}{r_b} \quad (2.23)$$

From the above equation, it is clear that decreasing the bubble size leads to an increase in the surface area. Therefore, the total interfacial area with bubble diameter (100  $\mu\text{m}$ ) is about 20 time more than with the fine bubble, if the diameter of the latter is 2mm. Therefore, enhancement of mass transfer, heat transfer and momentum transfer rate in gas-liquid systems is expected if the bubble size reduces.

Moreover the following Stokes equation suggests that the terminal velocity of microbubbles is much less than that with fine bubbles:

$$V_{\text{stokes}} = \frac{2}{9} \frac{g \Delta \rho D_b^2}{\mu_l} \quad (2.24)$$

Where  $V_{\text{stokes}}$  represents the terminal velocity of the gas bubbles,  $\Delta \rho$  is the density difference between gas and liquid,  $D_b$  is bubble diameter, while  $\mu_l$  is the viscosity of liquid. It can be clearly seen that the terminal velocity of the gas bubbles decreases with decreasing bubble size. Thus, the residence time with microbubbles is more than that with fine bubbles.

Therefore the heat transfer, mass transfer and momentum transfer rates increase when the bubble size decreases, due to the increase in the total interfacial surface area and residence time.

It is a common belief in relation to the generation of small bubbles that reducing the diameter of the aperture used for the generation of bubbles leads to reduction of the bubble size. However, the results obtained from these experiments contrasted with that view. They demonstrated that the bubble size was somewhat bigger than the aperture size, the reason being that a wetting force becomes attached that is effective in increasing the size of the bubbles. This force is called an anchoring force and is generated between the perimeter of the aperture and the walls of the bubbles generated. The magnitude of the anchoring force depends on the physical and chemical

characteristics of the diffuser. In other words, when the diffuser has hydrophobic properties, an attractive force is present, while it is absent when the diffuser has hydrophilic properties. Therefore, the size of the bubble continues to increase unless there is an external force to inhibit this growth or unless the buoyancy force increases with the bubble size increase and overcomes the anchoring force so as to allow the bubble to escape into the liquid.

In spite of successive developments of microbubble generation systems, the energy requirements are still reasonably high. Zimmerman et al. (2009, 2010, and 2011) have developed a novel aeration system through fluidic oscillation, which is capable of producing gas bubbles of micron size to achieve enhanced heat and mass transfer rates. As well as increasing the interfacial area, microbubbles offer hydrodynamic stabilisation, longer residence times and increased efficiency of mixing. The fluidic oscillation method has low energy demands compared to other methods for microbubble generation. The essential idea of this novel system is to use oscillatory flow to interrupt the air flow and limit the time available for growth of the bubbles, as shown in Figure 2.14.



(With fluidic oscillator)

(Without fluidic oscillator)

Figure 2.14: Bubbles generated by fluidic oscillation, and without fluidic oscillation

Microbubble generation by fluidic oscillator offers many benefits, including low cost, reliability and robustness. This technology can provide a range of bubble diameters depending on the type of application and diffuser used. In the present study, a two part ceramic diffuser is used in a form resembling a tablet. Each part of the diffuser has a diameter of 5 cm and is separated completely from the other part. The gas from the main supply terminal into the oscillator randomly stays attached to one of the two channels due to the Coanda effect. This creates a pressure difference in the feedback

loop and, as a result, the gas from the port on the non-flowing side (higher pressure) flows back to the lower pressure port with the current flow (Figure 2.15b). The gas pushed out from the low pressure port then hits the main passing flow and switches it to the opposite channel. This cycle is then repeated periodically to give oscillatory jet switching between the flow channels. The oscillation frequency can be easily adjusted by changing the feedback loop length in order to create bubbles of the required size when the outputs are fed to separate diffusers. The fluidic oscillator can be called an amplifier because the very weak flow input in the feedback process controls the powerful output flow. The frequency rate is 9.3 Hz per sec as shown in Figures 2.15 and 2.16.

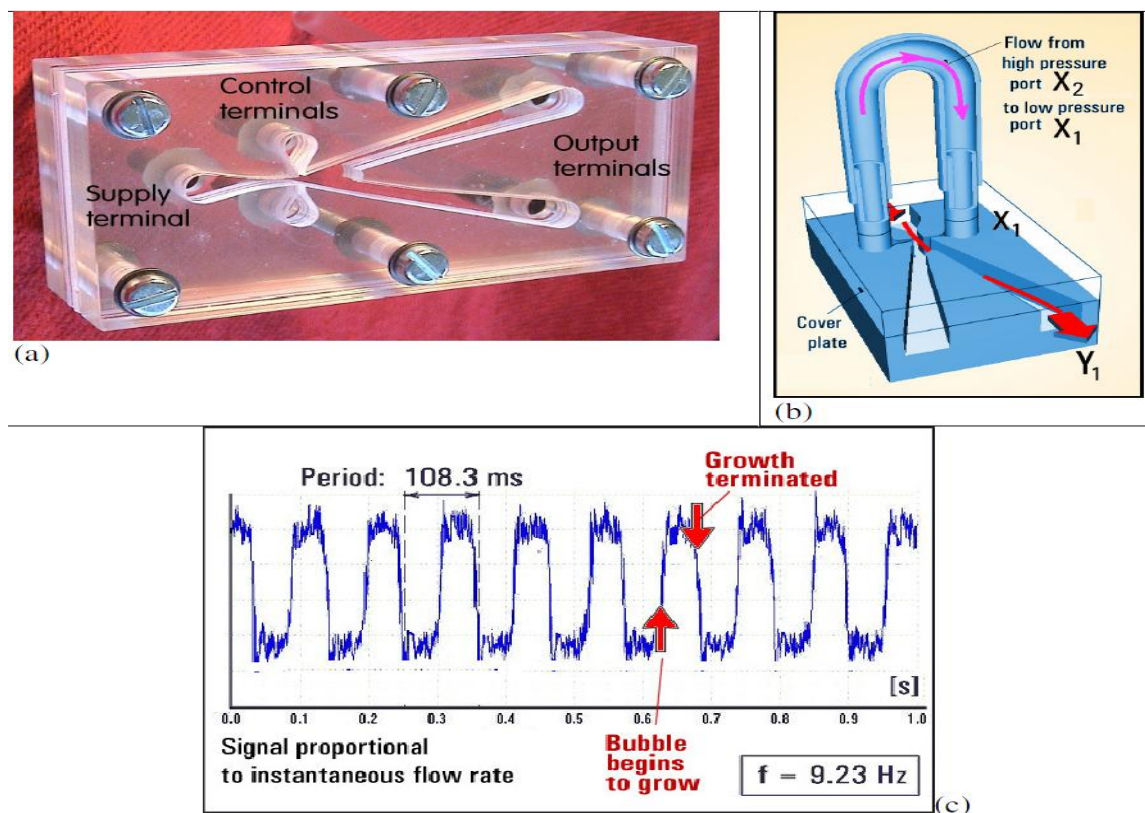


Figure 2.15: Fluidic oscillator system for microbubble generation (reproduced from Zimmerman et al. 2009). (a) Oscillator block containing no moving mechanical parts, with single input and two outputs. (b) Illustration of feedback loop connecting the two control terminals that causes gas pulses to be alternately emitted from each output. (c) Flow rate time history for the fluidic oscillator connected to a parallel percolation nozzle bank with apertures of  $600 \mu\text{m}$  diameter.

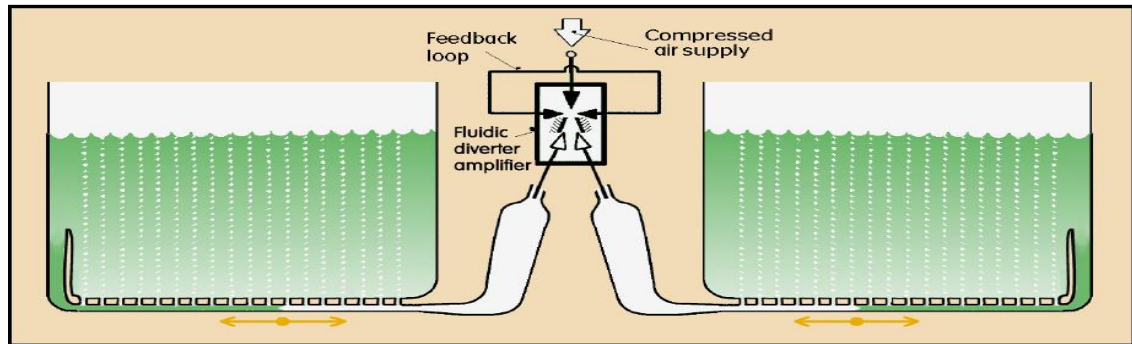


Figure 2.16: Fluidic oscillator system for microbubble generation. Each oscillating output is connected to a diffuser and the rapid interruptions in gas flow in each result in bubble diameters of the order of the aperture diameter.

## 2.10 Summary

The present study addresses the environmental and operational problems that facing the anaerobic digestion process. In spite of many attempts to treat some of these problems, there are some challenges still stand obstacles in the development of this process. The current research suggested use a new technology as a serious attempt to reduce the anaerobic digestion costs. Microbubble generated by fluidic oscillator is one of the most promising possible technologies that have several advantages, which can be used to address these problems.

In the present study, sparging system and microbubbles technology used to:

1. Design of bioreactor for biological applications.
2. Development of mixing systems in anaerobic digestion.
3. Removal of acid-gases from the digested sludge.
4. Increasing the amount of biogas produced from anaerobic digestion.
5. For development of heating systems in anaerobic digestion.
6. Integration of anaerobic digestion with upgrading of biogas unit and combined heat and power unit.

## 2.11 Hypothesis and Objectives of Current Research

The hypothesis of the current research can be summarized as follows: the use of microbubble technology in wastewater treatment plants (anaerobic digestion) reduces the cost of biogas production, improves the performance of anaerobic digestion, and increases the production of methane. In addition, using this technique to redact partial

pressure of methane in the biogas produced has a positive effect on the performance of the digestion process. Furthermore, microbubbles generated by fluidic oscillation contribute to the removal of acid-gases from the digested sludge. This technology can be used to improve the heating system in anaerobic digestion.

The potential benefits of this hypothesis are many, and include: reduction of the cost of production of bio-gas, protection of the environment from emissions of carbon dioxide that cause global warming and climate change, improved efficiency of anaerobic digestion and increased production of methane due to advantages offered by micro-bubble technology and its positive impact on the movement of material, mixing of the system, and reduction of the partial pressure of biogas.

In this research, we propose the design of a new reactor equipped with a dynamic mixing system, whose operation will be based on micro-bubble generation. The suggested design will solve many problems associated with previous designs.

This research consists of main four stages:

1. Investigation of the kinetics of carbon dioxide transfer by sparging with conventional fine bubbles and microbubbles.
2. Design and simulation of gaslift anaerobic digestion with microbubbles generated by fluidic oscillation using COMSOL multiphysics software to investigate the effect of this design on the efficiency of the mixing system in anaerobic digestion.
3. Application of the proposed design biologically to the removal of acid gases from the digested sludge using fine bubble and microbubble technology.
4. Application of the sparging system to anaerobic digestion using different gases (pure nitrogen, carbon dioxide, biogas generated by anaerobic fermentation).
5. Improvement heating system in anaerobic digestion.

#### **General Benefits of the Research:**

1. It is well known that biogas is a renewable source with many applications; therefore, one of the objectives of the current research is to enhance the operation of anaerobic digestion to produce methane that is cheaper and more readily available compared with other resources.

2. Reducing the cost of production of bio-gas by application of a sparging system in anaerobic digestion.
3. Protection of the environment from gas emissions which cause global warming and climate change that are produced in the wastewater treatment plant.

**Benefits of Using Microbubbles in Anaerobic Digestion (mass transfer):**

4. The large surface area provided by the microbubble technique will improve the mass transfer rate of biogas from the liquid phase to the gas phase, especially gas which becomes trapped in the bottom of the digester.
5. Reducing the partial pressure of hydrogen as a result of the high mass transfer rate, which makes some intermediate reactions thermodynamically favourable, allowing the reactions to proceed smoothly, and preventing the backlog of volatile fatty acid (VFA) in the digester and a fall in pH .
6. Increasing methane yield by reduction of partial pressure of methane, thus, encouraging methanogenic bacteria to produce more biogas and improving the performance of anaerobic digestion.

**Benefits of Using Microbubbles in Mixing System in Anaerobic Digestion:**

7. Using this design helps the substrate to move uniformly and gives sufficient time for bacterial consumption, leading to higher efficiency of digestion and increasing the production of biogas.
8. Using microbubbles as a mixer reduces hydraulic retention time, thereby making the treatment more efficient.
9. No moving equipment or parts inside the digester.
10. The electricity requirements for the new mixing system in anaerobic digestion are relatively low.
11. Low costs of installation and maintenance.
12. Assists in the removal of trapped gas from the bottom of the anaerobic digester.
13. Homogeneous distribution of temperature, pH and added chemicals to all parts of the anaerobic digester and prevention of the formation of the dead zones generated in traditional mixers.

14. The meeting of substrate and heat with microorganisms through intimate contact between feed sludge and active bacteria (active biomass).
15. Reduction in settling of the heavy solid materials at the bottom of the reactor and avoidance of the formation of scum (thick layer) on the surface of the sludge.

**Benefits of Using Microbubbles in the Digested Sludge**

16. An airlift (ALR) was used as an anaerobic digester in the present research to remove the generated gases, ( $\text{CO}_2$ , and  $\text{H}_2\text{S}$ ) thereby reducing odour.
17. Minimizing the corrosion in pipelines and pumps.

**Benefits of Using Microbubbles with Direct-Contact Heating Technique:**

18. Low maintenance and operation costs in heating system.
19. Avoidance of heat loss caused by “baking” of the sludge on the tube in traditional shell and tube heat exchangers.



CHEMICAL & BIOLOGICAL ENGINEERING

## **Chapter Three**

# **Materials and Methods**

### 3.1 Introduction

Applications of sparging system and microbubbles technology in anaerobic digestion process have investigated through several stages. The present chapter has listed and explained all the methodologies and materials due to difference the operational conditions and setup of experiments.

### 3.2 Materials and Methods for (Carbon Dioxide Mass Transfer Induced Through an Airlift Loop) (Chapter Four)

In this study, two reactors with 15 L and a working volume of 8.3 L of water are used in the experimental work. Each reactor is equipped with a heat controller to maintain temperature to within  $25\pm 1$  to prevent any effect on reading of pH. Tap water is sparged with carbon dioxide, while pH has recorded with certain periods of time until approaching saturation as the first, dosing, stage. In the second, stripping stage, nitrogen sparging with one of two different size bubbles is conducted. Conventional fine bubbles are produced by a nickel membrane diffuser, while microbubbles are generated by a ceramic diffuser and fluidic oscillation. Figure 3.1 and 3.2 illustrates the image of experimental work and schematic of reactor and equipment respectively. Table (3.1) gives the experimental operating conditions.

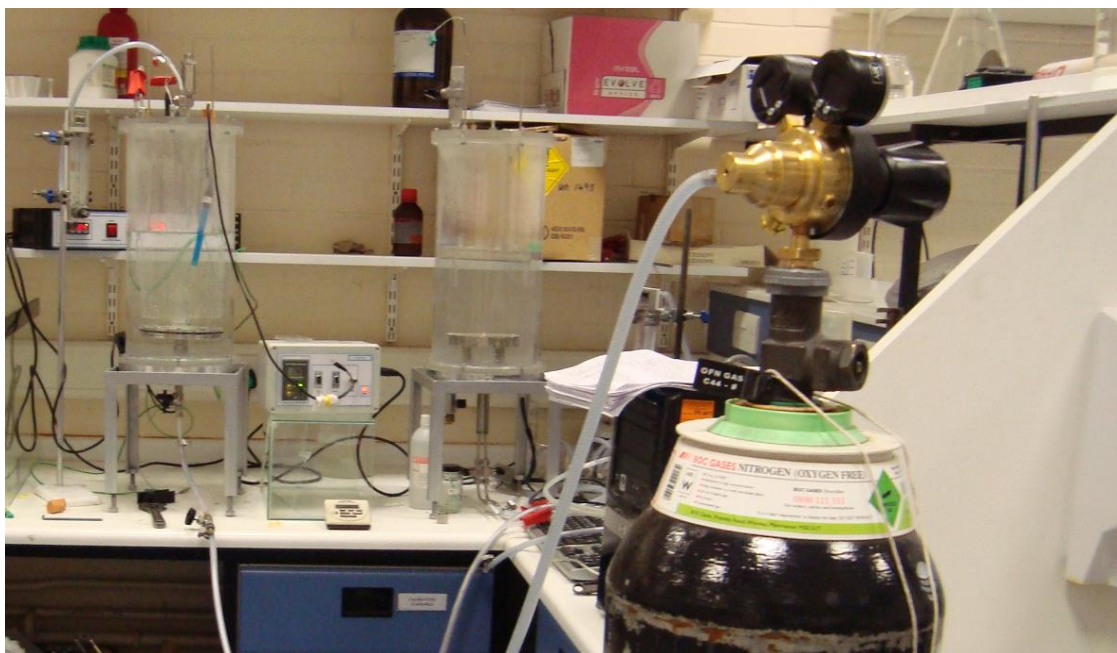


Figure 3.1: Image of experimental work

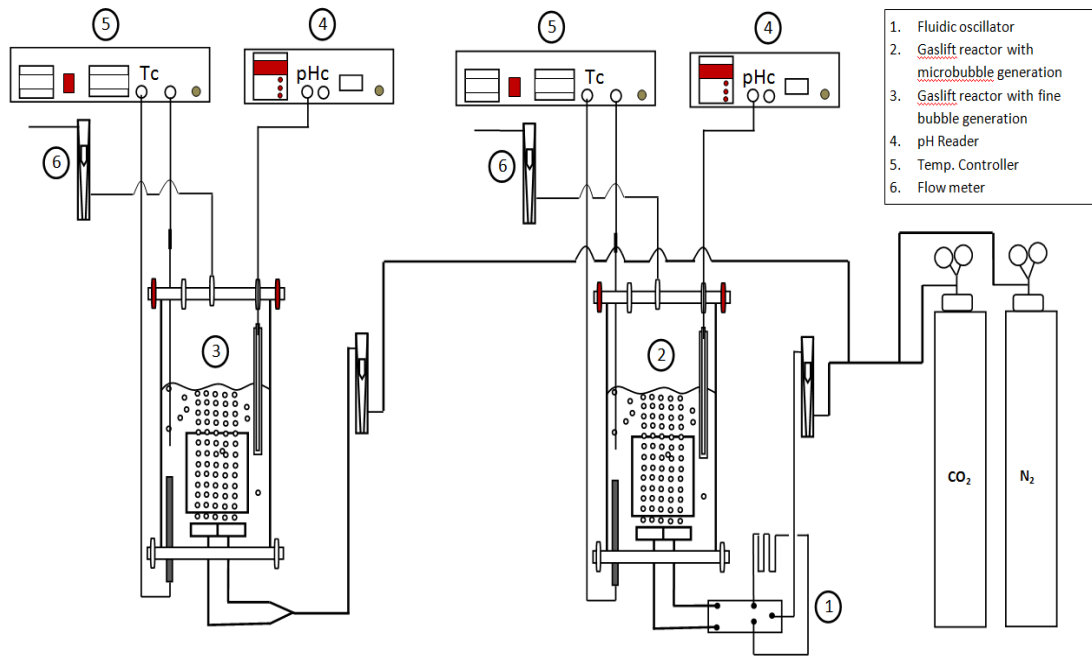


Figure 3.2: Process flow schematic for Carbon dioxide dosing and stripping experiments.

Table 3.1: Experimental Conditions

Name	Description	Value and type	units
<b>Reactor</b>	Type	Airlift	
	Inside diameter	20	cm
	height	45	cm
	height of draft tube	14	cm
	diameter of draft tube	12	cm
<b>Diffuser</b>	Inside diameter	10	cm
	Outside diameter	11	cm
	Area	78.5	cm <sup>2</sup>
	No. Of pores per cupic cē	10000	
	pore diameter	20	micron
<b>Operation condition</b>	Absolute pressure	1	bar
	Main flow rate	110± 5	L/min
	flow rate inlet and outlet	300± 5	ml/min
	Temperature	25±1	°C
	Volume of water	8300	Cm <sup>3</sup>
<b>Type of fluid</b>	Type of water	Tap water	
	Nitrogen	purity99%	source BOC
	CO2	purity99%	source BOC

### **3.3 Anaerobic digestion for laboratory purpose**

Health and environmental factors as well as operational difficulties are major challenges facing the development of an anaerobic digestion process by the present study. Some of these problems relate to the use of sludge collected from primary and secondary clarifier units in wastewater treatment plants, and the use of the traditional approach to biogas collection.

In the first part of this chapter the author suggests a new innovative methodology for collecting biogas produced from anaerobic digestion. This new technique allows the anaerobic digestion process to operate within one atmosphere, by utilisation of phenomena of communicating.

In the second part, the preparation of synthetic sludge and the use of a new method for collecting biogas for laboratory purposes are presented in two separate sections within this chapter. In the first part of this chapter, the author suggests a new procedure for simulation of the prepared sludge, which has been evaluated by means of biogas production based on environmental safety perspectives; especially this study's use of the sparging system.

The two suggested methods used in processing unit of digested sludge as well as in anaerobic digestion process.

#### **3.3.1 Collection of Biogas for Laboratory Purpose**

##### **3.3.1.1 Introduction**

Typically, the collection of biogas in wastewater treatment plant is done by using flexible covers. Although advances have been made in the methods for manufacturing these covers and their characteristics have been improved, the impact of these covers on the efficiency of anaerobic digestion still needs further investigation. Gas holders (GH) are manufactured worldwide in large quantities; however, there is an on-going need for development of biogas collection and storage systems. The GH is an essential part of an anaerobic digester and operates under a control system and ultrasonic sensor to run the gas utilisation plant (CHP).

There are numerous types of biogas holders for instance, moveable gasholder, plastic gasholder, and fixed-dome gasholder (Porras and Gebresenbet, 2003). These various

shapes and designs have advantages in terms of economic and operational benefits; however, many associated disadvantages also been reported:

1. Metal covers exposed to the atmosphere cause heat loss from the anaerobic digester.
2. Corrosion and cracking of the cover.
3. As a result of pressure generated due to accumulation of biogas, large amounts of biogas leak through the cracks or from sides of manhole cover.
4. Considerable quantities of biogas remain in the slurry, which being removed manually.

All conventional methods for biogas collection cause increase in pressure build-up in the headspace of anaerobic digestion. Thus, some of biogas could be re-dissolved into sludge again. The rate of solubility of  $\text{CO}_2$  and  $\text{H}_2\text{S}$  are relatively higher than that for  $\text{CH}_4$ , thus the produced  $\text{CO}_2$  dissolves in distilled water and converts in to  $\text{CO}_{2(\text{aq})}$ .



As mentioned earlier the conversion to carbonic acid is very slow as well as carbonic acid is a diprotic acid, thus it contains two hydrogen atoms ionisable in water and dissociates into bicarbonate and carbonate ions ( $\text{HCO}_3^-$ ,  $\text{CO}_3^{2-}$ ,  $2\text{H}^+$ ). Therefore, it can be concluded that the presence of dissolved carbon dioxide in liquid phase would produce a plenty of hydrogen ions which, in turn lead to lowering of the pH values.

In fact, this response is not limited to the impact of carbon dioxide ( $\text{CO}_2$ ) concentration, there is another gas could also re-dissolve into sludge. It is hydrogen sulphide ( $\text{H}_2\text{S}$ ) which is generated from anaerobic digestion as a trace gas. When  $\text{H}_2\text{S}$  dissolves in pure water, the pH, also, would drop due to releasing hydrogen ion and forming a weak acid. Indeed, the behaviour of the solubility of hydrogen sulphide is very similar to carbon dioxide because both gases form diprotic acid in water as shown in the following reactions:



Hydrogen sulphide is a corrosive and toxic gas. It is already heavier than air, as its specific gravity is 1.19 more than specific gravity of air, therefore any chock or a simple pressure can lead to re-dissolved to sludge again.

Sulphate dissolves with high concentrations can inhibit the generation of biogas produced from anaerobic digestion of wastewater. The most important reasons which lead to this inhibition, is that the sulphate dissolved in wastewater encourages growth the sulphate-reducing bacteria which consume the acetic acid and hydrogen that are consumed by methane bacteria to produce the biogas as well (Helton et al. 1988). This competition between the sulfate-reducing bacteria and the methane producing bacteria on consumption the hydrogen and acetic acid can be illustrated thermodynamically through the following equation:

**Methanogenesis:**



**Sulphate reduction**



From above equations, it can be seen that the sulphate-reduction reactions proceeding faster than methanogenesis, therefore methane production is inversely proportional to sulphate concentration. In addition, the generated gas ( $\text{H}_2\text{S}$ ) has a negative impact also on the methane production bacteria as reported by Karhadkar et al. 1986. The author also suggested that the concentration of  $\text{H}_2\text{S}$  in the digester can be taken as an indicator for inhibition of methanogenic bacteria.

### 3.3.1.2 Description of Suggested Biogas Collection

The collection of produced biogas needs space without any air or gases that affect its purity. The proposed idea of biogas capturing depends on phenomena of communicating vessels. Communicating vessels is an experimental or test, shows that the pressure of the liquid at the bottom of the container does not depend on the form or the size of the container, but depends on the height of the liquid in that container. Figure 3.3 shows level of water in several containers with different sizes and shapes. The level of liquid is similar at any vessel-end at constant pressure.

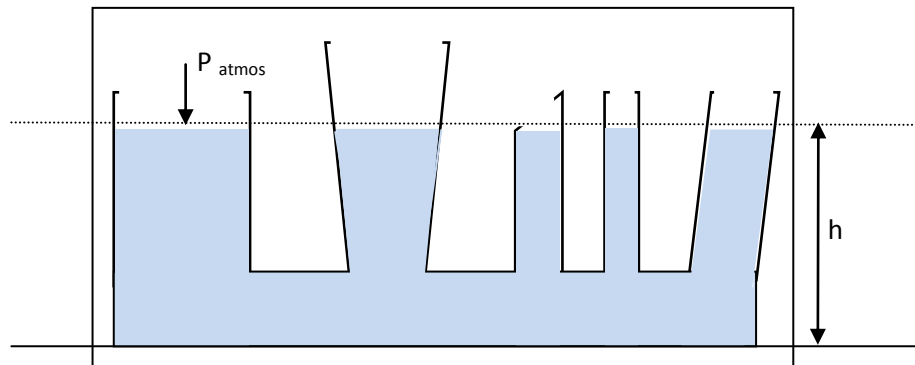


Figure 3.3: Communicating vessels

The above vessels are opened to atmosphere; however, everything would be different if these containers are closed. In this case, the pressure or vacuum pressure would occur at the closed ends of those containers.

The present research suggests utilisation the vacuum pressure build up to capture biogas from anaerobic digestion. The capturing equipment composes of two tubes; the first tube, 15 cm diameter and 1m height, is called the reference tube (balance tube), while the second tube, 30 cm diameter and 1m height, is called collector tube as shown in the Figure 3.4. The upper end of reference tube is opened to atmosphere, while the upper end of collector tube has four exits. Two of them used to withdraw samples to measure composition of biogas, which are closed during the collecting the biogas, while the third is connected to the reactor headspace for biogas flow. The fourth was for water supply.

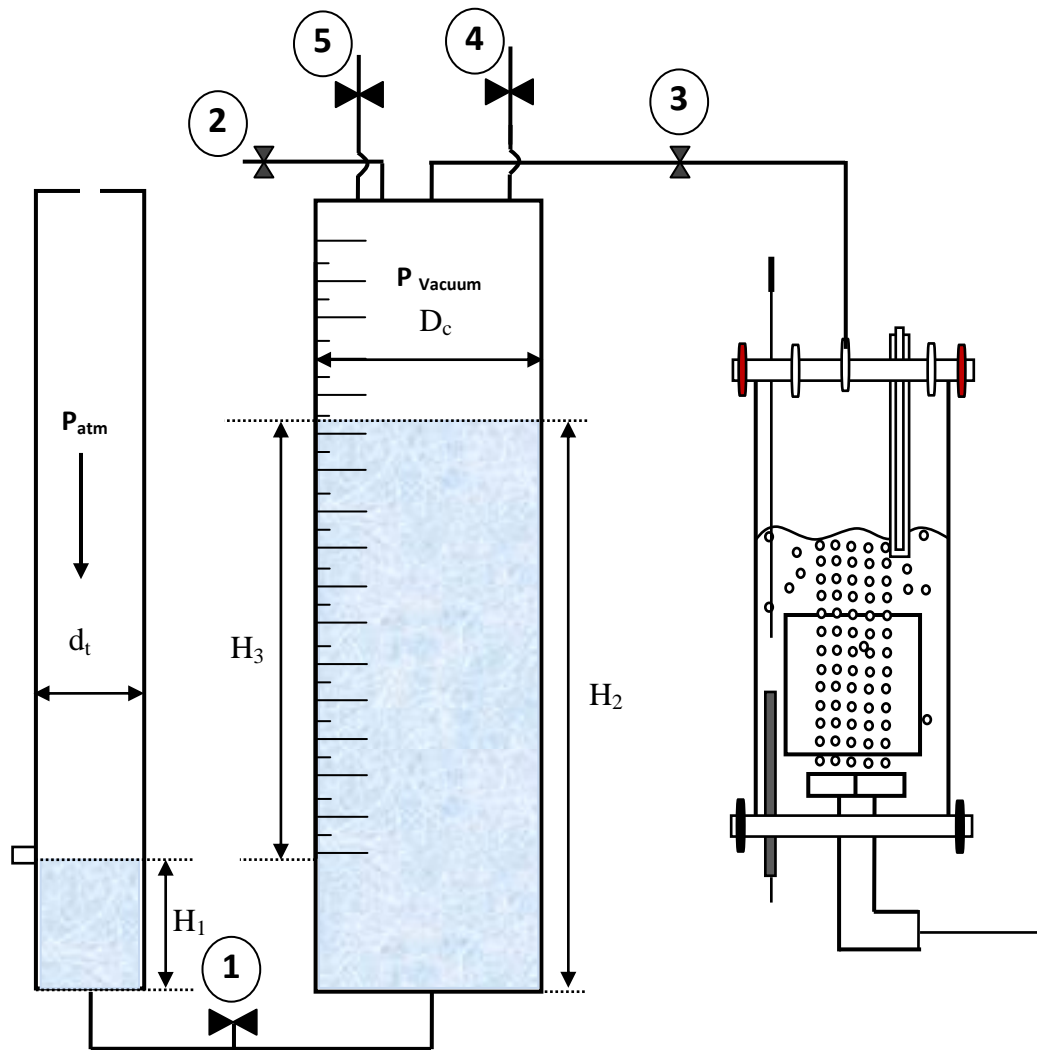


Figure 3.4: Schematic diagram of biogas collector by vacuum pressure as first stage.

The value of gauge pressure or vacuum pressure depends on the different level and can be expressed mathematically as the following:

$$P = \rho g \Delta H \quad (3.9)$$

Where  $P$  is hydrostatic pressure,  $\Delta H$  is different height between the two tanks,  $\rho$  is density of the fluid ( $\text{kg/m}^3$ ),  $g$  is gravitational acceleration ( $9.81 \text{ m/s}^2$ ).

The vacuum pressure decreases with increasing the differential level of water ( $\Delta h$ ) as shown in Figure 3.5. This response is found in collector tube and also in the head space of anaerobic digester when a closed end of collector tube is connected into the output stream of digester. This means that all gases leave the headspace in anaerobic digestion when it is being under vacuum pressure which causes decrease in the partial pressure of those gases. Another thing is worth to notice that the vacuum pressure would contribute

in removal of the dissolved gases from the sludge due to the mass transfer phenomena that plays an important role in this moment. Therefore, this technique should lead to increase the efficiency of removal gases.

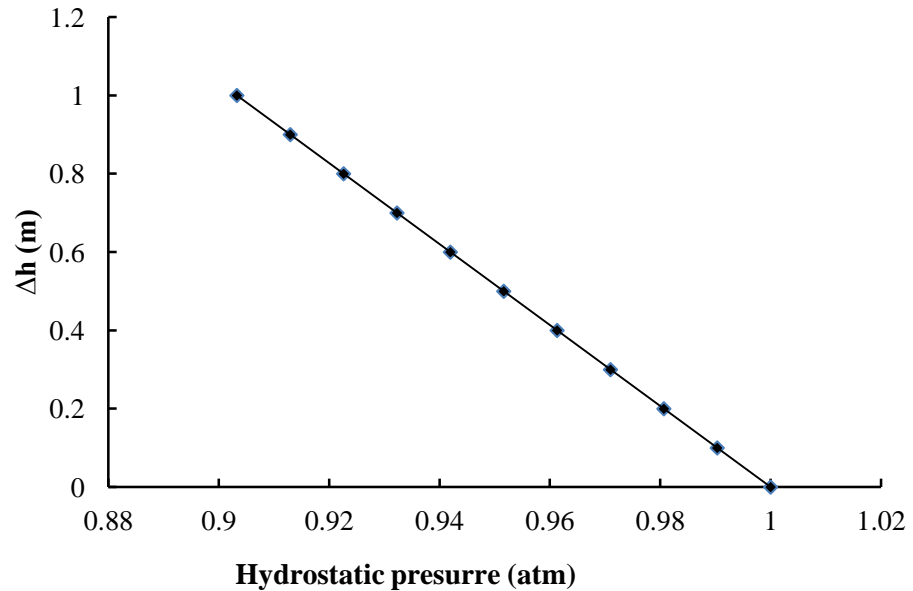


Figure 3.5: Hydrostatic pressure in the headspace of collector tube.

The value of vacuum pressure depends on the difference level between the two containers. However, the level of water will be the same in the both tanks, thus the pressure in the collector and headspace of anaerobic digestion will become 1 atm. Then, the pressure will increase in head space in anaerobic digestion if  $\Delta H$  was negative as shown in the Figure 3.6. Consequence re-dissolved of produced gas into medium again which influence negatively on activity of microorganism.

In laboratory research, use the capturing system with vacuum pressure and bubbling system may give us inaccurate results. The anaerobic digestion or any bio-reactor should work under normal pressure (i.e. 1atm). Indeed, it was difficult to distinguish that any change in biogas production, for example, was occurred due to bubbling or vacuum system. Each one can lead to removal of biogas produced. This scenario can be changed if the anaerobic digestion works under normal condition (i.e. 1atm). This condition can be obtained, if there would be a calibration between the anaerobic digestion and biogas collection.

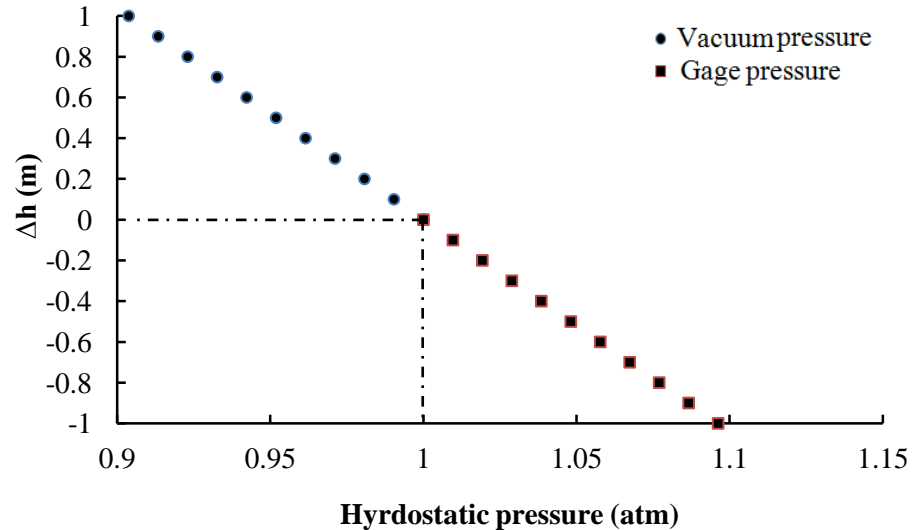


Figure 3.6: Vacuum and gage pressure at different level of water

If fact, the proposed method in this chapter is unique as it combines the two ideas to give an interesting design which helps to solve all the problems arose when using conventional methods. In other words, the vacuum pressure required to capture the biogas, should be faced by another pressure, which have the same value but with opposite direction.

The vacuum pressure is required for capturing the biogas; however, operating of an anaerobic digestion with standard conditions (1 atm) is more scientifically meaningful, since states are then comparable".

The present study suggested a new technique to capture biogas from anaerobic digestion. The schematic diagram of this method is given in the Figure 3.7.

The capture process as described earlier consists of two reservoirs with either similar or different diameters. Connecting the reservoirs together leads to creating vacuum pressure inside the collector tank. This pressure is treated by another hydrostatic pressure generated by lowered level of water inside the submerged tube as shown as in the Figure 3.8.

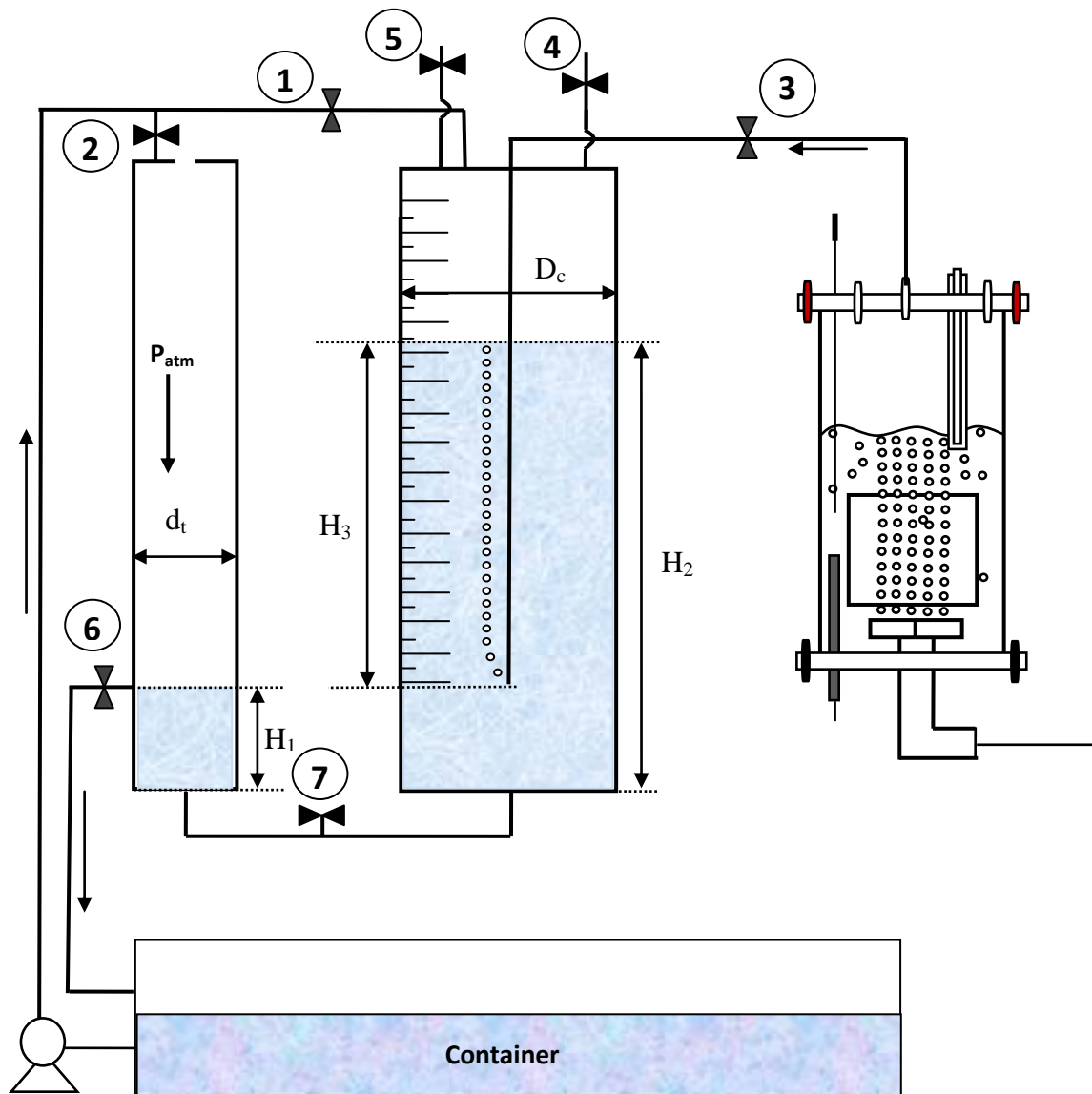


Figure 3.7: Schematic of collector of biogas

The situation can be represented mathematically:

$$P_c = \rho g (H_2 - H_1) \quad (3.10)$$

$$P_{\text{tube}} = \rho g (H_3) \quad (3.11)$$

Where  $H_1$ = level acidic aqueous solution in balance tank  
 $H_2$ = level of acidic aqueous solution in collector tank  
 $H_3$ = length of tube dispersed in collector tank  
 $P_c$ = pressure of collector biogas (mbar)  
 $P_{\text{tube}}$ = pressure inside tube dispersed in the collector tank (mbar)

The pressure balance:  $P_{\text{atmos}} + P_c = P_{\text{tube}} + P_{AD}$  (3.12)

The connection of the two tanks with anaerobic digester, the vacuum pressure created from different levels of tank is faced by pressured created from tube dispersed in collector tank.

In other word:

$$H_3 = H_2 - H_1 = \Delta H \quad (3.13)$$

$$P_c = P_{\text{tube}} \quad (3.14)$$

Therefore:

$$P_{\text{atmos}} = P_{\text{AD}} \quad (3.15)$$

Figure 3.8 clearly shows that there are two pressures ( $P_c$  and  $P_{\text{tube}}$ ) are created at any level of water ( $H_3$ ). The Two pressures have the same value but different direction. The final result will be one atmospheric pressure. Therefore; there isn't any pressure drop occurring in the headspace. For example at  $\Delta H$  of 0.5 ( $H_2-H_1$ ), the pressure in collector tank ( $P_c$ ) is 0.95. In the same time, there is another pressure will be created by submersed tube which has value of 1.05. Thus, the exceed pressure in one side is treated by vacuum pressure in another side. Therefore, the final result will be 1 atmos. Within these conditions, the biogas can moves freely without any resistance from the headspace to the collector.

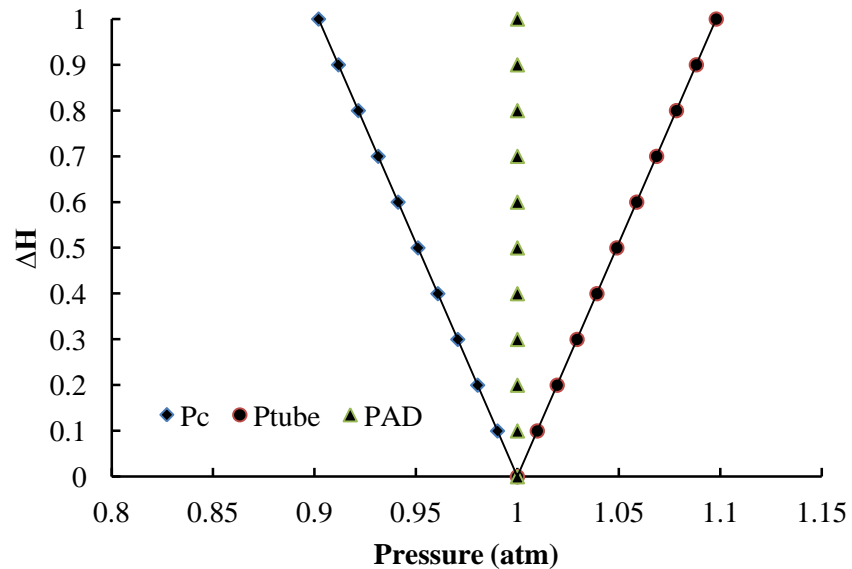


Figure 3.8: Pressures created in collection system

Therefore, the present study allows the anaerobic digester to operate with one atmosphere by utilisation of the phenomena of communicating vessels to create vacuum pressure as a first stage. The second stage treats this vacuum pressure by creation of hydrostatic pressure that has the same value but in different directions as action and reaction.

### **3.3.1.3 Water Used in Biogas Collection**

One of the goals of collection was to measure with accuracy the concentrations of methane and carbon dioxide. The solubility of methane in water is very low; therefore the methane production can be measured accurately, while carbon dioxide has high solubility. According to the literature, the solubility of carbon dioxide can be decreased by decreasing the pH in the solution. The present study suggested the use of acidic water (i.e pH <4). The acidic water was prepared by adding HCL to tap water to reduce the pH of 4.

### **3.3.1.4 Other Benefits of this Method**

The concentration of the collected biogas is carried out by different biogas analysers. Normally, these devices operate with one atmosphere and need large amounts of biogas. The lab-scale amount of biogas collected from the anaerobic digester is always less than that required for the biogas analyser. According to our experience with these types of biogas analyser, the optimum way of measuring to get an accurate reading is 4-5 min at 300 ml/min. Thus, the volume required for measuring is about 1200 ml plus 1000 ml to get a steady state value. Not all lab experiments yield such amounts (e.g. 2000 ml), therefore, the suggested collector allows the biogas analyser to operate with any volume of biogas with 1 atmosphere pressure. The biogas analyser was connected with the collector via valves 4 and 5 (Figure 3.7), while other valves were closed. Thus, the biogas was recycled between the collector and biogas analyser.

Although the anaerobic digester, which is connected with the suggested biogas collector, operates with one atmosphere, the collected biogas remains under vacuum pressure in the headspace of collector. Measuring the volume of biogas with vacuum pressure is inaccurate. In order to convert the vacuum pressure to one atmosphere pressure, the valves 1, 4, and 5 were kept closed, while valves 2 and 7 were open to allow the entry of acid water into the tube. The water supply to the collector was stopped when the level in the tube and the collector became equal. Then, according to

the level of the headspace in the collector, the volume of biogas was estimated according to the following equation:

$$V_{bg} = \frac{\pi}{4} D_c^2 H_{hs} \quad (3.16)$$

Where  $V_{bg}$  is volume of collected biogas ( $m^3$ ),  $D_c$  is diameter of collector (m), and  $H_{hs}$  is height of collected biogas (m).

### 3.3.2 Synthesis of the Sludge for Laboratory Purpose

#### 3.3.2.1 Introduction

The development of anaerobic digestion has been beset by many challenges. One of the most important of these challenges involves sludge collection from wastewater treatment plants. Sludge in anaerobic digesters consists of organic materials, inorganic materials and different types of bacteria. Its collection from either primary or secondary clarifier units has become unacceptable for health and environmental reasons, which have become a major concern for many researchers and being an additional burden when they are conducting their experimental work.

Even though several attempts have been made to resolve these problems through the use of simulated sludge, the results obtained from these experiments have been compromised by the use of simulated sludge, and the question of how closely it conforms to real sludge.

In most cases, the physical, chemical and biological properties of fresh sludge, collected from wastewater treatment plants, are unknown; in addition they continually change. Such changes can be influenced by, for instance, the type of wastewater, sampling and storage duration, handlings and transfers from wastewater treatment plant to the laboratory, weather conditions and seasonal changes, variation of water treatment equipment design and operating conditions. Biologically, many types of anaerobic bacteria exist in wastewater (Baudez et al., 2007). The activity and type of these bacteria mainly depend on the characteristics of wastewater and weather conditions at the time of sampling, as well as on the collection method used. These parameters, for instance, would strongly affect the biogas production rate and the efficiency of biodegradation of the organic matter in the sludge. Chemical and physical properties of

sewage sludge vary with time; this makes it difficult to link the results obtained from experiments carried out using different sludge batches (e.g. starter inoculums).

Therefore, in an attempt to prevent this problem occurring, the author of the present study considered using an identical sampling procedure for the sludge by taking sludge samples from one pre-identified source. The sludge inoculums which been simultaneously taken from a wastewater treatment plant would have been introduced into the two reactors under similar operating conditions, in an attempt to produce the most accurate results possible; as is reported in this chapter. However, the collection of sludge samples from primary and/or secondary clarifiers for lab-tests has become unacceptable due to numerous health and environmental restrictions.

Hence, a process for the simulation of sludge samples has been adopted in an attempt to overcome these restrictions. In earlier studies, a synthesised sludge consisting of organic and inorganic synthetic components has been used (Baudezal, 2007; Muller and Dentel, 2002; Dursun *et al.*, 2004). However, the suggested methods still need to be further clarified through simpler procedures for preparation and use.

This chapter suggests using a mixture of digested real sludge (which pose less danger than sludge collected from primary and secondary clarifiers) and simulated sludge formed from kitchen waste.

### **3.3.2.2 Materials and Methods**

Achieving secure discharge of the kitchen waste collected from households, restaurants, and residues from the food industry, which makes up about 70% of the total municipal solid waste, has become a major challenge for the environment. Several methods have been used for the treatment of kitchen waste. Although landfill dumping of kitchen waste has been the most common method of reducing the volume, pathogens and odour of such waste, the incurred costs and comparatively large areas taken up by landfill sites are serious drawbacks of this method. Utilisation of kitchen waste as a source of energy generation has become the best practice both, environmentally and economically, through the use of biological processes such as anaerobic digestion. Such treatments have the combined benefits of reducing the effects of kitchen wastes as well as producing biogas and digested sludge (compost) which can be used as soil fertiliser. The different types of organic matter which make up kitchen waste are presented in

Table 3.2. The table below shows the substrates and nutrients which are required for the anaerobic digestion process.

The simulated sludge, which was suggested in this chapter, consists of a mixture of anaerobic digested sludge mixed with kitchen wastes. The components and quantities of the kitchen wastes constituents used in the present study are presented in Table 3.3.

Table 3.2: Type of organic matters in kitchen waste

Organic materials	Description	Source
<b>Lipids</b>	Fat-like substances that are important parts of the membranes found within and between each cell. They include oils, fatty acids, waxes, steroids and cholesterol. Lipids are stored in the fatty tissue, organs and cells of the body. There are certain foods that contain a high amount of lipids	<i>butter, cheese, whole milk, ice cream, cream and fatty meats</i>
<b>Polysaccharides</b>	Polysaccharides are common sources of energy. Many organisms can easily break down starches into glucose. Starch is a carbohydrate consisting of a large number of glucose units joined together by glycosidic bonds. This polysaccharide is produced by all green plants as an energy store.	<i>potatoes, wheat, maize (corn), rice, and cassava</i>
<b>Protein</b>	Protein is a macro nutrient composed of amino acids that is necessary for the proper growth and function of the cell. While the body can manufacture several amino acids required for protein production, a set of essential amino acids needs to be obtained from animal and/or vegetable protein sources	<i>lamb, egg, beef, marmite etc</i>
<b>Nucleic acids</b>	The nucleic acids are made up of purines and pyrimidines, which are carbon- and nitrogen-containing molecules derived from carbon dioxide and amino acids like glutamine. Because they are formed in the body, nucleic acids are not essential nutrients	<i>plant and animal foods like meat, certain vegetables and alcohol</i>

Table 3.3: Details of materials which was used in the synthetic sludge

Item	Name	Organic content	Quantity (g)
1	Rise	<i>Carbohydrates (80%), Fat, Protein, Vitamin B1,2,3,5,6,9,C, Calcium, Phosphorus, Potassium, Iron</i>	1250
2	Meat	<i>Protien</i>	400
3	Red bean	<i>Protien, Carbohydrates, Fat</i>	600
4	Peas	<i>Carbohydrates, Fat, Protein, Vitamin A, B1,2,3,5,6,9,C, Iron</i>	
5	Lentils	<i>Protien, Sugars, Carbohydrates, Fat, Vitamen B1,9, Caciium, Iron, Phosphorous, Potassium, Sodium</i>	
6	White bean	<i>Protien, Carbohydrates, Fat</i>	
7	Chickpea	<i>Carbohydrates, Fat, Sugar, Protein, Vitamin A, B1,2,3,5,6,9,12,C,E, K Iron, Phosphorus, Potassium, Sodium</i>	
8	Carrot	<i>Carbohydrates, Fat, Sugar, Protein, Vitamin , Iron, Phosphorus, Potassium, Sodium</i>	

Fresh meat, red beans, peas, lentils, white beans, chickpeas, carrots, and rice are the principle materials used in the sludge in the present study, since these materials have the

organic material (lipids, polysaccharides, proteins and nucleic acids) necessary for anaerobic bacteria. The first six materials were initially boiled at 100 °C for 1 hour, before being added to the rice, which has been soaked in water for 24 hours. Then, the product from the previous stage was thoroughly mixed for 30 min to make a simulated kitchen waste with more slurry after adding the water.

According to the recommendations provided by earlier studies, feeding the digester with nutrients or trace metals was not necessary (Perez-elvira et. al. 2011, Chamy and Ramos 2011, Braguglia et. al. 2011, Kim et. al. 2011, Siggins et al 2011). The studies reported that sludge taken from WWTP did not require the addition of any supplementary nutrients or trace metals, as the used sludge already contained lipids, polysaccharides, proteins and nucleic acids that are required for the digestion process.

The digested sludge, used in these experiments, was collected from an outlet stream of a full-scale mesophilic digester at “Woodhouse wastewater treatment plant” in Sheffield city in the UK.

Many experiments with different conditions and methods were conducted in order to achieve the best simulation process. The experiments were carried out starting with using raw sludge collected from WWTP, followed by the direct use of the kitchen waste and the digested sludge. Although many experiments have given negative results, some of the experiments which have given positive results have encountered environmental problems (e.g. producing huge amounts of H<sub>2</sub>S gas). For instance, when the kitchen waste was used as a sole feed stock with no added digested sludge, huge amounts of biogas were produced with comparatively high H<sub>2</sub>S content, which was out of the range of the biogas analyser used in this experiment. This problem, consequently led to a full shut down of the digestion process.

Two main setup procedures were applied in this experiment. The first procedure was experimental testing of the suggested mixture, which was used in the first setup trial. This mixture consisted of a portion of the digested sludge collected from our earlier experiments and a portion of the digested sludge collected from the anaerobic digester from wastewater treatment, in addition to the kitchen waste which was simulated and prepared in the present study. The aim of the second setup practice was to analyse the prepared simulated sludge in order to create a semi-continues process for long operation periods.

In this experiment, two identical bench-scale anaerobic digesters were setup. The digester has an overall volume of 15 litres, with a working volume of 9 litres. The working days of this experimental work were 19 and 35 days in digester 1 and 2, respectively. The digesters were operated under mesophilic conditions ( $36^{\circ}\text{C}$  to  $38^{\circ}\text{C}$ ). Continuous measurement of biogas produced from both digesters was achieved by downward displacement of acidic aqueous solution (0.2 M HCL,  $\text{pH} < 4$ ). All volumes of biogas given in this chapter have been corrected to 1atm pressure and  $20^{\circ}\text{C}$ . Continuous measurement of methane, carbon dioxide and hydrogen sulphide concentrations in the biogas mixture was carried out daily by biogas analyser (Data gas analyser, Model 0518) at 1atm pressure. A schematic diagram of the experimental apparatus is shown in Figure 3.9.

A PID controller was used in the present study to maintain the temperature in the reactor at  $35^{\circ}\text{C}$ . The digester was fitted with a pH controller, type ON/OFF controller (model BL931700 pH minicontroller) to monitor pH values in the digester.

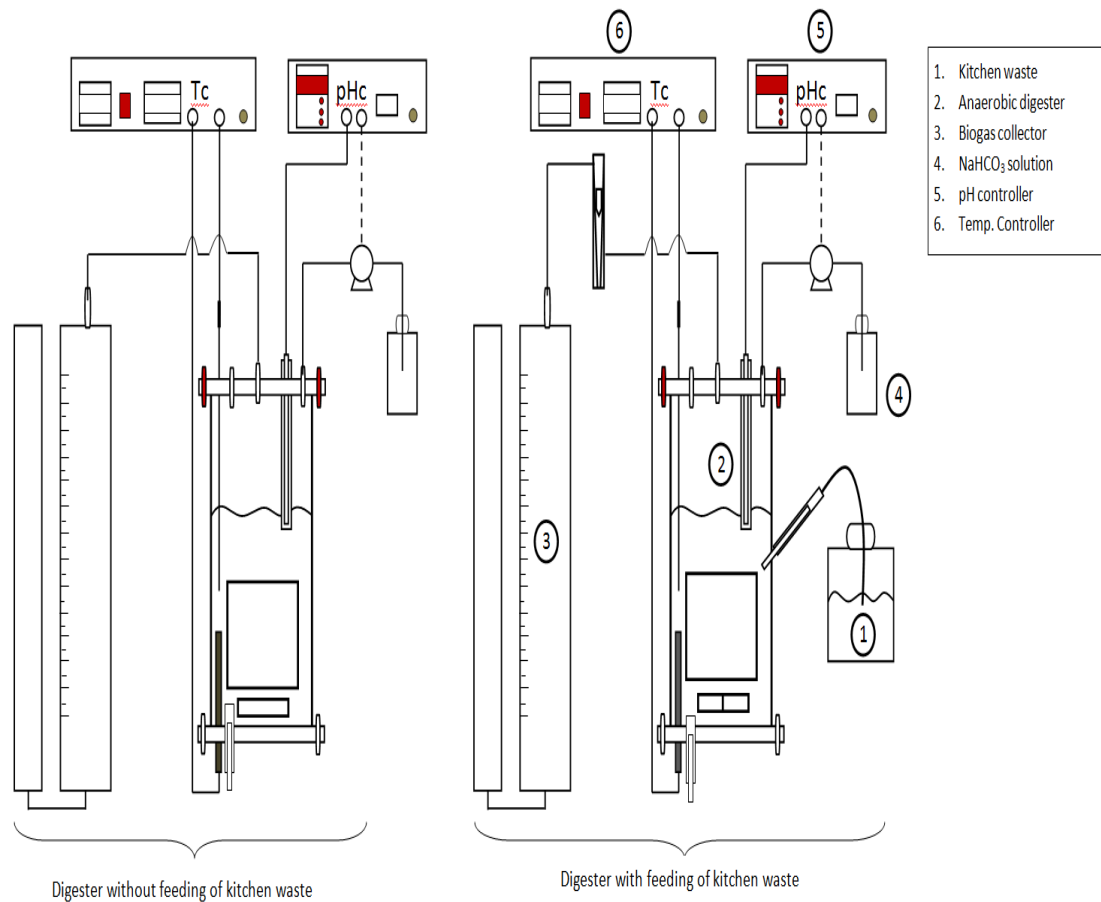


Figure 3.9: Process flow schematic for synthesis of the sludge for laboratory purpose

Volatile fatty acids (VFAs) content was measured according to Hanch Lange for Water Quality (HLWQ) procedure, in which the sample was filtered by centrifugal device (Eppendorf centrifuge 5810) at 2000 rpm for 10 min. Then, an aliquot of 0.5 ml of centrifuged sample was pipetted into a dry 25 ml sample cell. While the second dry sample cell has 0.5 of deionised (DI) which was prepared to calibrate the spectrometer device. Ethylene glycol (1.5 ml) and sulphuric acid (0.2 ml and 19.6 N) were also introduced into each sample cell. The hydroxylamine hydrochloride solution (0.5 ml), sodium hydroxide (2.0 ml and 4.5 N) and ferric chloride sulphuric acid solution (10 ml) are used in the evolution of VFAs. The details are illustrated in Appendix A.2.

### 3.3.2.3 Results and Discussion

In this experiment, the efficiency of the simulated sludge prepared for use in this study was evaluated by measuring the biogas production rate from anaerobic digestion as methane gas. The latter is produced by methanogenic bacteria through the anaerobic digestion process, which when it encounters any problem, prevents or slows biogas production (methane and carbon dioxide). Lower concentrations of hydrogen sulphide in the produced biogas from an anaerobic digestion process were an indicator of the success or otherwise of the process (Karhadkar et al., 1986). Methane, carbon dioxide and hydrogen sulphide, as well as oxygen, were continuously monitored during the experimental operation period.

The effect of addition of kitchen waste supplement to the feed substrate on biogas production through anaerobic digestion process has been investigated in this section. Figures 3.10 and 3.11 show yield of biogas from two anaerobic digesters fed with and without kitchen waste supplementary substrate, respectively. It can be clearly seen that the amount of biogas produced from the first digester, which is fed with kitchen waste supplementary, is more than that produced from the second digester (e.g. fed with only digested sludge).

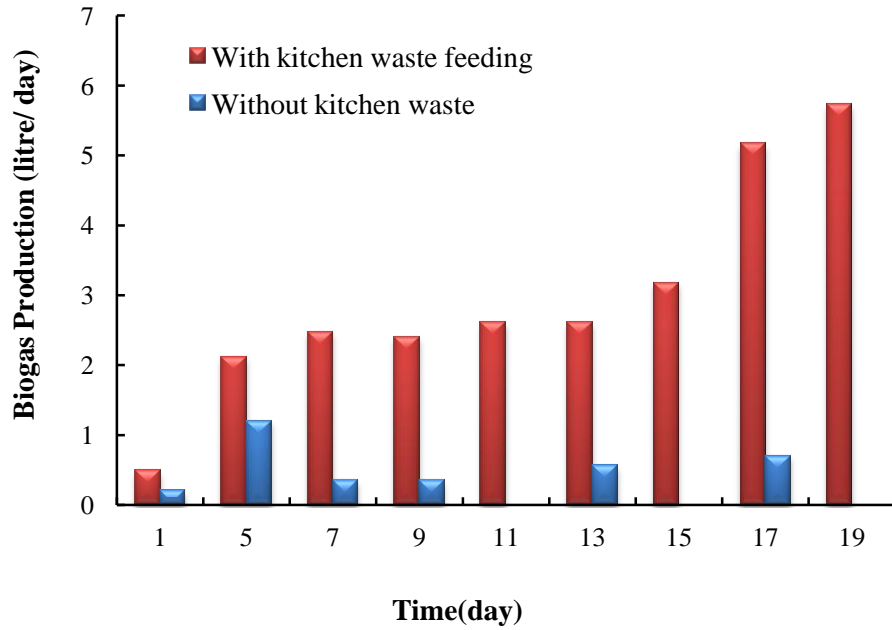


Figure 3.10: Methane production from anaerobic digester from the both digester

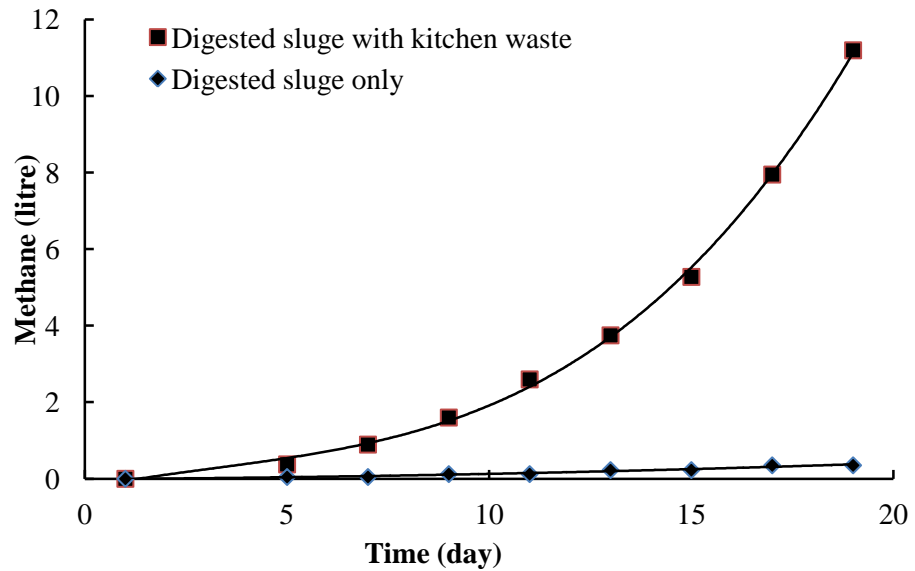


Figure 3.11: Cumulative methane production from anaerobic digester with and without kitchen waste

Figure 3.12 shows the biogas concentration produced from the digester that is fed with 15 ml of kitchen wastes. During the first six days of experiments time, the carbon dioxide produced from the digester is more than methane. The main reason of this situation is that the big production of carbon dioxide takes place in the second stage of the anaerobic digestion process via converting the propionate and butyrate to acetate,

hydrogen and carbon dioxide as shown the following equation. Moreover, the acidogenesis bacteria are faster growing than methanogenesis bacteria.

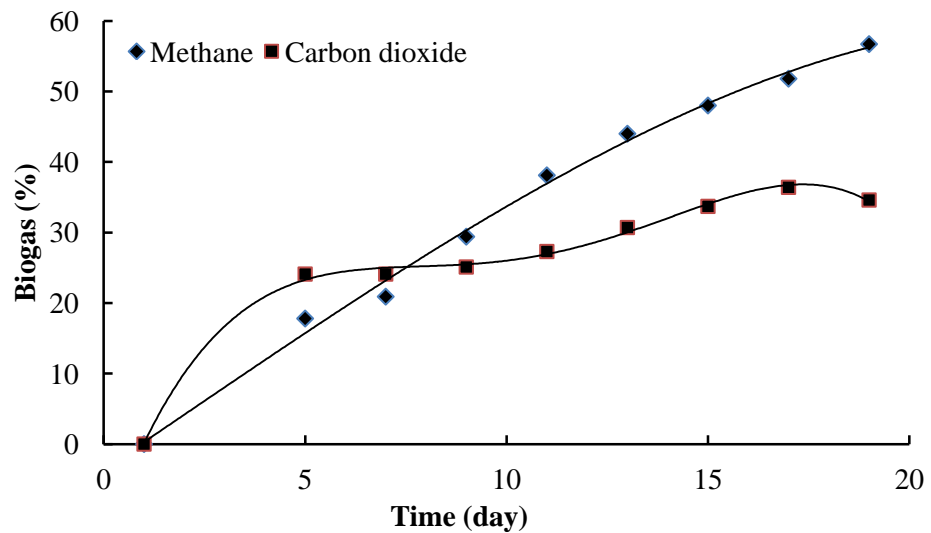
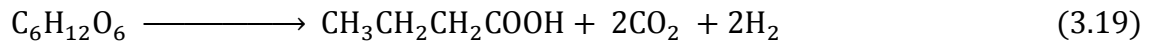
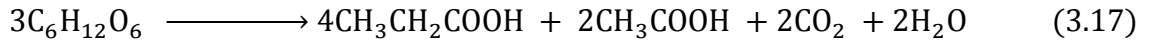


Figure 3.12: Percentage of methane (CH<sub>4</sub>) and carbon dioxide (CO<sub>2</sub>) in biogas produced from anaerobic digester contains digested sludge and fed by kitchen waste

As some of the produced carbon dioxide remains as a dissolved gas in the sludge, another portion of CO<sub>2</sub> gas strips up of the digester to biogas collector.

In addition, in this stage, the methanogenic bacteria have a very slow growth and they need time to complete the fermentation process. These bacteria convert a part of the produced carbon dioxide to methane by reducing of partial pressure of hydrogen produced from the second phase into  $10^{-4}$ . Reduction of hydrogen concentration to this level allows ensuring the success the whole process by reducing the accumulation of volatile fatty acids, as well as increasing the production of methane. The amount of methane produced from the reaction of hydrogen with carbon dioxide is estimated by

30% (Appels, et al. 2008; Sahlstrom 2003; Birgitte, 2003; Metcalf & Eddy, 2003). Thus, the methane production usually increases day per day until reaches to a known-value (e.g.  $\approx 60\%$ ).

During operating the anaerobic digestion process, the kitchen waste slurry was fed into digester with 15 ml every day. Equally, similar quantities of sludge been removed daily from the digester in order to maintain the working volume of the anaerobic digester constant.

In order to evaluate the efficiency of the degradation process of organic material (kitchen waste) at different stages, the concentration of volatile fatty acid (VFAs) was measured in different intervals during the operation period, considering that the VFAs are raw materials to produce the acetates molecules by acetogenic bacteria. Figure 3.13 below indicates that the concentration of VFAs in the digester fed with sludge and kitchen waste show higher values than that in the digester with sludge only. Moreover, there were no significant variations in pH values throughout the experiments, and the pH values were kept at optimal conditions as shown in Figure 3.14. Thus, this finding evidently support the fact that the increase in VFAs was not because of an accumulation process, but these values would be converted into acetate by acetogenic bacteria and then to the methane by methanogenic bacteria.

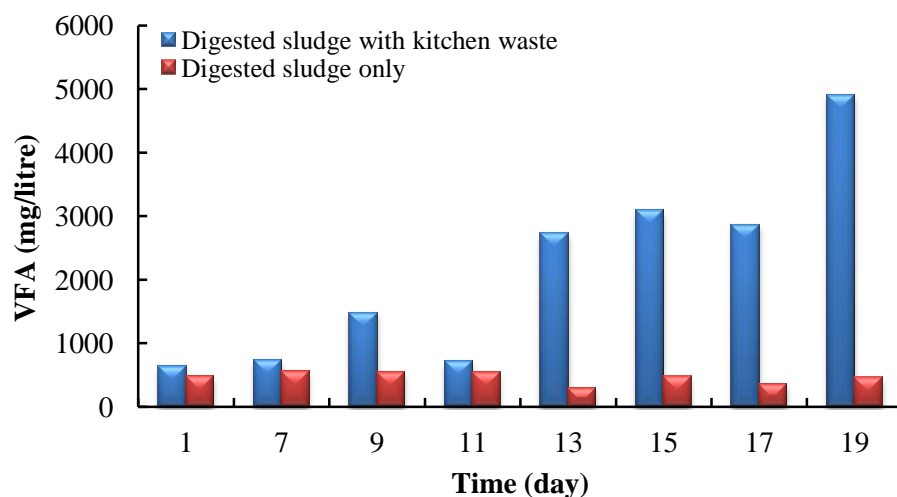


Figure 3.13: Variations in volatile fatty acids concentration in the digester fed with kitchen waste and the digester contains only digested sludge.

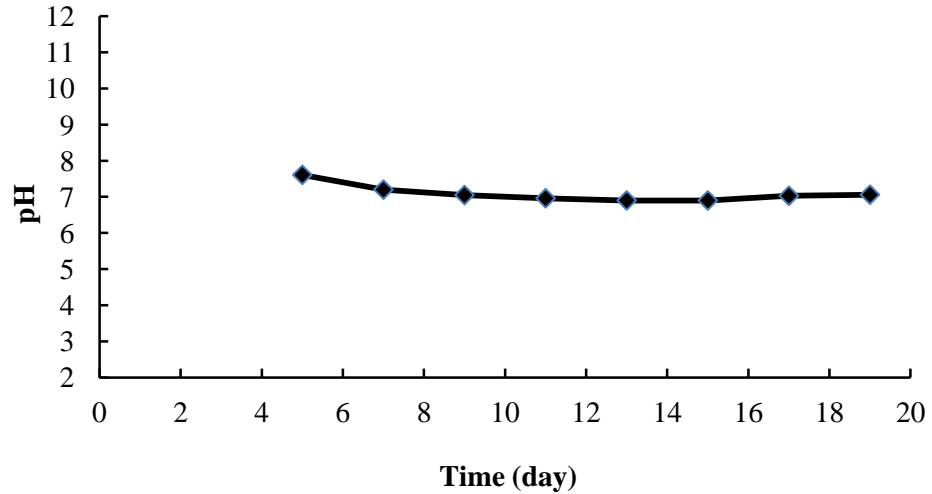


Figure 3.14: pH values in the anaerobic digester that contains simulated sludge. The pH value remained stable at optimum conditions.

Although the experiment in the first stage has shown encouraging results with both digested sludge and kitchen waste, this experiment was repeated but for longer operation in an attempt to ensure confirms the obtained results and the behaviour of the process. The digested sludge collected from Woodhouse Wastewater Treatment Plant (WWTP) in Sheffield city in United Kingdom, was used with the same preparation procedure that was used in first stage. Figures 3.15 and 3.16 show the methane and carbon dioxide produced from the anaerobic digester, respectively, over 35 days of operation. The trend of methane production has been stable during the operation period.

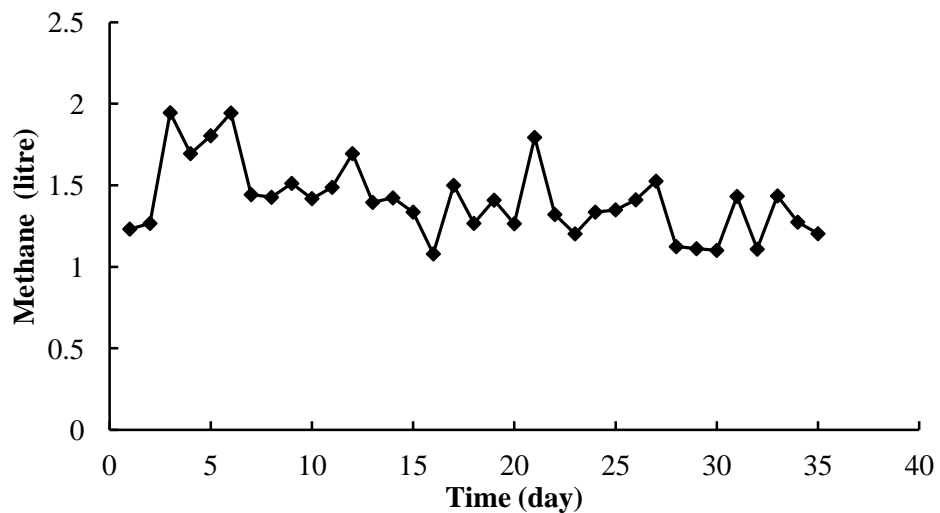


Figure 3.15: Methane production from anaerobic digester fed with digested sludge and kitchen waste.

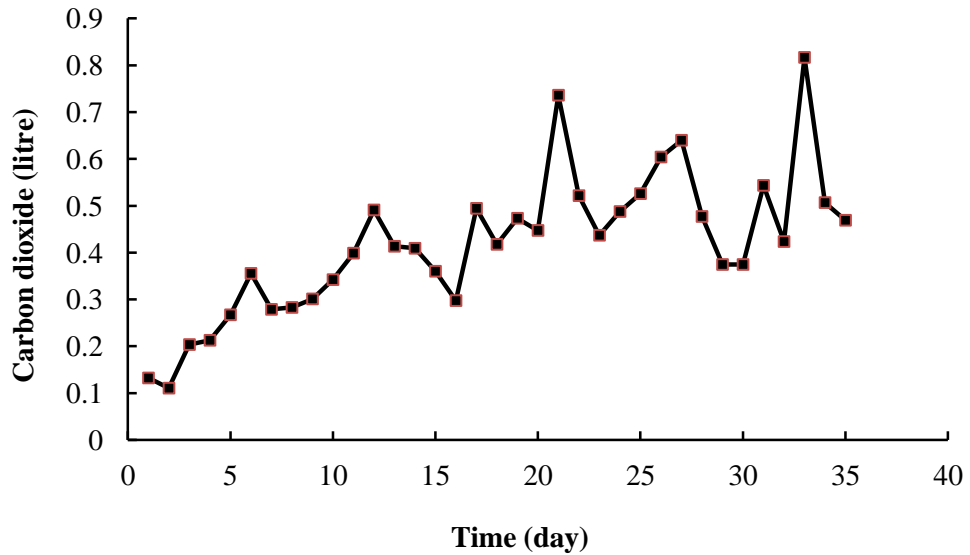


Figure 3.16: Values of carbon dioxide produced from anaerobic digester fed with simulated sludge

Figure 3.17 below shows percentages of biogas components (e.g.  $\text{CH}_4$  and  $\text{CO}_2$ ) produced from the anaerobic digester fed with a simulated sludge. It can be seen that the percentages of methane and carbon dioxide were around 60-70% and around 20%, respectively. The data obtained from the experiments shows that use the suggested simulated sludge keeps operation of the anaerobic digestion with desired results, providing that  $\text{H}_2\text{S}$  values are kept low as shown in Figure 3.18.

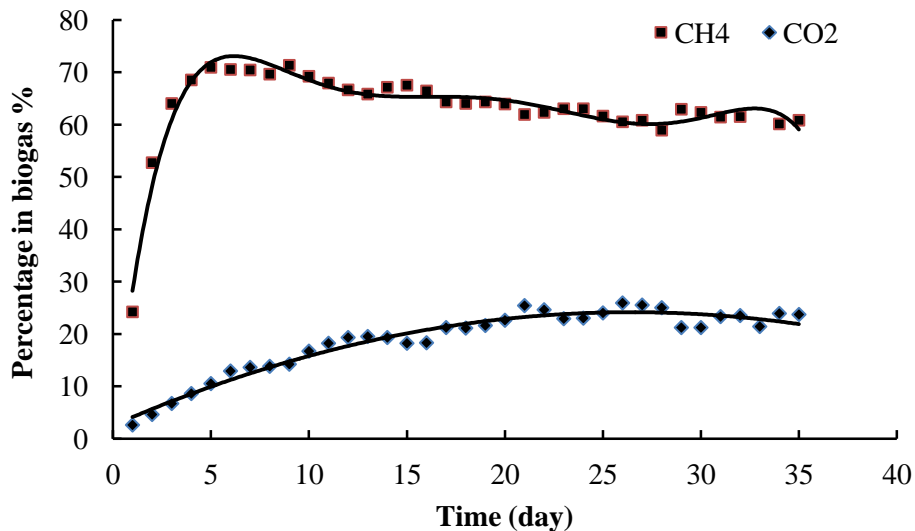


Figure 3.17: Percentage of methane and carbon dioxide in the biogas produced from anaerobic digester fed with simulated sludge

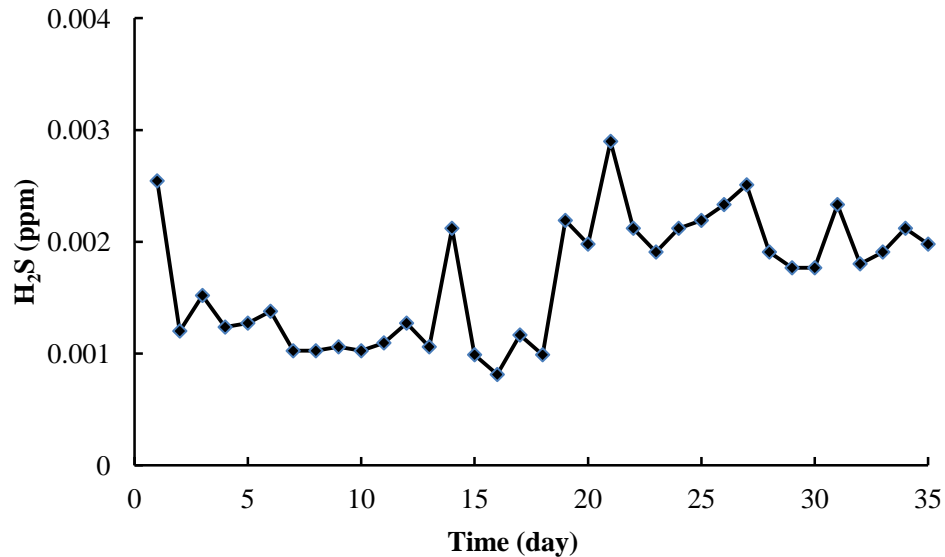


Figure 3.18: Hydrogen sulphide produced from anaerobic digester fed with simulated sludge

It would, therefore, be expected that any accumulation of dissolved CO<sub>2</sub> in the digesters without pH control would lead to lowering of pH, however, as shown in Figure 3.19, the results showed the capability of the used pH control system to maintain the pH within an ideal range in both digesters. It should also be noted that there was also a natural buffering effect whereby acids produced can immediately react with ammonia produced from biodegradation of proteins.

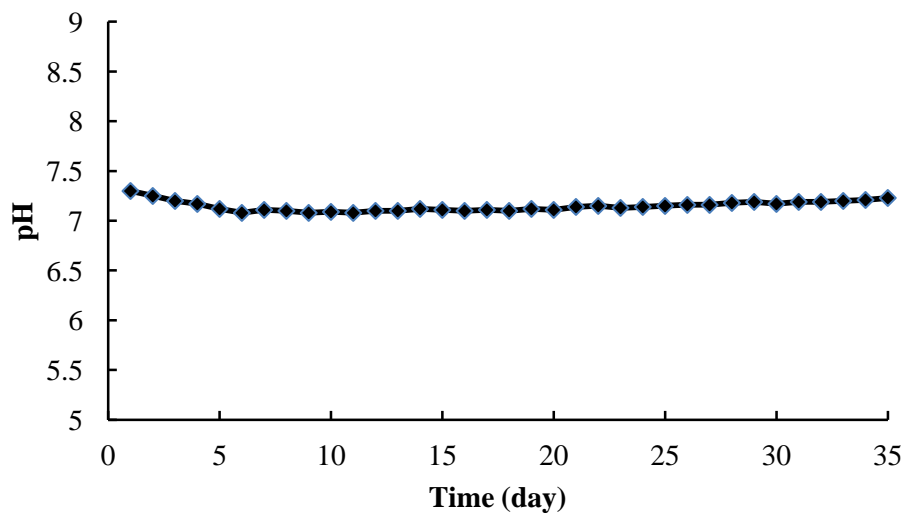


Figure 3.19: pH value in the anaerobic digester that contains simulated sludge.

Finally, it can be concluded that the present experiments show a steady methane production rate from the anaerobic digester which used the suggested sludge, with

comparatively lower H<sub>2</sub>S gas content. Whilst, the produced methane from the digester that used only the digested sludge, has been decreasing during the experiment period.

### **3.4 Materials and Methods for (Removal of Acid-gases from Digested Sludge using Periodic Sparging in an Airlift Bioreactor with Microbubble Generated by Fluidic Oscillation) (Chapter Six)**

Two identical lab-scale airlift anaerobic digesters were used in this study. Each one has a total volume of 15 litres and a working volume of 9 litres, with the remaining volume used as head-space.

The sparging gas was nitrogen which generated by a nitrogen generator (Peak Scientific Ltd) with a purity of 99.8%. Both digesters were operated for 170 hours with a under mesophilic conditions at a temperature of 35°C. The digesters were simultaneously sparged with nitrogen following seeding with sludge for several hours to provide an anaerobic environment. The sparging with 300±50 ml/min of nitrogen was performed for one hour daily on the airlift bioreactor only. The total biogas production rate was measured continuously by downward displacement of acidified (0.2 M HCL, pH<4) water. Collection of biogas produced from anaerobic digester was carried out according method suggested in section 3.2.1. The concentrations of CH<sub>4</sub>, CO<sub>2</sub> and H<sub>2</sub>S were measured by a biogas analyser (Data gas analyzer, Model 0518) at 1atm pressure. This device gives the composition of CH<sub>4</sub>, CO<sub>2</sub> and O<sub>2</sub> as percentages and H<sub>2</sub>S in ppm. The total volume of the gas in both collection vessels  $V_t$  and its composition  $y_t^i$  was measured at the same time each day (immediately before sparging of the airlift digester) to calculate the daily production of each gas. For example, the daily production of carbon dioxide for each day =  $y_t^{CO_2}V_t - y_{t-1}^{CO_2}V_{t-1}$ . For the collection vessel fed by the gaslift digester, the present setup also made an additional set of measurements immediately following the 60 minute sparging period in order to calculate the production of gas during the sparging period only. Figure 3.20 shows the schematic diagram of the experimental work.

Fresh sludge to seed the bioreactors was taken from the outlet stream of full-scale mesophilic digester from the Woodhouse wastewater treatment plant in Sheffield city operated by Yorkshire Water.

The key motivation for constructing two bioreactors and seeding with the same sludge is the inherent variability in the physical, chemical and biological properties of sludge.

These properties can differ widely depending on time of sampling, weather conditions and operating conditions. There are also many types of anaerobic bacteria that exist in the wastewater (Baudez et. al. 2007) in rather variable abundances depending on the characteristics of the wastewater and weather conditions at the time of collection. These factors will affect the production of biogas and the efficiency of biodegradation of the organic matter. Therefore, the present study uses the same sludge distributed into both reactors at the same time with the same operating conditions.

The digested sludge used in this study has methanogenic bacteria but a low concentration of substrates and the present experiments did not include addition any more nutrients. Consequently, the production of biogas falls substantially over the course of this experiment.

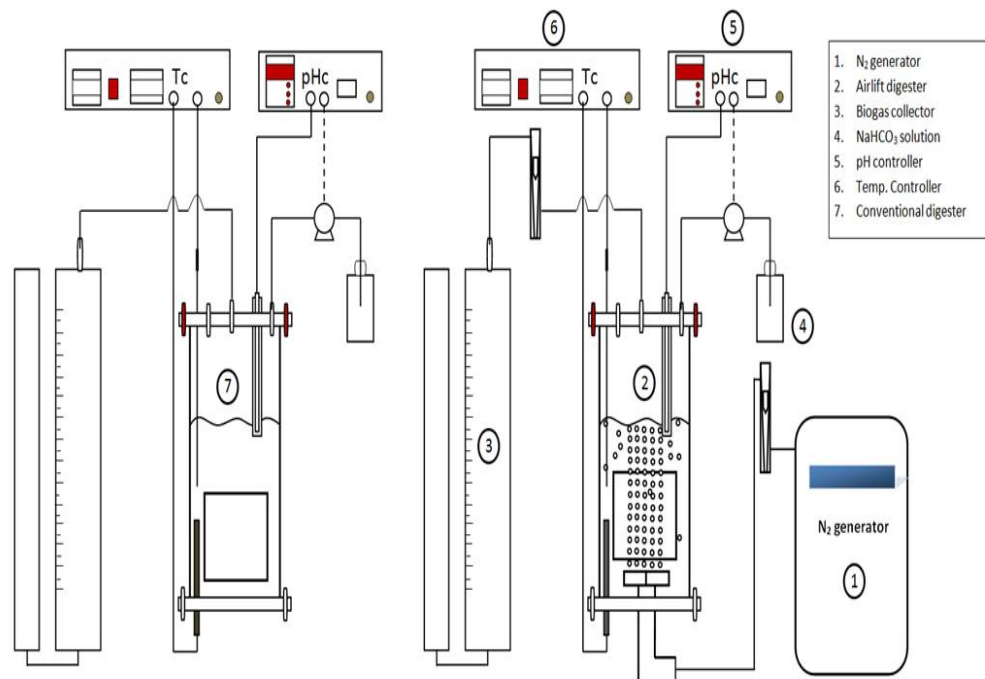


Figure 3.20: Process flow schematic for removal of acid-gases from digested sludge using pure nitrogen. Two digesters were used; the sparged digester in right side operates without fluidic oscillator, and the digester in left side operates without sparging system

Many researchers (Perez-elvira et. al. 201; Chamy and Ramos 2011; Braguglia et. al. 2011; Kim et. al. 2011; Siggins et al 2011) do not introduce any nutrients or trace metals into digestion sludge in their experimental work because the digestion sludge for anaerobic digestion is mainly composed of lipids, polysaccharides, protein and nucleic acids which are bio-degraded by anaerobic bacteria to produce the biogas and effluent,

which used as fertilizer. For the successful operation of anaerobic digestion, facultative anaerobes, anaerobes including methanogenic bacteria and organic particulates should be present in the sludge. The primary clarifier provides particulates and many anaerobes including methane-producing bacteria, while the secondary clarifier provides many facultative anaerobes.

Good pH control is a vital aspect of maintaining efficient digester operation and yet it is notoriously difficult to achieve due to its inherently non-linear nature. In this study, however, we were able to achieve a pH value within quite a tight range of 6.8-7.5 which provided a suitable environment for the growth of the methanogenic bacteria (note that other bacteria such as acidogenic bacteria can grow at lower pH values of 5-6). Due to the importance of pH control, the present study comments briefly on the implementation of pH control loop used.

The pH controller system used in the current study is ON/OFF relay controller. It consists of main three parts: controller, peristaltic pump and pH probe sensor. The low flow rate of peristaltic pump (1 ml/min) gave enough time distribution of the solution through the sludge and minimised any resulting overshoot in pH value. The type of pH controller system used was the BL931700 pH minicontroller. The solution which is used to adjust with by pH control is 0.2M sodium bicarbonate ( $\text{NaHCO}_3$ ). Using the sodium carbonate to adjust the pH in anaerobic digestion is more efficient compared with other bases such as NaOH for several reasons, which include this solution, is less corrosive and toxic, it also tends not to cause any precipitation; and therefore minimises maintenance and cleaning. Most importantly,  $\text{NaHCO}_3$  is a mild base that does not cause big jumps in pH value even for excessive doses.

### **3.5 Materials and methods for (Investigation of the Effects of Sparging in Anaerobic Digestion using Various Gases and Microbubbles Generated by Fluidic oscillation)(Chapter Seven)**

#### **3.5.1 Using Pure Nitrogen**

Three lab-scale gaslift anaerobic digesters, whose designed and simulated, were used in this study as is shown in Figure 3.21. Each had a total volume of 15 litres and a working volume of 10 litres, with the remaining volume used as head-space.  $\text{N}_2$ -generated (Peak scientific Ltd) nitrogen with a purity of 99.9% was sparged through a micro porous ceramic diffuser (HP technical ceramics) with  $20\mu\text{m}$  size pores. The diffuser was fitted

at the bottom of the digester. Sparging with  $300\pm 50$  ml/min of pure nitrogen for a fixed duration each day was performed for 27 days. All digesters were simultaneously sparged with nitrogen following seeding with sludge for several hours to provide an anaerobic environment. The different periods of sparging used in the gaslift digesters are illustrated in Table 3.4. Each digester contains digested sludge, which was collected from the outlet stream of a full-scale mesophilic digester at the Woodhouse wastewater treatment plant in the city of Sheffield in the UK. In each digester kitchen waste was as a substrate for bacteria, 15 ml was fed daily to the digester on the basis of the results presented in chapter seven. In order to maintain the volume of sludge in each anaerobic digester, 12-15 ml was discharged daily from each reactor. Additional losses due to evaporation were reason why less than 15 ml were sometimes discharged to keep a constant level in the digester. The chemical oxygen demand (COD) of the digested sludge and kitchen waste were 33 and 127 g/L respectively (see Appendix A.1 for method).

In the present chapter, a proportional-integral-derivative (PID) controller was used to maintain the temperature in the digester at  $35\pm 1^\circ\text{C}$ . A temperature control system was constructed using a 500 W heater and thermocouple sensor type K with a range of  $-128^\circ\text{C}$  to  $539^\circ\text{C}$ .

Table 3.4 Operational conditions for conducting the experiments.

Number of stage	Flow rate of nitrogen (ml/min)	Time of sparging (min)	Working days
<b>First stage</b>	300	100	12
<b>Second stage</b>	300	60	4
<b>Third stage</b>	300	30	4
<b>Fourth stage</b>	300	15	3
<b>Fifth stage</b>	300	5	4
<b>Sixth stage</b>	300	0	11

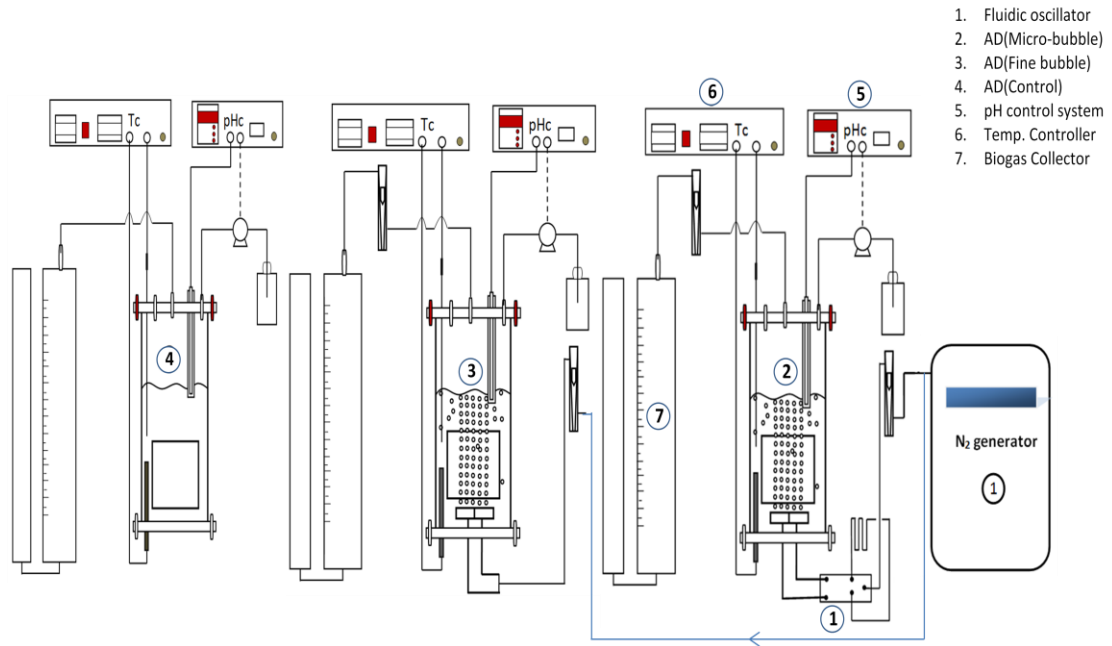


Figure 3.21: Process flow schematic for sparging the digester with pure nitrogen. Three digesters were used; the sparged digester in right side operates with fluidic oscillator, the sparged digester in the middle operates without fluidic oscillator, and the digester in left side operates without sparging system

Continuous measurement of biogas yield was accomplished by means of the downward displacement of acidic aqueous solution (0.2 M HCL, pH<4). Methane, carbon dioxide and hydrogen sulphide concentration were measured daily using a biogas analyser (Data gas analyser, Model 0518). Each digester was provided with a pH controller. The optimum pH value is between 6.8 and 7.4 which provide a suitable environment for growth of the anaerobic bacteria.

The biogas produced from anaerobic fermentation is captured using the collection process described and explained earlier.

Methane is a final product of digestion by anaerobic microorganisms and therefore any inhibitory effect on any preceding stage has an effect on the methane yield. The study focuses on the biogas produced from the anaerobic process (methane, carbon dioxide and hydrogen sulphide), while the oxygen was measured merely to check the anaerobic conditions.

### 3.5.2 Using Nitrogen and Carbon Dioxide

The same lab-scale anaerobic digesters used in the previous part of the study were used in this part, although certain changes were made to render them suitable for the intended

procedure. The digesters were operated for 65 days and under mesophilic conditions ( $35 \pm 1$  °C). The biogas was collected continuously before and after the application of the sparging system, while the concentrations of methane, carbon dioxide, and hydrogen sulphide were measured using a biogas analyser (data biogas analyser model 0518). The gaslift digesters were sparged with  $N_2$ -generated nitrogen ((Peak scientific Ltd), with a purity of 99.9% through a ceramic diffuser for 12 min, while carbon dioxide with purity of 99.9% (from BOC) was sparged into the same diffuser for 3 min, as shown in the Figure 3.22. the digesters operate under the optimum pH condition (6.8-7.8). An adjustable solution of sodium bicarbonate was used in the pH buffering system. Kitchen waste, used as the substrate for the bacteria, was fed daily at doses of 15 ml into each digester, as recommended earlier. In order to maintain the volume of sludge in each digester, about 12-15 ml was collected daily from each reactor. The different sparging regimes used are summarised in the Table 3.5.

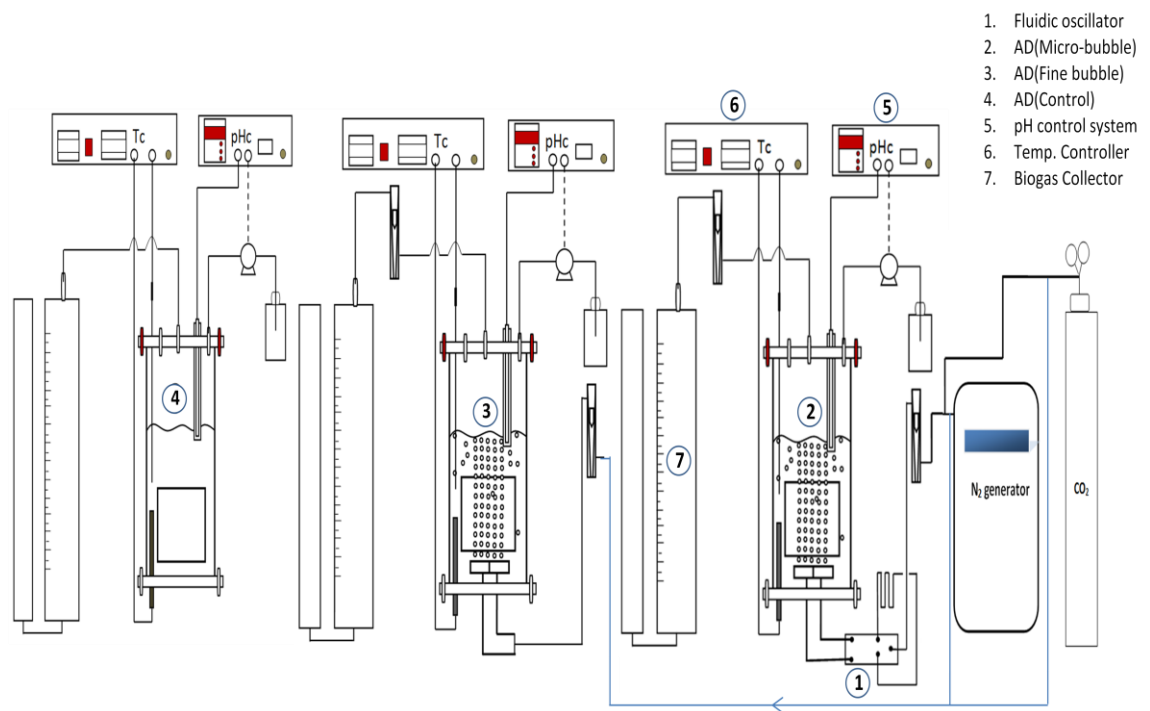


Figure 3.22: Process flow schematic for sparging the digester with nitrogen and carbon dioxide. Three digesters were used; the sparged digester in right side operates with fluidic oscillator, the sparged digester in the middle operates without fluidic oscillator, and the digester in left side operates without sparging system

Table 3.5 Operational conditions applied in present study

Number of stage	Flow rate N <sub>2</sub>	Time (min)	Flow rate CO <sub>2</sub>	Time (min)	Duration days	Periodicity
First stage	300	12	300	3	7	1
Second stage	300	12	300	3	10	2
Third stage	300	12	300	3	12	3
Forth stage	300	12	300	3	15	5
Fifth stage	300	12	300	3	8	8
Seven stage	300	12	300	3	13	13
<b>Total</b>					65	

The collected biogas and concentration of methane and carbon dioxide are estimated according to the following equation:

$$[\text{CH}_4]_T = [\text{CH}_4]_i \times V_i + [\text{CH}_4]_{\text{N}_2} \times V_{\text{N}_2} + [\text{CH}_4]_{\text{CO}_2} \times V_{\text{CO}_2} \quad (3.21)$$

Where  $[\text{CH}_4]_T$  is total amount of methane produced from anaerobic digestion,  $[\text{CH}_4]_i$  is the percentage of methane in the biogas produced before the sparging of any gas,  $V_i$  is the volume of collected biogas before the sparging of any gas,  $[\text{CH}_4]_{\text{N}_2}$  is the percentage of methane after sparging the nitrogen into the digester,  $V_{\text{N}_2}$  is the volume of biogas collected after sparging the nitrogen into digester,  $[\text{CH}_4]_{\text{CO}_2}$  is the percentage of methane after sparging the carbon dioxide into the digester,  $V_{\text{CO}_2}$  is the volume of biogas collected after sparging the carbon dioxide into the digester.

### 3.5.3 Recycling of the Biogas in Anaerobic Digestion

Two identical lab-scale gaslift anaerobic digesters were used in this study. Each had a total volume of 15 litres and a working volume of 10 litres, while the remaining volume served as head-space. The sparging gas was biogas generated from the same digester. Both digesters were operated for 64 days under mesophilic conditions at a temperature of 35°C. The digesters were left unsparged to ensure that the methane production was the same in each digester. The sparging system operated at 1000±50 ml/min of biogas. Biogas produced from the digesters was collected based on the suggested method in present study. The concentrations of methane, carbon dioxide, and hydrogen sulphide were measured using a biogas analyser (Data gas analyser, Model 0518) at 1atm pressure. This device gives the composition of CH<sub>4</sub>, CO<sub>2</sub> and O<sub>2</sub> as percentages and H<sub>2</sub>S in ppm. The total volume of the gas in collection vessel and its composition was

measured at the same time each day (immediately before sparging of the airlift digester) to calculate the daily production of each gas.

#### 3.5.3.1 The procedure for recycling the pure biogas as shown in Figure 3.23.

- a) Biogas produced from the gaslift digester under non-sparging conditions is accumulated in collector No.1.
- b) Methane, carbon dioxide and hydrogen concentrations are measured using the gas analyser (Data gas analyser, Model 0518), after balancing the system in the headspace of the collector.
- c) Acidic aqueous solution was supplied to create pressure in the collector, allowing recycling of the biogas back into the digester for stripping of the produced biogas and for mixing purposes.
- d) The biogas produced in the digester during the sparging process, was accumulated in collector No.2 by downward displacement of the acidified (0.2 M HCL, pH<4) aqueous solution.
- e) The concentrations of CH<sub>4</sub>, CO<sub>2</sub> and H<sub>2</sub>S were measured by a biogas analyser at 1 atm pressure in collectors no.1 and No. 2, after balancing the system in the headspace of the collector.

#### 3.5.3.2 The procedure for recycling the diluted biogas as shown in Figure 3.24

Recycling of the diluted biogas comprised the following steps.

- a) Biogas collected from the gaslift digester under non-sparging conditions is accumulated in collector No.1.
- b) Pure carbon dioxide is added to collector no.1 to reduce the concentration of methane to around 20%.
- c) Methane, carbon dioxide, and hydrogen sulphide concentration are measured using the gas analyser, after balancing the system in the headspace of the collector.
- d) The pressure inside the collector is increased by introducing acidified aqueous solution enabling the biogas to be sent to the digester for stripping of the biogas produced and mixing of the sludge.
- e) The biogas produced from that digester during the sparging process is collected in collector No.2 by downward displacement of the acidified (0.2 M HCL, pH<4) aqueous solution.

- f) The concentrations of CH<sub>4</sub>, CO<sub>2</sub> and H<sub>2</sub>S are measured again using a biogas analyser at 1atm pressure in collectors No.1 and No.2, after balancing the system in the headspace of the collector.

These experiments faced several challenges and problems, for example, the digestion process did not produce enough biogas to use the fluidic oscillator. This device (fluidic oscillator) needs a flow rate of 60-80 L/min with 5 atm pressure to generate microbubbles, while biogas produced by the lab-scale anaerobic digester was insufficient to meet this requirement. Therefore the fluidic oscillator was not used in this part of the study. In addition, recycling biogas to the digester also requires pressure. Although pressure was supplied by acidic aqueous solution as mentioned in step 2 of the experiment's procedures, it was difficult to measure the amount of biogas that entered the digester exactly, since some of the gas remained below pressure and some was returned to the water tank through pumping. Therefore, some degree of calculated estimation was necessary to determine the amount of biogas that was entering the digester. The equation used for this purpose is:

$$V_i = \frac{1 - X_{oCH_4} - X_{oCO_2}}{1 - X_{iCH_4} - X_{iCO_2}} \times V_o \quad (3.22)$$

Where:

$V_i$  = Inlet gas volume to digester

$V_o$  = Outlet gas volume to digester

$X_{iCH_4}, X_{oCH_4}$  = Inlet and outlet fraction of methane to digester

$X_{iCO_2}, X_{oCO_2}$  = Inlet and outlet volume of carbon dioxide to digester

Moreover, the suspended solids in the unsparged digester became sedimented because the digester was operated without a mixing system for a long time. Therefore the sludge in that digester became more dilute than that in the other digesters as shown, in the Figure 3.25.

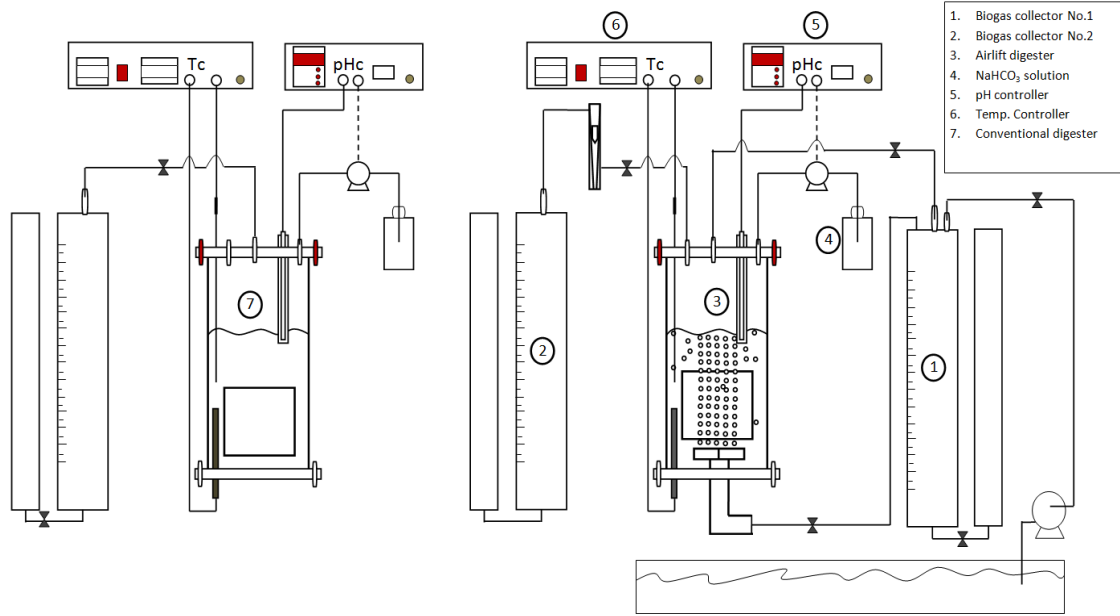


Figure 3.23: Process flow schematic for sparging the digester with recycling the biogas. Two digesters were used; the sparged digester in right side operates with recycling the biogas but without fluidic oscillator, and the digester in left side operates without sparging system

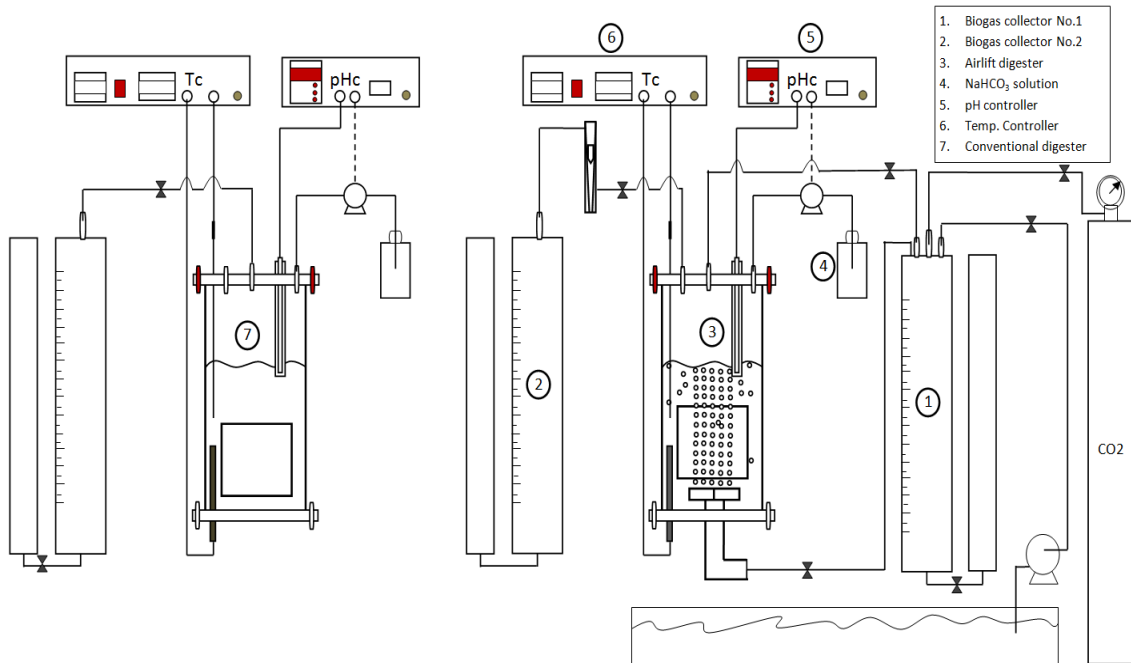


Figure 3.24: Process flow schematic for sparging the digester with recycling the diluted biogas by carbon dioxide. Two digesters were used; the sparged digester in right side operates with recycling the diluted biogas but without fluidic oscillator, and the digester in left side operates without sparging system



Figure 3.25: Snapshot of the digesters in the experiments showing the dilution in the unsparged digester (light colour on left picture), while the sludge in the other digesters (middle and right) is thicker (dark colour)

Therefore, an increase in the temperature of the sludge was observed in the unsparged digester, because the heat flux from the heater to the solution became faster than in previous days, when the sludge was thicker. This increase in the temperature caused an increase in biogas production. The control system was working very well, however; and when the change in temperature was observed, the setting on the controller was adjusted to ensure that all digesters were working at 35 °C.

#### 3.5.4 Using Pure Carbon Dioxide

Two lab-scale digesters were used in the present study: a conventional digester and a digester provided with a ceramic diffuser to sparge the carbon dioxide with microbubbles generated by fluidic oscillation as shown in Figure 3.25. Both digesters were operated for 19 days under mesophilic conditions. The biogas was collected continuously before and after bubbling, while the concentrations of methane, carbon dioxide, and hydrogen sulphide were measured using a biogas analyser. The gaslift digester was sparged with carbon dioxide for 5 min to prevent a drop in the pH value.

The flow rate used in the current experiments was 300-400 ml/min.

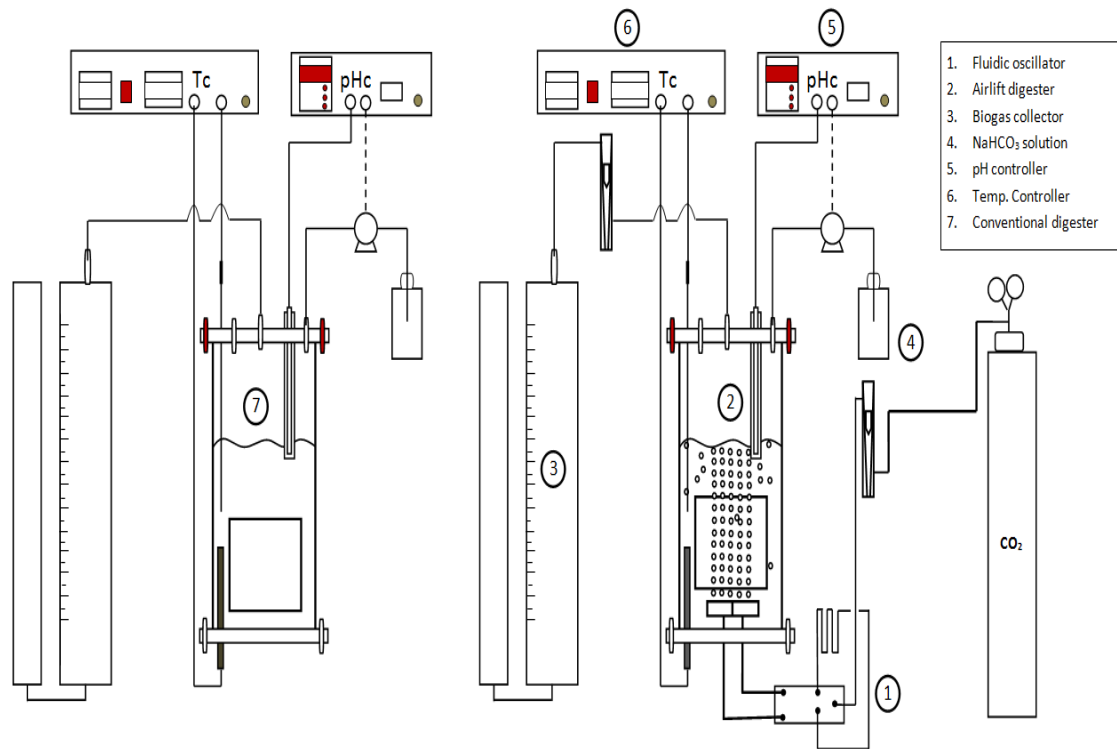


Figure 3.26: Process flow schematic for sparging the digester with pure carbon dioxide. Two digesters were used; the sparged digester in right side operates with fluidic oscillator, and the digester in left side operates without sparging system

### 3.6 Materials and Methods for (Direct-contact Evaporation to Direct-Contact Heating as a Step to Improve Heating in a Biological Application) (Chapter Eight)

#### 3.6.1. Setup of the Experiments

Direct contact heating experiments were performed in a laboratory scale bubble column set-up as shown in Figure 3.26. A cylindrical tank (0.14m inner diameter and 0.34m height) is filled with liquid, while gas bubbles are sparged from the bottom of the reactor through a micro porous Ceramic diffuser produced by HP Technical ceramics with  $20\mu$  size pores. Here, the right and left half discs are separated chambers. Due to buoyancy, the air bubbles rise through the water. The ceramic diffuser consists of two parts with a total diameter 0.1m. Each part has an inlet stream for hot air.

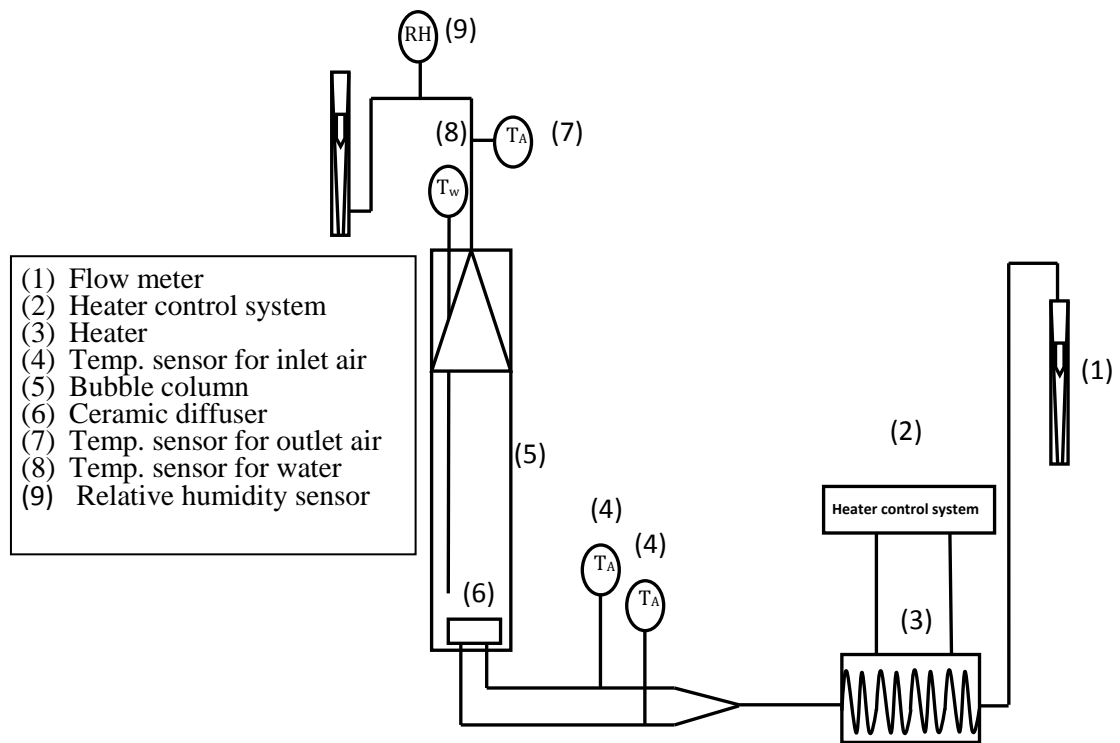


Figure 3.27: Schematic diagram of the experimental set up

The air was heated in an electrical oven with a total power 1000 W. The gas temperature was controlled by a PID controller. All the pipelines that connected the tank and heating system were thoroughly insulated with fibre glass to minimise heat losses. The air temperature was recorded in two positions; at heater outlet and outlet stream of the tank using thermocouples type K. Water temperature and relative humidity was measured continuously. The air flow rate was controlled by a flow meter. For high air flow rate, 40 l/min was used with different level of water (2, 4, 8, and 12 cm) above the diffuser. However, experimental design (Central composite rotatable design) has used in the present part of the thesis to study effect of the different operational conditions on the liquid temperature and percentage of evaporation, which can be calculated by following equation:

$$\text{Evaporation (\%)} = \frac{\text{Amount of evaporated of liquid (as volume)}}{\text{Initial amount of liquid (as volume)}} \times 100 = (\%) \quad (3.23)$$

In bioreactors, the medium is typically 90- 95% water, depending on the type of bioprocess. For instance, water content in sludge is around 95%, while 5% consists of

micro-organisms, organic matter, bio-chemicals, and suspended solids. Therefore, pure water was used as liquid phase, and air was taken as gas phase. The relative humidity (measured using a relative humidity and temperature meter, N18FR, precision GOLD, Humidity 0%-100% RH) is located at outlet stream.

Effect of the variables (flow rate, height of water, time of heating) on the process heating and percentage of evaporation have been investigated in present experiments. In addition, CCRD was used to create a numerical equation that describes the entire process.

### 3.6.2 Experimental Design used in Chapter Eight

#### 3.6.2.1 Central Composite Rotatable Design (CCRD)

If a response ( $y$ ) from a factorial experiment depends on a number of quantitative variables e.g. time, flow rate and volume, then the value for  $y$  may be expressed as a function of the levels of such variables, which can be written as:

$$y_u = \Phi(x_{1u}, x_{2u}, \dots, x_{ku}) + e_u \quad (3.24)$$

Where  $\Phi$  = Response surface function,  $u = 1, 2, \dots, N$  represents the  $N$  observations in the experiment,  $x_{iu}$  = level of the  $i^{\text{th}}$  variable in the  $u^{\text{th}}$  observation,  $e_u$  = experimental error of the  $u^{\text{th}}$  observation,  $k$  = number of  $x$ - variables i.e.  $x_{iu}$   $\{i = 1, 2, \dots, k\}$  (Cochran & Cox, 1992, p335).

For a second order design, the relation between  $y$  and  $x$  variables could be approximated satisfactorily, within an experimental region, by the following polynomial (Fakheri *et al*, 2012).

$$y_u = \beta_0 + \sum_{i=1}^k \beta_i x_{iu} + \sum_{i=1}^k \sum_{j=2}^k \beta_{ij} x_{iu} x_{ju} + \sum_{i=1}^k \beta_{ii} x_{iu}^2 + e_u \quad (3.25)$$

Where  $B_0, B_i, B_{ii}$  and  $B_{ij}$  are the parameter of general equation  $X$  code (1, -1, 0, -1.682, 1.682), and  $k$  is the number of variables to be studied.

These parameters can be estimated using the following equations (Cochran & Cox, 1992):

$$B_0 = 0.166338 (Y_0) - 0.056791 \sum(iiy) \quad (3.26)$$

$$B_i = 0.073224(iy) \quad (3.27)$$

$$B_{ii} = 0.0625(iiy) + 0.006889 \sum (iij) - 0.056791 (Yo) \quad (3.28)$$

$$B_{ij} = 0.125 (ijy) \quad (3.29)$$

This second order equation represents a multiple linear regression. Central composite design (CCD) can be used to obtain the coefficients of the multiple regression that fits a given data and it has the advantage of significantly reducing the number of experiments required compared to a full factorial design (Aslan, 2007 and 2008).

### 3.6.2.2 Experimental Error in CCRD

A CCD (Central composite design) begins with a standard  $2^k$  factorial design. In addition to the  $2^k$  factorial, CCD requires an additional factor of  $2k + 1$ , bringing the total number of experimental runs for a CCD design to  $(2^k + 2k + 1)$ . A CCD design of this kind requires the assumption that time trends do not change the level of response ( $y$ ) between the first and second experiment. A CCD can be given the property of being rotatable in which case it is known as a central composite rotatable design (CCRD). A rotatable design ensures that the standard error of the model is the same at all points that are of equal distance from the centre of the design region (Aslan, 2007, Cochran & Cox, 1992, p345).

A CCRD design for any number  $k$  of  $x$ -variables requires the standard  $2^k$  factorial points, extra  $2k$  axial points with axial spacing  $(\alpha) = 2^{k/4}$  and replicate tests at the centre of design region. These replicates are useful for estimating the standard error of the developed model.

For three  $x$ -variables, a total number of 6 replicates are recommended at the centre point. Closeness in the results obtained from replicates tests are a clear indication of the accuracy of the results and this is what has already been obtained in this study. Therefore, the total number of experimental runs for a design consisting of three  $x$ -variables is  $2^3 + (2 \times 3) + 6 = 20$  *experimental runs*.

For CCRD, design calculations are simplified by coding each  $x$ -variable. Codification of variables refers to the transformation of the original or real values for  $x$  into coordinates inside a scale of dimensionless values. For CCRD designs, the  $x$ - variables are normally coded to lie at  $\pm 1$  for the factorial points,  $\pm \alpha$  for the axial points and 0 for the centre points.



CHEMICAL & BIOLOGICAL ENGINEERING

## Chapter Four

# Carbon Dioxide Mass Transfer Induced Through an Airlift Loop

---

*This study published as paper in Ind.&Eng.Chem. research ( Mahmood K. H. Al-Mashhadani, Hemaka Bandulasena and William B. Zimmerman).*

## 4.1 Introduction

The physical chemistry of carbon dioxide is of widespread public interest due to the concerns posed by increasing annual emissions and the longevity of atmospheric carbon dioxide. Carbon abatement programmes typically require mass transfer interfacial transfer of gaseous carbon dioxide for dissolution into a carrier liquid. For instance, the common design of a carbon capture and storage system dissolves carbon dioxide in a carrier liquid such as monoethanolamine (MEA) by atomization of the liquid into the gas stream in an absorber unit. To release the carbon dioxide, the carbon dioxide-rich MEA liquid is heated in a regenerator, causing the degassing of the carbon dioxide (Abu-Zahra et al., 2007). The speed of this process is controlled by the mass transfer kinetics of the interfacial transport in both processes (Clarke 1964; Jou et al., 1995). The energy cost depends largely on the mechanical energy of the atomization of liquid into droplets, and of the heat losses in the heat exchanger for degassing the carbon dioxide. Although MEA is a cheap solvent, there is still a substantial raw material cost in using it as a carrier liquid. Similar issues exist for ionic liquids in natural gas sweetening (Astarita et al., 1983, Bates et al. 2002).

By comparison, water is a much cheaper carrier liquid for carbon dioxide scrubbing. Its use is becoming widespread in biogas scrubbing from anaerobic digesters and landfill sites (Ofori-Boateng and Kwofie, 2009), typically with large water scrubbing towers to enhance the phase contacting. Water has a lower carbon dioxide solubility than MEA, hence also a much lower driving force for mass transfer in dissolving carbon dioxide and in degassing in the thermal regeneration phase. So as a carrier liquid for CCS, it has distinct disadvantages to MEA (Weiss, 1974). With the same processing methodology, it will take more water to scrub the carbon dioxide from the gas stream and more heat to regenerate it due to the slower kinetics. Biogas sweetening does not require a regeneration step necessarily if the water supply is cheap. Reduction of the water requirement is massively reduced by reactive dissolution (Caldeira and Rau, 2000, Gunter et al., 1993), whereby acid-base reaction is fast, and it is expected that mass transfer of the carbon dioxide gas is the rate limiting step.

Clearly, for dissolution and regeneration using water as the carbon dioxide carrier liquid to be viable, energy efficiency of mass transfer would have to be comparable to that of MEA. Since mass transfer is crucially dependent on the interfacial surface area, one

would have to improve on the surface area per unit volume of atomization of liquid droplets. Atomization can routinely generate microdroplets with less than 50  $\mu\text{m}$  diameter (Hartman, et al., 2000), so it would be very difficult to increase on the surface to volume ratio significantly. The major difficulty with atomization is that it is achieved by flowing liquid, which has approximately a thousand-fold density ratio to gases. So if improvement on the energy efficiency of dissolution and degassing are going to be achieved, it would be with microbubbles of similar surface to volume ratio, but radically different energy cost of generation. Recently, such a microbubble generation approach has been developed (Zimmerman et al 2008 and 2011(a)), exploiting the ability of no-moving-part fluidic oscillators (Tesar et al, 2006) to produce short sharp bursts, with packets of gas that shoot out of apertures like “bullets”. So far, the methodology has been reported to achieve clouds of fairly uniformly spaced and sized microbubbles as small as an average diameter of 28  $\mu\text{m}$  from 20  $\mu\text{m}$  pores in a metallic membrane (Zimmerman et al. 2011(a)). Measurements of power consumption show an 18% reduction of electricity over that of steady flow with the same volumetric flow rate. As multiple small bubbles are produced in the same time period as a conventional larger bubble, which spreads out and slowly detaches from the same aperture with steady flow, it is clear that the inertia of the small bubbles is preserved, whereas the conventional large bubbles are much more dissipative, accounting for the improved energy efficiency of the microbubble generation by the fluidic oscillation mechanism.

Clearly, energy efficient microbubble generation is a significant competitor to microdroplet atomization on the level of surface area per unit volume achievable, but with a much lower pumping cost. Whether or not microbubbles alone are sufficient for the gas exchanges in dissolution and degassing (dosing and stripping) as a carbon dioxide carrier fluid depends on transfer rates and driving forces, as well as the mixing and contacting time. Achieving mixing with microbubbles has proven to be an almost “cost free” bonus. An airlift loop bioreactor (Figure 4.1), implemented at the lab scale with 250 L volume (Zimmerman et al. 2009) and at the pilot scale (2200 L) (Zimmerman et al., 2011(b)), has been designed for and tested on the growth of algal biomass. The true cost of insertion of the internal baffle which creates the airlift loop and makes the draft tube effect possible is the additional friction loss on the rise of the bubbles in the riser region. The upshot of this slower average rise rate is that the contact time of the microbubbles is somewhat longer, permitting a closer approach to

equilibrium mass transfer before the bubble bursts. The strength of the recirculation flow induced in the airlift loop bioreactor increases with decreasing bubble size, hence so does the rate of mixing. The feature suggests that microbubbles generated by fluidic oscillation can provide efficient mixing at low energy cost, since the bubble must rise and can be injected at lower cost than conventional fine bubbles, and hence be introduced for mixing in systems that have never been sparged before.

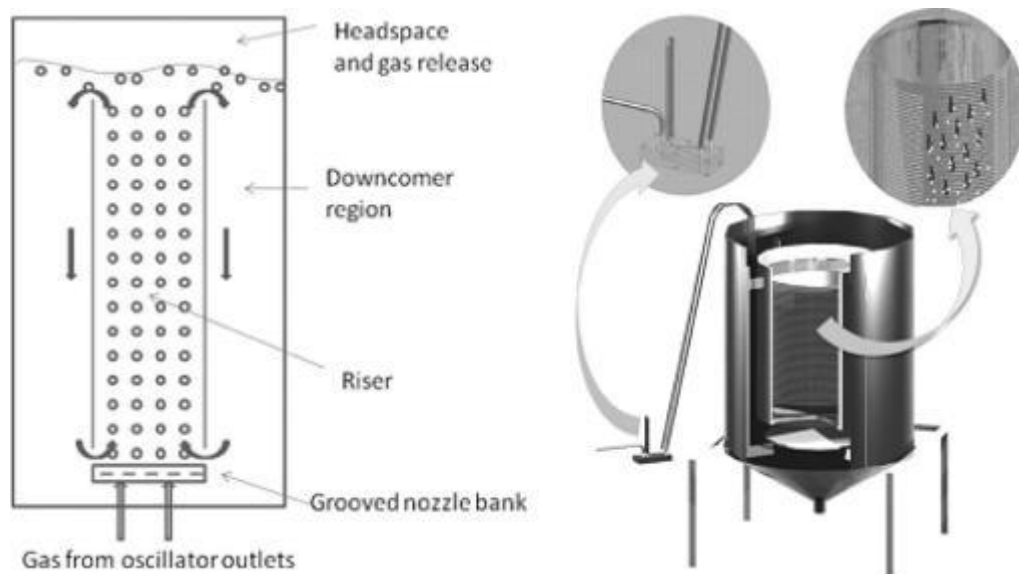


Figure 4.1: Use of energy efficient microbubbles to generate airlift loop effect, suspension of algae by flotation, and gas exchange—CO<sub>2</sub> dosing and O<sub>2</sub> stripping. The operating regions of the flow structure induced by the microbubble rise and liquid released by the bursting of the bubbles causes the downcomer flow. The fluidic oscillator is external to the device. The “draft tube” effect produces mixing because the microbubble cloud drags a significant amount of liquid with it—due to all the surface area—and as the bubbles spread out across the top surface, the liquid is released when the bubbles burst. In the downcomer region, there are practically no bubbles, so it is solely a liquid flow (Zimmerman et al. 2011).

The purpose of this study was to explore, both experimentally and with computational modeling, the hypothesis that microbubbles not only accelerate the rate of carbon dioxide dissolution, but also the rate of carbon dioxide removal under the stripping conditions where the carrier gas has initially practically no carbon dioxide content, in the airlift loop configuration. It is possible conjecture that given the strength of the solubility of carbon dioxide in comparison to other gases, particularly O<sub>2</sub> which is commonly dosed in aeration systems, microbubbles are required to strip carbon dioxide. The typical experience is that carbon dioxide can be dosed into, for instance, algal bioreactors, faster than metabolic uptake, hence is not a major obstacle in biomass production. The energy efficiency offered by fluidic oscillator microbubble dosing may

be secondary to the mixing effects and suspension of the algae, which also influence vitality positively. The surprising result from the airlift loop bioreactors was the stripping of O<sub>2</sub> from the liquid media, as attested by the inlet and outlet gas traces. Without the O<sub>2</sub> inhibition, super exponential biomass growth was observed in the pilot scale trial. Because microbubbles were never used before in algal bioreactors, this increased vitality was more attributable to the O<sub>2</sub> stripping than the more rapid carbon dioxide dosing. Since O<sub>2</sub> is soluble up to 10-12 mg/L in aeration, and much higher with pure O<sub>2</sub> dosing as is done by algal secretions, stripping of O<sub>2</sub> should require the greater surface area per unit volume possible with microbubbles but not with other gas exchange systems, let alone natural diffusion or modest mixing with small paddle wheels, for instance.

In this Chapter, we test the analogous conjecture that stripping carbon dioxide requires microbubble levels of surface area to volume ratios for effectiveness. Although motivated in terms of carbon capture systems, the target has other applications as well. For instance, oxygenation in aquaculture is a relatively mature technology with well-established operational principles, techniques, and equipment. Carbon dioxide control has become an important issue only recently as aquaculture operations have intensified, and the technology is still evolving (Summerfelt et al., 2000). Section 2 presents the experimental program from a lab bench-scale airlift loop bioreactor (15 L), purpose-built to visualize microbubble dynamics from a well-distributed cloud injected from an external fluidic oscillator. Section 3 presents numerical simulation of the target system using a bubbly flow model adapted for microbubble clouds that are uniformly distributed, nearly monodispersed, and hence noncoalescent, in order to compare with experimental observations of the flow structure and carbon dioxide mass transfer rates. Discussion is presented within each section. Conclusions are drawn in section 4.

## **4.2 Experiments for Mass Transfer of Carbon Dioxide with Microbubbles.**

### **4.2.1 Physical Chemistry of Carbon Dioxide Gas Exchange.**

One of the most powerful design tools in the chemical engineer's arsenal is reactive separation, which restates Le Chatelier's principle in terms of simultaneous reaction and separation. The Gibbs free energy of a binary reaction with two products in the gaseous phase is illustrated in chapter two (equation 2.10 and 2.11).

Clearly, removal of products decreases the denominator in equation (2.11) with the accompanying decrease in the Gibbs free energy of reaction. This removal of products has the effect of driving the reaction in the direction of greater product formation, but is essentially an entropic effect. Replacing the removed products increases the entropy of the product-depleted state, which is why this effect becomes more important at higher temperature as entropy creation then dominates the standard Gibbs free energy of reaction. This principle applies equally well for equilibrium reactions in biochemistry (Gary, 2004).

For instance, the production of biohydrogen from glucose has been the subject of considerable investigation for the efficacy of gaseous product removal (Tanisho, et al. 1998, Park et al. 2005, Alshiyab, et al. 2008).

#### 4.2.2. Absorption of Carbon Dioxide in the Water.

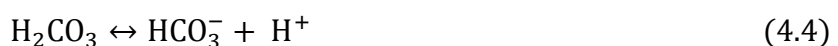
In bioreactors, the medium is typically 90–95% water, depending on the type of bioprocess. For instance, water content in sludge is around 95%, while 5% consists of micro-organisms, organic matter, biochemicals, and suspended solids. Produced carbon dioxide reacts with water to produce carbonic acid.



Kinetically, the conversion to carbonic acid is very slow, with just 0.2% of CO<sub>2</sub> converting to carbonic acid and its ions, while 99.8% of the CO<sub>2</sub> remains as a dissolved gas, as shown by the association equilibrium constraint

$$K_h = \frac{[\text{H}_2\text{CO}_3]}{[\text{CO}_{2(\text{aq})}]} \quad (4.3)$$

Carbonic is a diprotic acid, thus it contains two hydrogen atoms ionizable in water and dissociates into bicarbonate and carbonate ions:



### 4.2.3. Relationship between pH and Dissolved Carbon Dioxide.

Clearly, it is possible to infer the dissolved carbon dioxide concentration from the pH presuming equilibrium and a well mixed system. The equilibrium constraint for each dissociation reaction 4.4 and 4.5 is

$$K_{a1} = \frac{[\text{HCO}_3^-][\text{H}^+]}{[\text{H}_2\text{CO}_3]} \quad (4.6)$$

$$K_{a2} = \frac{[\text{CO}_3^{2-}][\text{H}^+]}{[\text{HCO}_3^-]} \quad (4.7)$$

Electroneutrality imposes another constraint

$$[\text{H}^+] = [\text{OH}^-] + [\text{HCO}_3^-] + 2[\text{CO}_3^{2-}] \quad (4.8)$$

As does the dissociation reaction of water to hydrogen and hydroxide ions and the association reaction of CO<sub>2</sub>. These five equations and the definition of pH relate the six unknowns [H<sup>+</sup>], [OH<sup>-</sup>], [HCO<sub>3</sub><sup>-</sup>], [H<sub>2</sub>CO<sub>3</sub>], [CO<sub>3</sub><sup>2-</sup>], [CO<sub>2(aq)</sub>], through a set of readily solvable nonlinear algebraic equations in standard packages such as Mathematic. Hence, all species concentrations, including our target dissolved carbon dioxide as shown below, can be inferred from pH measurement.

$$[\text{H}^+][\text{OH}^-] = 10^{-14} \quad (4.9)$$

$$\text{pH} = -\log[\text{H}^+] \quad (4.10)$$

Therefore, the relationships between pH and dissolved carbon dioxide and its ions will be as following:

$$[\text{CO}_{2(\text{aq})}] = \frac{(10^{-\text{pH}})^2 (10^{-\text{pH}} - \frac{10^{-14}}{10^{-\text{pH}}})}{K_{a1} K_h [10^{-\text{pH}}] + 2K_{a1} K_{a2} K_h} \quad (4.11)$$

$$[\text{H}_2\text{CO}_3] = \frac{(10^{-\text{pH}})^2 (10^{-\text{pH}} - \frac{10^{-14}}{10^{-\text{pH}}}) K_h}{K_{a1} K_h [10^{-\text{pH}}] + 2K_{a1} K_{a2} K_h} \quad (4.12)$$

$$[\text{HCO}_3^-] = \frac{(10^{-\text{pH}})^2 (10^{-\text{pH}} - \frac{10^{-14}}{10^{-\text{pH}}}) K_h K_{a1}}{[K_{a1} K_h [10^{-\text{pH}}] + 2K_{a1} K_{a2} K_h] (10^{-\text{pH}})} \quad (4.13)$$

$$[\text{CO}_3^{2-}] = \frac{(10^{-\text{pH}})^2 (10^{-\text{pH}} - \frac{10^{-14}}{10^{-\text{pH}}}) K_h K_{a1} K_{a2}}{[K_{a1} K_h [10^{-\text{pH}}] + 2K_{a1} K_{a2} K_h] (10^{-\text{pH}})^2} \quad (4.14)$$

#### 4.2.4. Thin Film Theory of Mass Transfer Coefficients.

Liquid-gas film theory for mass transfer coefficients is well documented (Bailey and Ollis 1986), for the canonical situation as shown in Figure 4.2. In general, the mass transfer rate is proportional to the concentration driving force (the difference between two concentrations, say  $C_L$  and  $C_G$ ) at the interface and interfacial area.

$$N_A = K_L a (C_L - C_G) \quad (4.15)$$

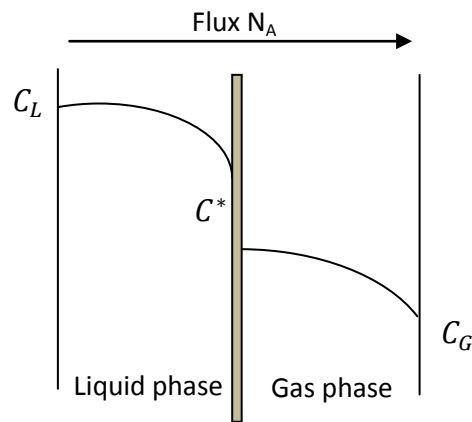


Figure 4.2: Interfacial dynamics of mass transfer for gas exchange

From the mathematical relationships between liquid - gas phases and direction of mass transfer flux  $N_A$ , it is possible to posit the following equations:

$$N_A = K_L a (C_L - C_E) \quad (4.16)$$

Where  $C_L$  is the concentration of the dissolved gas in the bulk liquid phase, and  $C_E$  is the concentration that is in equilibrium with the initial bubbles gas concentration. This is often called the saturation concentration, but that commonly refers to the equilibrium concentration of the dissolved gas with its concentration in the header space. As our carrier gas and header space compositions are substantially different, the distinction is worth making.

$$\frac{dC_L}{dt} = K_L a (C_L - C_E) \quad (4.17)$$

Integration gives the mass transfer coefficient explicitly

$$K_L a = \frac{1}{t} \ln \left( \frac{C_L - C_E}{C_L^0 - C_E} \right) \quad (4.18)$$

$C_L^0$  is the initial concentration of the dissolved gas in the liquid. The usual technique for determining  $K_L a$  is graphical with a semi-log plot, yielding it through the slope of the supposed straight line. As traditionally helpful a concept as this semilog plot has proven, with microbubbles, the approach has been demonstrated to be inherently flawed (Bredwell and Worden 1998; Worden and Bredwell and 1998). Microbubbles have a small, finite capacity of excess gas that they carry, hence the large surface area per unit volume depletes this capacity down to the equilibrium level far more rapidly than coarse bubbles (diameter 10 mm) or fine bubbles (diameter 1–2 mm). Microbubble mass transfer is inherently transient as the excess gas concentration in the bubble phase must also be accounted for, rather than treated as a pseudosteady, infinite reservoir. In the semilog graphical approach, the slope varies with time, hence the inferred  $K_L a$  is not a constant. If an effective, time averaged  $K_L a$  is employed, it is merely a convenient comparator, rather than the theoretical  $K_L a$ , which must be determined following more precise inference (Bredwell and Worden 1998; Worden and Bredwell and 1998).

Figure 4.3 shows the microbubble generator used in these experiments, based on the fluidic oscillator approach (Zimmerman et al., 2008 and 2011 (a)). The investigation

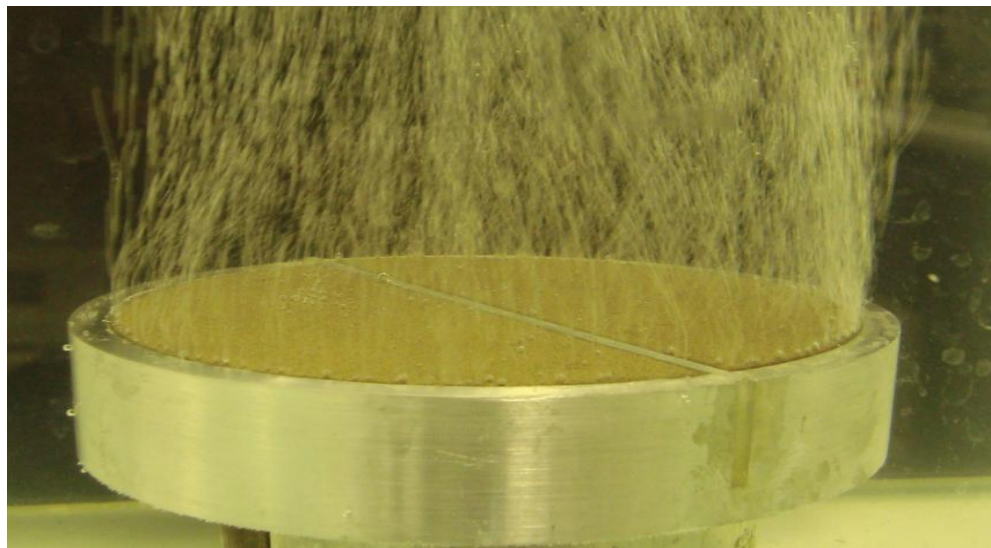


Figure 4.3: Microbubble cloud generated from a two-chamber microporous ceramic diffuser with fluidic oscillation leading to a more uniform bubble size distribution and spatially regular bubble separation.

seeks to determine the effective mass transfer coefficients for microbubbles in the near millimeter range from this diffuser in comparison with fine bubbles, for the case of dosing and stripping carbon dioxide. In this regime, the traditional semilog slope approach could be expected to be a good estimator, particularly at high volumetric flow rates and bubble phase gas holdup, where the bubble phase still has a substantial non-equilibrium excess gas.

#### 4.2.5 Bubble Analysis

This study includes analysis of bubble sizes in different diffusers (Nickel and ceramic diffuser) using water as a liquid and air as a gas with flow rate 300 ml/min. The study was achieved using a high speed camera. The reactor used in the experiments was cylindrical in shape in order to increase efficiency of mixing; however, it was difficult to measure bubble size in the cylinder because it gives an image bigger than reality. Therefore, the cylindrical reactor was replaced with a rectangular reactor. Measuring of bubble size was carried out by image analysis software, which gives the area of the bubbles with two dimensions.

Figure 4.4 shows the bubble size distribution using the nickel diffuser and air flow rate of 300 ml/min. The average bubble diameter was around 1300  $\mu\text{m}$ . It can be noticed that the bubbles diameter with range 1000-2200  $\mu\text{m}$  have higher relative frequency than other. It can be seen that about 85% of the bubbles were in the range 1000-2600  $\mu\text{m}$ , while only 15% was for bubbles that had a diameter less than 1000  $\mu\text{m}$ . This means that the majority of fine bubbles had a diameter between 1000  $\mu\text{m}$  and 2200  $\mu\text{m}$ .

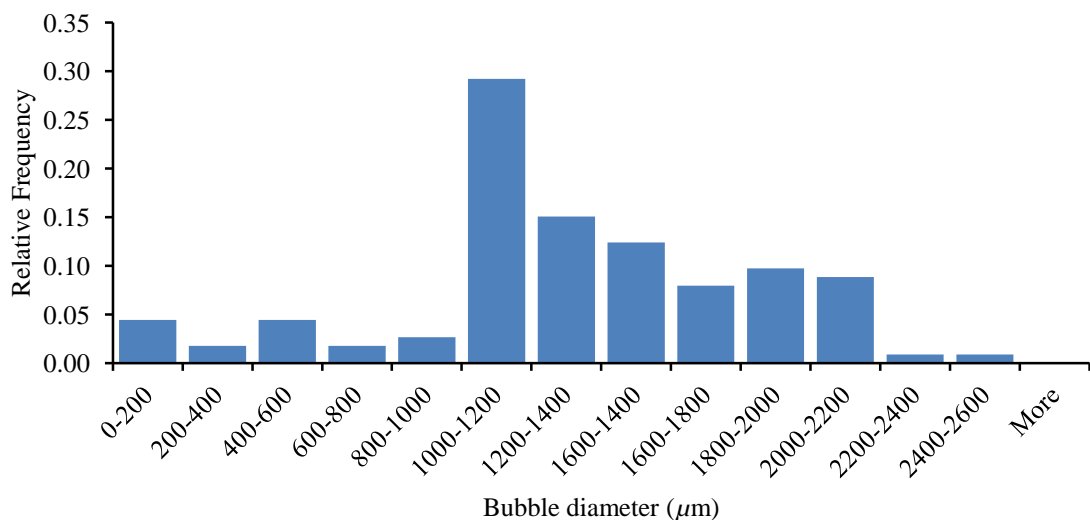


Figure 4.4: Bubble size distribution using nickel diffuser

Study of distributed size analysis for micro-bubbles was achieved using a ceramic diffuser and fluidic oscillator (Zimmerman et al, 2009) with same air flow rate (300 ml/min). Figure 4.5 shows the micro-bubbles diameter distribution. An image containing more than 130 bubbles was analysed. The average diameter of these bubbles was 550  $\mu\text{m}$ . The micro-bubbles with diameter 400-500  $\mu\text{m}$  have relative frequency of 0.37 higher than other diameter. The lowest relative frequency was in the range 0-400  $\mu\text{m}$  of bubble diameter. It can be seen that the range 400-600  $\mu\text{m}$  was more dominant than any other as shown in this figure with about 60%.

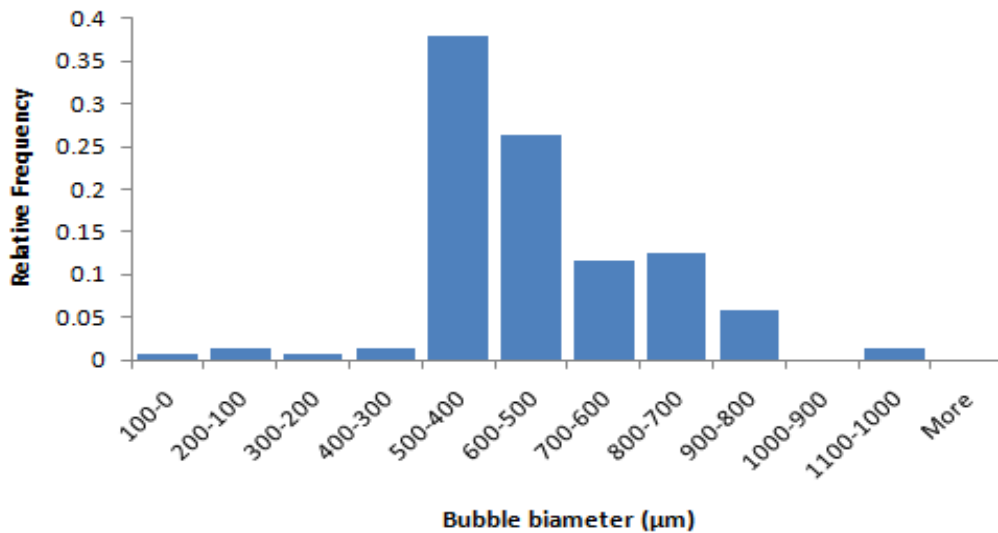


Figure 4.5: Bubble size distribution using ceramic diffuser

Finally the analysis gave a clear idea about the dominant sizes in the process and average diameter for micro-bubbles and fine bubbles using different diffusers but with the same flow rate.

#### 4.2.6 Results and Discussion

The results in current study were obtained according to the materials and methodology that has been explained in section 3.2 of chapter three. The effect of bubble size on dissolution rate of carbon dioxide was investigated through a series of tests using the relationship between dissolved carbon dioxide and pH derived earlier. Figure 4.6 shows the effect of dissolved carbon dioxide on the pH value of water.

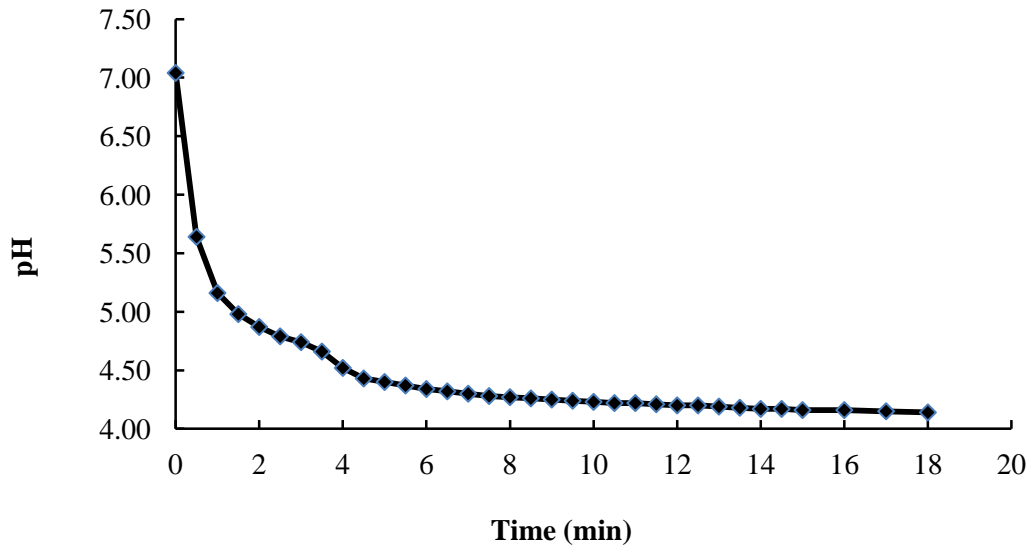


Figure 4.6: Response of pH during bubbling of carbon dioxide into water with fine bubbles (1.3 mm diameter).

It shows a rapid decline of pH value until it reaches the solubility limit. The pH of the initial water was close to 7. A time of 6 min is enough to drop the pH value from 7 to 4.5 for 8.3 L of water. Similarly, Figure 4.7 shows the response curve for stripping out fully saturated carbon dioxide in water by sparging with pure N<sub>2</sub>. It is clear by comparison that the stripping time is substantially longer than the dosing time.

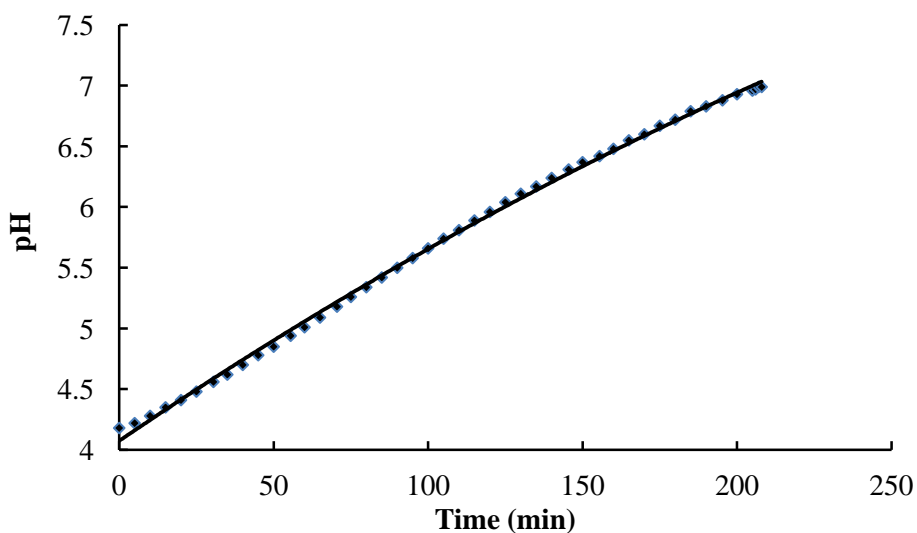


Figure 4.7: Response of pH with time during stripping of carbon dioxide by sparging with pure N<sub>2</sub> with fine bubbles (1.3 mm diameter).

This is illustrated clearly in Figure 4.8, where the concentration which combines both experiments with computed dissolved carbon dioxide concentration.

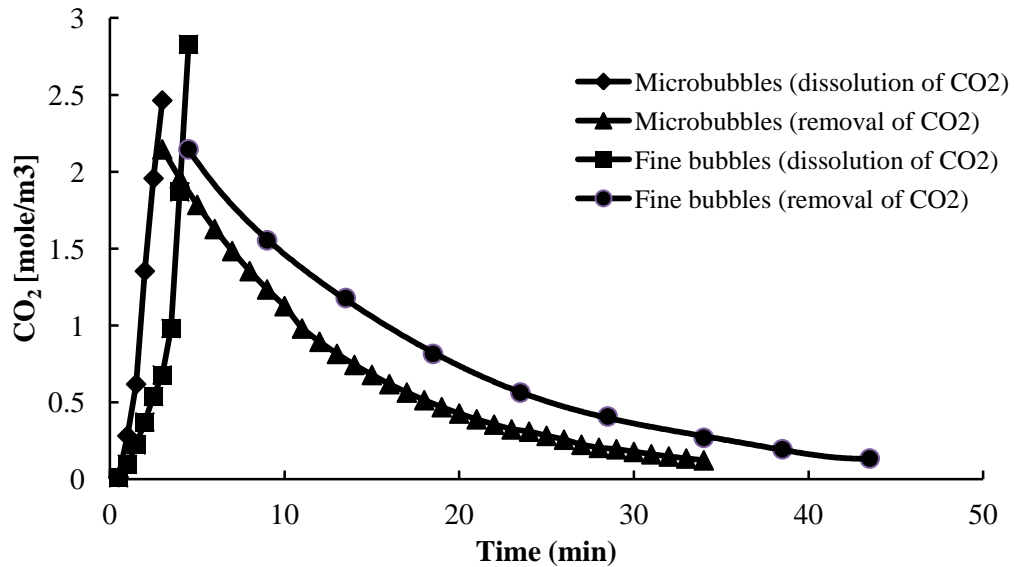


Figure 4.8: Concentration time profile of carbon dioxide in both dissolution and removal processes for fine bubbles and microbubbles.

The common assumption that it is much harder to strip dissolved carbon dioxide than dose it is borne out in this study. The behaviour of both response profiles is qualitatively the same with fine bubbles (c. 1.3 mm diameter) and the microbubbles studied here, with 550  $\mu\text{m}$  diameter.

Figure 4.9 demonstrates that the comparison achieves precisely the expected increase in mass transfer with microbubbles, or does it? The expected increase should follow equation 4.18 if thin film theory holds, which requires a reduced coordinate graph as in Figure 4.10.

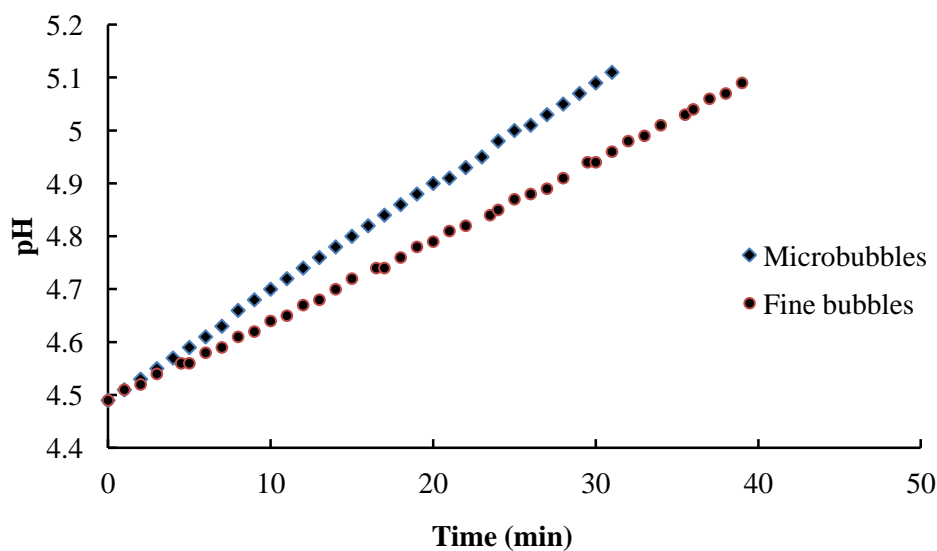


Figure 4.9: Response of pH with time during stripping of CO<sub>2</sub> by sparging with pure N<sub>2</sub> for both microbubbles (550  $\mu\text{m}$ ) and fine bubbles (1.3 mm diameter).

The best fit lines in Figure 4.10 lends confidence to the assumption that thin film theory holds with the canonical assumption of a pseudosteady reservoir in the bubble of the solute being transferred.

The average slope captures the overall behaviour of the response curve well. The canonical estimate of overall mass transfer coefficient ( $K_L a$ ) of carbon dioxide has been estimated  $0.092 \text{ min}^{-1}$  for microbubbles size of  $550 \mu\text{m}$  compared with  $0.0712 \text{ min}^{-1}$  for fine bubble sparging. It is observed that the efficiency of carbon dioxide removal has increased up about 29% by microbubble sparging compared with fine bubble sparging. This exercise was chosen to illustrate that microbubbles that are only slightly submillimeter in diameter are still well analyzed by canonical thin film theory. Worden and co-workers (1998(a) and 1998 (b)) studied substantially smaller microbubbles, and found that the mass transfer response was inherently transient.

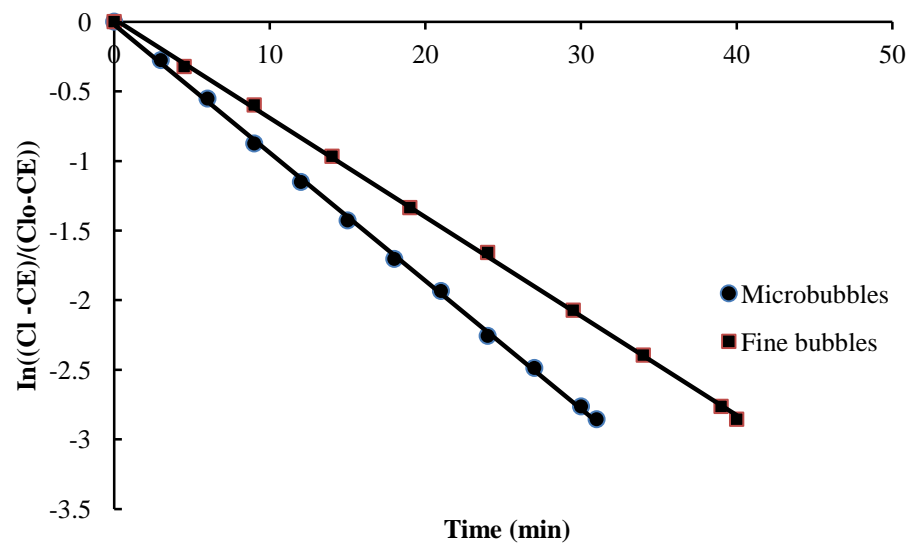


Figure 4.10: Canonical thin film theory semilog plot for determining  $K_L a$  by the slope of the supposed line.

The rationale for the transient response is that the transfer is sufficiently fast so that the internal gas concentration of carbon dioxide in the microbubble is reduced, therefore reducing the nonequilibrium driving force. Eventually, if the bubble composition is in equilibrium with the bulk liquid concentration, the driving force for mass transfer vanishes. If the system were not well mixed due to the airlift loop effect, the conclusion would be that bubbles in this size range are either too large for the increased mass

transfer rate to diminish the internal bubble carbon dioxide gas composition, or that the layer height is too low to have sufficient contact time for this to occur. However, as the airlift loop does achieve very good internal mixing, the bulk concentration is nearly uniform for dissolved carbon dioxide; hence whether the rising bubble has achieved equilibrium by diminishing the internal carbon dioxide gas composition cannot be assessed from bulk measurements. That assessment can only come from changing the liquid layer height or from computational modeling with concentration bubble phase profiles averaged horizontally only.

### **4.3. Computational Modeling of Carbon Dioxide Dissolution in a Batch Airlift Loop Mixer**

In the development of their essentially transient thin film theory, Worden and Bredwell, 1998(a) and 1998(b), developed a computational model, which is difficult to implement for spatially distributed systems. Our target system, the airlift loop bioreactor (Figure 4.1) has demonstrated some remarkable properties in the production of algal biomass (Zimmerman et al. 2011), which contributed to super exponential growth that was essentially free of O<sub>2</sub> inhibition by stripping. The suspension of algae which parades about the lighted surfaces was certainly instrumental in achieving high survivability (no observed dead algae) and regular photosynthesis. These are attributes of the airlift loop effect, which as discussed earlier provides “mixing for free.” Given that the mass transfer of carbon dioxide dissolution and stripping has been demonstrated to be intrinsically transient, the modeling of either process in an airlift loop mixer/bioreactor is necessarily transient too. There are two common modeling scenarios to consider: (i) steady state fluid dynamics where the draft tube effect mixing has been set up by a practically insoluble gas, such as N<sub>2</sub>, but where at time  $t = 0$  the gas supply is switched to the carbon dioxide rich stream; (ii) fully transient fluid dynamics, where the liquid in the vessel is initially at rest, and the carbon dioxide rich microbubble stream is introduced at time  $t = 0$ .

Scenario ii is represents the idealization of the experiments conducted in the previous section and so is the appropriate target for model development here. Scenario i is appropriate for intermediate dosing in a system in which microbubbles are regularly used for mixing and intermittently used for dosing of nutrients or stripping of product.

### 4.3.1. Chemical Kinetics Model

The kinetics of dissolution, association, and dissociation of reactants can be modeled in two different ways. It is commonly adopted that fast kinetic reactions are treated as in pseudoequilibrium. This has the effect that the resulting differential-algebraic system is very difficult to treat algorithmically. Mchedlov-Petrossyan and co-workers (2003(a), 2003(b) and 2007) have demonstrated a differential coordinate transform that reduces the differential-algebraic system arising in well-mixed or dispersed heterogeneous reactions to a differential equation system in the new coordinates, thereby removing the difficulty in efficient numerical analysis. As this transformation must be analyzed for each differential-algebraic system individually, generalization is problematic.

Cao and co-workers, 2002, developed a generic differential-algebraic solver which does not require analysis of the specific dynamics for adaptation. To our knowledge, the Petzold DAE solver (Cao et al. 2002) is only commercially available in Comsol Multiphysics, which is used in the computational modeling presented here. The alternative to the assumption of pseudoequilibrium implemented as algebraic constraints is to model the transient kinetics of the chemical reactions with the effects of both forward and reverse reactions explicitly accounting for accumulation. It follows that the system of equations is fully evolutionary-all differential and no algebraic constraints. Such evolutionary equations are treatable by ordinary numerical analysis, but, if the pseudoequilibrium approximation was justifiable, suffer from a different numerical analysis pathology-stiffness. A stiff system has a large time scale separation between slow processes of interest (mass transfer in our case) and rapid processes (dissociation reactions or acid-base chemistry, for instance). The latter processes may rapidly equilibrate, but the solution of the system dynamics is limited by the resolution of the shortest time scale process. Large time steps are simply not possible to accurately resolve in the fast time scale dynamics. Stiff systems can be treated so that the fast time scale dynamics are effectively ignored (Shampine and Gear, 1979) by stiff solvers, but this is problematic if the fast time scales dynamics manifest as fundamental changes to the slow time dynamics.

The canonical example of this is the Kapitsa pendulum, which is rapidly oscillated and the fast time scale oscillations actually stabilize the pendulum standing upside down. In this system, the fast kinetics of the reverse reactions create the rapid equilibration and hence either the differential-algebraic or stiff system pathologies inherently. Given that

it is our intention to extend the modeling work eventually to acid-alkali rapid kinetics; it is strategically ill-advised to adopt the differential-algebraic numerical analysis when the next stage of development requires resolving the transient dynamics. Whether or not the stiff system approximate methods (Shampine and Gear, 1979) provide an accurate solution in either the current dissolution model, or future rapid acid-alkali chemistry models, can only be addressed by comparison with the fully time-resolved model. Hence there is little point in starting with a stiff system numerical analysis.

Table 4.1 makes clear that the dynamics of carbonate and bicarbonate ions are practically an irrelevance with regards to the dissolution of carbon dioxide. This is evident from our experimental results (for instance Figure 4.11).

Table 4.1: Reactions modelled in dissolution, dissociation, and association reactions for CO<sub>2</sub> aqueous chemistry, at room temperature and atmospheric pressure

Chemical Reaction	Reaction rate constant	Unit	Reference
$H_2O \xrightarrow{K^f} H^+ + OH^-$	$K^f = 5.5 \times 10^{-6}$	1/s	Charterjee et al, 1983 Zhang and Houk, 2005 Garrett et al 2005.
$H^+ + OH^- \xrightarrow{K^r} H_2O$	$K^r = 3 \times 10^{10}$ $K_{eq} = 1.8 \times 10^{-16}$ $K_w = 1 \times 10^{-14}$	l/mole/sec	
$CO_2 + H_2O \xrightarrow{K^f} H_2CO_3$	$K^f = 0.043$	l/mole/sec	
$H_2CO_3 \xrightarrow{K^r} CO_2 + H_2O$	$K^r = 14.98$ $K_{eq} = 2.87 \times 10^{-3}$	1/s	Zhang Y., 2008
$H_2CO_3 \xrightarrow{K^r} HCO_3 + H^+$	$K^f = 10^{6.9}$	1/s	
$HCO_3 + H^+ \xrightarrow{K^r} H_2CO_3$	$K^r = 4.67 \times 10^{10}$ $K_{eq} = 1.7 \times 10^{-4}$	l/mole/sec	
$HCO_3 \rightleftharpoons CO_3 + H^+$	$K_{eq} = 5.62 \times 10^{-11}$		

The kinetics of this system can be studied independently of the mass transfer and mixing dynamics-essentially the continuously stirred tank reactor-which determines that the time scale for equilibration is faster than  $10^{-5}$  s, the smallest time step practically meaningful in the numerical integration of a system with macroscopic changes 6 orders

of magnitude slower, that we were prepared to simulate from the initial conditions of Table 4.2.

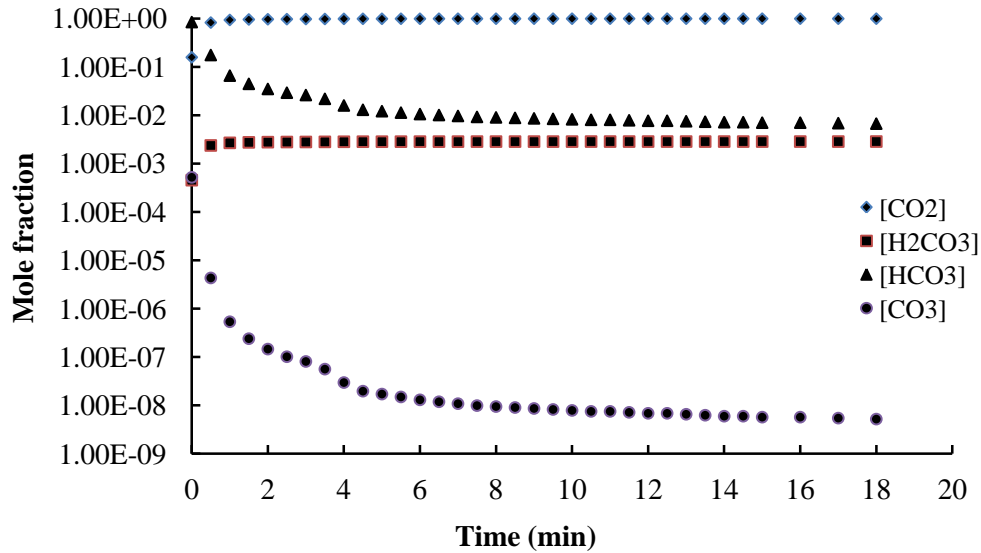


Figure 4.11: Mole fraction of ionic and dissolved species inferred from pH measurements for dissolution of carbon dioxide with fine bubbles.

The carbonate ion formation, with such a small equilibrium coefficient, could not be practically treated as anything but a differential algebraic constraint, if at all. With such a small mole fraction, it can be estimated parametrically from the other variables without being back-coupled to their dynamic changes. Including it, however, is essential to the planned application to mineralization chemistry.

### 4.3.2. Dilute Species Chemical Transport Model

The equations of mass transport and distributed reaction are well-established for dilute systems with single component Fickian diffusion. For species  $i$  with concentration  $c_i$ , the convective-diffusion-reaction mass transport equation take the classical form:

$$\frac{\partial c_i}{\partial t} + \mathbf{u} \cdot \nabla c_i = \nabla \cdot D_i \nabla c_i + R_i \quad (4.19)$$

Where  $R_i$  is the reaction rate term using the mass action kinetics of the elemental reactions with coefficients from Table 4.1. The bicarbonate dissociation term (last reaction, Table 4.1) is treated artificially with a  $K_r = 1$  and  $K_f = K_{eq}$  which will rapidly equilibrate to an insignificant carbonate concentration as indicated by the equilibrium

coefficient anyway. Table (4.2) gives the initial, uniform concentrations in the liquid for  $c_i$ . Table (4.3) catalogues the diffusion coefficients  $D_i$  and references for their values in dilute aqueous solution.

Table 4.2: Initial species conditions for the kinetics only (CSTR) and distributed system model

Species	Initial concentration (mol/m <sup>3</sup> )
CO <sub>2</sub>	0
H <sub>2</sub> O	55600
H <sub>2</sub> CO <sub>3</sub>	0
H <sup>+</sup>	1e-7
OH <sup>-</sup>	1e-7
HCO <sub>3</sub> <sup>-</sup>	0
CO <sub>3</sub> <sup>2-</sup>	0

Table 4.3: Diffusion coefficients for the six species treated in the computational model

Diffusivity Coefficient	Value	Unit	Reference
CO <sub>2</sub>	1.97e-9	m <sup>2</sup> /s	Frank et al. 1996
H <sub>2</sub> CO <sub>3</sub>	1.3e-9	m <sup>2</sup> /s	Nesic et al. 1996
HCO <sub>3</sub> <sup>-</sup>	9.23e-10	m <sup>2</sup> /s	Gupta et al. 2006
CO <sub>3</sub> <sup>2-</sup>	1.19e-9	m <sup>2</sup> /s	Gupta et al. 2006
H <sup>+</sup>	9.31e-9	m <sup>2</sup> /s	Nesic et al. 1996
OH <sup>-</sup>	5.3e-9	m <sup>2</sup> /s	Polle and Jung, 1989

### 4.3.3. Laminar Bubbly Flow Model

In two-fluid modeling, both the bulk liquid and bubble phase are treated as interpenetration continuum media, which is preferable in process modelling and applied research because of its computational convenience. In the model, constitutive equations describing the fluid stresses are treated fundamentally, with the exception of the exchange momentum terms, which assume that the drag on the bubble phase removes momentum from the bulk liquid and transfers it to the bubble phase (Crowe et al. 1989). The drag law (or slip velocity) explicitly depends on the average bubble size, presuming that the distribution of bubble sizes is a secondary and negligible effect. In the case of the microbubble clouds generated with fluidic oscillation, the nearly uniform spacing and monodispersity of the bubble size should render this an excellent approximation.

In this chapter, we have used the laminar bubbly flow interface of Comsol Multiphysics, which permits the expression of the slip velocity through the slip velocity Hadamard-Rybczynski method, which is appropriate for bubbles of all sizes, but corrects the significant error from the older Stoke's drag law for microbubbles smaller than 100  $\mu\text{m}$

(Parkinson et al. 2008). The two-fluid model for bubbly flow is appropriate for a dilute bubble phase, less than 10% by volume fraction, as it assumes that the flow field is solenoidal; that is, the density of the gas is negligible in comparison to that of the liquid, and the system's density as a whole remains constant. The other major assumption is that the two phases share the same mechanical pressure field.

Based on these assumptions, the sum of the momentum equations for the two phases gives a momentum equation for the liquid velocity, a continuity equation, and a transport equation for the volume fraction of the gas phase (Sokolichin et al. 2004). The liquid phase momentum equation is given by

$$\varphi_1 \rho_l \frac{\partial \mathbf{u}_l}{\partial t} + \varphi_1 \rho_l \mathbf{u}_l \cdot \nabla \mathbf{u}_l = -\nabla p + \nabla \cdot [\varphi_1 \mu_l \cdot \nabla \mathbf{u}_l] + \varphi_1 \rho_l \mathbf{g} + F \quad (4.20)$$

Where  $\mathbf{u}_l$  is the velocity field for the liquid phase,  $\varphi_1$  is the liquid volumetric phase fraction, and  $\rho_l$  and  $\mu_l$  are the phase density and viscosity, respectively.  $F$  represents the net forces for phase momentum exchange. Owing to the dilute bubble phase fraction, both fluids are nearly incompressible to good approximation, hence

$$\nabla \cdot \mathbf{u}_l = 0 \quad (4.21)$$

The velocity difference between the two fluids is defined as the slip velocity:

$$\mathbf{u}_{\text{slip}} = \mathbf{u}_g - \mathbf{u}_l \quad (4.22)$$

The slip velocity is computed via the drag force on the bubble phase:

$$\frac{3C_d}{4d_b} \rho_l |\mathbf{u}_{\text{slip}}| \mathbf{u}_{\text{slip}} = -\nabla P \quad (4.23)$$

Where  $C_d$  is the Hadamard drag coefficient of a bubble of diameter  $d_b$ . The model computes the solution to the field variables  $\bar{\rho}_g = \rho_g \varphi_g$ ,  $\mathbf{u}_l$ , and  $P$ , and infers the effective gas phase density from

$$\rho_g = (p + p_{\text{ref}}) \frac{M}{RT} \quad (4.24)$$

From which it is a simple matter to infer the bubble phase fraction

$$\rho_g = \frac{\bar{\rho}_g}{\varphi_g} \quad (4.25)$$

$$\varphi_1 = 1 - \varphi_g \quad (4.26)$$

to complete the description of the field variables. The laminar bubbly flow model can be extended to nondilute systems by explicitly computing the compressibility effects on the momentum equations and the continuity equation, as well as keeping track of solubility effects from mass transfer changing the phase densities.

The mass transfer rate from liquid to gas is computed using two-film theory (Bailey, J. E.; Ollis, 1986):

$$\dot{m}_{lg} = K_L a (C^* - C) M \quad (4.27)$$

Where  $\dot{m}_{lg}$  is a mass transfer rate in gas-liquid system,  $K_L a$  is the overall mass transfer coefficient and  $M$  is the molecular weight of species transferred across the interface (same as equation 4.16),  $C^*$  represents the equilibrium concentration while  $C$  represents instantaneous concentration of species transferred.

On reactor walls and draft tube, no slip BCs were used for the liquid phase while “no gas flux” BCs were used for the gas phase.

$$u_l = 0, \quad n(\phi_g u_g) = 0 \quad (4.28)$$

For the diffuser bubbling surface, no slip BCs were used for liquid with “gas flux” BCs for gas.

$$-n(\bar{\rho}_g u_g) = N_{\rho_a \phi} \quad (4.29)$$

At the top liquid surface, “gas outlet” boundary conditions were used. These BCs imply gas leaving the reactor at  $u_g$  with no other constraint at the boundary. For the liquid phase, slip boundary conditions were used.

$$u_l n = 0 \quad (4.30)$$

At the low gas flow rates used in this study, it is not clear whether the flow becomes turbulent or not. A preliminary study was carried out with turbulent flow to compute the flow field. To alleviate convergence issues at low Reynolds numbers, the model was first solved with laminar flow until sufficiently high liquid flows were reached. Then the model equations were substituted to a k-epsilon turbulent flow with last solution as an initial guess. Reynolds number calculated from the flow field hardly exceeded 2500. It should also be mentioned that visual inspection of rising microbubbles indicated a highly ordered flow. With above justification, we assumed the flow to be laminar for the rest of our study.

The mass transfer coefficients measured in our experiments were used as inputs to the computational model to account for mass transfer. The enhancement of mass transfer with microbubbles suggested by  $K_L a$  values will be reflected in carbon dioxide concentration plots later (Figures 4.19 and 4.20).

#### 4.3.4 Results and Discussion: Computational Study

One of the key features of an airlift-loop bioreactor is global mixing induced by its draft tube and bubbles rising in the aerated region. Designing such a reactor requires careful consideration of the flow patterns within the reactor to optimize mixing while fulfilling the purpose for which it is built. The reactor used in this study was designed to process sludge in future experiments; hence a dead volume exists below the diffusers. Velocity fields for the computational domain with time are shown in Figure 4.12.

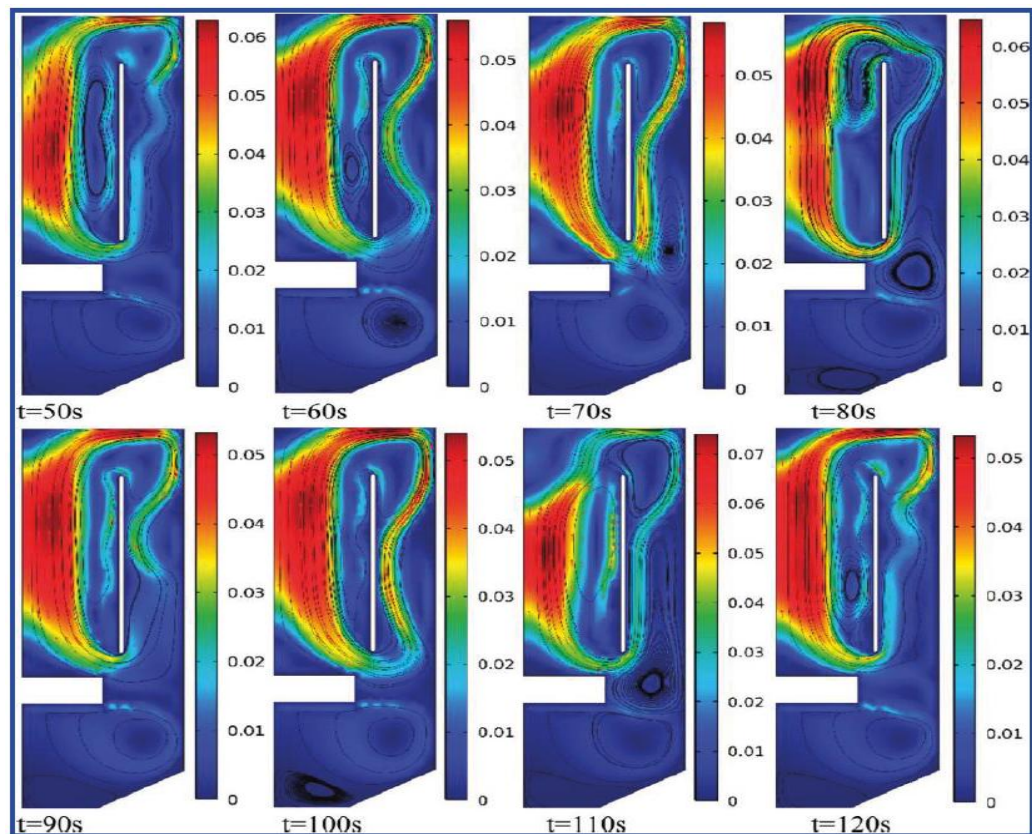


Figure 4.12: Velocity profiles in the reactor predicted by the CFD model. Velocity magnitude of the liquid phase is shown by the greyscale, while streamlines depict fluid structure. Simulation times are 50, 60, 70, 80, 90, 100, 110, and 120 s from top left. The flow structure is apparently transient, from observation of the animation, with the first and last frame practically periodically reproduced.

The computational domain was created considering axial symmetry of the reactor to reduce computer resources required to carry out the work. Maximum velocity is

observed at the center of the riser region as expected. A main liquid recirculation loop is generated by the rising bubbles around the suspended baffle promoting vertical mixing. The flow spreads at the top surface reducing the liquid velocity above the baffle, while liquid returning via the down-comer region rejoins through the gap between the baffle and the diffuser.

Vortices are created at several points within the reactor where flow turns around solid boundaries. Figure 4.13 shows a cross-sectional plot of liquid velocity across the midbaffle region. Figures 4.12 and 4.13 confirm that the main vortex is in the riser region closer to the baffle. The vortex formed on top of the baffle to the down-comer region cause the downward liquid flow to attach to the bottom half of the baffle from outside. This behaviour causes another vortex to form in the mid-downcomer region closer to the outer wall. Study of vortex positions with time suggests that this vortex moves downward into the dead space below the diffuser periodically. Lateral and vertical movement of vortices demonstrated by both Figures 4.12 and 4.13 suggest good overall mixing within the reactor.

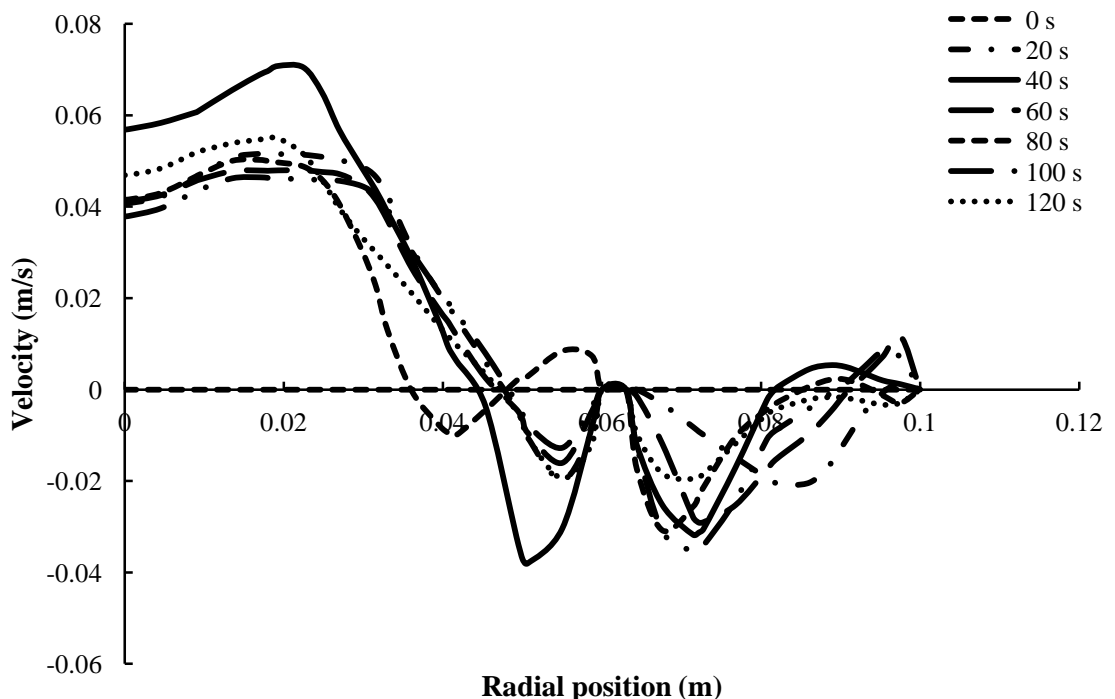


Figure 4.13: Horizontal profile of velocity across the reactor 12 cm below the water level is shown.

However, it can be clearly seen that the region below the diffuser is poorly mixed due to flow separation. In addition to enhancement of mass transfer, microbubbles cause

significantly stronger liquid recirculation compared to larger bubbles at the same flow rate. This is due to higher drag force imparted by rising bubbles on the liquid contents. Mass flux of liquid rising in the aerated region of the reactor is shown in Figure (3.14). For computations presented in this Study, a fixed gas mass flux of  $0.0012 \text{ kg m}^{-2} \text{ s}^{-1}$  was used as the gas inlet boundary condition to match our experiments. Even though microbubbles have lower rise velocities, liquid velocity reaches its average in approximately 3s with microbubbles compared to 9s for fine bubbles. According to Figure (4.14), mass flux in the riser region for the microbubble aerated case is almost twice that of the fine bubble aerated case. This not only increases mass transfer coefficients, but also helps suspension of biological matter and good mixing. This effect will be further investigated experimentally using particle image velocimetry (PIV) in a future study. One of the key objectives in modelling here is to investigate the effect of microbubbles on removal of dissolved carbon dioxide by nitrogen bubbling.

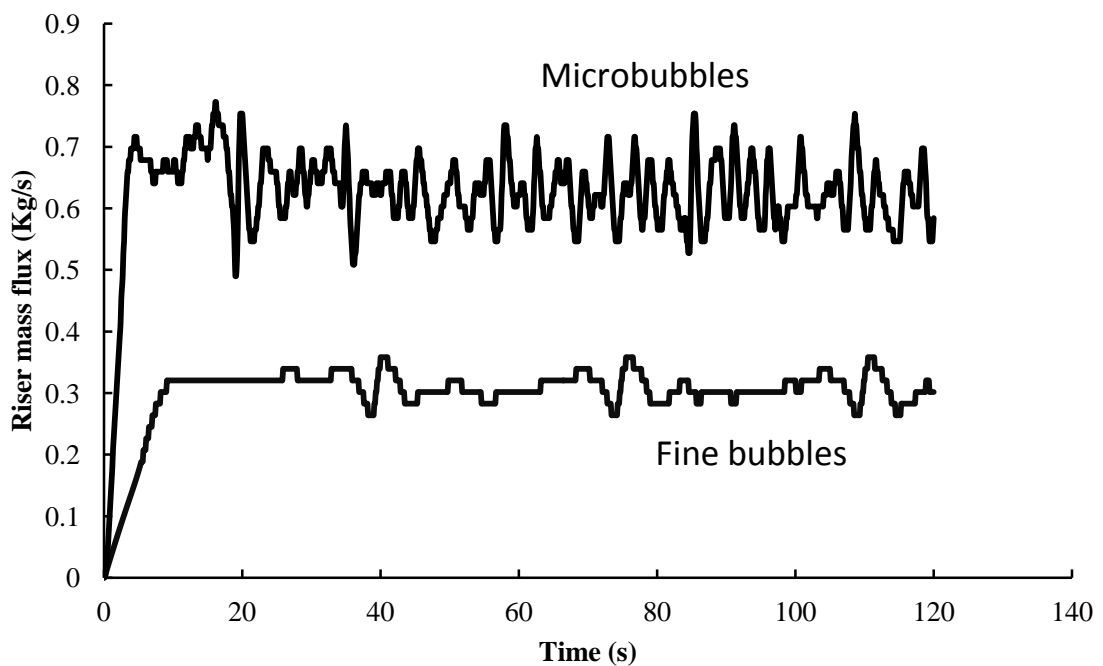


Figure 4.14 Mass flux of liquid rising in the riser region of the reactor for microbubble and fine bubble aeration

Average bubble size calculated from measured bubble size distribution was used in the model, that is, microbubbles with diameter  $550 \mu\text{m}$  and fine bubbles with diameter  $1300 \mu\text{m}$ . Since most of the carbon dioxide exists as dissolved carbon dioxide, removal rate is least affected by the chemical reactions mentioned previously. However, all reactions

were included for completeness and for future use with impurities that consume dissolved carbon dioxide to form other products. Plots of concentration of dissolved carbon dioxide within the computational domain are presented in Figure 4.15. Carbon dioxide transferred in the aerated region is carried around the top part of the reactor via the main flow recirculation loop.

Convection currents change their path due to vortices; hence mixing improves. The bottom part of the reactor below the diffuser is badly mixed and separated by a stationary vortex. Diffusion alone is far too slow to raise the carbon dioxide concentrations in the bottom part of the reactor to match that of the upper section.

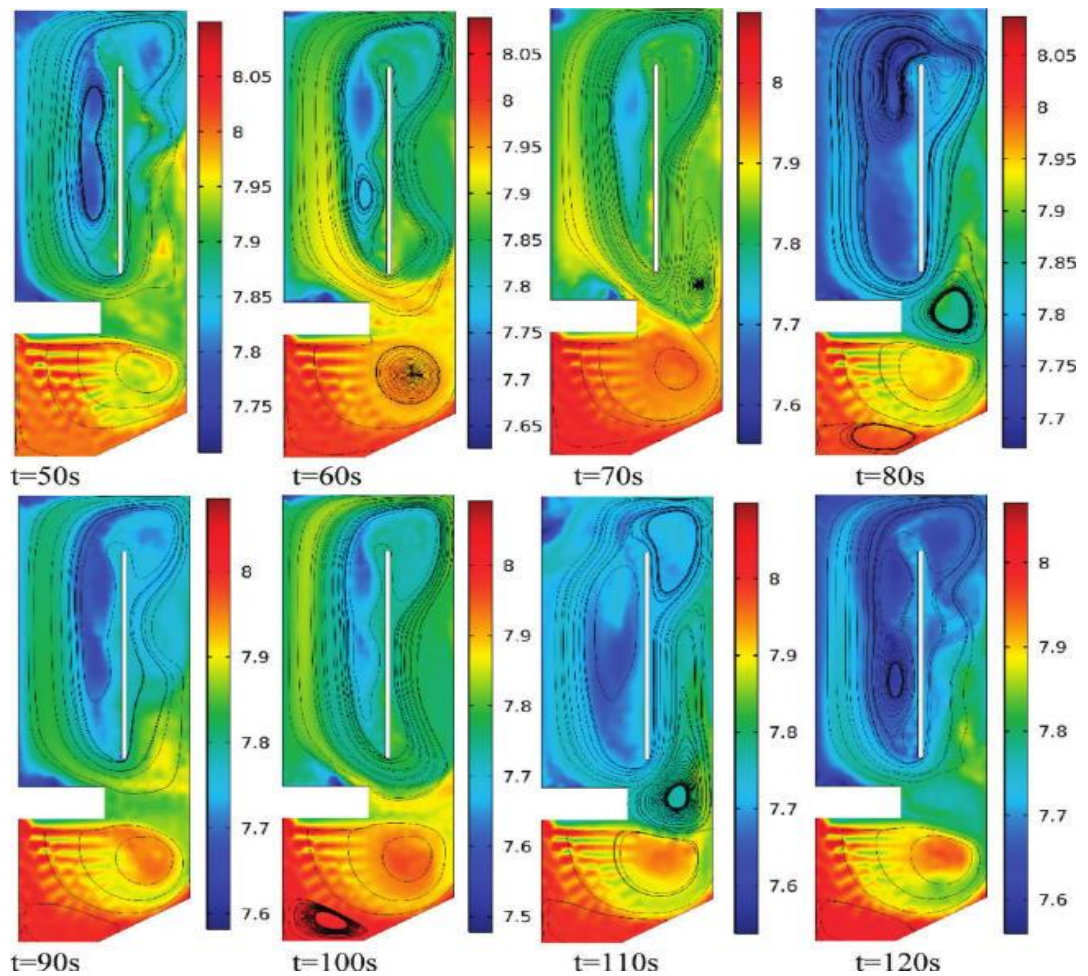


Figure 4.15: Dissolved carbon dioxide concentration in the liquid phase predicted by the CFD model. Concentration is shown by greyscale and streamlines depict flow currents. Simulation times are 50, 60, 70, 80, 90, 100, 110, and 120 s from top left.

Figures 4.16 and 4.17 show change in dissolved carbon dioxide concentration in the riser region for microbubbles and fine bubbles. The model was solved for 2 min of the

process with initial carbon dioxide concentrations at  $2\text{mol/m}^3$  and  $8\text{mol/m}^3$  for both microbubbles and fine bubbles. As demonstrated by both Figures 4.16 and 4.17, microbubbles show greater performance due to enhanced removal rate. Figure 4.17 shows a higher mass transfer rate compared to that of Figure 4.16 due to larger concentration driving force.

The removal rates predicted by the model are considerably lower compared to experimentally measured values for all cases, but within an order of magnitude. Mass transfer for the model was defined using classical thin film theory. Overall mass transfer coefficients measured in our experiments were used with interfacial areas calculated from the model to account for carbon dioxide removal. Worden and Bredwell (1998) discuss change in instantaneous mass transfer coefficient with time. Bubbles shrink as they rise due to mass transfer from gas to liquid. This will improve mass transfer coefficients as surface to volume ratio and Laplace pressure increases. However, they concluded that the average mass transfer coefficients are sufficient to define mass transfer from microbubbles. Current study, carbon dioxide is stripped from the liquid by gas so that bubbles are expected to increase in diameter.

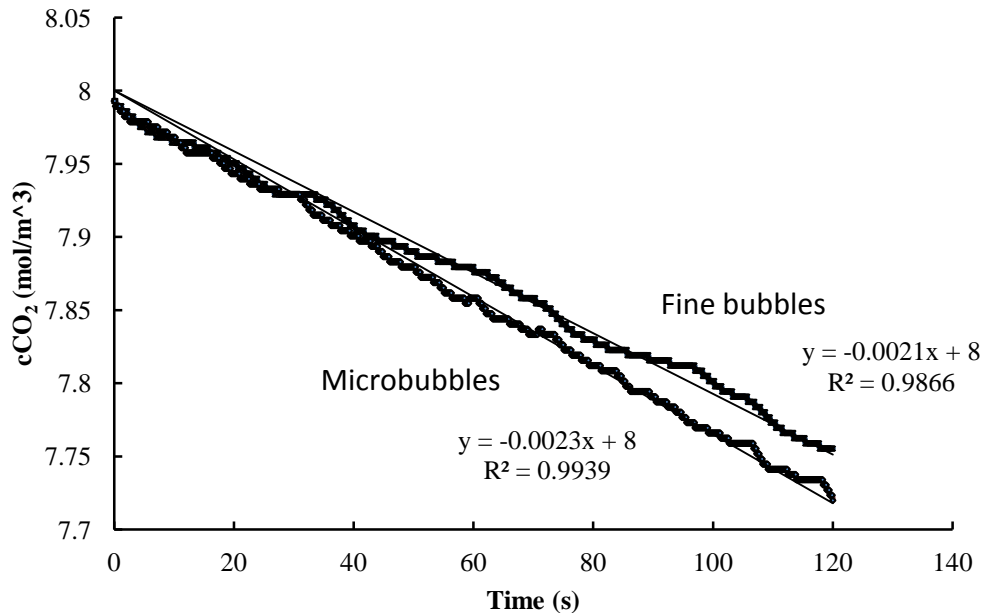


Figure 4.16: Dissolved carbon dioxide concentration in the reactor during nitrogen bubbling predicted by the computational model. Initial concentration of carbon dioxide was taken as  $8\text{mole/m}^3$ .

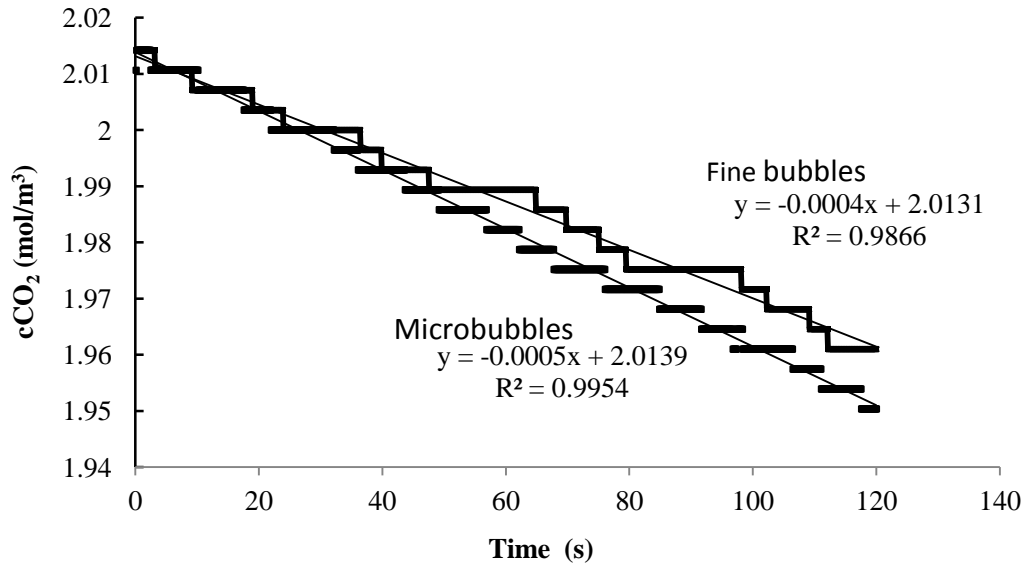


Figure 4.17: Dissolved carbon dioxide concentration in the reactor during nitrogen bubbling predicted by the computational model. Initial concentration of CO<sub>2</sub> was taken as 2 mole/m<sup>3</sup>.

In contrast to dissolution of a gas, this suggests that the instantaneous mass transfer coefficient should decrease with time. Here our assumption of suitability of the overall mass transfer coefficient is questionable as experiments deviate from model predictions, although the trends match direction. This begs the question whether one can confidently estimate the overall mass transfer coefficient for a microbubble-aerated process using conventional methods used for larger bubbles. It should be noted that there is no universally accepted model for the bursting of bubbles at the gas-liquid interface, so that the actual mass and momentum exchange could be substantially different from the idealized assumptions commonly made, leading to higher transfer and mixing rates.

Another issue that needs to be mentioned is the flow regime within the reactor. For a given reactor at certain operating conditions, some sections of the reactor may undergo turbulent flow such as the bubble riser column. The spreading and bursting of bubbles at the gas-liquid surface of the vessel is visually more rapid than their rise and much more disordered. However, other parts of the reactor may still remain in the laminar flow regime. If a turbulence model is used throughout the domain, convergence issues could be expected. In such cases, from our experience in exploring turbulence models, we recommend using different model equations in each domain to satisfy appropriate flow conditions. Earlier, it was mentioned that whether the flow investigated in this study should be treated as turbulent or not is an open question. Had it been considered, the prior turbulent mass transfer should be accounted for by adding a turbulent diffusion

coefficient. This will enhance the mass transfer within the turbulent region and could have reduced the difference. However, an initial computation carried out with a turbulent model suggests no turbulence at operating conditions used. Perhaps this is an important issue that needs to be investigated in detail in future studies, in order to accurately predict performance of the reactor. A state of the art flow visualization technique such as particle image velocimetry (PIV) can be used to validate the flow field condition where reasonable doubt exists. The smaller bubbles used in this study had a mean diameter of 550  $\mu\text{m}$ . It is likely that miniaturization shown possible in other studies (Zimmerman et al. 2011) will be well within the bubbly laminar flow regime, with the potential exception of the to surface-spreading dynamics.

#### 4.4 Summary

Carbon dioxide is one of the most common gases produced from biological processes. Removal of carbon dioxide from these processes can influence the direction of biological reactions as well as the pH of the medium, which affects bacterial metabolism. Kinetics of carbon dioxide transfer mechanisms are investigated by sparging with conventional fine bubbles and microbubbles. The estimate of the concentrations of CO<sub>2(aq)</sub>, H<sub>2</sub>CO<sub>3</sub>, HCO<sub>3</sub><sup>-</sup>, and CO<sub>3</sub><sup>2-</sup> from pH measurement in an airlift loop sparged mixer is derived. The canonical estimate of overall mass transfer coefficient of carbon dioxide has been estimated as 0.092 min<sup>-1</sup> for a microbubble size of 550 $\mu\text{m}$  compared with 0.0712 min<sup>-1</sup> for a fine bubble (mean bubble size of 1.3 mm) sparging. It is observed that the efficiency of carbon dioxide removal has increased up to 29% by microbubble sparging compared with fine bubble sparging. Laminar bubbly flow modeling of the airlift loop configuration correctly predicts the trend of the change in overall mass transfer in both gas stripping with nitrogen and gas scrubbing for carbon dioxide exchange, while demonstrating the expected separated flow structure. The models indicate that the macroscale flow structure is transient and pseudoperiodic. This latter feature should be tested by flow visualization, as preferential frequencies in the flow can be exploited for enhanced mixing.



CHEMICAL & BIOLOGICAL ENGINEERING

## Chapter Five

# Gaslift bioreactor for biological applications with microbubble mediated transport processes

### *Design and Simulation*

## Chapter Five

### Gaslift bioreactor for biological applications with microbubble mediated transport processes

#### *Design and Simulation*

#### 5.1 Introduction

In spite of the accelerated development of bioreactors due to their widespread use, there are still difficulties in maintaining stability and rates of bioprocesses. It is believed that the most important causes of that failure have been poor construction and design, leading to inadequate mixing, which may jeopardize the stability and performance of the process (Karim et al., 2005; Monteith and Stephenson, 1981; Karim et al., 2003)

Mixing in fermentation processes is required to prevent thermal stratification, maintain uniformity of the pH, increase the intimate contact between the feed and microbial culture, and prevent fouling and foaming. The importance of mixing in bioreactor design has encouraged numerous studies for many bioprocesses, including those producing biogas by anaerobic digestion (Stroot et al., 2001; Stafford, 1982; Bello-Mendoza and Sharratt, 1998).

Bello-Mendoza and Sharratt (1998), concluded that the insufficient mixing can cause a remarkable decrease in both the efficiency of the fermentation process as well as the amount of biogas it produces. More importantly, efficient mixing can speed up reaction rates and therefore reduce the hydraulic retention times required (i.e. reduce the size of the reactor) or increase the throughput of medium (Monteith and Stephenson, 1981).

In bio-hydrogen production processes, for example, the mixing factor plays an important role according to Lay (2000 and 2001). This author reported that the hydrogen produced from anaerobic fermentation of microcrystalline cellulose increased with increasing the agitation speed. Equally, the characteristic of good mixing in bio-hydrogen processing results in decreasing the mass transfer resistance (Majizat et al. 1997). Therefore, the mixing process in bioreactors is an important and critical factor in determining the efficiency of fermentation process and the nature of design which plays an active role in providing a suitable environment for micro-organisms.

Traditional mixing using stirred tanks may give better biogas yields but, when the process energy requirement is weighed against the extra energy obtained, these processes become economically unviable. Therefore, the reduction of the energy required for mixing is one the most challenging targets that is faced in large-scale bioenergy production.

The present study proposes the use of an airlift bioreactor as an alternative to stirred tanks for bioprocess applications as can be seen in Figure 5.1. The airlift (gaslift) reactor (ALR) has been used in several industrial applications requiring gas-liquid contacting. (Chisti 1989, Mudde and Van 2001).

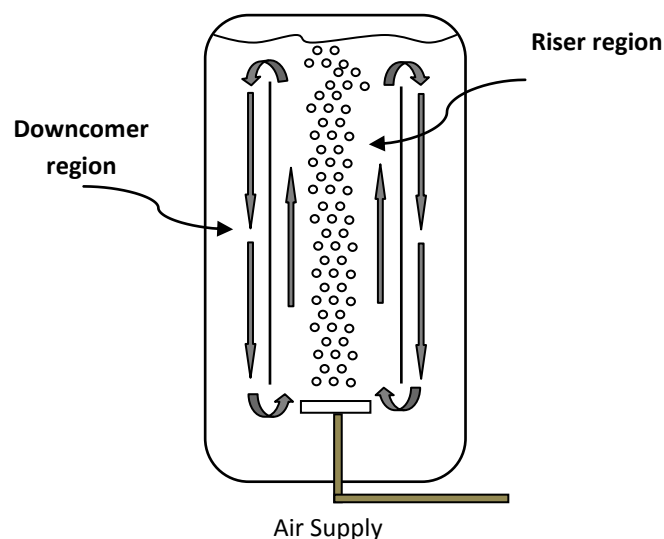


Figure 5.1: Schematic of airlift bioreactor with internal recirculation

In addition to good mixing, ALRs have long times for gas-liquid contacting and do not cause shear damage to cells. This has seen their widespread use in various biological processes, for example: biomass from yeast, vinegar, bacteria, etc. These advantages can be considerably further improved by equipping the ALRs with a fluidic oscillator

for generating micro-bubbles which, compared to traditional stirred tanks, can dramatically increase the interfacial area between gas and liquid phases.

Traditionally, enhancement of mass and heat transfer rates in gas-liquid interface have always been accomplished by increasing the interfacial area between gas and liquid phases. Due to their high maintenance cost and energy requirements, use of traditional methods (e.g. stirred tanks) to achieve certain preset goals is not economically convincing. However, this scenario could be changed if microbubbles systems are used in chemical and biochemical processes. These systems would highly make improvements of mass flux by increasing surface-area-to volume rates of a bubble.

In spite of the successive developments of microbubble generation systems, the energy requirements are still reasonably high. Zimmerman et al. (2009, 2011(a) and 2011(b)) have developed a novel aeration system by fluidic oscillation, which is capable of producing gas bubbles with micron size to achieve enhanced heat and mass transfer rates. As well as, increased interfacial area, microbubbles offer hydrodynamic stabilisation, longer residence times and an increased mixing efficiency. The fluidic oscillation method has low energy demands compared to other methods for microbubble generation.

Microbubble generation by fluidic oscillator offers many benefits including low cost, reliability and robustness. This technology can provide a range of bubble diameters depending on the type of application and diffuser used. In the present study, the type of diffuser used is made of ceramic and its form resembles a tablet, which is divided into two parts. Each part of the diffuser has a diameter of 5 cm and is separated completely from the other part. It is equipped with two entries to enter the gas

The gas from the main supply terminal into the oscillator randomly stays attached to one of the two channels due to the Coanda effect. This creates a pressure difference in the feedback loop and, as a result, the gas from the port on the non-flowing side (higher pressure) flows back to the lower pressure port where the current flow is currently passing. The gas, pushed out from the low pressure port, then hits the main passing flow and switches it to the opposite channel. This cycle then repeats periodically to give oscillatory jet switching between the flow channels. The oscillation frequency can be easily adjusted by changing the feedback loop length in order to create bubbles of the required size when the outputs are fed to separate diffusers. Al-Mashhadani et al. (2012)

used this technology for stripping carbon dioxide. They reported that the efficiency of CO<sub>2</sub> stripping was about 29% more than that for fine bubble sparging.

## 5.2 Airlift Bioreactor Design and Simulation

The geometry of bioreactor is influenced by the complexity of the biological medium. This is generally a multiphase solution consisting of cells and nutrients in solid, liquid and gas forms. A fundamental understanding of bioreactor flow mixing patterns helps to provide optimal conditions for growth and product formation when assisted by reliable control systems for pH and temperature monitoring. There are many possible shape options of the bioreactor configuration, which depend on several parameters (e.g. efficiency of mixing, cost etc). Cylindrical is a conventional German design and egg-shaped configurations have been widely used in the world, whereas rectangular cross-section reactors have more limited uses due to poorer mixing efficiency (Metcalf & Eddy 2003).

An actual cylindrical bioreactor with airlift gas injection was modelled in the current simulation study (Figure 5.2). The diameter of the bioreactor to draught tube diameter ratio ( $D/d$ ) is 0.7 and the angle of the conical bottom is 25°. The total volume of the reactor is 15 litres with a working volume of 8-9 litres. The remaining volume of the bioreactor is used as headspace volume, which is necessary to condense the vapour water and return it to the medium as shown in the Figure 5.2.

The biological medium in a working bioreactor is typically thick, opaque slurry containing organic materials, solids, bacteria and dispersed gas bubbles. It is difficult to visibly see the efficiency in the mixing process even when using high-speed cameras. Computer simulation provides a powerful means for optimising bioreactor design for two reasons. Firstly, for a specific bioreactor configuration such as that described above, it enables the internal flow patterns to be mapped to a level of precision that is beyond experimental techniques. Secondly, it allows the effect of key design decisions on overall bioreactor performance to be rapidly evaluated. Computational Fluid Dynamics (CFD) software is increasingly being deployed to simulate, trouble-shoot and design bioreactors.

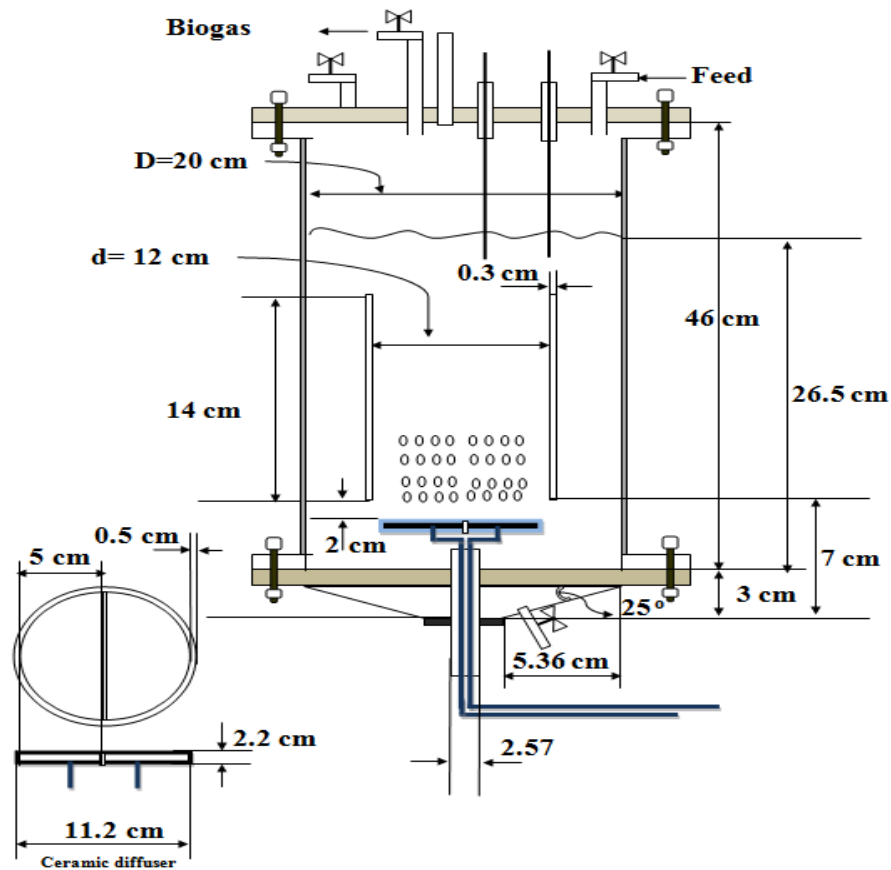


Figure 5.2: Dimensions of airlift bioreactor used in this study.

Previous work on anaerobic digestion is the progenitor of this more general work on the simulation of airlift bioreactors presented here. Other researchers have used simulation to contribute to the development and design of the bioreactors. These authors include, Vesvikar and Al-dahhan,(2005); Wu and Chen, (2008); Meroney and Clorado, 2009;Wu 2009 and 2010; Terashima et al. 2009; OEY et al. 2001 and Šimčík et al. 2011; Becker et al. 1994; Calvo 1989; Calvo and Leton 1991; Moraveji et al. 2011. CFD has been used in two ways: firstly to improve the performance of the mixing regime in the reactor and, secondly, to investigate the effect of an existing design on the efficiency of bioprocess. Meroney and Clorado (2009) studied the impact of changing dimensions of the mixing parts on the efficiency of mixing in the digester. In a different study, Wu (2009) has used many different types of mixing methods in order to identify the effect of each of these on the performance of the bioprocess. Wu and Chen (2008); Karim et al. 2007; Vesvikar and Aldahhan (2005) have developed a design of a mixing system and have tested all the variables that would lead to a higher efficiency of the developed system in the anaerobic digester using CFD software. Huang et al. (2010) studied the hydrodynamic and local mass transfer in the airlift bioreactor. The authors mentioned

that the mass transfer rate in the riser region is higher than any other region of the reactor.

In the current study, COMSOL Multiphysics software (Version 4.1) was used, which is considered as the best programme choice as an efficient way to evaluate and description the flow dynamic in gaslift bioreactor. The gas holdup and liquid velocity are investigated in the present study as a main flow dynamic parameter (Calvo et al. 1991). In addition, the simulation study was carried out at pre-determined conditions and structures.

### 5.3 Flow Modelling of the Airlift Bioreactor

A simulation process of the airlift bioreactor carried out using COMSOL Multiphysics software (Version 4.1). The airlift bioreactor configuration that was used in the simulation is illustrated in Figure 5.2, while the properties of the process are presented in Table (5.1).

Table 5.1: The properties of flow modelling

- Range of microbubble diameter between 40-1000  $\mu\text{m}$
- Low gas concentration
- Low flow rate (300 ml/min)
- Liquid phase is water
- Gas phase is air
- The temperature is 298.15 K, the pressure is 1 atm.

A laminar bubbly flow model interface was used for modelling of the two-fluid flow regimes (e.g. mixture from gas bubbles and liquid). Thus, the momentum transport equation is given by:

$$\phi_1 \rho_l \frac{\partial u_l}{\partial t} + \phi_1 \rho_l u_l \cdot \nabla u_l = -\nabla P + \nabla \cdot [\phi_1 \eta_l (\nabla u_l + \nabla u_l^T)] + \phi_1 \rho_l g \quad (5.1)$$

Where  $\phi_1$  is liquid volume fraction ( $\text{m}^3/\text{m}^3$ ),  $\rho_l$  is density of liquid,  $u_l$  the velocity of liquid phase (m/s),  $t$  is time (sec),  $P$  is pressure (Pa),  $\eta_l$  is dynamic viscosity of liquid phase (Pa.s) and  $g$  the gravity ( $\text{m/s}^2$ ).

For low gas concentration, the liquid holdups coefficient ( $\phi_1$ ) is about one. Therefore, the change of  $\phi_1$  can be neglected in the following equation.

$$\frac{\partial \phi_l}{\partial t} + \nabla \cdot (\phi_l u_l) = 0 \quad (5.2)$$

$$\nabla \cdot u_l = 0 \quad (5.3)$$

The equation of gas phase is illustrated as follows:

$$\frac{\partial \rho_g \phi_g}{\partial t} + \nabla \cdot (\phi_g \rho_g u_g) = -m_{gl} \quad (5.4)$$

Where  $\rho_g$  is the density of gas phase ( $\text{kg}/\text{m}^3$ ), gas volume fraction ( $\text{m}^3/\text{m}^3$ ),  $u_g$  is velocity of gas and  $-m_{gl}$  the mass transfer rate ( $\text{kg}/\text{m}^3 \cdot \text{s}$ ).

As the approximation of the present paper, there is no mass transfer between gas and liquid phases. Thus the  $m_{gl} = 0$ . Therefore, the continuity equation can be arranged for two phases (e.g. gas and liquid) but without mass-transfer terms as follows:

$$\frac{\partial \rho_g \phi_g}{\partial t} + \nabla \cdot (\phi_g \rho_g u_g) = 0 \quad (5.5)$$

The ideal gas law was used to calculate the density of gas ( $\rho_g$ ):

$$\rho_g = \frac{P M_w}{RT} \quad (5.6)$$

Where  $M_w$  is the molecular weight of the gas bubble,  $R$  is the ideal gas constant ( $8.314 \text{ J}/(\text{mol} \cdot \text{K})$ ) and  $T$  the temperature of gas ( $\text{K}$ ).

The gas volume fraction is estimated by the following equation:

$$\phi_g = 1 - \phi_l \quad (5.7)$$

The gas velocity can be determined as  $u_g = u_l + u_{slip}$ , since  $u_{slip}$  is relative velocity between two-phases fluid (gas and liquid).

Pressure-drag balance, obtained from slip model, was used to calculate the  $u_{slip}$ . The assumption of this model suggests that there is momentum balance state between viscous drag and pressure forces on the gas microbubble:

$$\frac{3C_d}{4d_b} \rho_l |u_{slip}| u_{slip} = -\nabla P \quad (5.8)$$

Where  $C_d$  is the viscous drag coefficient (dimensionless),  $d_b$  is bubble diameter (m). Owing that the microbubbles diameter used in the simulation are equal or less than  $1000 \mu\text{m}$ , the Hadamard-Rybczynski drag law was used, and hence:

$$C_d = \frac{16}{Re_b} \quad (5.9)$$

Where:

$$Re_b = \frac{d_b \rho_l |u_{slip}|}{\eta_l} \quad (5.10)$$

Where  $Re_b$  is Reynolds number

On the draft tube and internal airlift bioreactor walls, no slip ( $u = 0$ ) was used in boundary conditions (BCs) for liquid phase, whilst no gas flux values were used for the gas bubble phase, hence the values of  $u_l$  and  $n(u_g \phi_g)$  equal to zero. In the other hand, the ‘‘Gas outlet’’ and the slip ( $n \cdot u = 0$ ) BCs were used at the top of liquid phase for both liquid phase and gas phase, respectively. On the top of the diffuser, no slip boundary conditions were used for liquid phase and the ‘‘gas flux’’ boundary conditions for the gas phase.

## 5.4 Results and Discussion of Simulation Study

The distribution of gas volume fraction and the liquid velocity streamlines at different bubble diameters (40, 100, 200, 400, 600, 800, and  $1000 \mu\text{m}$ ) are presented in Figure 5.3. The simulation time required for each run to achieve steady state increased with decreasing bubble size as can be seen in Figure 5.3. The  $40 \mu\text{m}$  bubble simulation had reached a steady state in around 900 seconds but we found the  $20 \mu\text{m}$  bubble simulation did not reach a steady state after by this time. The current study concludes that the  $20 \mu\text{m}$  bubble simulation requires a significantly longer time and therefore much more computational effort in order to converge to a steady state.

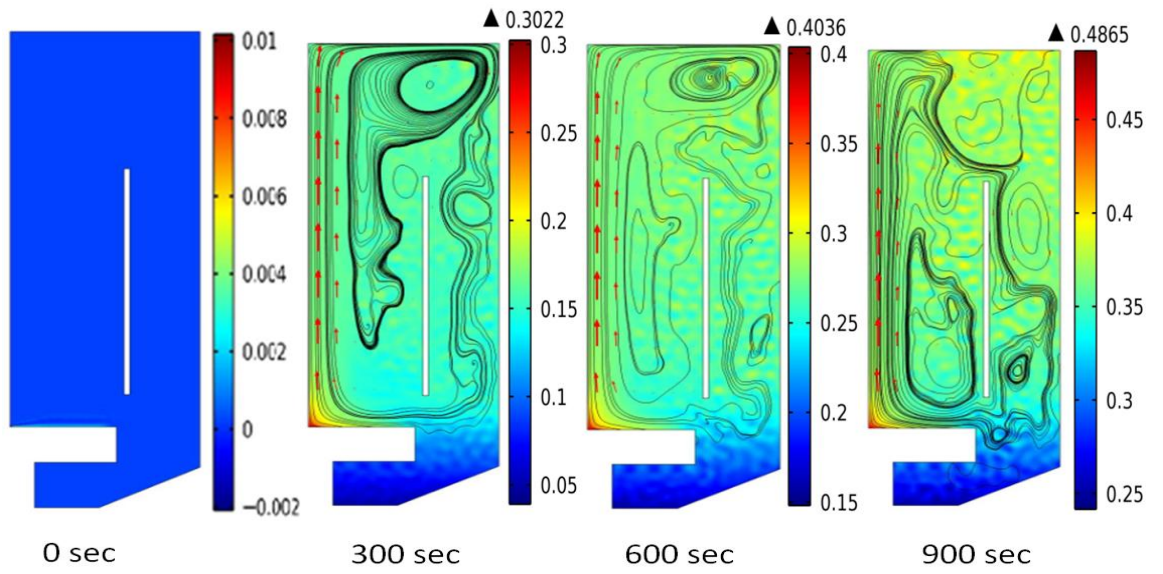
It can be observed in Figure 5.3 that gas bubbles are not present in the downcomer for bubble sizes of  $200 \mu\text{m}$  or greater (i.e. the volume gas fraction is zero in this region of the reactor). However, in simulations using bubble diameters of  $40 \mu\text{m}$  and  $100 \mu\text{m}$ , there is recirculation of gas bubbles in the downcomer in which the steady state volume gas fractions are 0.12 and 0.01 respectively (Figure 5.4). For bubbles exceeding  $200 \mu\text{m}$ , therefore, both mass and heat transfer are confined to the riser region, because the

downcomer region, which is equivalent to more than 60% of overall working volume of the reactor is free of gas bubbles. The liquid circulation is unable to overcome the higher buoyancy of bigger bubbles so they make no further circulations.

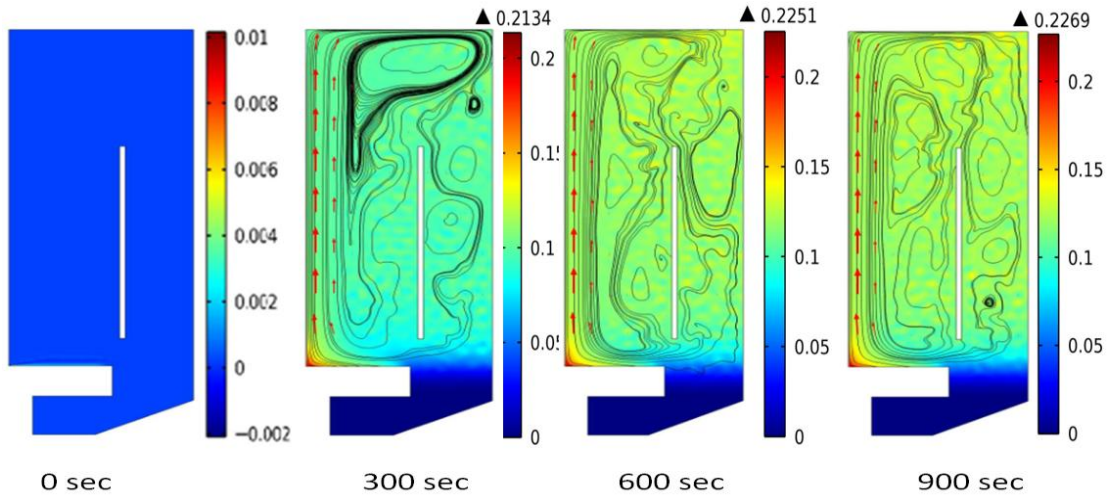
However, as just discussed, this situation is different for bubbles that are  $100\ \mu\text{m}$  or smaller. For example, for a bubble diameter of  $40\ \mu\text{m}$ , the volume gas fraction of 0.12 is extremely high compared to other experimental work in similar airlift reactors using larger bubble sizes such as results reported by Rengel et al. 2012. These authors give a maximum downcomer volume fraction of around 0.045 but to achieve this they require a superficial gas velocity of 0.047 m/s which is two orders of magnitude greater than that used in this work (0.00044 m/s). This gives an indication of the huge benefits in mass transfer performance that microbubbles can achieve. To put it another way, a volume gas fraction of 0.12 corresponds to an enormous high interfacial area of  $18,000\ \text{m}^2\ \text{per}\ \text{m}^3$  which is around three orders of magnitude greater than experimental values reported for typical bubble columns using standard bubble sizes of a few millimetres (Maceiras et al. 2010). In addition Calvo (1989) mentioned that the gas hold up in the riser region increases with increasing the flow rate of gas. Thus big amount of gas are lost leading to make this process inefficient economically. But, the present study demonstrates that the gas fraction in both two regions of reactor (riser region and downcomer region) can be achieved, but with much lower gas inflow, if the microbubble technology is used in the sparging system.

It should also be noted that presence of bubbles in the downcomer region for the smaller bubble sizes allows significant mass transfer to occur in this region. Furthermore, the higher rates of gas recirculation give longer gas residence times and so, along with the higher interfacial area, provide even further benefits for gas-liquid mass transfer. Experimentally, we have observed the presence of micro-bubbles generated by fluidic oscillation in the downcomer, and the disappearance of these bubbles when the oscillator is turned off (increasing bubble size).

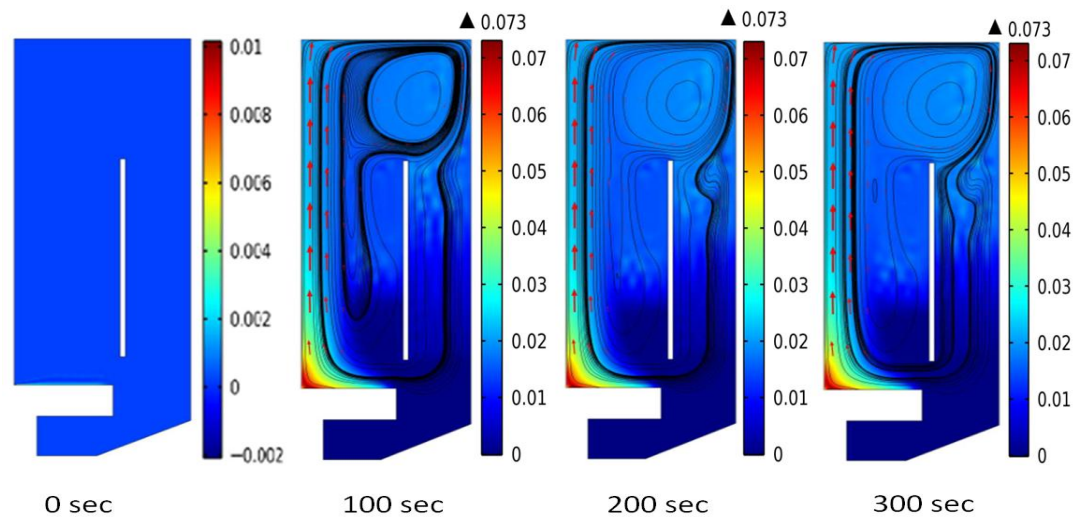
Microbubble prevents coalescence, however, some surfactants and salts also oppose coalescence (Ribeiro and Lage 2004; Francis and Pashley, 2009), so that this model is appropriate when coalescence is suppressed.



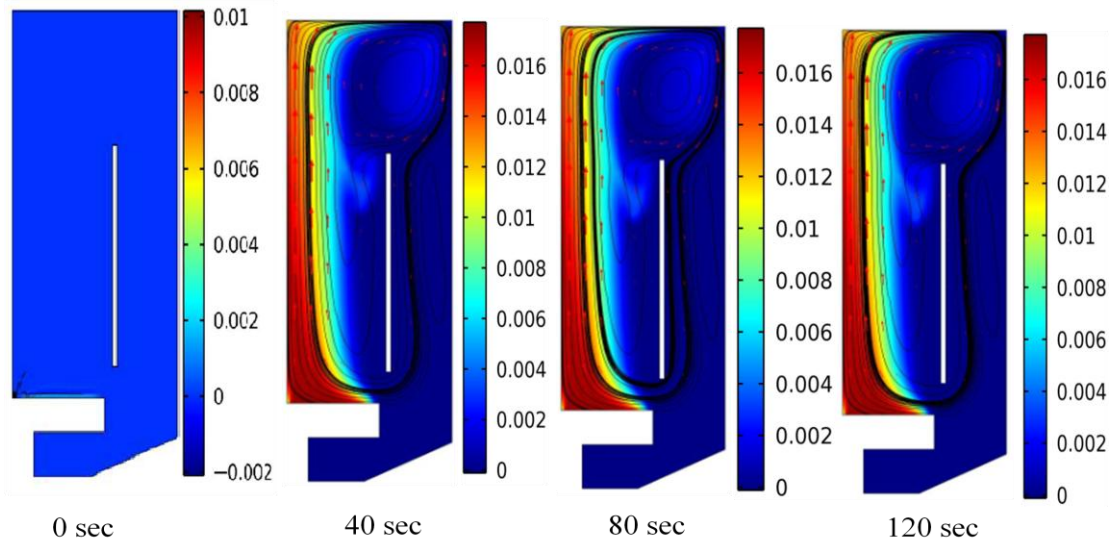
(a)



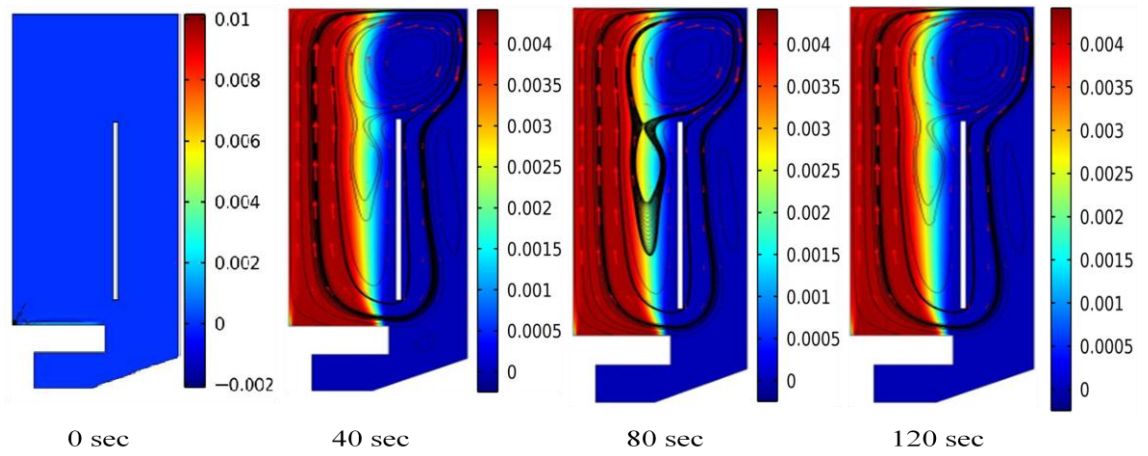
(b)



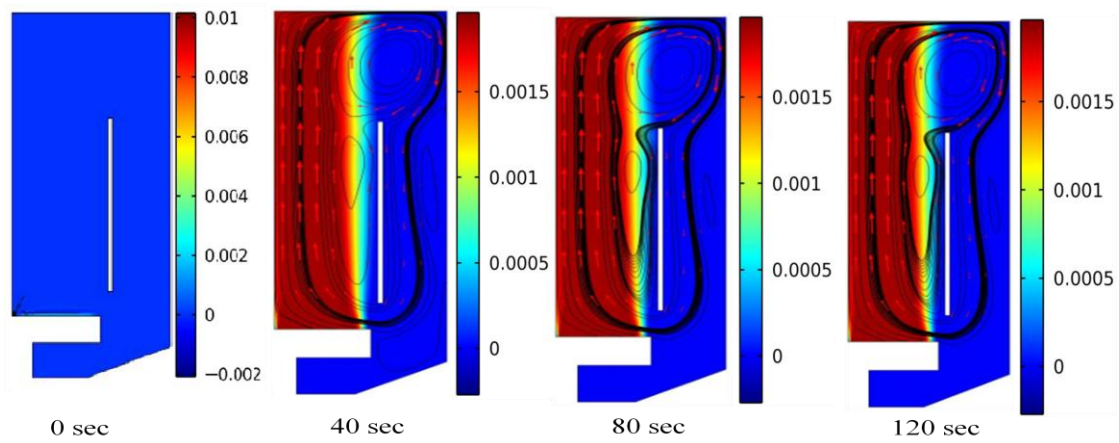
(c)



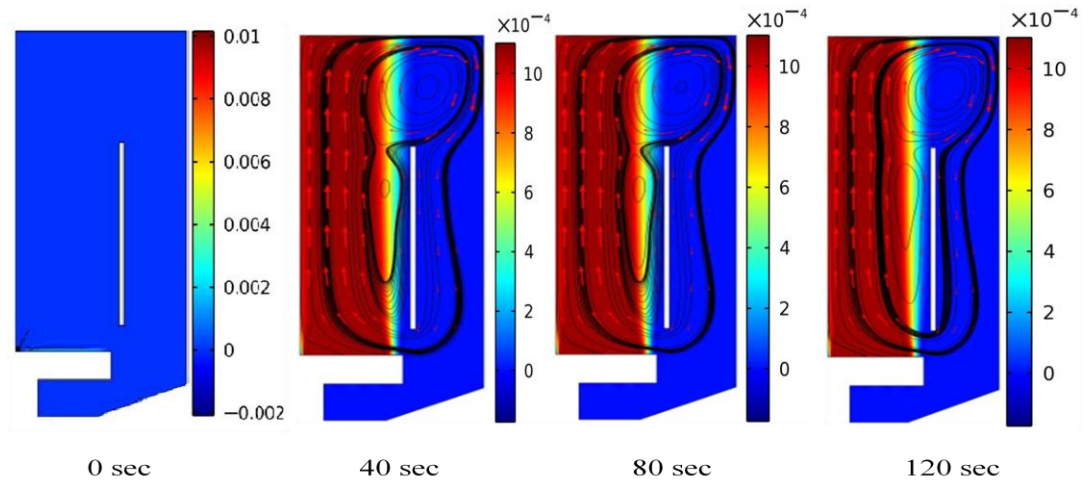
(d)



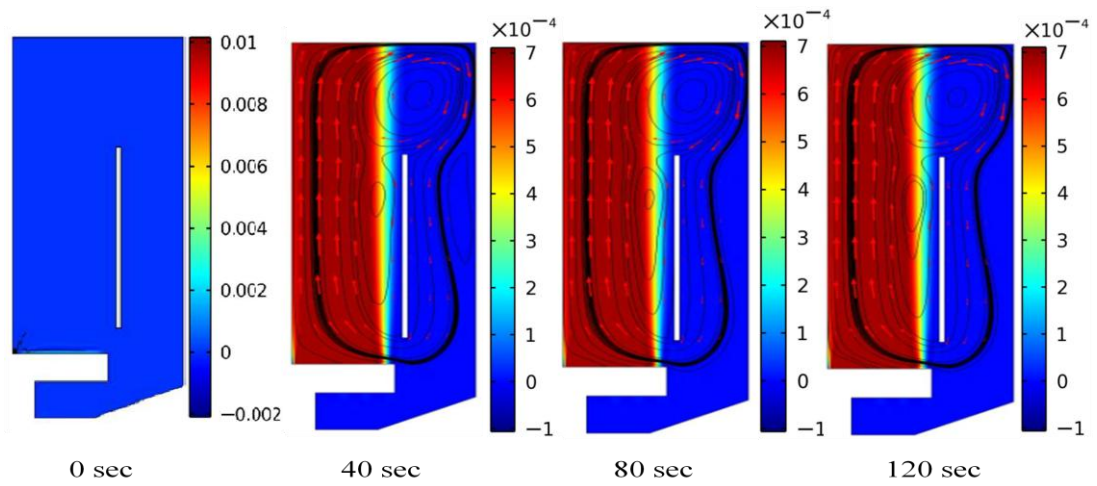
(e)



(f)



(g)



(h)

Figure 5.3: Snapshots of gas concentration at different bubble diameter after 120 sec a) bubble diameter  $20 \mu\text{m}$ , (b) bubble diameter  $40 \mu\text{m}$ , (c) bubble diameter  $100 \mu\text{m}$ , (d) bubble diameter  $200 \mu\text{m}$ , (e) bubble diameter  $400 \mu\text{m}$ , (f) bubble diameter  $600 \mu\text{m}$ , (g) bubble diameter  $800 \mu\text{m}$ , (h) bubble diameter  $1000 \mu\text{m}$ .

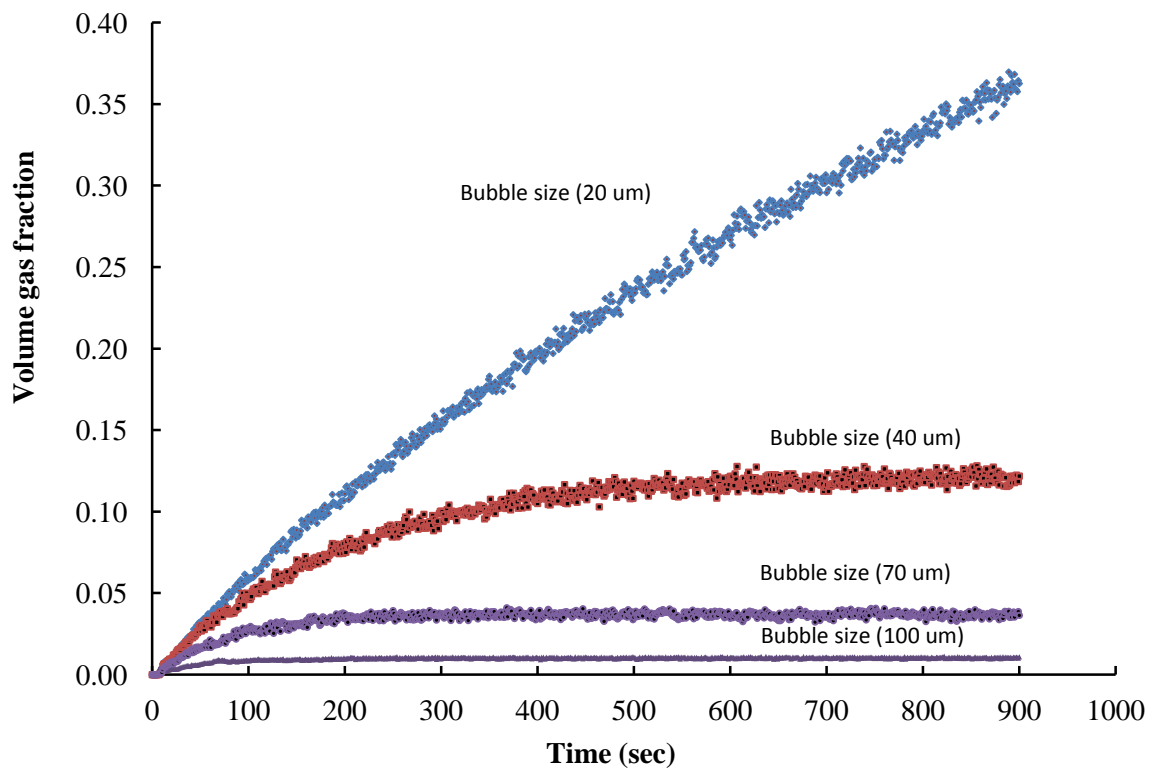


Figure 5.4: Volume gas fraction in cross section downcomer at different bubble diameter (20, 40, 100 $\mu$ m) after steady state.

## 5.5 Liquid and Gas Velocity Profile

The goals of the mixing system in biological processes include prevention of the formation of thermal stratification, maintaining uniformity of the pH, increase of contact between feed and microbial culture, and preventing fouling and foaming. As described earlier, some of biological media are viscous liquids, of high density, and contain solids, grits etc, thus, mixing of these materials thoroughly in order to achieve the desired objectives requires a great effort and energy. In fact, using a bubbling system for mixing of such media is inefficient at certain flow rates. Owing to generation of foams at the top of the culture surface, increase induced gas flow rate is become necessary, thus, the whole bioprocess would be uneconomical. Changing this scenario is possible, if micro-bubbles technique is being used in this process, because, the rising velocity of gas bubbles dependent on the pressure drag-coefficient and bubble diameter. For example, decrease of bubble diameter causes decreasing in the values of Reynolds number, and then pressure drag-coefficient increases based on Equation 5.10.

Consequently, rise in velocity of the microbubbles would decrease the drag coefficient according to (Equation 5.9).

Figure 5.5 shows, for different bubble sizes, the gas velocity profiles across the radius of the riser zone at a level of 0.12 m from the bottom of the reactor. Figure 5.6 shows the centreline gas velocities in the Y (vertical) direction in the riser zone. The corresponding the liquid velocity profiles are shown in Figure 5.7 and Figure 5.8. The simulation data shows that at this low gas flow rate (300 ml/min), the gas velocity decreases with decreasing bubble size, as would be expected, due to the increased drag force (Figure 5.5 and 5.6). A more surprising finding is that liquid velocity increases with decreasing bubble size for bubbles larger than 200  $\mu\text{m}$ .

But Figure 5.8 shows also that the liquid velocity decreases when the bubble diameters decrease less than 100  $\mu\text{m}$ . Indeed, when the sparging started, the liquid velocity for 40  $\mu\text{m}$  bubbles was larger than liquid velocity for 100  $\mu\text{m}$  bubbles. But this behaviour changed, since the liquid velocity for 40  $\mu\text{m}$  bubbles decreases with time to become less than its velocity when diameter of bubble is 100  $\mu\text{m}$  by 25%. It can be also noticed that this unexpected decrease in liquid velocity in riser region (for 40  $\mu\text{m}$  bubbles) has occurred when the gas concentration increased in downcomer region, as can be seen in Figure 5.9. Hence, these results indicates that the presence of high concentration of microbubbles in downcomer region obstruct the recirculation of the liquid around the draft tube in the bioreactor due to increasing buoyancy force in that area (downcomer region).

The simulations show a fivefold increase in centreline liquid velocity for 100  $\mu\text{m}$  bubbles as compared to 1000  $\mu\text{m}$  bubbles for the same gas flow rates. Micro-bubbles, therefore, are able to move the liquid quite rapidly upwards even at low gas flow rates. The fact that micro-bubbles can provide strong liquid circulation at very low gas flow rates shows that they could give a very big reduction in the energy required to provide adequate mixing in bioreactors.

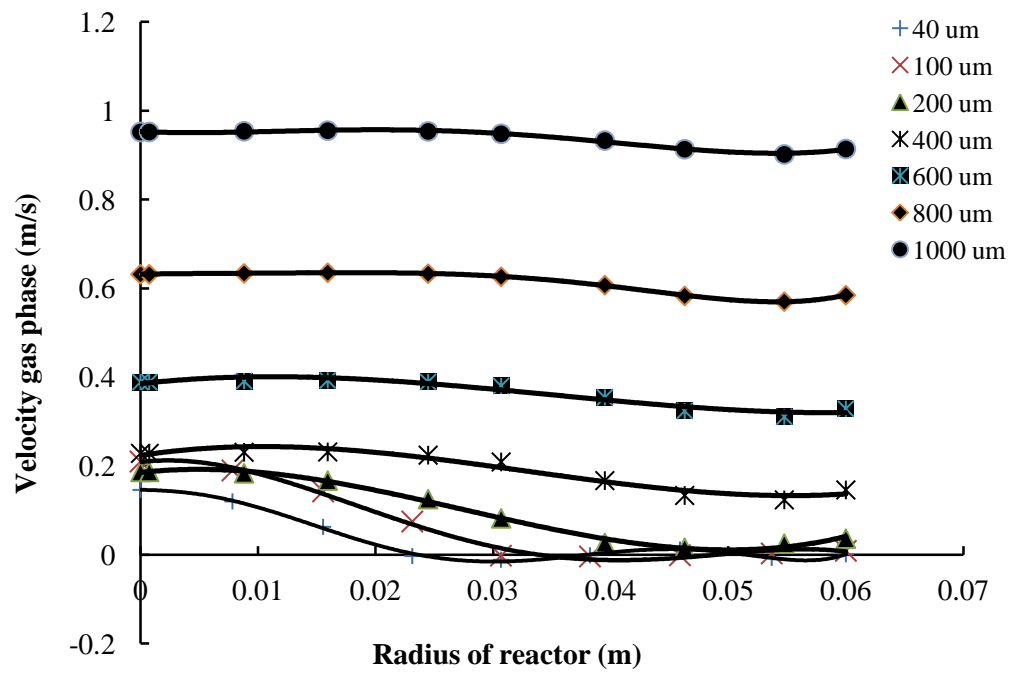


Figure 5.5: Velocity gas profile in cross-section riser zone after steady state at different gas bubble diameter (40,100, 200, 400, 600, 800, 1000  $\mu\text{m}$ ) after steady state.

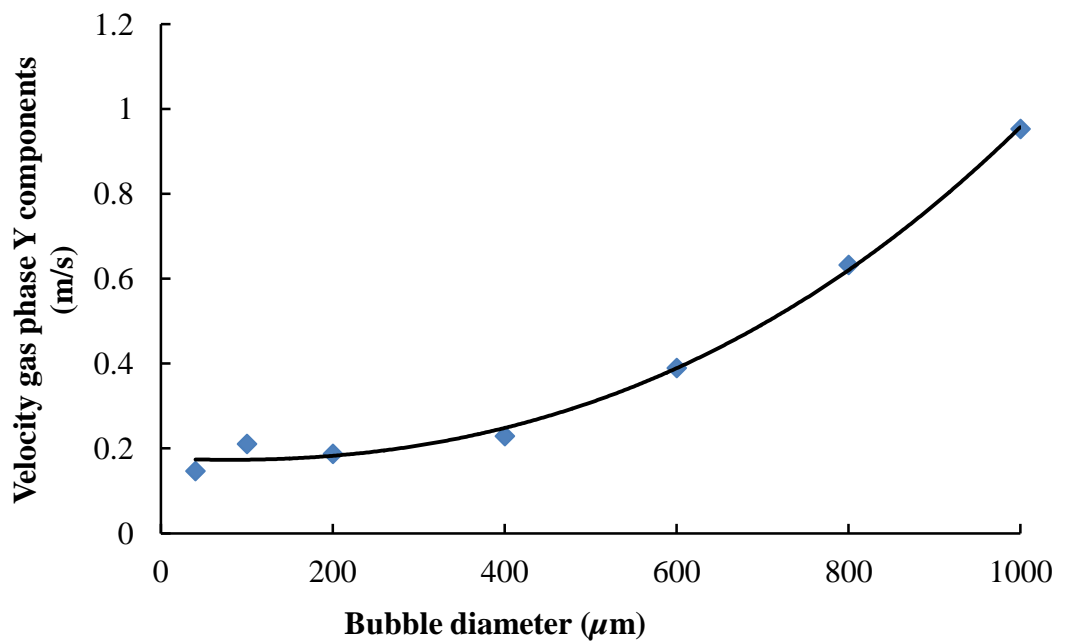


Figure 5.6: Velocity profile in certain point riser zone after steady state.

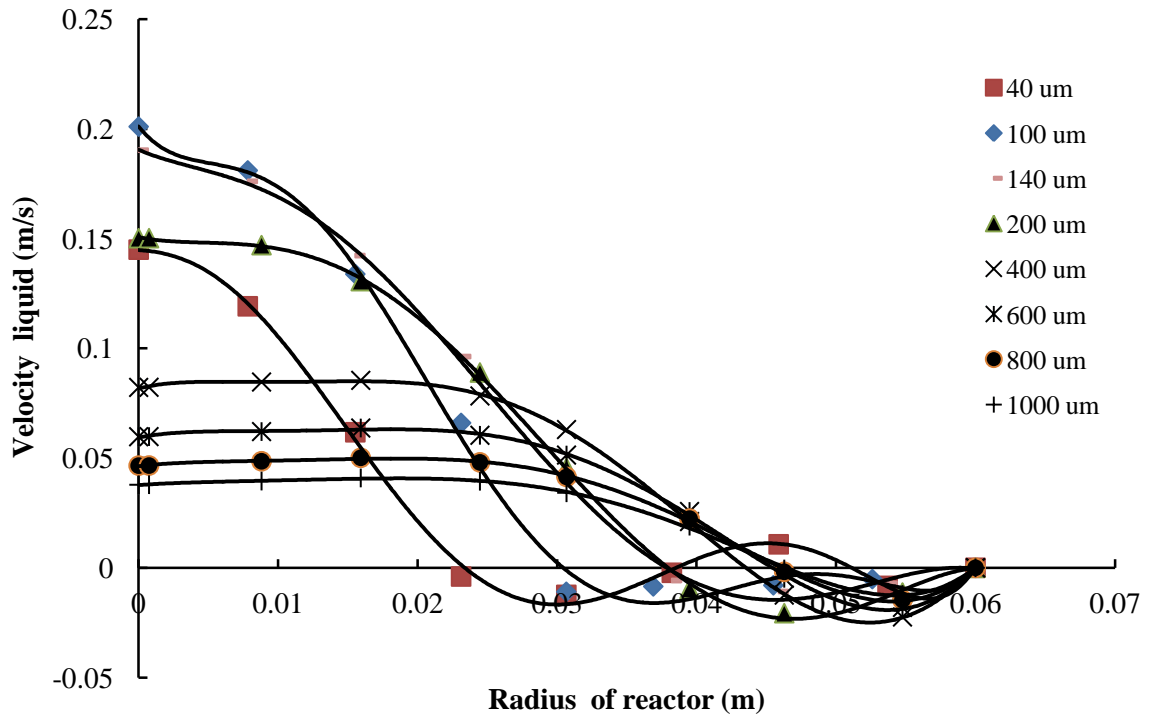


Figure 5.7: Velocity liquid profile in cross-section riser zone after steady state at different gas bubble diameter (40, 100, 140, 200, 400, 600, 800, 1000  $\mu\text{m}$ ) after steady state.

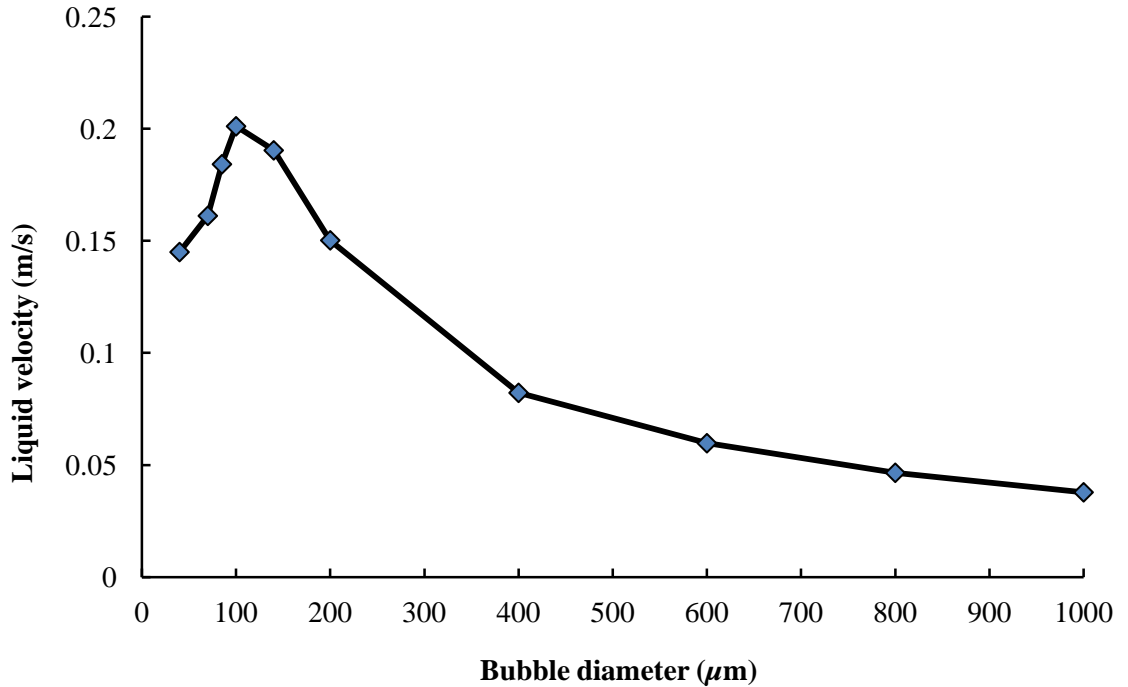


Figure 5.8: Velocity profile in certain point in riser zone after steady state.

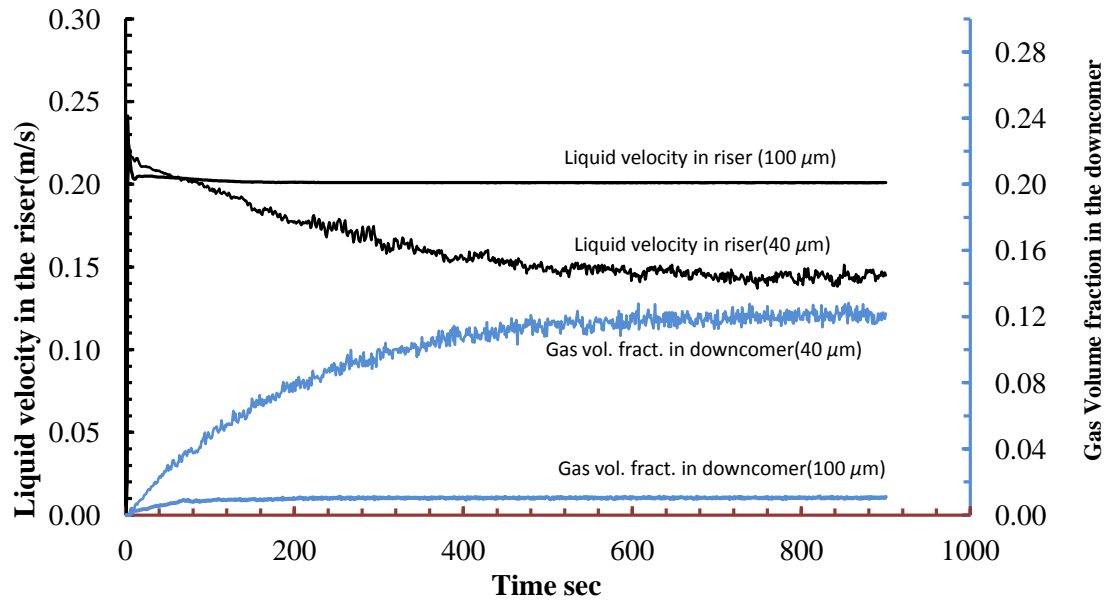


Figure 5.9: Velocity of liquid phase in riser region and gas volume fraction in downcomer region for  $40 \mu\text{m}$  and  $100 \mu\text{m}$  bubble diameter after steady state. It can be seen that the velocity of liquid in left side of chart, while gas velocity in right side of the chart.

## 5.6 Penetration of the Microbubbles

The penetration depth of micro-bubbles into the downcomer zone was also investigated in the present study. The depth of penetration influences the rate of heat and mass transfer in the reactor since it effects the overall residence time of gas bubbles in the reactor and also the total interfacial area. The simulation data shows that the depth of penetration of the microbubbles increases with decreasing bubble size. Figure 5.10 presents the gas volume fraction profiled in the downcomer region for various bubble diameters ( $40$ ,  $70$ ,  $85$ ,  $100$  and  $140 \mu\text{m}$ ). The distribution of gas in the reactor is shown in Figure 5.11. The position of the gas diffuser in the reactor is an important design factor in this context. The gaslift bioreactor was simulated with four different locations of gas sparger. The ratio of height of gas sparger to height of gaslift bioreactor ( $h_d/H$ ) was varied from  $0.17$  to  $0.37$ . Figure 5.12 and Figure 5.13 show that with similar bubbles diameter (i.e.  $40 \mu\text{m}$ ), the deeper penetration could be achieved at lower  $h_d/H$  ratio.

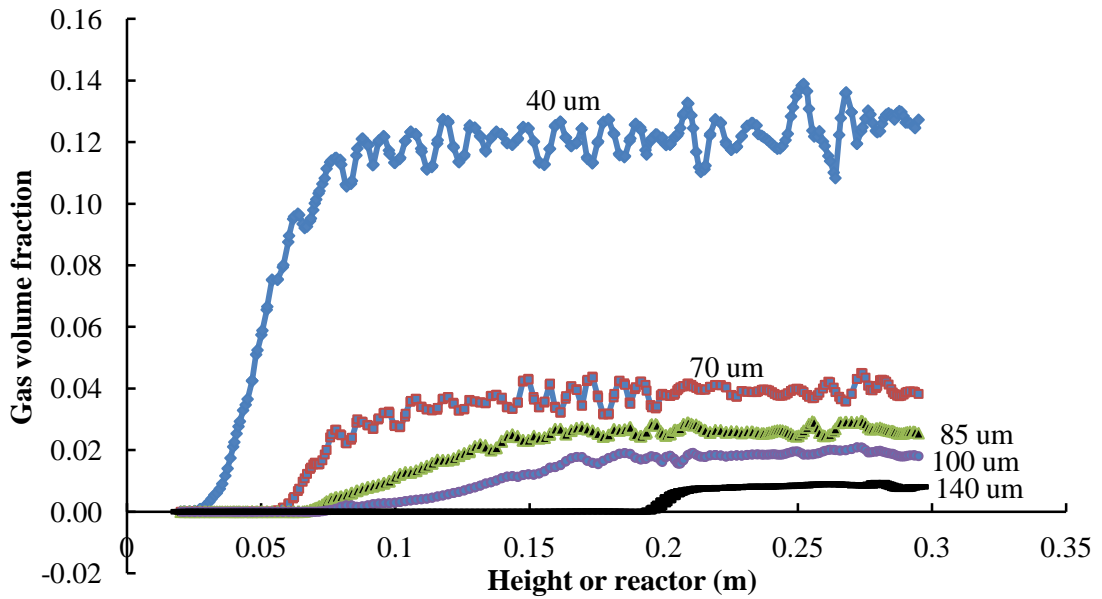


Figure 5.10: Gas volume fraction versus height above bottom of reactor in the downcomer for (40, 70, 85, 100, 140  $\mu\text{m}$ ) after steady state. Note that the diffuser position for these simulations is 0.05 m above the bottom of the reactor

The settling velocity of soot, dust, heavy metals and suspended matter, which affect on the fermentation efficiency and block the porous of diffuser, has been one of the important parameter that should be taken into consideration when designing the bioreactor. Therefore, the  $h_d/H$  ratio of 0.17 has been found as the best position to mount diffusers in airlift digester.

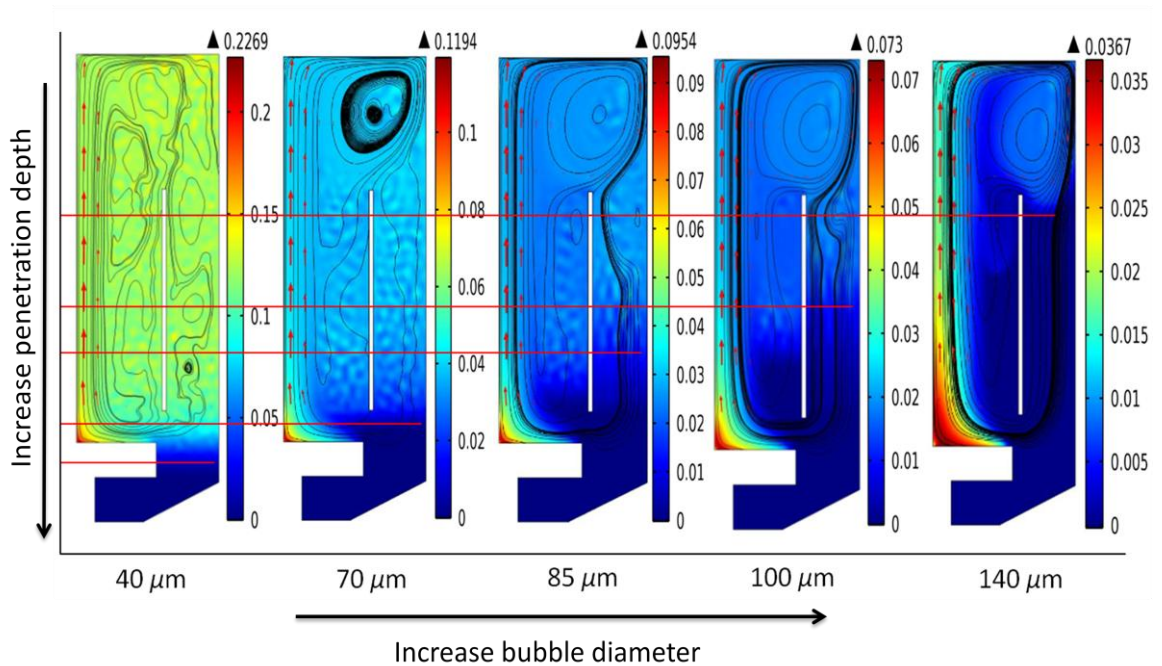


Figure 5.11: Steady state distributions of gas concentration in the reactor for different bubbles sizes (40, 70, 85, 100 and 140 $\mu\text{m}$ ).

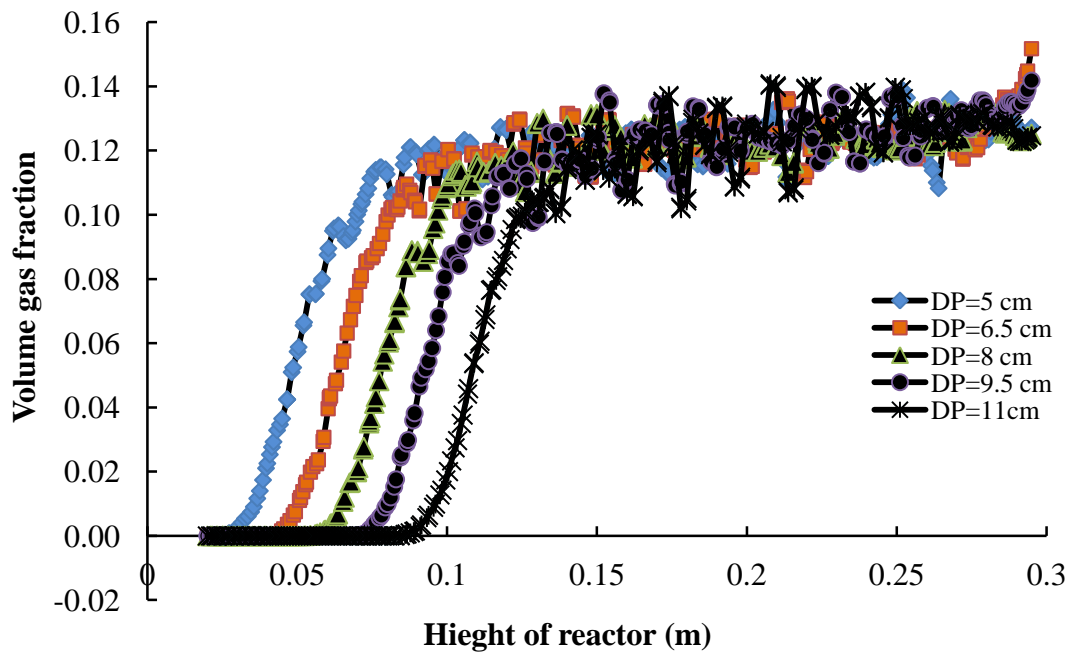


Figure 5.12: Volume gas fraction with height of airlift digester at different diffuser position (5, 6.5, 8,9.5,11 cm) at  $40 \mu\text{m}$  and after steady state.

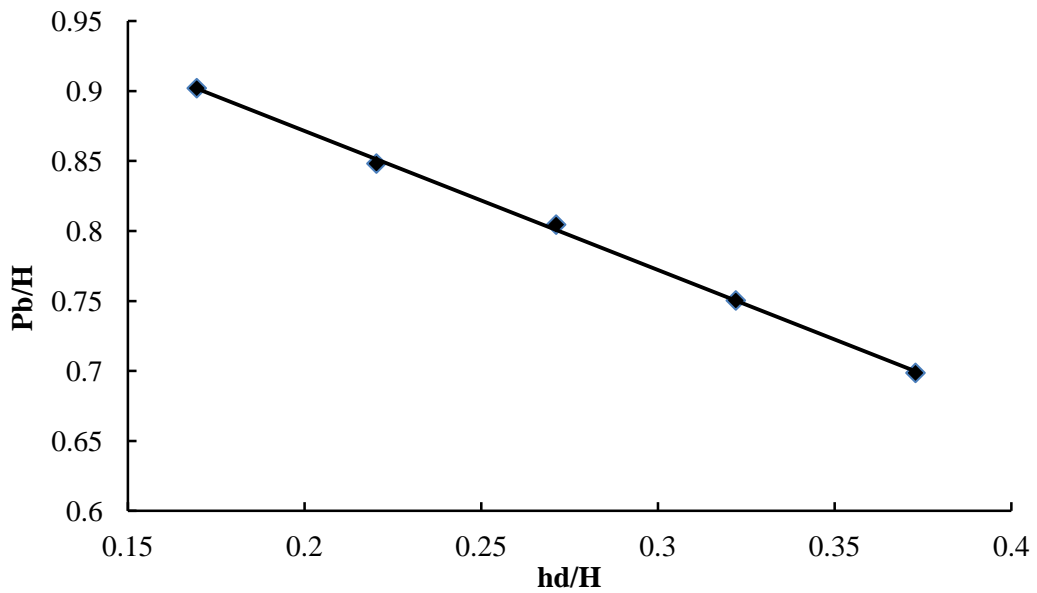


Figure 5.13: Height of diffuser and height of reactor ratio ( $hd/H$ ) with height of penetration and height of reactor ratio ( $Pb/H$ ) at micro-bubble diameter of  $40 \mu\text{m}$ .

## 5.7 Dead Zones in Gaslift Bioreactor

Dead zones in gaslift bioreactor are the part of the bioreactor in which no transfer of heat and mass occur in them, as well as those parts whose fluid flow less than 5%. Thus, thermal layers and non-homogeneous of pH is being formed in these areas. Increased size ratio of the dead zones inside the reactor increases the likelihood of failure of the anaerobic digester. These areas have very low velocities of the liquid (e.g. less than 0.0001m/s), which is very small in comparison with liquid velocities in the other parts of the reactor. Gentle increase in the flow rate of gas in the reactor has shown very little effect on reducing those areas in the bioreactor. In addition, increasing gas flow rate causes an increase in the bubble size that would ultimately reduce the transfer rate of heat and mass.

Another important design parameter is the height of the diffuser above the bottom of the reactor. Figure 5.14 and Figure 5.15 show the steady state distribution of gas concentration in the reactor at various diffuser positions (0.05, 0.065, 0.08, 0.095, 0.11 m above the bottom of the reactor) for the 40  $\mu\text{m}$  bubble size. The results confirm that, for each diffuser position, there is negligible gas volume fraction and liquid circulation below the level of the diffuser.

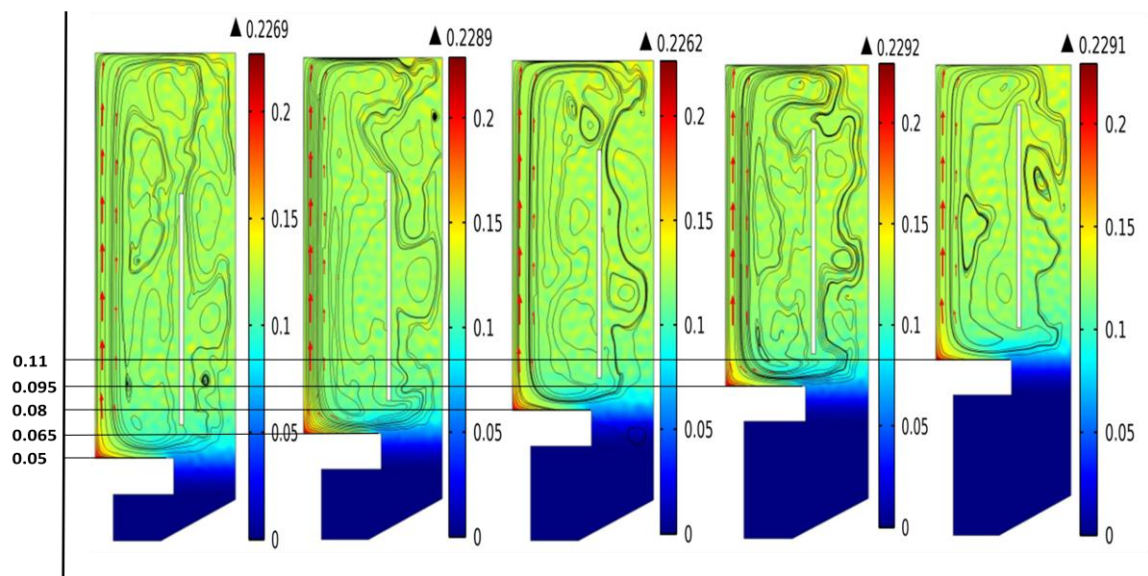


Figure 5.14: Snapshots of gas concentration after steady state condition different diffuser position (0.05, 0.065, 0.08, 0.095, 0.11 m)

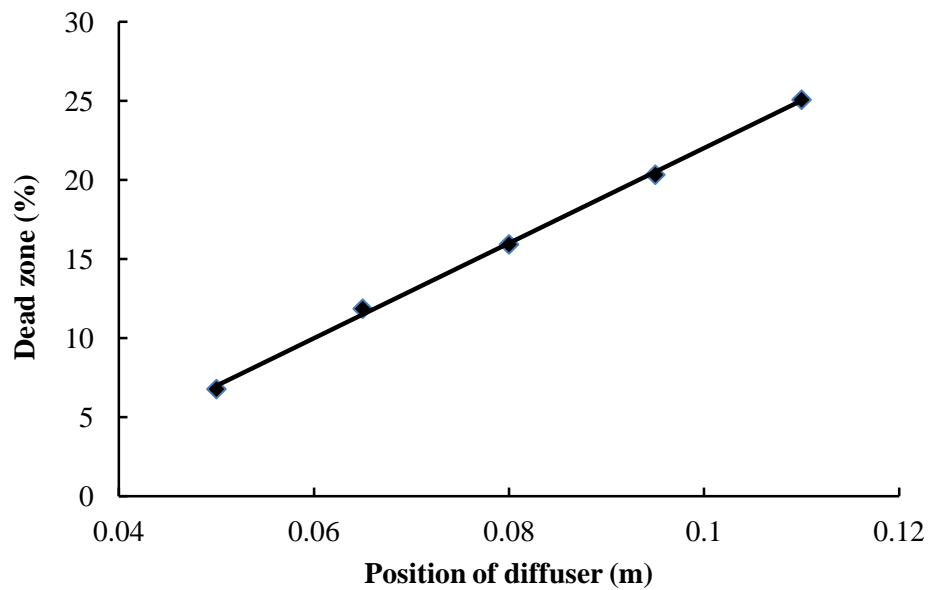


Figure 5.15: Percentage of dead zone after 120 sec, microbubble diameter 20  $\mu\text{m}$ , and at different diffuser position (0.05, 0.065, 0.08, 0.095, 0.11 m)

This region can therefore be considered to be a dead zone. Although in general, dead zones are to be avoided a practical consideration in anaerobic digesters in the settling of solids directly on the sparger surface that can inhibit its performance. This is the reason that the experimental bioreactor discussed in section 5.6 has the diffuser at a slightly elevated level of 0.05m above the reactor bottom ( $h_d/H=0.17$ ). The simulation results therefore confirm that improper location of the diffuser can give poor bubble distribution and may have a deleterious effect on the performance of anaerobic digester.

## 5.8 Effect of Draft Tube Diameter

Since the relative flow area of the riser compared to the downcomer is an important design parameter for internal airlift reactors, the present study simulated four different draft tube diameters. The ratio of draft tube diameter to the bioreactor diameter ( $d/D$ ) was varied from 0.6 to 0.9. Two bubble diameters (40  $\mu\text{m}$ , 400  $\mu\text{m}$ ) were used for investigating effect the draft parameter on mixing efficiency. Figure 5.16 shows the liquid circulation patterns and the steady state distribution of gas volume fraction for.  $d/D = 0.6, 0.7, 0.8,$  and  $0.9$ ) when the bubble diameter is 400  $\mu\text{m}$ , while Figure 5.17 shows the corresponding velocity liquid profiles across the cross section of the riser

region. An interesting aspect of these results is that the liquid circulation in the downcomer is very low for the largest riser diameters ( $d/D = 0.8$  and  $0.9$ ) with most liquid circulating downwards in the riser. The reactor is therefore operating as a simple bubble column in these simulations. Indeed, for  $d/D = 0.8$  and  $0.9$ , it can be seen in Figure 5.18, that this stagnant region extends beyond the downcomer well into the riser. Our simulation results therefore show a marked transition from a liquid circulation pattern that has good mixing for  $d/D = 0.6$ , to one that has a large annular dead zone of poorly mixed liquid.

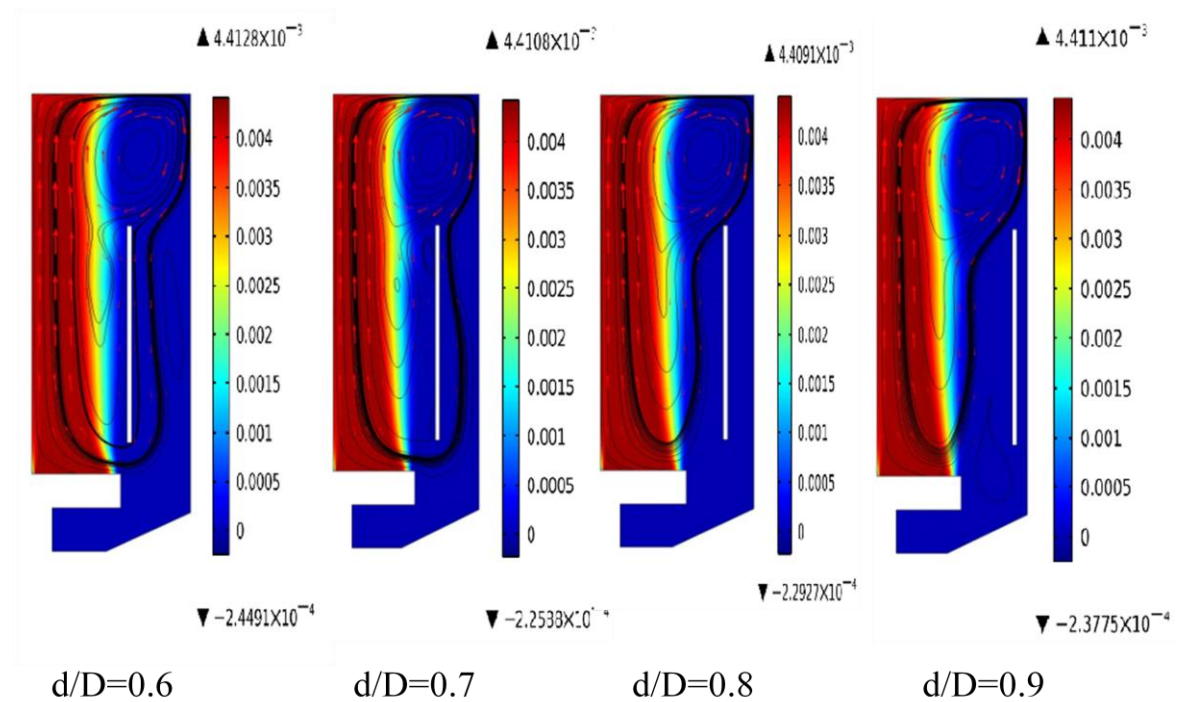


Figure 5.16: Snapshots of gas concentration at different  $d/D$  ( $d/D = 0.6, 0.7, 0.8,$  and  $0.9$ ) when microbubble diameter is  $400 \mu\text{m}$  and after 120 sec

In order to assess the effect of much smaller microbubbles size, simulations were performed for the  $40 \mu\text{m}$  bubble size and the results are shown in Figure 5.19 and Figure 5.20. It can be seen that the increase in draft tube diameter has very little effect on the liquid velocity profile (Figure 5.20), but may causes slightly more swirling flow in the reactor (Figure 5.19).

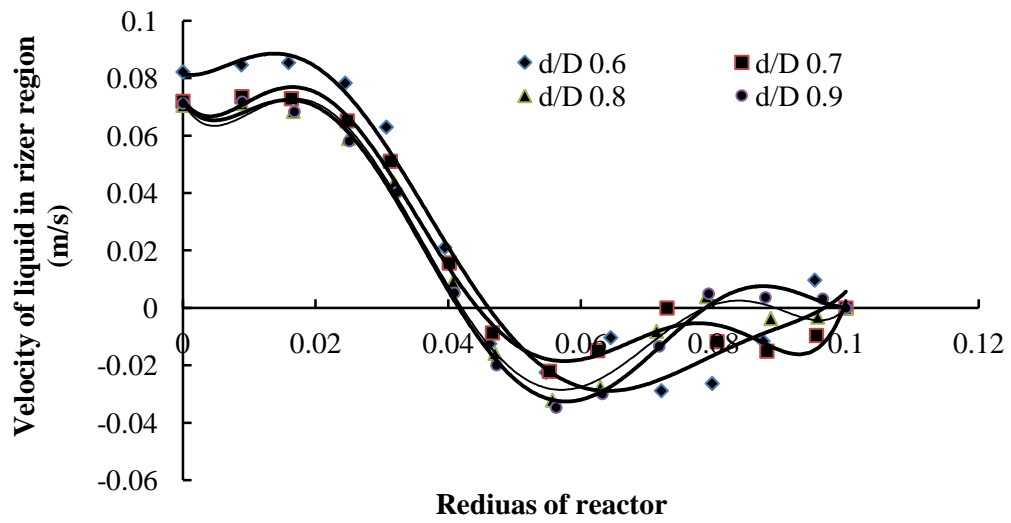


Figure 5.17: Velocity liquid profile in cross-section after 120 sec

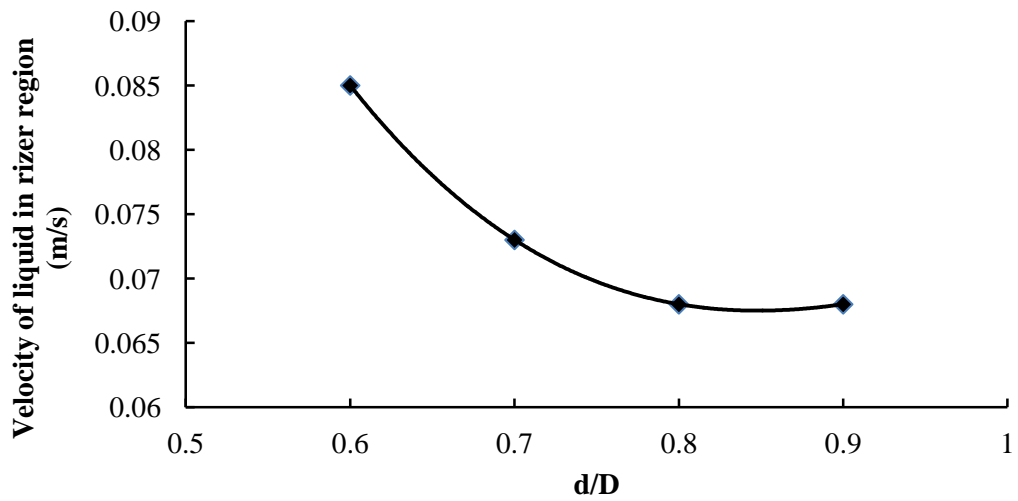


Figure 5.18: Velocity liquid in cross-section riser region at different draft tube diameter after steady state.

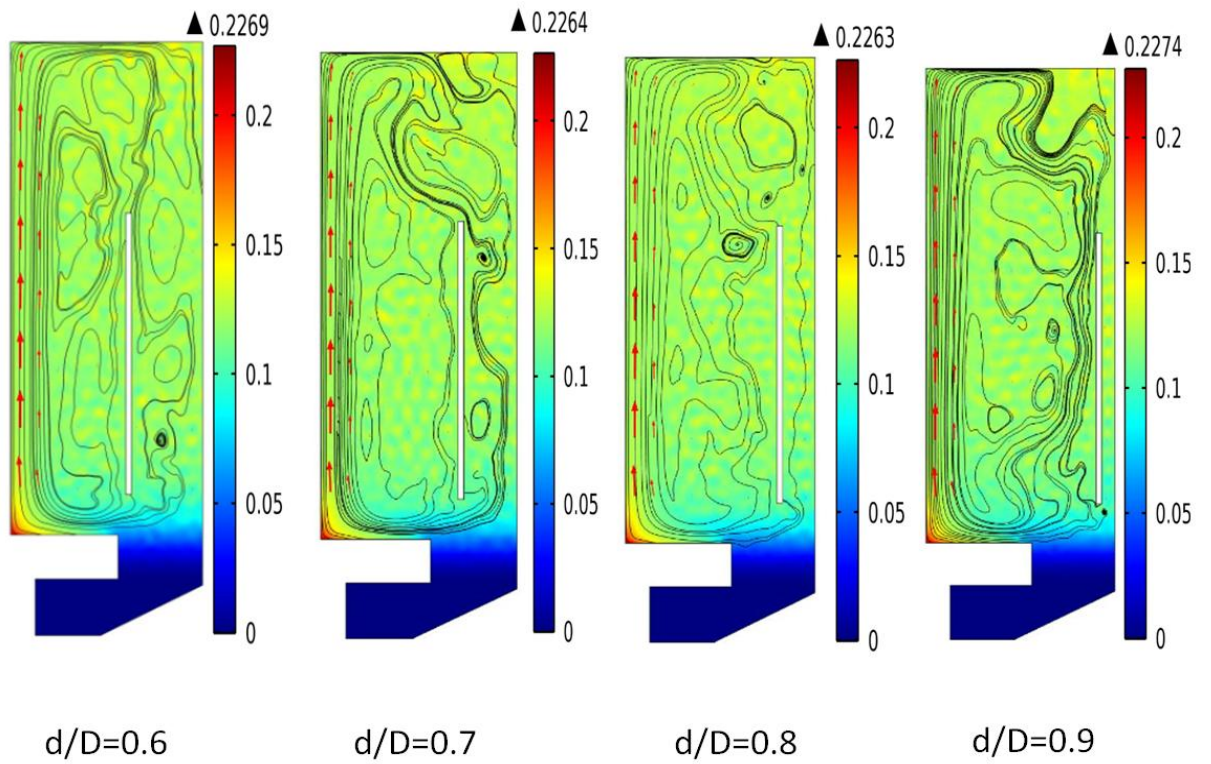


Figure 5.19: Snapshots of gas concentration at different  $d/D$  ( $d/D = 0.6, 0.7, 0.8,$  and  $0.9$ ) when microbubble diameter is  $400 \mu\text{m}$  and after 900 sec

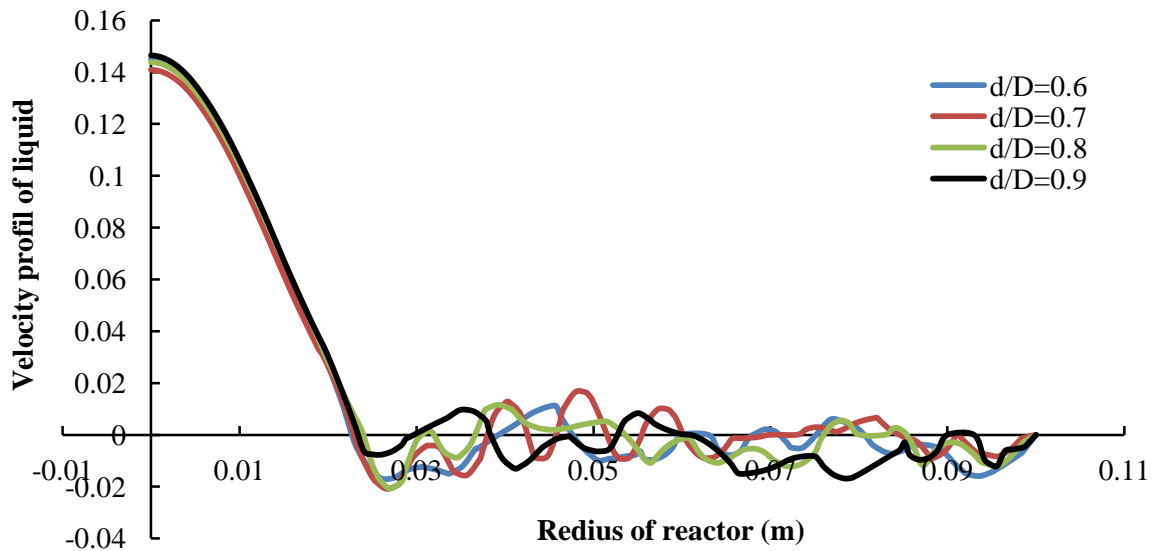


Figure 5.20: Velocity liquid profile in cross-section after 120 sec

From the above results, the study concluded that following:

1. The diameter of the produced bubbles exceeded  $200\ \mu\text{m}$ , the downcomer region, which is equivalent to about 60% of overall volume of the reactor, is free from gas bubbles.
2. The simulation data showed, also, that below certain constant flow rate (e.g. 300 l/min), the gas velocity decreases with decreases in bubble size, due to increased drag force against the buoyancy force.
3. At similar conditions and flow rates, liquid velocity increases corresponds to decreases in bubble size. The results showed that the depth of penetration of the microbubbles increases with decreasing the bubbles size due to a bigger downward drag force compared to the buoyancy force.
4. The volume of dead areas has increased with increasing the height of diffuser location. Therefore, based on the calculated simulation data, it can be concluded that poor gas bubbles distribution, occurred due to improper location of the diffuser, may have a marked deleterious effect on performance of bioreactor.

Overall, the results obtained suggest enormous potential for microbubble aeration for improving the efficiency of mixing and mass transfer. They also demonstrate the power of computational modelling for the analysis and design of the next generation airlift bioreactors for bioprocess applications. According to the results obtained from the simulation study, gaslift anaerobic digester is assembled for our experiments as can be seen in Figure 5.21.



Figure 5.21 Actual airlift bioreactor modelled in this study and used in the current experiments

## 5.9 Summary

Airlift bioreactors have many advantages over stirred tanks. For instance, there are no moving parts inside the reactor which often results in lower costs of installation and maintenance as well as lower energy consumption. However, these bio-reactors still need further technical developments in order to increase the efficiency of mass and heat transfer rate in gas-liquid processes. Bioprocesses with gaseous reactants or products that are operating at high cell densities are particularly susceptible to being mass transfer limited. Enhancement of the mass transfer rate can be accomplished by smaller bubbles that increasing the interfacial area between the gas and liquid phases. Microbubbles generated by fluidic oscillation provide an effective, low energy means of achieving high mass transfer rates. This study presents the design and simulation of a gaslift bioreactor with microbubbles generated by fluidic oscillation.

The simulation results show that when the diameter of the microbubbles exceeded 200  $\mu\text{m}$ , the “downcomer” region, which is equivalent to about 60 % of overall volume of the reactor, is free from gas bubbles. The results also demonstrate that the use of microbubbles not only increases surface area to volume ratio, but also increases mixing efficiency through increasing the liquid velocity circulation around the draft tube. In addition, the depth of downward penetration of the microbubbles into the downcomer increases with decreasing bubble size due to a bigger downward drag force compared to the buoyancy force. The simulated results indicate that the volume of dead areas increase as the height of diffuser location is increased. We therefore hypothesise that poor gas bubble distribution due to the improper location of the diffuser may have a markedly deleterious effect on the performance of the bioreactor used in this work.



CHEMICAL & BIOLOGICAL ENGINEERING

## Chapter Six

# Removal of Acid-gases from Digested Sludge Using Periodic Sparging in an Airlift Bioreactor with Microbubble Generated by Fluidic Oscillation

---

*Part of this chapter published in (The Sixth International Conference on Environmental Science and Technology, Volume 1, 2012, page 223, ISBN 9780976885351, American Science Press). In addition, was chosen as best paper of the conference.*

## Chapter Six

### **Removal of acid-gases from digested sludge using periodic sparging in an airlift bioreactor with microbubble generated by fluidic oscillation**

#### **6.1 Introduction**

The hydraulic retention time (HRT) applied in conventional mesophilic anaerobic digesters is normally 20 days. The digested sludge (effluent) contains biodegradable organic matter, inert solids, anaerobic bacteria and some dissolved gases: both those with high solubilities such as carbon dioxide (CO<sub>2</sub>) and hydrogen sulphide (H<sub>2</sub>S); and also those that are sparingly soluble such as hydrogen (H<sub>2</sub>) and methane (CH<sub>4</sub>). The aim of this chapter was to investigate the effect of stripping these dissolved gases using an air-lift reactor. We show that this leads to increased methane production, perhaps because the aforementioned dissolved gases inhibit biogas production. The presence of these dissolved gases in the effluent can also have a negative impact on the pipelines and the downstream processing units. Corrosion is one potential problem in piping metals. In addition, the generation of biogas continuously, in the digested sludge during its transfer and handling could lead to a creation of gas-liquid mixture; which, even if a small fraction of dissolved gas can degrade the performance of pumps due to creating cavitation phenomena. In addition, and due to large density differences between the two

phases, the gas and liquid tend to separate in pipelines and the pumps, consequently, handling with this mixture will become a difficult task and inefficient (William and Bohr, 2010; Lester and Phil, 1970; Garber and Ohara, 1972).

Airlift reactors (ALR) have been used in several industrial applications for many gas-liquid contacting processes (Merchuk and Siegel, 1969). ALRs have several advantages over stirred tanks. In addition, it has been observed that use of airlift reactor can enhance mixing efficiencies compared to agitation by conventional stirred tanks. Because of these benefits the airlift reactor was used as the unit for the anaerobic digester in this study. The efficiency of ALRs for stripping CO<sub>2</sub> from liquid was demonstrated by Al-mashhadani et.al. (2012). They reported that the bubble size in the airlift reactor plays an important role in removal of dissolved gases from the liquid. In this study, the contact between the liquid sludge and the nitrogen gas bubbles leads to a reduction of the partial pressure of the biogas produced due to gas exchange. The low partial pressure of the products contributes to the Gibbs free energy with a negative sign; hence the reaction becomes thermodynamically favourable and provides impetus for the formation of more products (Gary, 2004). Investigations that depend on the mathematical relationship between partial pressure and Gibbs free energy are many and with widespread applications (Tanisho et. al.1998; Park et.al. 2005; Alshiyab et. al. 2008; Liang et. al. 2002; Mizuno et. al. 2000; Kim et al 2006; Kraemer et. al. 2008). This process has raised debate among researchers about controlling the partial pressure of hydrogen or carbon dioxide and its effects on the production of hydrogen.

It should be noted that hydrogen is an important intermediate in anaerobic digestion for methane production since it is produced by the acetogenic bacteria from degradation of organic acids and is consumed by the carbon dioxide-reducing methanogenic bacteria. However, low H<sub>2</sub> partial pressures ( $<10^{-4}$  atm) are essential for acetogenic reactions to be thermodynamically favourable (Schink, 1997; Stams et. al. 2005). So the effects of removal of hydrogen on methane production are not clear since it could enhance acetogenesis but decrease the rate of methane produced from hydrogen and carbon dioxide - hydrogenotrophic methanogenesis. The other route to methane, aceticlastic methanogenesis, uses only acetate as the substrate and is therefore independent of dissolved hydrogen (Schink, 1997).

Although we did not measure hydrogen in this study it is likely that it is at low level since we did not add any additional substrate. Several previous studies have found a close correlation between higher hydrogen levels and more organic loading with readily fermentable substrates (Mosey and Fernandes, 1989) but in this study the system is substrate limited so hydrogen levels are not likely to be high enough to be limiting. The reduction of the partial pressure of gases can be achieved by different methods with different implications for removal efficiency and cost. The current research has been conducted on a hypothesis that using airlift bioreactor (ALR) as anaerobic digester would lead to an increase in the stripping of the biogas produced.

## 6.2 Results and Discussion of Using Gaslift Digester

Study of removal of acid-gases from the digested sludge was carried out according to the setup of experiments that discussed in part 3.4 of chapter three. Figure 6.1 shows that, over 170 hours, the cumulative methane production from the gaslift anaerobic digester was 29 % higher than that observed in the conventional anaerobic digester. The production of methane in both digesters decreased each day indicating an exhaustion of substrate as can be expected since we used digested sludge in this experiment with no additional feeding.

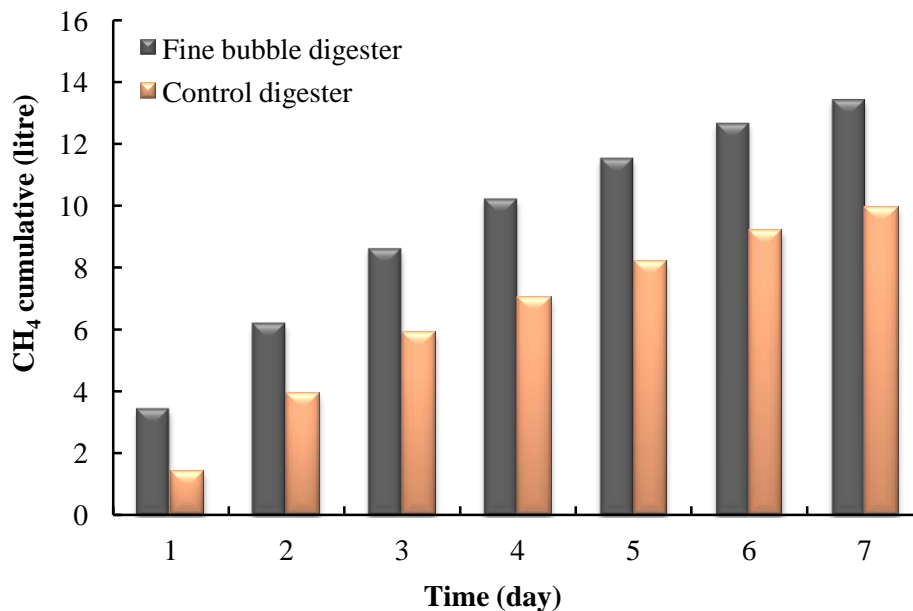


Figure 6.1: Cumulative methane production in the airlift digester vs. the unsparged digester.

It can be also being seen in Figure 6.2 that the vast majority of methane was obtained from the airlift anaerobic digester during the daily one hour period of sparging with nitrogen. This indicates that the biogas produced by the biological processes remains either dissolved in solution or is perhaps trapped as small bubbles in the digested sludge. During sparging the trapped gases are released, either by mass transfer from solution into the fine nitrogen bubbles, or possibly by physical dislodging of the bubbles.

The reduced methane production for the unsparged digester suggests that metabolic activity is limited by high concentrations of dissolved gases in the bulk solution. Indeed, a rough calculation shows that prior to sparging, the methane concentration is highly super-saturated, particularly in the early stage of culture.

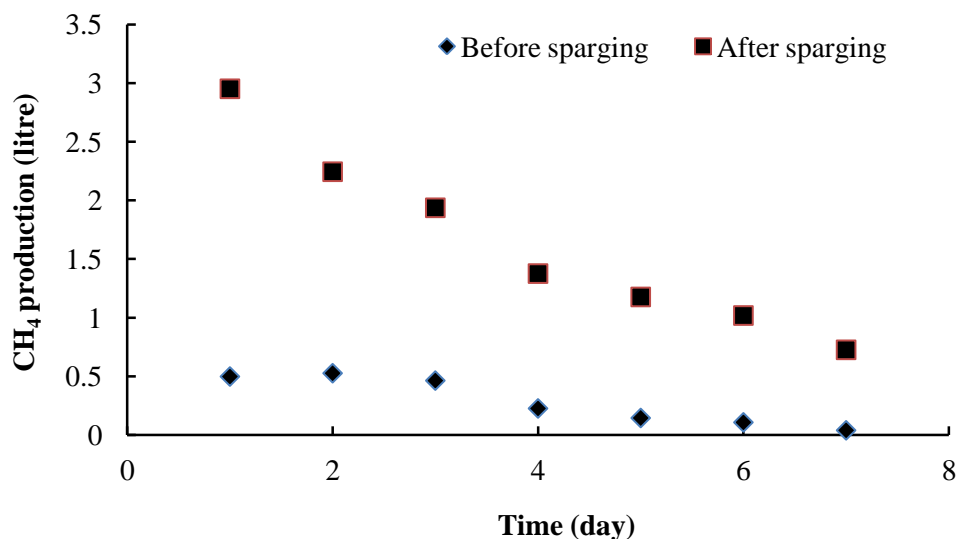


Figure 6.2: Comparison of methane production in the airlift digester during the daily one hour sparging period versus that in the preceding 23 hours unsparged operation.

A volume of around  $0.003 \text{ m}^3$  (3 litres) of methane were released from the  $0.009 \text{ m}^3$  (9 litres) working volume digester on day 1 whereas only  $0.00024 \text{ m}^3$  (0.24 litre) of methane could be dissolved in 9 litres of distilled water at  $35^\circ\text{C}$  (assuming solubility of  $0.017 \text{ g/l}$  at this temperature). The methane hold-up in the digester liquid, either in dissolved form, as small trapped bubbles, or in the head space is equivalent 30% of digester volume suggesting a high degree of super-saturation that possibly limits its production. In fact, the degree of supersaturation /overconcentration is likely to be even

higher than this calculation suggests since the solubility of methane in the fermentation liquid is almost certainly less than that in distilled water due to the competition from other dissolved ions. This supersaturated extracellular concentration of methane has been found in previous studies (Pauss et. al. 1990) on mass transfer limitations in anaerobic digesters. Such high concentrations outside the cell imply even higher concentrations inside the methanogenic cells since the driving force for passive transport of methane product out of the cell is the concentration gradient. We hypothesise the intracellular/extracellular concentrations of methane or other biogas constituents ( $\text{CO}_2$ ,  $\text{H}_2\text{S}$ ,  $\text{NH}_3$ ) in the comparatively crowded conditions of the digester may be higher than that found in the cells' natural environment and thus limit biogas production. This is due to the simple chemistry of making the Gibbs free energy of the final step in methane production less negative and perhaps also by active metabolic regulation. Stripping with an inert gas such as nitrogen can correct this effect by removing gaseous products to make gas producing reactions thermodynamically more favourable. These results suggest, somewhat counter intuitively, that even sparging with pure methane will reduce the concentration of methane – i.e. from the super-saturated concentration towards saturated concentration. This raises the possibility of sparging with, for example, recycled mixtures of  $\text{CO}_2$  and  $\text{CH}_4$  which will not dilute the energy content of the biogas rather than nitrogen used in this research.

After methane, the next most abundant gas produced from the anaerobic fermentation is carbon dioxide which is some 70 times more soluble in water than methane at  $35^\circ\text{C}$ . A small fraction (0.2%) of aqueous  $\text{CO}_2$  exists as carbonic acid ( $\text{H}_2\text{CO}_3$ ) which is a diprotic acid with two ionisable hydrogen ions which can sequentially dissociate to form bicarbonate and carbonate ions.

It would therefore be expected that accumulation of dissolved  $\text{CO}_2$  in the digesters without pH control would lead to a lowering of pH but Figure 6.3 shows the ability of pH control system to maintain the pH within a reasonable range in both digesters. It should also be noted that there is also a natural buffering effect whereby acids produced can immediately react with ammonia produced from biodegradation of protein.

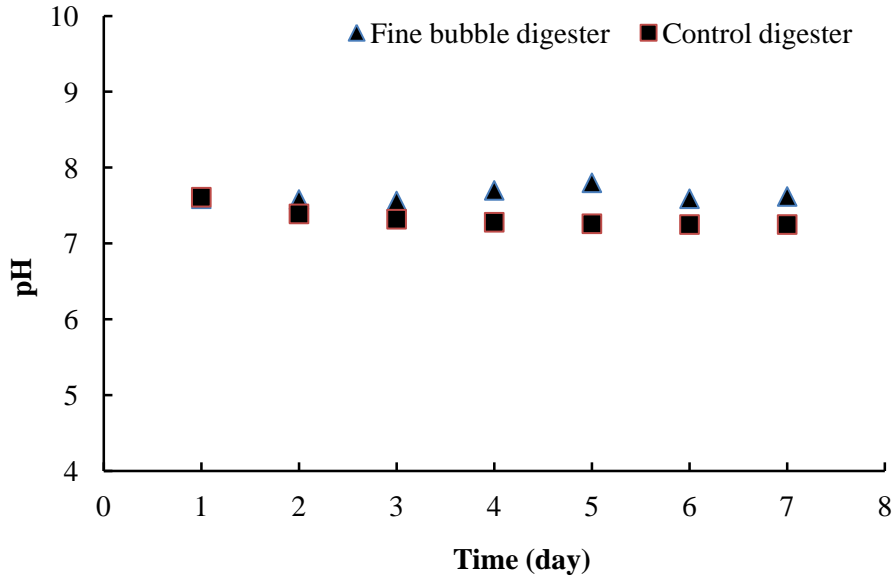


Figure 6.3: pH values of both Airlift digester and the conventional digester

Figure 6.4 compares the production of carbon dioxide from airlift digester with and without conventional unsparged digester. It can be clearly seen that there is a significantly greater removal of carbon dioxide in gaslift digester over the conventional digester. It is clear that the higher solubility of  $\text{CO}_2$  allows it to remain in solution at much higher levels than the  $\text{CH}_4$  until it is stripped out by the nitrogen sparging.

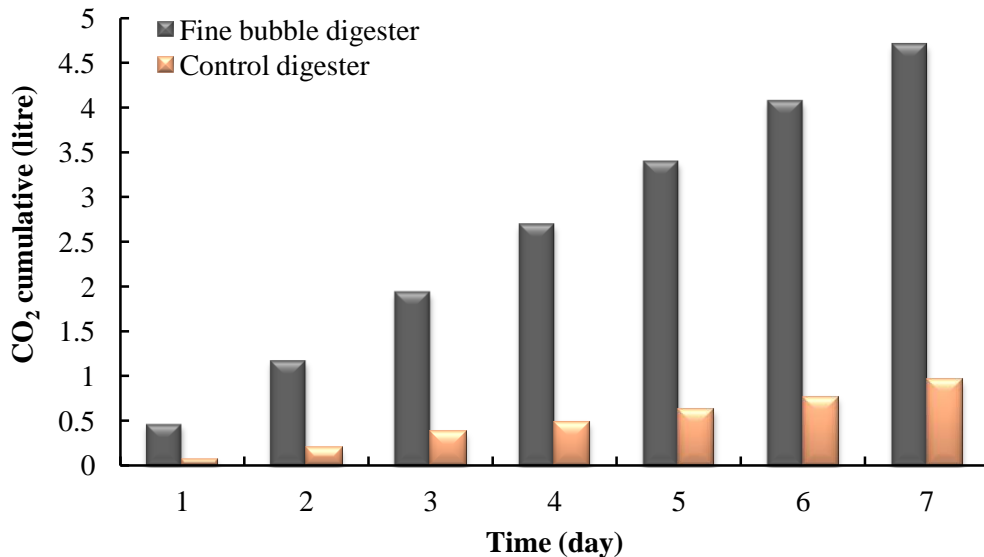


Figure 6.4: Cumulative carbon dioxide production in the airlift digester with periodic nitrogen bubbling compared to the conventional unsparged digester

Figure 6.5 shows the hydrogen sulphide removal from digested sludge during nitrogen bubbling. Since the solubility of  $H_2S$  is more than twice that of  $CO_2$  and it is produced in much smaller quantities, there is very little produced from the unsparged digester when compared to that stripped by using one hour per day sparging in the airlift digester.

Sulphate can inhibit the generation of biogas produced from the anaerobic digestion of wastewater since it encourages the growth of the sulphate-reducing bacteria which consume the acetic acid and hydrogen used by methanogenic bacteria to produce methane (Hiltan and Archer 1988). As well as competition between the sulphate-reducing bacteria and the methane-producing bacteria there is also a direct inhibitory effect. Sulphide produced from sulfate reduction has inhibitory effect at concentrations of 0.002 M of  $H_2S$  (Speece 1996). In fact, the concentration of  $H_2S$  can be taken as an indicator of the degree of inhibition of methane production by methanogenic bacteria Karhadkar (Gerardi 2002). The removal of dissolved  $H_2S$  from the sludge can therefore prevent inhibition of methanogenic bacteria and also reduce the odour of the digested sludge.

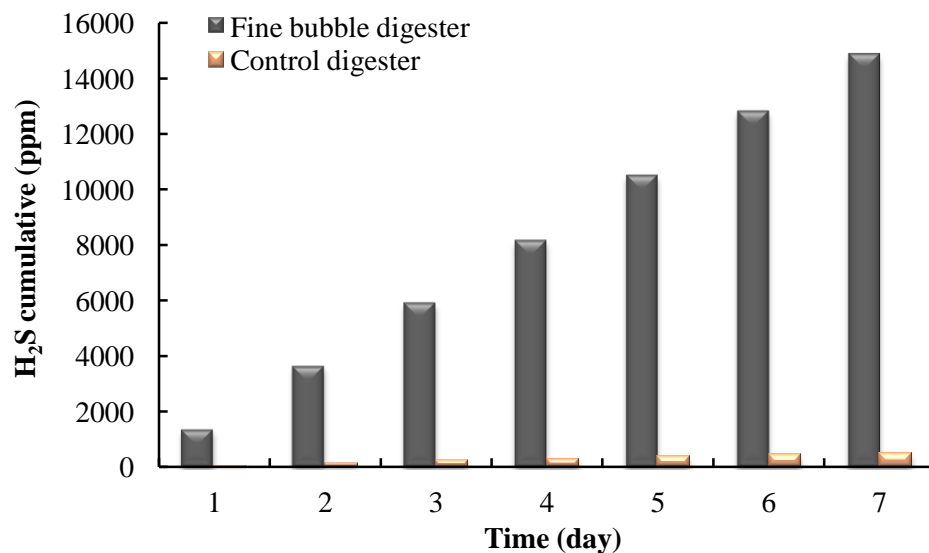


Figure 6.5: Cumulative hydrogen sulphide production in the airlift digester with periodic nitrogen bubbling compared to the conventional unsparged digester.

Without any additional sparging, there is a very modest stripping effect from the other evolved gases-primarily  $CH_4$  which is produced in the largest quantities and is relatively insoluble. There is also some direct mass transfer between the liquid and the headspace

at the top of the digester. This can be further improved by mixing of the digested sludge to provide intimate contact between sludge and bubbles of biogas or headspace. However, the rheological characteristics of digested sludge at high solid loading require a high energy input for mixing. The airlift digester with gas sparging can provide better gas transfer with lower energy requirements.

The stripping of two other gases, hydrogen and ammonia not measured in this study, may also have contributed to the improved performance of the airlift digester. Hydrogen has a very low solubility in water (more than one order of magnitude less than that of methane) and its effects were discussed earlier. Ammonia, on the other is highly soluble and has been shown to be an inhibitor of methanogenesis (Sung and Liu, 2002). A few industrial and lab studies have demonstrated the feasibility and efficacy of stripping ammonia from the digester supernatant using air columns (Siegrist et. al. 2005; Katehis et. al. 1998) In summary, whichever dissolved gas species (or combination of gases) is limiting, the enhanced productivity demonstrated in these results provide a clear motivation for using the better mass transfer of the airlift digester.

The results presented here demonstrate that enhanced removal of gases in the airlift reactor can lead to significant increase in methane productivity and this is therefore a fruitful area of further research.

The present chapter addresses also utilization of microbubble generated by fluidic oscillator with a gaslift bioreactor (GLR) for removal of acid gases ( $\text{CO}_2$  and  $\text{H}_2\text{S}$ ) from digested sludge. The hydrodynamic stabilisation, longer residence times, and low energy demands could be achieved by using this technique. Al-Mashhadani et al.(2012) used this technology for stripping carbon dioxide. They reported that the efficiency of  $\text{CO}_2$  stripping was about 29% more than that for fine bubble sparging. Therefore, the present chapter suggested, also, using this technique with gaslift digester for removal the acid cases.

Anaerobic digester, which operates with fluidic oscillator, was added to previous setup that illustrated in section 3.3 of chapter three.

### **6.3 Results and Discussion of Using Microbubbles Technology**

Figure 6.6 shows trends of carbon dioxide production rate in the anaerobic digester with and without  $\text{N}_2$  gas sparging. It is obvious that the bubbling system in the gaslift

digester, highly contributed in stripping of produced carbon dioxide. With the use of micro-bubble technology of  $N_2$  gas sparging, the  $CO_2$  production has increased compared to that for the conventional digester.

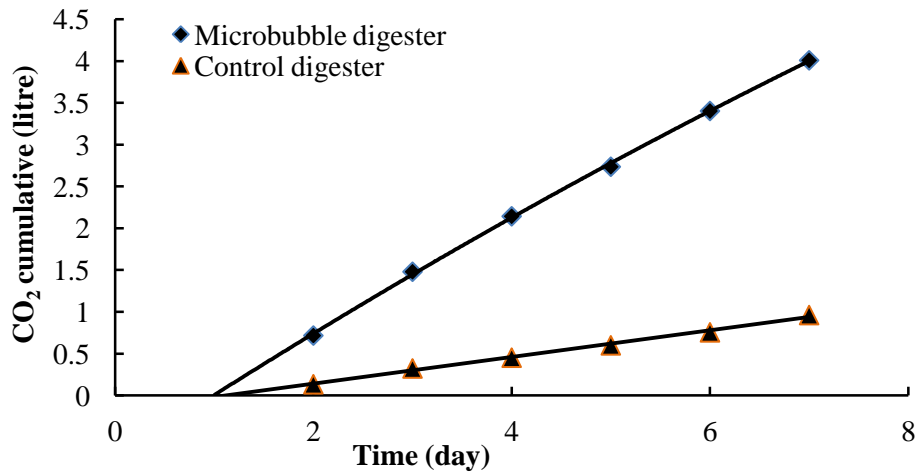


Figure 6.6: Cumulative carbon dioxide production in airlift digester with and without nitrogen bubbling

Experimentally, the characteristic complexity of the sludge has played an important role in enhancement of biogas stripping. The characteristics of digested sludge require a high energy to achieve good mixing. Using a gaslift digester with microbubble generated by fluidic oscillation, with low energy requirements, can contribute to remove most of the generated hydrogen sulphide. Figure 6.7 shows the hydrogen sulphide removal from digested sludge during nitrogen bubbling. The figure indicates with one hour of nitrogen, sparging as microbubbles increased removal of hydrogen sulphide as order of magnitude more than the unsparged conventional digester.

From above, it can be summarised that the benefits of a gaslift bioreactor with microbubbles are illustrated through above results. Low energy, good mixing, and enhancement of gas stripping are the most important of characteristics of the gaslift bioreactor that were utilized in this study. More stripping of carbon dioxide and hydrogen sulphide were obtained from this utilization. Finally, the current study has shown one of important applications, which utilized the proposal design and micro-bubble generated by fluidic oscillator with great mixing for stripping with lower energy requirements. In addition, there are various applications which take advantage of this technology. The results which obtained from this study, showed, also, that using the gaslift bioreactor with microbubble technology can leads to increase the efficiency of mass transfer between gas-liquid contact systems.

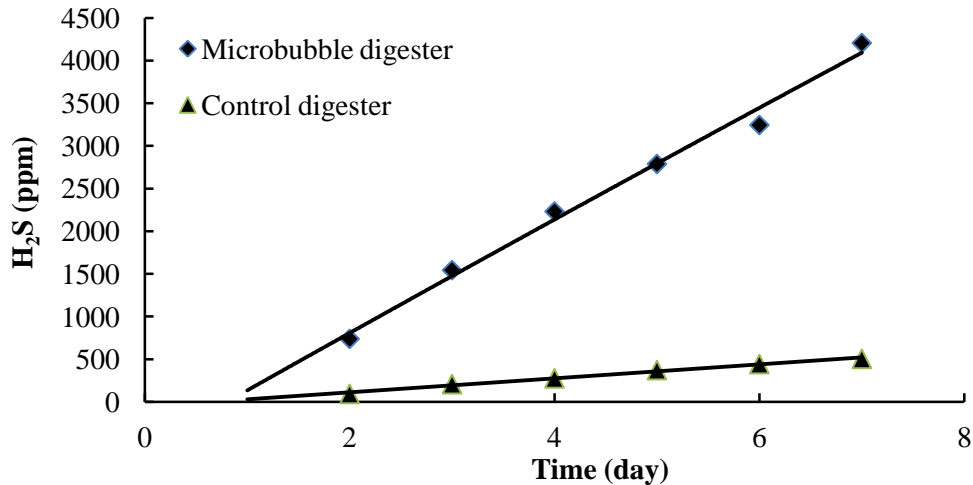


Figure 6.7: Cumulative hydrogen sulphide production in anaerobic digestion with and without nitrogen sparging

## 6.4 Summary

This chapter addresses further anaerobic digestion of already digested sludge by processing in an airlift bioreactor and, in particular, the effect of periodic sparging using nitrogen gas. As mentioned earlier the organic matter is broken down through four biodegradation stages into methane ( $\text{CH}_4$ ), carbon dioxide ( $\text{CO}_2$ ), varying amount of hydrogen sulfide ( $\text{H}_2\text{S}$ ), and the digested sludge, which can be used for fertilizer. The remaining dissolved gases in the digested sludge have a pejorative effect on the environment when they are eventually released, as well as causing operational difficulties. Moreover, the continuous generation of biogas in the sludge increases cavitation phenomena and the accompanying pump load. Removal of these gases is investigated by a bubbling system. An airlift (ALR) was used as an anaerobic digester in the present research to remove the generated gases, (e.g.  $\text{CH}_4$ ,  $\text{CO}_2$ , and  $\text{H}_2\text{S}$ ) thereby reducing odour. The experimental data shows that the cumulative methane production from the airlift anaerobic digester is 29% more than observed in the conventional anaerobic digester. We also find that the methane hold-up in the unsparged fermentation medium, either in dissolved form, as small trapped bubbles, or in the headspace is equivalent 30% of digester volume suggesting a high degree of supersaturation that possibly limits its production. Throughout 170 hours of processing, there was also a significantly greater removal of carbon dioxide and hydrogen sulphide in airlift digester over the conventional digester.

The present chapter studies also the mechanism of post anaerobic digestion of digested sludge for removal of acid gases ( $\text{CO}_2$  and  $\text{H}_2\text{S}$ ) using microbubbles generated by fluidic oscillator. Throughout seven days of processing, the experimental data showed that the removal of carbon dioxide and hydrogen sulphide were more than that for the conventional digester.



CHEMICAL & BIOLOGICAL ENGINEERING

## Chapter Seven

### **Investigation of the Effect of Sparging in Anaerobic Digestion Using Various Gases and Microbubbles Generated by Fluidic Oscillation**

- 1. Sparging using nitrogen: Part I**
- 2. Sparging using nitrogen and carbon dioxide: Part II**
- 3. Recycling the diluted and undiluted biogas: Part III**
- 4. Sparging using carbon dioxide: Part IV**

## Chapter Seven

### **Investigation of the effect of sparging in anaerobic digestion using various gases and microbubbles generated by fluidic oscillation**

#### **7.1 Introduction**

Convincing results from previous investigations have shown the importance of the removal of gases from biological processes in increasing production of hydrogen and improving the overall efficiency of the process. Reduction of the partial pressure of gas can be achieved by a variety of means. Selection of the appropriate method depends on many parameters, such as the efficiency of the removal process, the type of gas that requires removal, and the cost of installation and maintenance. Park et al. 2005 and Alshiyab et al. 2008 have used *C. acetobutylicum* NCIMB 133357 and KOH, respectively, to remove carbon dioxide from the headspace of the bioreactor. Other researchers (Tanisho et al. 1998; Mizuno et al. 2000; Kim et al. 2006; Kraemer and Bageley, 2008; Nath and Das 2004; Hussy et al. 2005; and Kyazze 2006) have used a range of sparging gases (e.g. N<sub>2</sub>, H<sub>2</sub>, and CO<sub>2</sub>) in bio-hydrogen production process to remove H<sub>2</sub> and CO<sub>2</sub>. Corte et al. 1988, used *Rhodospirillum rubrum* ATCC 17100 bacterium, which utilizes hydrogen and carbon dioxide, in reducing both gases and also used sulfate-reduction bacteria to remove hydrogen gas only.

This chapter discusses the use of a sparging system to remove the biogas produced from anaerobic digestion under mesophilic conditions (35°C). Over an experimental period of more than 200 days, an airlift anaerobic digester was employed to investigate the effects

of the sparging system on the efficiency of biogas production using different gas types, such as pure nitrogen, a mixture of nitrogen and carbon dioxide, biogas (methane and carbon dioxide), and finally, pure carbon dioxide. These experiments were carried out using microbubbles generated by fluidic oscillation except, for technical reasons, in the case of the recycling of biogas (methane and carbon dioxide). The chapter presents and discusses the results obtained from the experiments using different concentrations of different gases and their effects on biogas production in anaerobic digestion. The study comprised the following stages:

**Part I :** Sparging using nitrogen

**Part II:** Sparging using nitrogen and carbon dioxide

**Part III:** Recycling biogas in anaerobic digestion and diluting biogas with carbon dioxide

**Part IV:** Sparging using carbon dioxide

## 7.2 Sparging Using Pure Nitrogen

The bubbling system has been widely used in single stage biological processes. However there have been very few, if any, applications in multistage processes that use different bacteria in more complex biological transformations. One such application that requires further investigation is anaerobic digestion. This process, as mentioned earlier, uses a number of stages to produce hydrogen, carbon dioxide, and methane. In addition, there is a mutually beneficial relationship between the bacteria since the product of one type of bacteria produces the feed for another type.

The main hypothesis of this part is that the use of inert gas in a bubbling system leads to an increase in biogas production by reducing the partial pressure of methane and carbon dioxide. As mentioned in the literature survey, reduction of the partial pressure of products contributes to a change in the Gibbs free energy value leading to an increase in the yield of those products.

The benefits of using microbubbles generated by a fluidic oscillator are investigated in this chapter as well as the effects of sparging time as a parameter on biogas production.

### 7.2.1 Results and Discussion: Part I

Stripping the biogas produced from the fermentation process is done in order to convert unfavourable reactions into favourable reactions by maintaining low partial pressure of these gases or providing a convenient environment to produce more gases. This aim is achieved through sparging of inert gases in the fermentation processes. As mentioned above, previous researchers have demonstrated that there is a significant increase in bio-hydrogen yield if nitrogen is used as an inert gas in this sparging process. However, this does not mean that sparging with inert gases will lead to an increase in biogas production in all bioprocesses. Some bioprocesses are more complex than bio-hydrogen processes because they comprise multiple stages and use multiple types of bacteria. Moreover, each stage is dependent on previous stages of the same bioprocess.

This chapter deals specifically with the anaerobic digestion process which is important in wastewater treatment plant and takes place by means of multiple stages. Conflicting requirements among the bacteria in these stages complicate decisions on which gases should be removed to increase the biogas yield. For example the hydrogen produced in the fermentation stage is used by another type of bacteria (methanogenic bacteria) in a syntrophic relationship. Stripping the hydrogen allows the products of the reaction in the fermentation stage to be increased and reduces the amount of volatile fatty acid. On the other hand, the methanogenic bacteria are affected by this removal process, since hydrogen is required for the production of methane. In order to investigate this situation, six different operational conditions were used in this part of this study.

The materials and methodology used in the present study was explained in part 3.5.1 of chapter three. Figure 7.1 shows the cumulative methane production from three anaerobic digesters: a gaslift digester operating with fluidic oscillator, a gaslift digester operating without fluidic oscillator and a conventional digester. All three digesters were operated for 12 days. The time taken for sparging with pure nitrogen in this stage was about 100 min daily, while the flow rate was about  $300\pm 50$  ml/min. The figure indicates that during the first eight working days, the accumulated methane production from the sparged digesters was more than that produced from the control digester. But this does not mean that methane production increased throughout the entire period. Figure 7.2 illustrates that the methane produced from the sparged digesters decreased from day to day, while the amount of methane produced by the traditional digester remained more or less stable throughout the test period. Therefore, there was slightly

more total methane production in the traditional digester than in the other digesters. On the other hand, the sparged digesters produced more carbon dioxide than the control digester throughout the test period although production decreased daily, as is shown in the Figures 7.3 and 7.4. It seems that the stripping process removed all the biogas found in the digester: either as dissolved gas, bubbles, or in the headspace and, in addition the growth of anaerobic bacteria was slow. Therefore, extra processing time is needed as compensation for the shortfall in biogas.

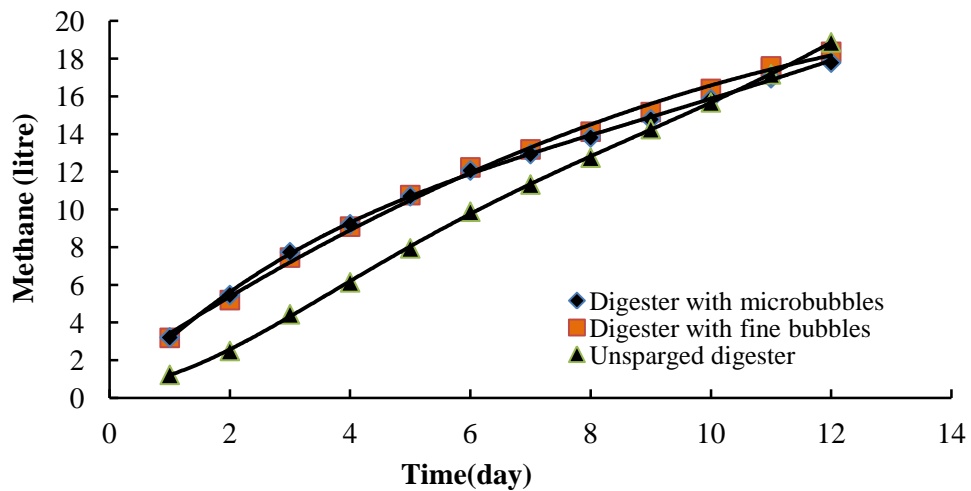


Figure7.1: Cumulative methane production from the sparged digesters and unsparged digester in the first stage

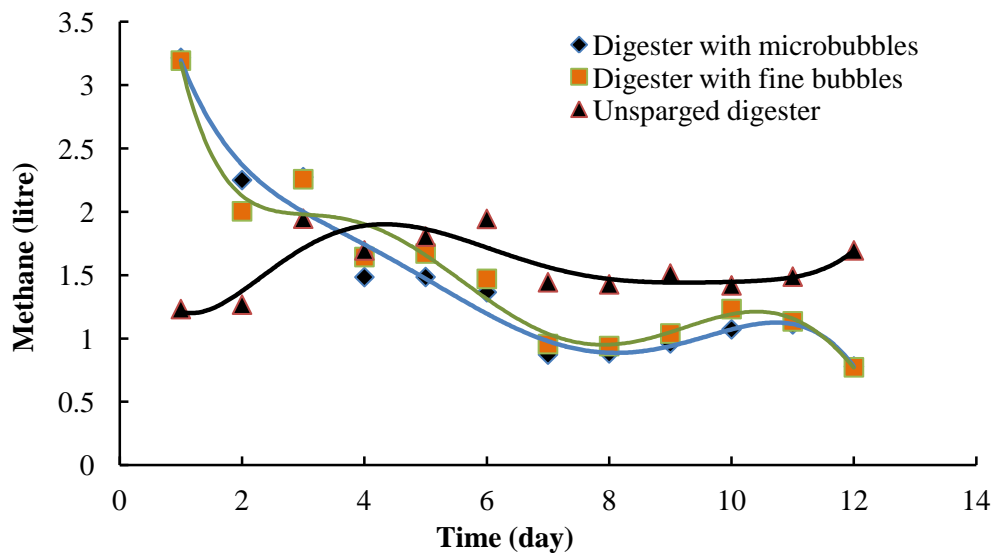


Figure7.2: Methane produced from the sparged digesters and unsparged digester in the first stage

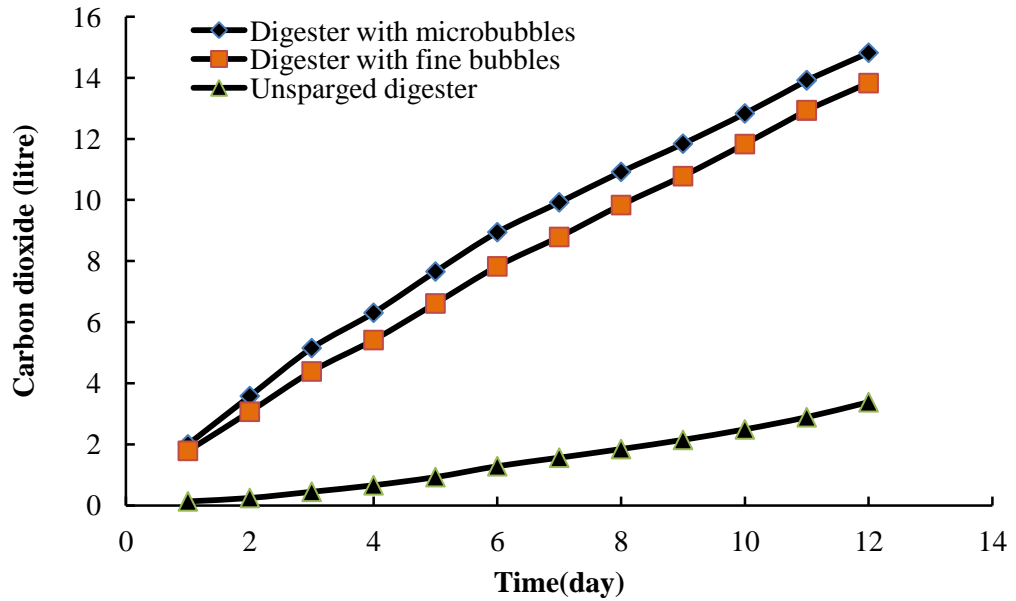


Figure 7.3: Cumulative carbon dioxide production from the sparged digesters and unsparged digester in the first stage

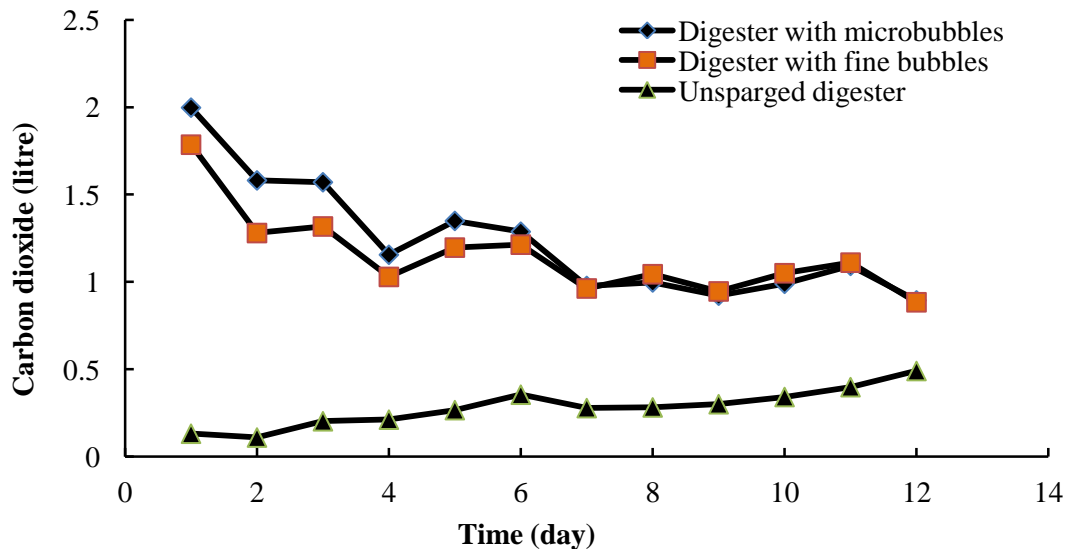


Figure 7.4: Carbon dioxide produced from the sparged digesters and unsparged digester in the first stage

To investigate the decline in methane production in the first stage, the bubbling time of the nitrogen was reduced from 100 minute to 60 minute in both digesters (i.e sparged digesters). Figure 7.5 displays the amounts of methane produced by the three digesters when 60 min of sparging with pure nitrogen was applied. The results indicate that the amount of methane produced remained unchanged during the process, thereby rendering

unnecessary the additional 40 of minute stripping in the previous experiment. In addition, the decline in methane production was less than that in the first stage as is shown in Figure 7.5; however, the cumulative methane production in the traditional digester still exceeds that of the other digesters according to Figure 7.6.

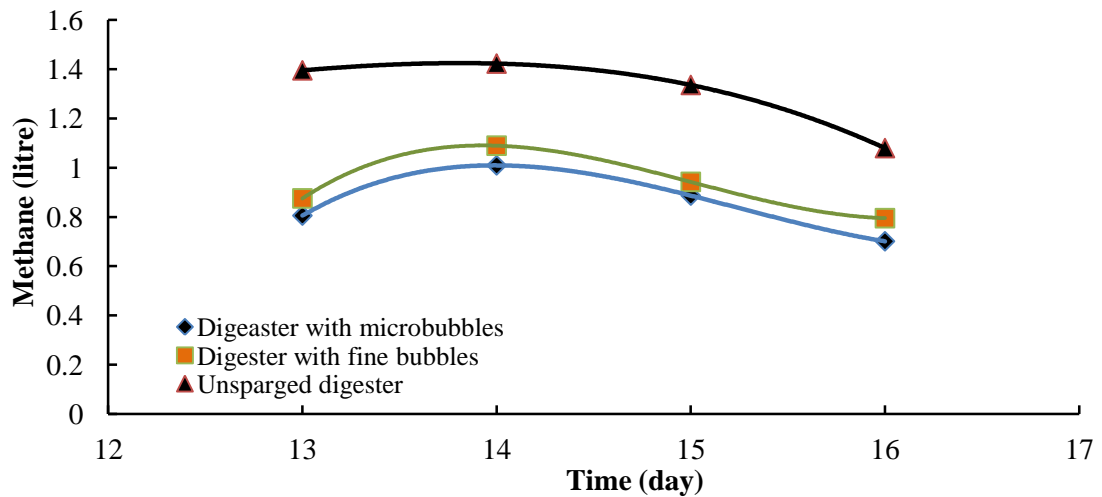


Figure 7.5: Methane produced from the sparged digesters and unsparged digester in the second stage

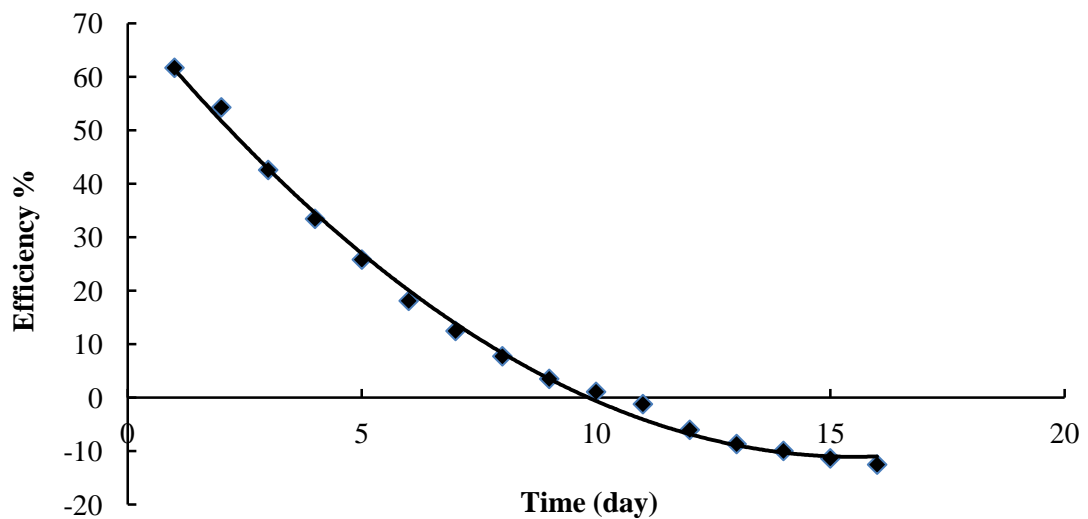


Figure 7.6: Efficiency of cumulative methane produced from the sparged digesters and unsparged digesters in the second stage

Then, the nitrogen sparging time was decreased into three periods. In the first period, the sparging period lasted for 30 min on each of four subsequent days; the second period of sparging lasted for 15 min on each of three days, and the third sparging period lasted for 5 min on each of four days. During these periods, the methane produced by the sparged digesters increased significantly. However, they both produced less methane than the unsparged digester (control digester), as can be seen in Figures 7.7 and 7.8.

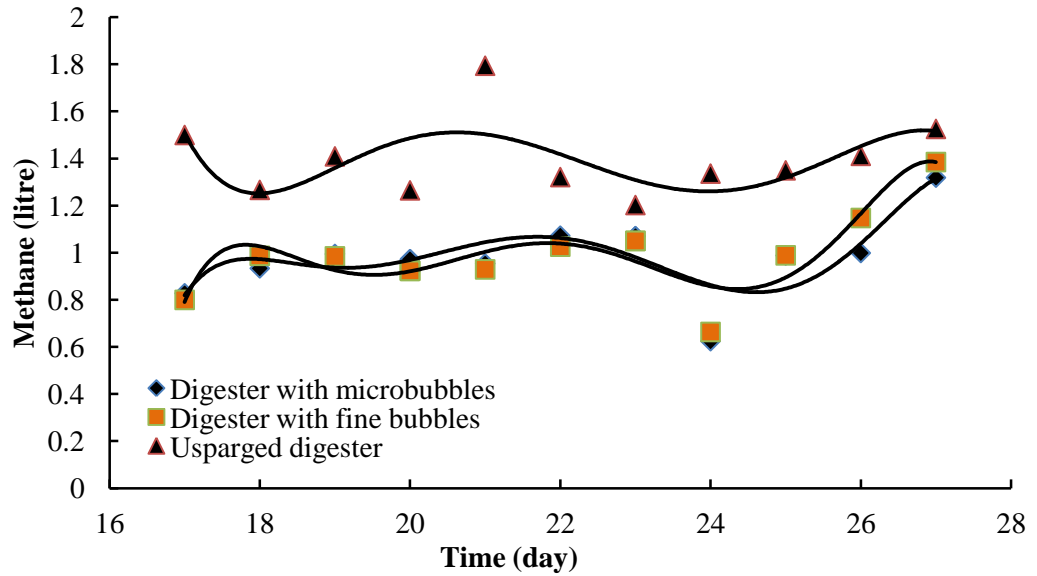


Figure 7.7: Methane produced from the sparged digesters and unsparged digester in the third, fourth, and fifth stages

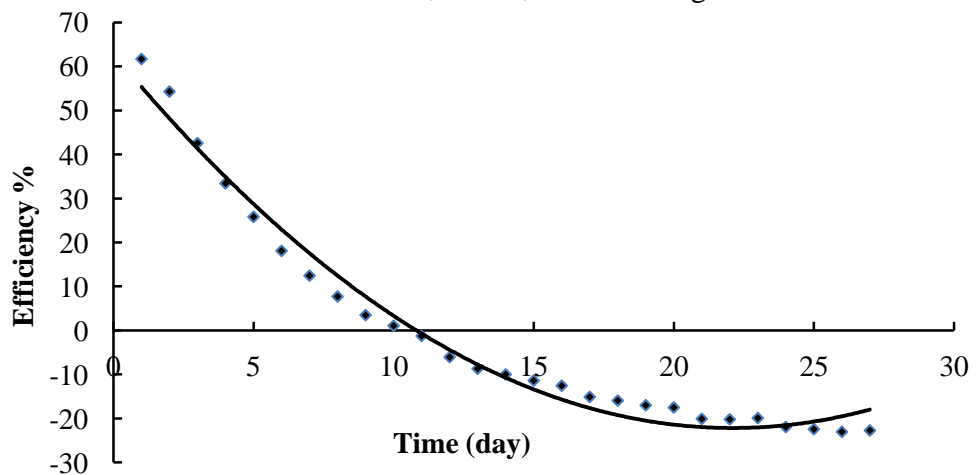


Figure 7.8: Efficiency of cumulative methane production from sparged digesters and unsparged digester third, fourth, and fifth stage

In the final stage of this part of the experiment, there was no sparging of pure nitrogen in either sparged digester. As evidenced by the methane remaining in the digester, the amount of methane produced was relatively small. Subsequently, the production of methane increased significantly due to saturation of the sludge with methane, as shown in the Figure 7.9. This increase minimized the difference between the amount of methane produced in both gaslift digesters and that produced in the control digester, as shown in the Figure 7.10.

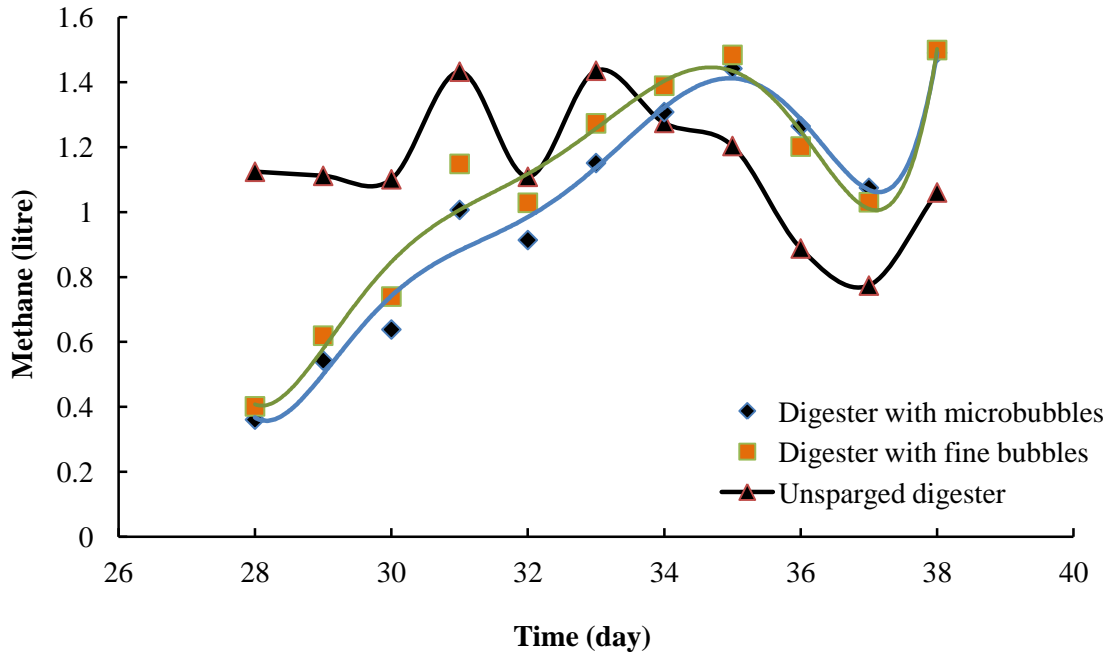


Figure 7.9: Methane produced from the sparged digesters and unsparged digester in the sixth stage

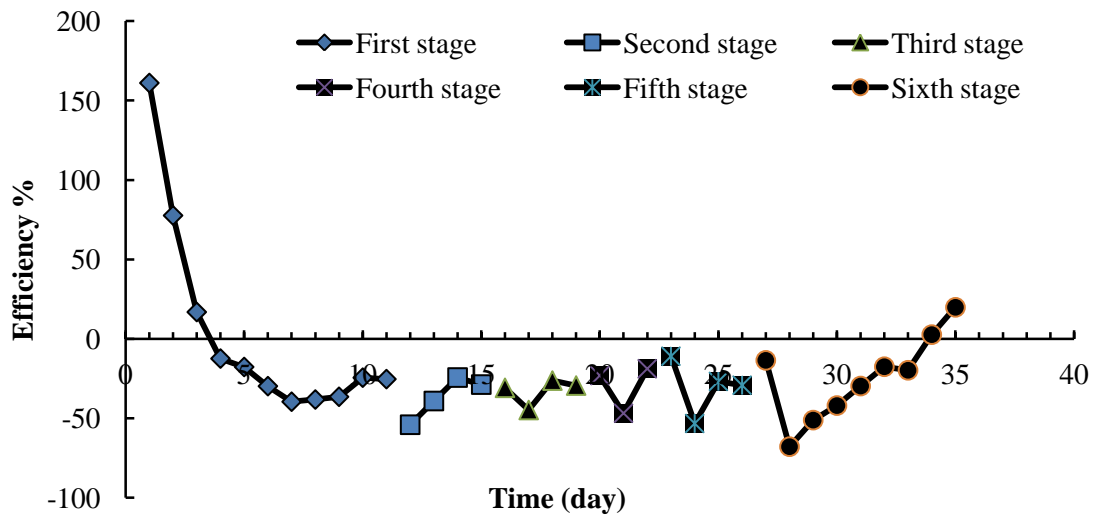


Figure 7.10: Efficiency of cumulative methane production from the sparged digesters and unsparged digester during the sixth stage

If these responses are collated with the same figure, a clear vision can be gained about the impact of sparging with nitrogen on methane production. Figure 7.11 shows the production of methane in the three digesters during different sparging periods across 38 days. It can be clearly seen that the decline in methane production occurred in the early

stages of the experiment, especially when the sparging time was 100 or 60 min. This decline then started to slow down when the sparging period was reduced to 30, 15 and 5 min. A big increase in methane production was achieved when the sparging with nitrogen was stopped completely.

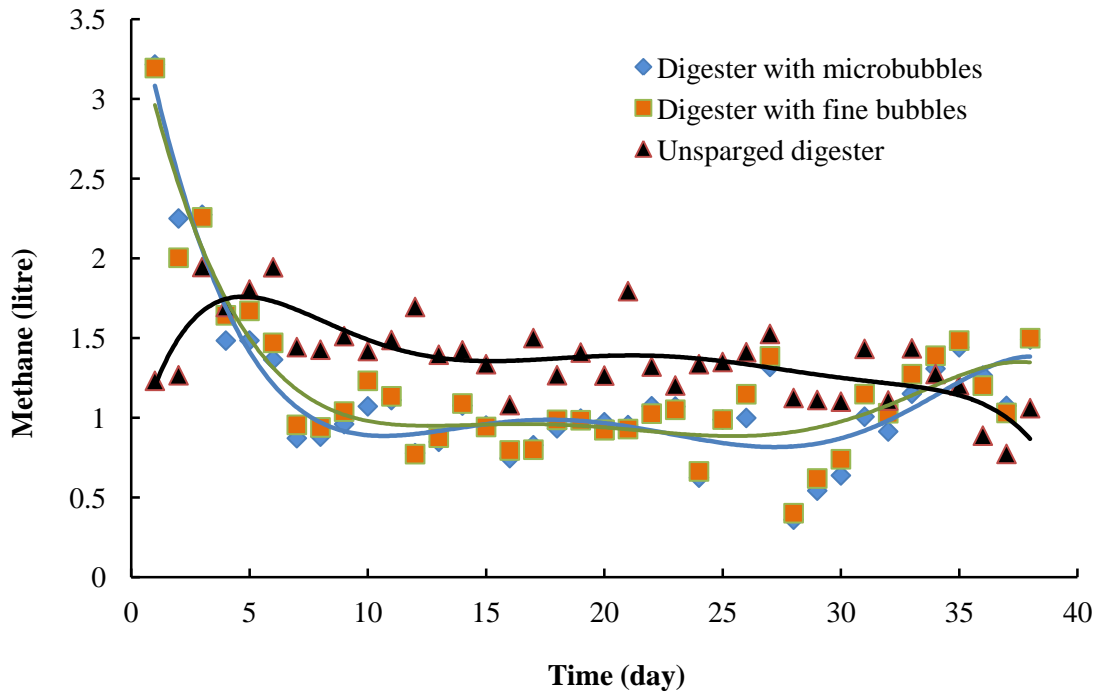


Figure 7.11: Methane produced from the sparged digesters and unsparged digester

Figure 7.12 shows the methane production before and after the sparging process in the gaslift digester. The results were compared with those for methane production in the control digester. The results indicate that the use of nitrogen for sparging in the gaslift digester leads to a decrease in methane production, with a subsequent return to normal methane production when the sparging process is stopped.

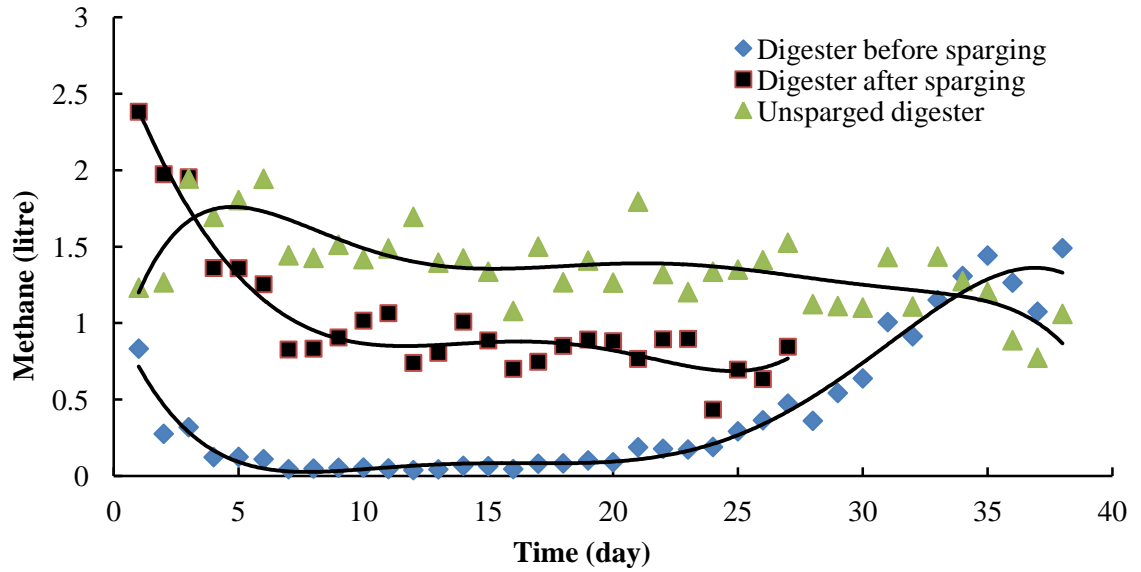


Figure 7.12: Methane produced from the sparged digester (before and after sparging the process) and in the unsparged digester

Figure 7.13 shows that the methane to carbon dioxide ratio reduces since the carbon dioxide produced in the acidogenesis stage and the acetogenic stage is stripped directly from the sludge by the sparging process. However, it should be noticed that the rate of which the ratio increased when sparging was stopped depends on the activity of the bacteria.

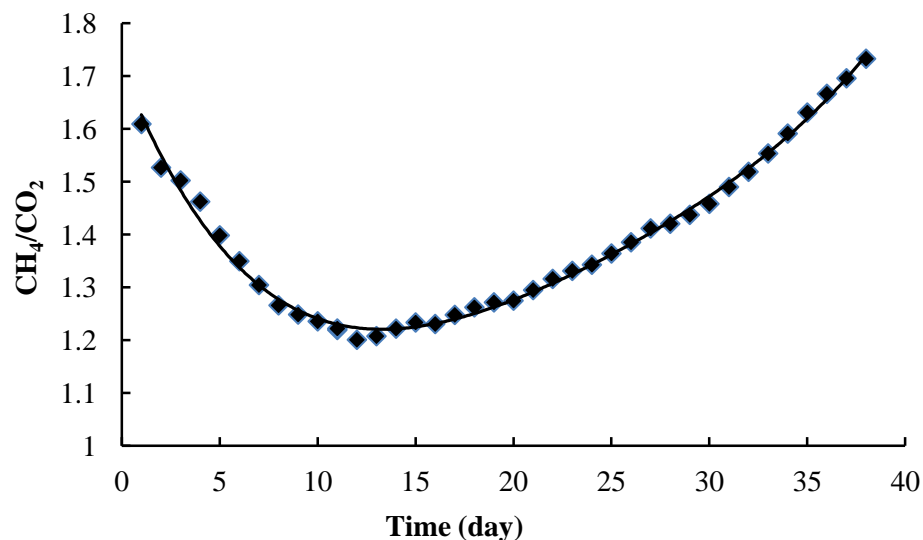


Figure 7.13: Methane to carbon dioxide ratio throughout the experiments

### 7.2.2 Effect of Microbubbles Generated by a Fluidic Oscillator

It has become known that using microbubbles generated by a fluidic oscillator in gas-liquid systems increases the contact area and residence time and thus improves the mass transfer rate between the two phases. This behaviour was demonstrated theoretically and experimentally in chapter three. However, the results obtained from this part of the study did not clearly distinguish the effects of micro-bubble and fine bubble systems on the production of methane using gaslift anaerobic fermentation system.

It can be seen that the effect of fine bubbles is roughly similar to that of the microbubbles. This is due to the fact that there was “excess” sparging in the experiment so the benefits of microbubbles compared to fine bubbles are not apparent. In other words, both technology (fine bubble and microbubble) provided similar stripping of gases for the relatively long sparging durations used.

We speculate that most of the gases were stripped in a short time which is why the length of bubbling times has little effect in this experiment.

### 7.2.3 Conclusion: Part I

Application of an airlift bioreactor for anaerobic fermentation was explored in this part of the investigation. Pure nitrogen was used for sparging using fine bubble and microbubbles generated by fluidic oscillator. The results obtained from the experiments show that the sparging process, using pure nitrogen in anaerobic fermentation to breakdown organic matter, has a negative effect on biogas production generally and on methane production especially. Less methane was produced in the airlift digester, with or without microbubbles than produced from the unsparged digester. Even when the sparging time was changed, the situation remained the same, although the decline in methane production was less when the sparging period decreased. Cessation of sparging led to a return of the production of methane to expected levels. It can be concluded that the use of sparging has an effect across the different stages of methane production, since the process does not just strip methane gas produced in the final stage, but also strips the carbon dioxide and hydrogen that are necessary for other bacteria involved methane production. The effects of sparging are therefore more complex than in bio-hydrogen fermentation, since anaerobic digestion involves gaseous intermediates ( $H_2$ ,  $CO_2$ ).

## 7.3 Sparging Using Nitrogen and Carbon Dioxide: Part II

Based on thermodynamic fundamentals, reducing the partial pressure of a product leads to an increase in the yield due to an increase in the absolute Gibbs free energy. This finding has been reported by many researchers. However, the data reported in the previous part of the current chapter demonstrated different results when the sparging system was applied to give a reduction of the partial pressure of the product gases in the anaerobic digester. The production of methane from the sparged digesters was less than in the conventional digester (control digester). The results indicated that stripping of methane was accompanied by removal of carbon dioxide, which is necessary for secondary production of methane by methanogenic bacteria. Therefore, when the sparging with pure nitrogen was stopped, the production of methane returned to normal levels.

The current part of the investigation aims to explore further the impact of sparging on methane production in anaerobic digestion. During 65 days of continuous experiments, the effects of sparging were studied based on different periods of sparging time under mesophilic conditions.

### 7.3.1 Results and Discussion: Part II.

The results obtained from the experiments in the first part indicated that a potential reason for the reduction of methane is that sparging the digester with pure nitrogen leads to stripping of the carbon dioxide, which is then not present in sufficient quantities for the hydrogen reducing bacteria to produce methane. Therefore, when the sparging process ceased for many days, the production of methane returned to normal levels.

The idea of this experiment was to sparge with carbon dioxide after nitrogen to replenish any carbon dioxide stripped out during the nitrogen sparging. The results in current study were obtained according to the materials and methodology that has been explained in part 3.5.2 of chapter three. The first regime of sparging ever day lasted for 7 working days. Figure 7.14 shows the cumulative methane production during this stage. The cumulative methane production from the gaslift digester was about 120% more than that from the control digester. Figure 7.15 shows that large amount of methane was obtained during sparging with pure nitrogen and carbon dioxide. However, the yield of methane fell from day to day as shown in the Figure 7.16.

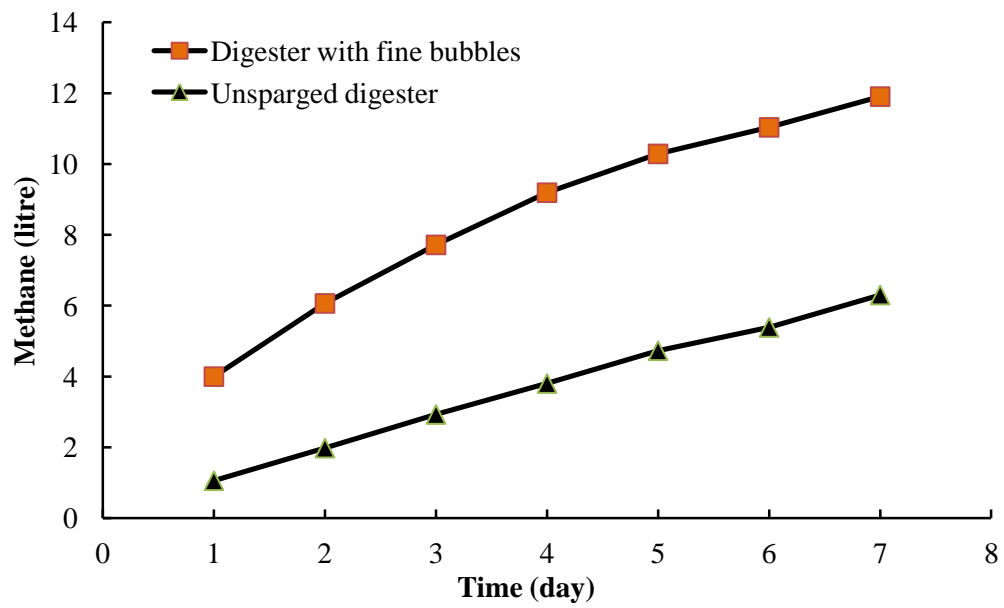


Figure 7.14: Cumulative carbon dioxide produced from the sparged digester and unsparged digester in the first stage

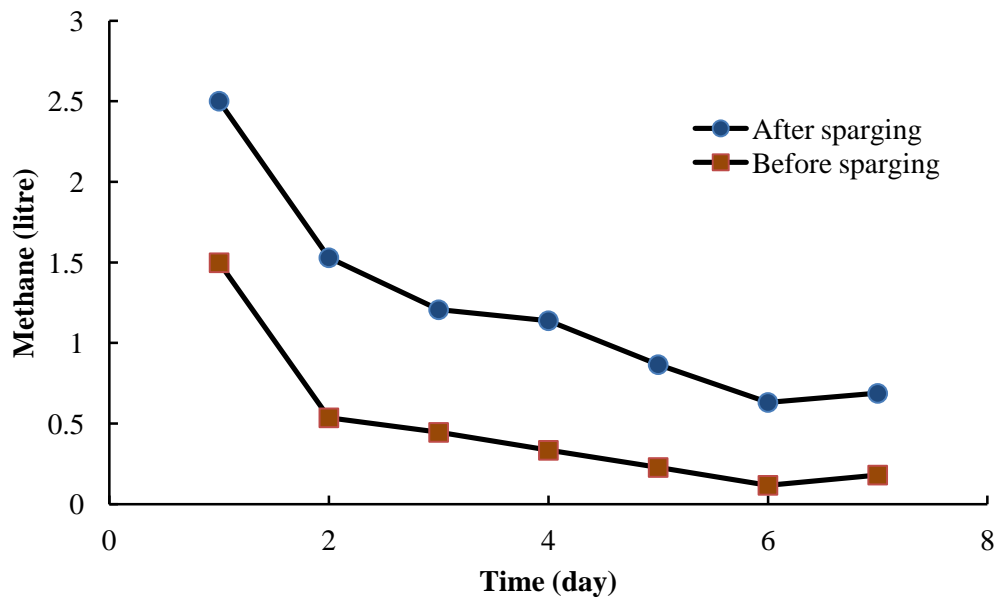


Figure 7.15: Methane produced from the sparged digester (before and after the sparging process)

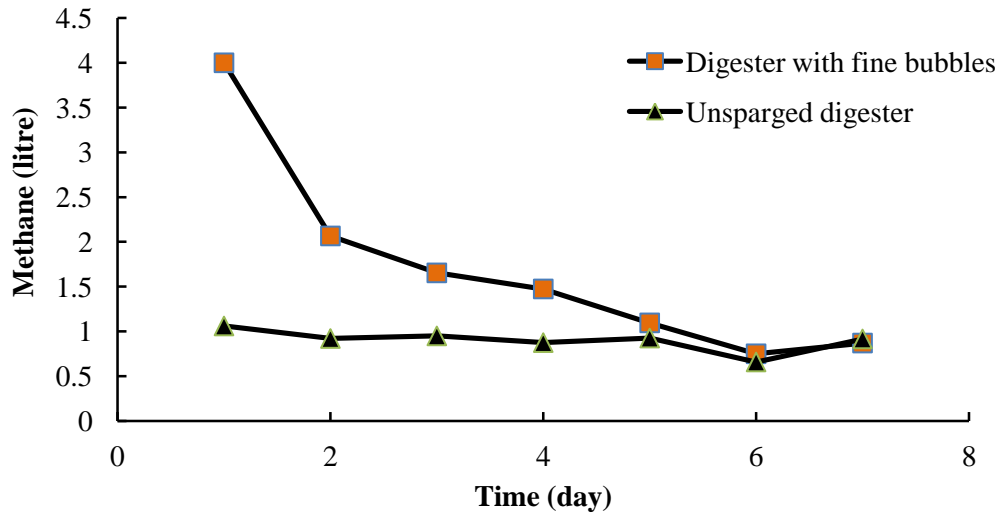


Figure 7.16: Methane produced from sparged digester and unsparged digester in the first stage

The current study hypothesized that daily sparging was recovering too much hydrogen and therefore having deleterious effect on methane production. Therefore the decision was to reduce the frequency of sparging.

For the sparging regime in the second stage, sparging of the gaslift digester with pure nitrogen and carbon dioxide was carried out every 48 hours. Figure 7.17 indicates that the production of methane increased slightly during these periods of operation.

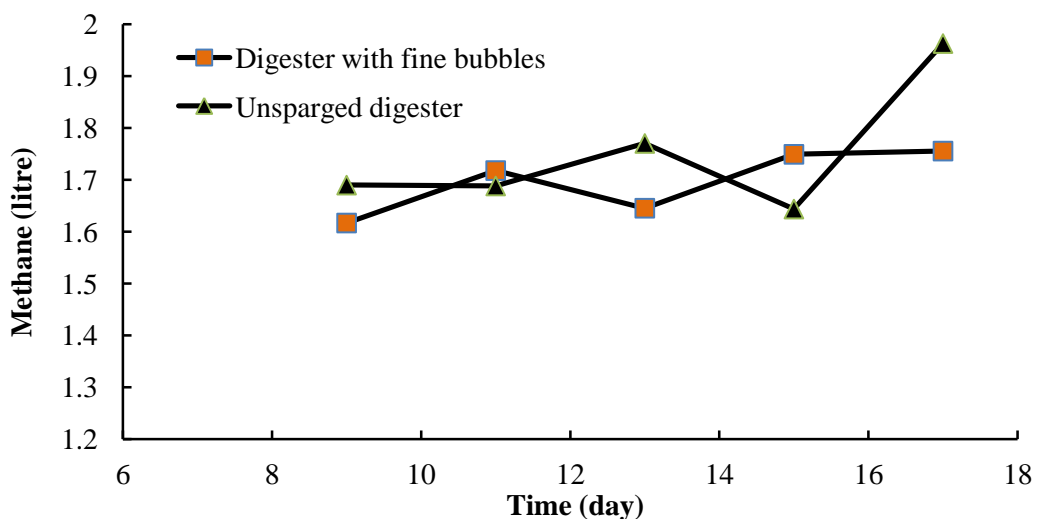


Figure 7.17: Methane produced from sparged digester and unsparged digester in the second stage

The efficiency of methane production in both digesters (i.e. gaslift reactor and unsparged digester) was estimated for the first stage and second stage and the results are collated in the same Figure 7.18. Although the efficiency of methane production in the gaslift digester in the first stage was greater than that of the unsparged digester, the efficiency decreased continuously. However in the second stage, the decline in the efficiency of methane production was reduced.

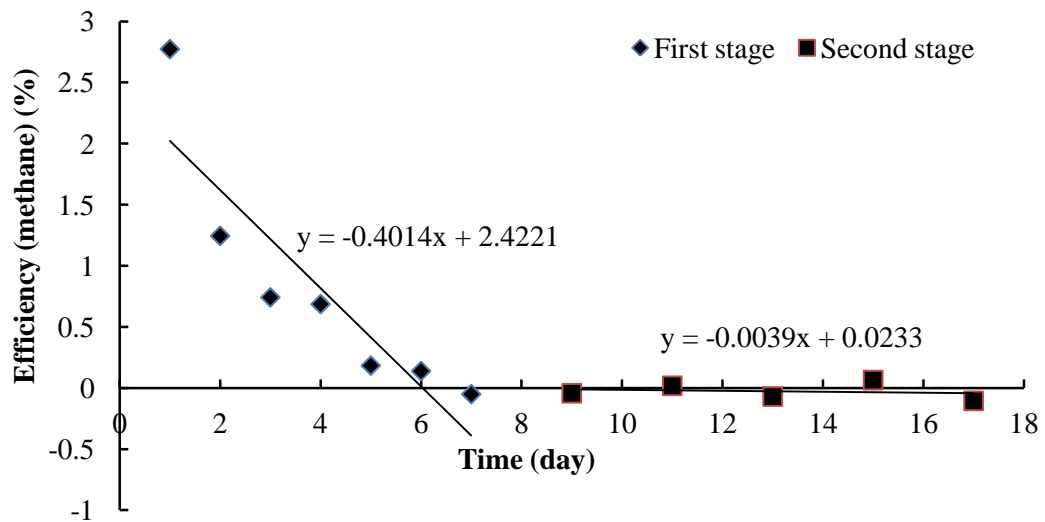


Figure 7.18: Efficiency of cumulative methane production from sparged digester and unsparged digester in second stage

As discussed above, the production of methane in anaerobic digestion requires the presence of carbon dioxide and hydrogen, as reactants, at the same time. The period of bubbling was therefore increased to allow the bacteria to produce more hydrogen to react with the carbon dioxide. However, stopping the sparging process in the gaslift anaerobic digester for 48 hours did not achieve the effect of increasing methane production within this digester. According to the results, the production of methane was stable at 1.7 litres per day. This equalled the amount of biogas produced in the conventional digester; thus, the efficiency was about zero during this period. However, cumulative methane production by the gaslift digester was about 52% more than that of the unsparged digester due to the increased rate of production in the initial daily sparging stage as can be seen in the Figure 7.19.

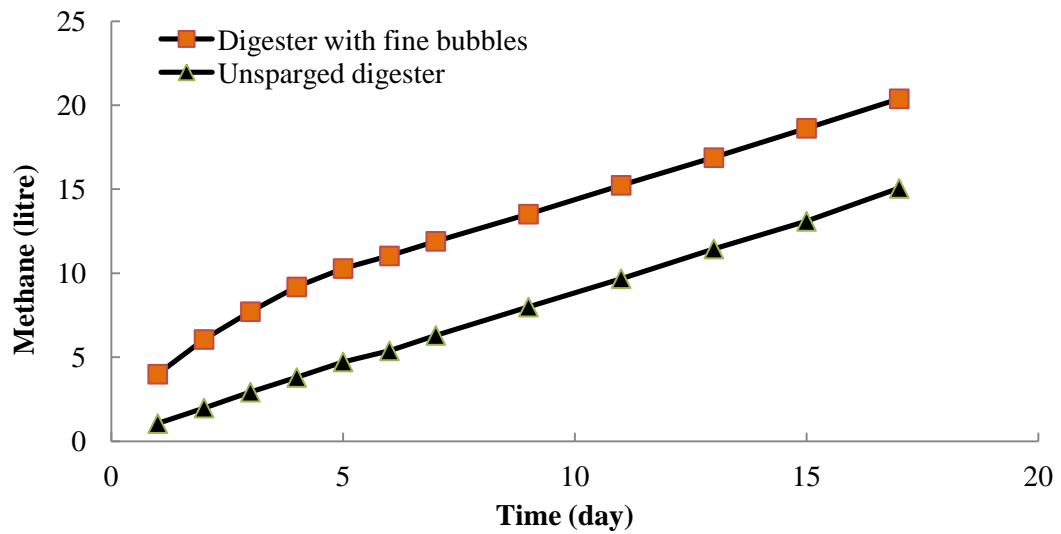


Figure 7.19: Cumulative carbon dioxide production from the sparged digester and unsparged digester up to the second stage

In the third stage, the gaslift digester was sparged every 72 hours (3 days). The period of operation was 12 days. Again, the target of this stage was to provide enough time to generate hydrogen to react with carbon dioxide via methanogenic bacteria to produce methane. Figure 7.20 displays methane production from the gaslift and conventional digesters, while Figure 7.21 shows the efficiency of methane production in the gaslift digester compared with the unsparged digester for days 21 to 29 of the period of operation.

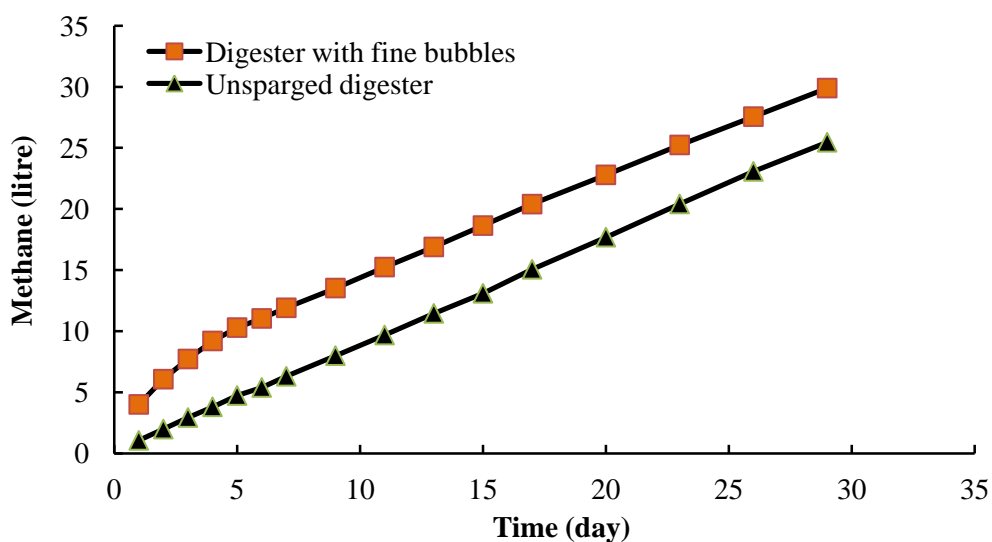


Figure 7.20: Cumulative carbon dioxide production from the sparged digester and unsparged digester up to the third stage

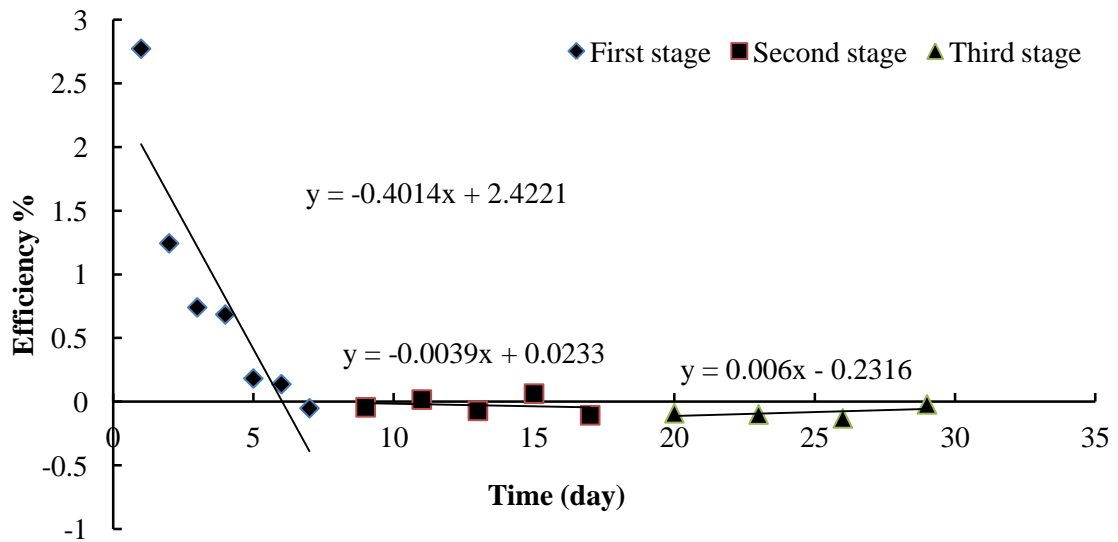


Figure 7.21: Efficiency of cumulative methane production from the sparged digester and unsparged digester up to the third stage

It can be seen that the effect of sparging once every three days is to give stable daily methane production at a very similar rate to the unsparged reactor. Indeed, when the frequency of sparging was reduced still further to once every five days and lower, the same results was observed. In other words, the daily production rates of the sparged and unsparged digester are very similar and quite constant over time.

The gaslift digester produced less methane than the conventional digester. The efficiency remained at around -6%. Although the unsparged digester produced more methane than the gaslift digester, cumulative methane production from the gaslift digester still exceeded that of the conventional digester because methane production in the unsparged digester was less than the cumulative methane production in the gaslift digester in the first days, as shown in the Figure 7.22. It seems that stopping the sparging for a longer period increases the amount of methane stripped from the sludge; however, it is difficult to strip more methane than the amount found originally in the digester, either as bubbles, dissolved, or in the headspace of the digester. This is evident from the results obtained from the subsequent tests whereby the sparging process was stopped for 8 and 13 days as illustrated in Figure 7.23.

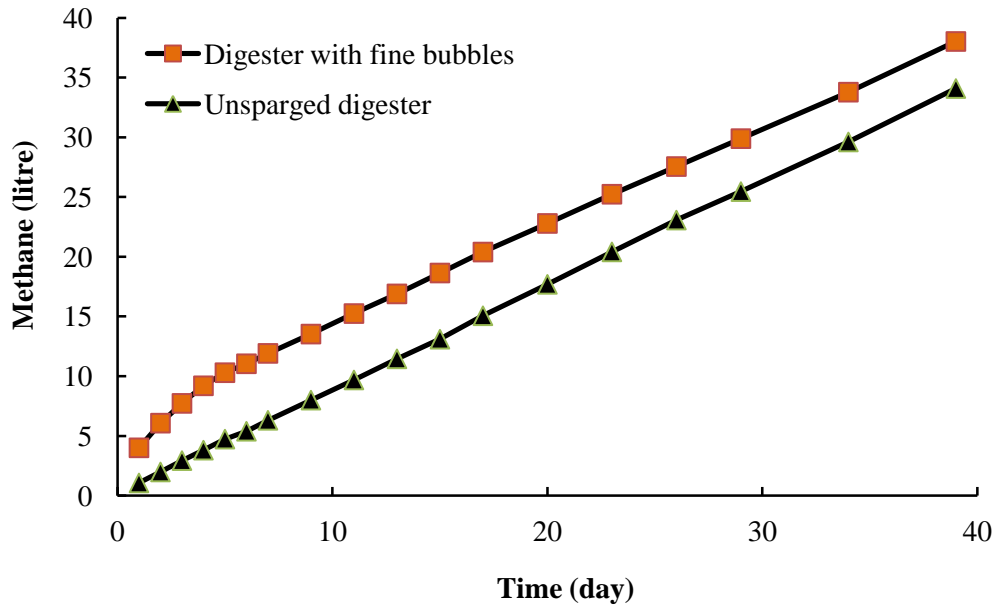


Figure 7.22: Cumulative carbon dioxide production from the sparged digester and unsparged digester up to fourth stage

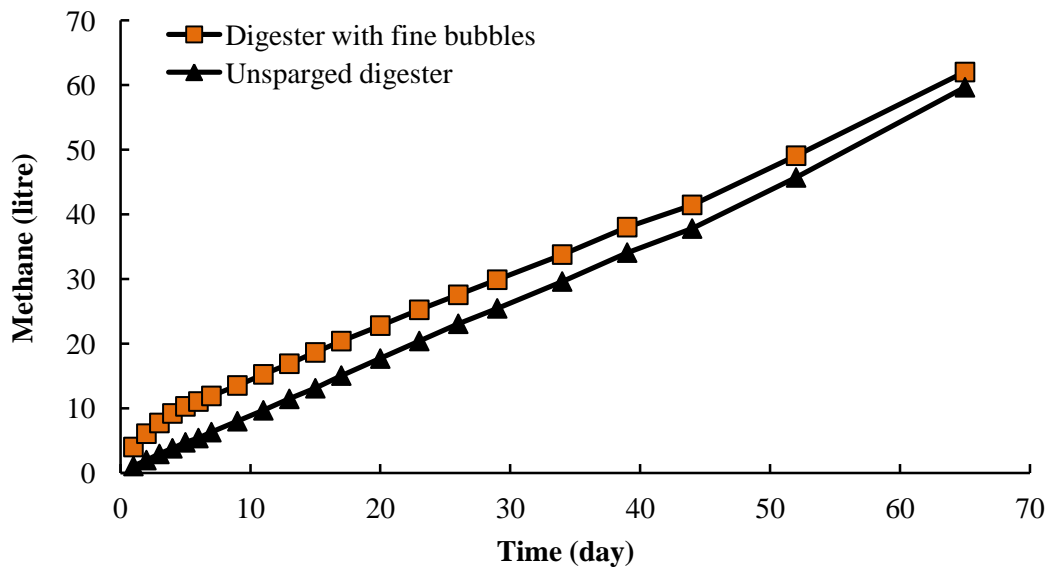


Figure 7.23: Cumulative carbon dioxide production from the sparged digester and unsparged digester up to fourth stage

For example, in first the bubbling process (i.e. at the beginning of the experiment), the amount of methane stripped was approximately 2.5 litres, whilst daily continuing of the sparging led to a decrease in the methane stripped from the digester as shown in the Figure 7.24. However, stopping the bubbling process gave the bacteria time to

compensate the stripped biogas. Therefore, it can be seen that the amount of methane increases when the non-sparging time increases.

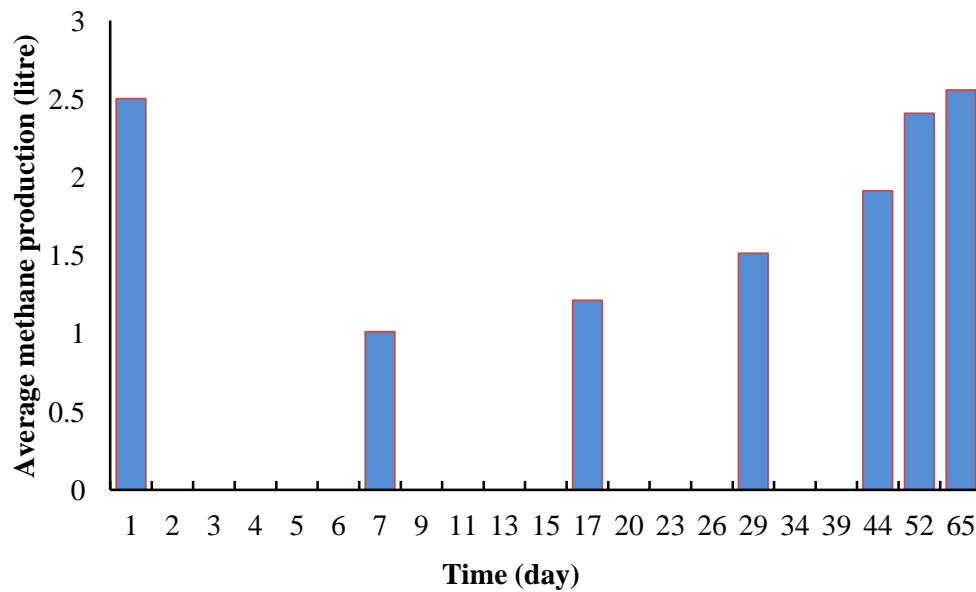


Figure 7.24: Average methane production from sparged digester

As is well-known, the solubility of methane in distilled water is about 0.017 mg/l, this means that the amount of methane that can dissolve in each digester is no more than 0.24 L. However, the volume of methane stripped from the sludge was about 2.5 L (i.e. 25% of the gaslight digester's volume). This means that methane held in the unsparged digester, either in dissolved form or as small trapped bubbles was the equivalent of up to 12 times its solubility in distilled water. In fact, density, viscosity, and bubbles size are important parameters in determining the terminal velocity of the bubbles in the fluid, according to Stok's equation. In addition, the suspended solids in the sludge present obstacles that significantly hamper even the big bubbles from rising to the top. The sparging process contributes to moving the suspended solids away from the big bubbles, thus the effect of suspended solids on the rising biogas bubbles is reduced, whilst, the small bubbles become attached (by coalescence) to nitrogen bubbles to form big bubbles that are able to overcome the effects of the physical properties of the sludge. Thus, when the bacteria produce biogas, that biogas dissolves in the sludge until a state of equilibrium is achieved, and then the remaining bubbles either stay as bubbles or rise upward and leave the sludge.

In the conventional digester, because the sludge is already over-saturated, the methane produced from the anaerobic bacteria will leave the digester directly in bubbles, and go

into the collector. Therefore, the sparging process will help to remove all methane (dissolved or remaining bubbles) from the sludge. Meanwhile, the anaerobic bacteria will continue to produce methane until the sludge reaches a state of saturation. Then, the sparging process can be repeated. The time required to reach a state of saturation with methane depends on the activity of the anaerobic bacteria.

The headspace also contains some biogas, since the pressure in this area of the reactor is 1 atm, as mentioned in chapter six part II; therefore, the biogas exiting from the sludge in the gaslift digester remains in the headspace until the pressure increases to more than 1 atm. In addition, biogas can be stripped if the digester is sparged with pure nitrogen or any other gas, whilst increasing the sparging time does not lead to the stripping of any more methane than that originally found in the sludge or in the headspace. In addition, the growth of anaerobic bacteria is very slow, as was demonstrated in our separated experiments. The aim of those experiments was to discover how long a period of anaerobic digestion was needed to produce normal concentrations of methane in mesophilic conditions. Same lab-scale digesters were used for this process and under the conditions shown in the Figure 7.25.

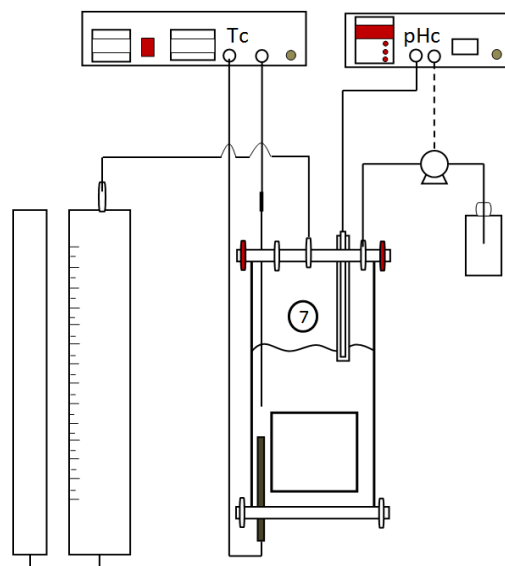


Figure 7.25: Schematic of experimental work used in the separated tests

Figure 7.26 shows methane produced from the anaerobic digester in the separated experiment, while Figure 7.27 illustrates the concentration of methane and carbon dioxide in the biogas produced from the same digester. It can be seen that 19 days were required to achieve the desired concentration of methane and carbon dioxide when depending on the activity of the bacteria.

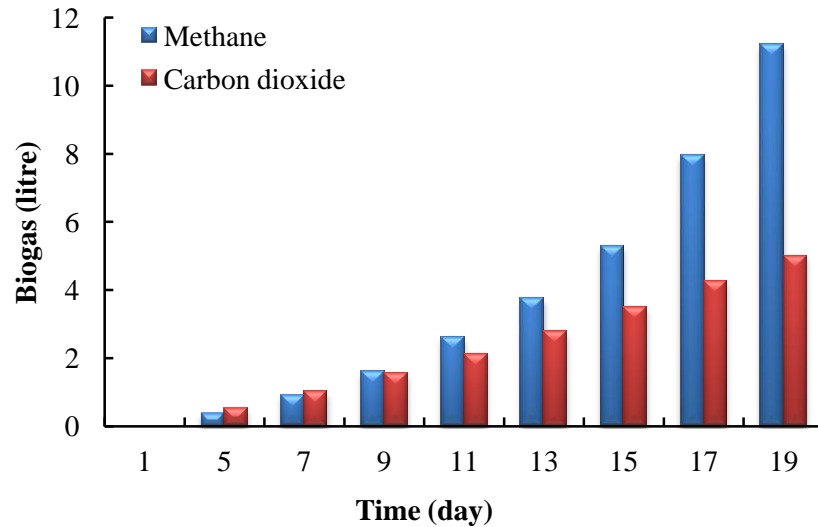


Figure 7.26: Methane and carbon dioxide produced from anaerobic digestion

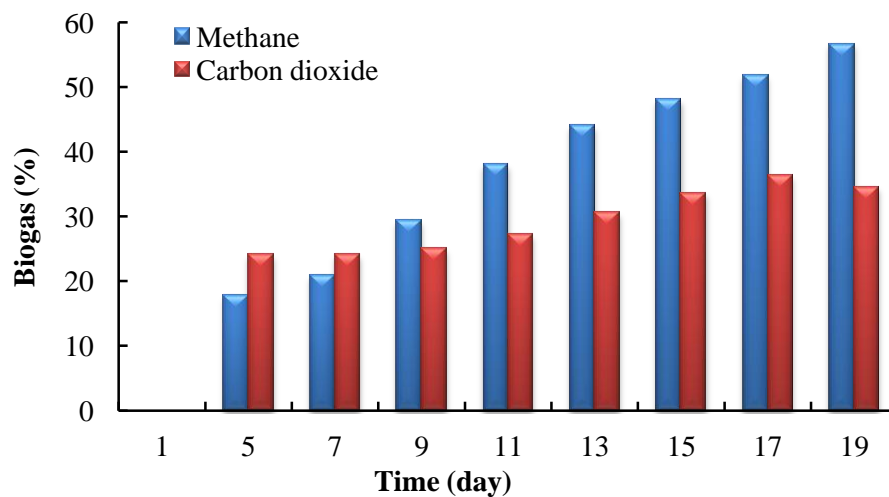


Figure 7.27: Percentage of methane and carbon dioxide in the biogas

From above, it can be concluded that sparging the digester with pure nitrogen did not cause any more methane to be stripped than was present at that moment. Compensation of the stripped methane or biogas by the anaerobic bacteria takes a long time.

Figure 7.28 illustrates the methane production *before* the sparging process in the gaslift digester and the conventional digester. The methane concentration in the biogas produced by the gaslift digester decreases in the first stage, whilst it begins to increase in the following stages (stages 2, 3, 4, 5, and 6).

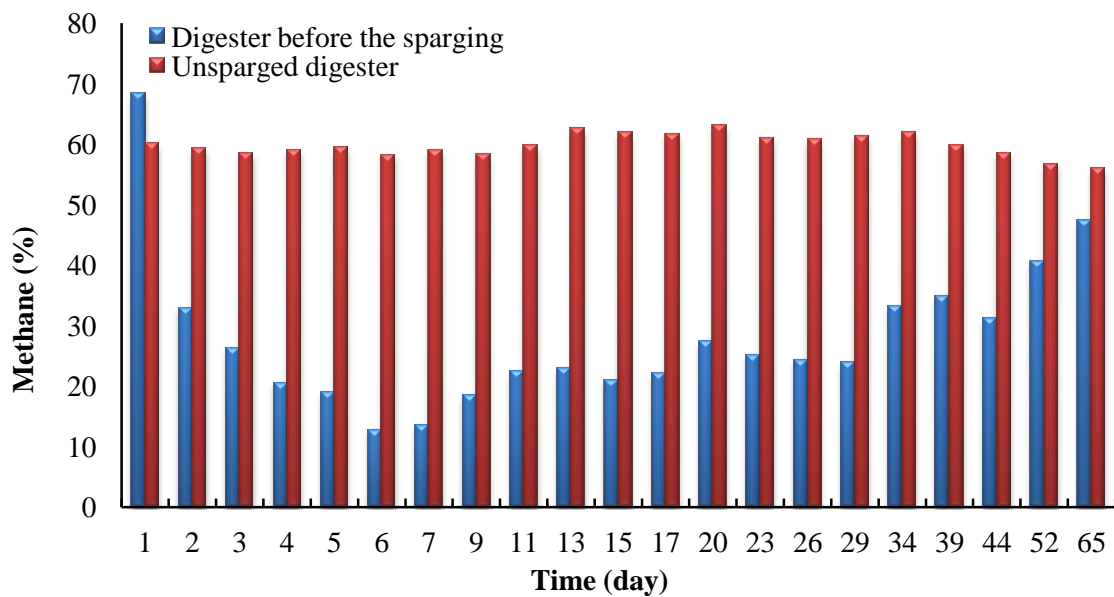


Figure 7.28: Percentage of methane produced in the sparged digester and unsparged digester

The lower methane production of the first stage was particularly apparent in the first six days (about 12%), while in the fifth stage, the percentage of methane in the biogas rose to about 40%. This increase in the concentration of methane in the produced biogas reduces the difference in the amount of methane produced in the gaslift and conventional digesters.

### 7.3.2 Application of Microbubbles Technology

The innovative approach of using microbubbles generated by a fluidic oscillator was applied in the experiments in this part of the study. The experiments gave positive results on the rate of transfer of gases from the sludge to the gas bubbles, as shown in Figure 7.29. The cumulative methane production from the digester operated with microbubbles is larger than that of the digester operated with fine bubbles. However when results were compared with those obtained from the conventional digester, it was found that application of this innovative approach to a sparging system in anaerobic digestion did not lead to an increase methane production as is illustrated in Figure 7.30. The figure suggests that efficiency of methane production decreases significantly, even when the microbubble technique is used in anaerobic digestion.

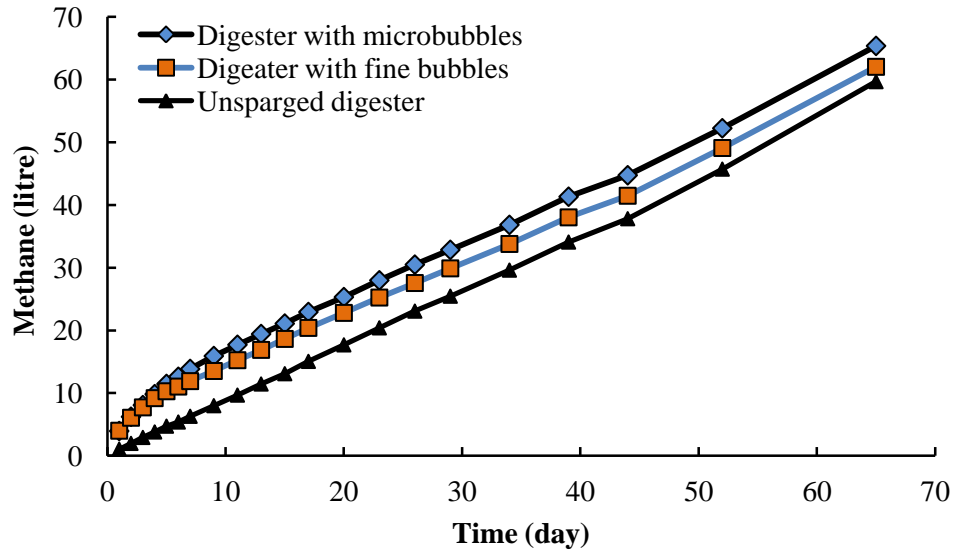


Figure 7.29: Cumulative methane production from the gaslift digester using microbubbles generated by a fluidic oscillator, gaslift digester without fluidic oscillator, and unsparged digester

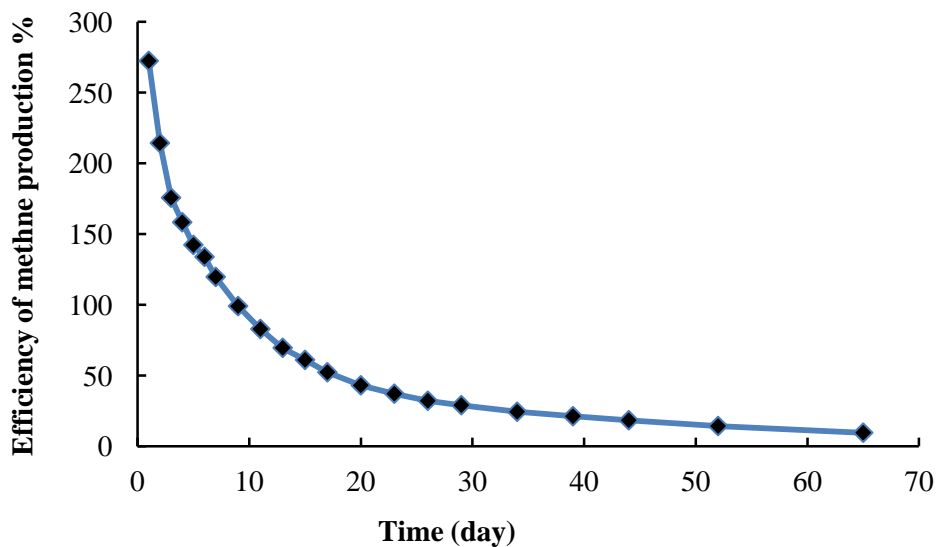


Figure 7.30: Efficiency of methane production from a gaslift digester using microbubbles generated by a fluidic oscillator and in an unsparged digester

### 7.3.3 Conclusion: Part II

This part of the study has tested the hypothesis that compensation of carbon dioxide stripped by sparging using pure nitrogen can increase methane production. The results obtained were based on seven stages of testing, with different sparging frequencies. The data illustrated that the sparged digester produced less methane than the unsparged digester, even when the non-sparging periods were increased. The results indicated that

compensation of carbon dioxide in the sparged digester does not lead to increased production of methane, even for very infrequent patterns of sparging.

It was found in this part of the study that the application of microbubbles generated by a fluidic oscillator in a sparging system does not give a sustainable increase in methane production in comparison to methane production in a conventional anaerobic digester.

## **7.4 Recycling the Undiluted Biogas in Anaerobic Digestion and Diluted Biogas with Carbon Dioxide: Part III**

According to our previous experiments, sparging in anaerobic digestion leads to an initial increase in methane yield, whilst a subsequent reduction in methane yield is then observed. It seems that the stripping process leads to the stripping of other gases, for instance, carbon dioxide and hydrogen, which are required in order for the bacteria present to produce methane. In fact, stripping the carbon dioxide from the digestion process not only affects the ability of hydrogen-reducing bacteria to produce methane, but also affects acetogenic bacteria that convert propionate and butyrate to acetate, which is consumed by methanogenic bacteria to form methane. Therefore the stripping system using pure nitrogen in anaerobic fermentation can inhibit the activity of these two types of bacteria (acetogenic and methanogenic bacteria).

As was discussed in the second part of this chapter the additional sparging with carbon dioxide after nitrogen sparging in order to replenish it did not produce a sustained increase in methane yield as compared with that in the unsparged digester.

However the carbon dioxide sparging did have some compensatory effect since the reduction in methane production between the unsparged digester and sparged digester was less than that observed in the experiments in the first part of this chapter, where pure nitrogen was used in the sparging system.

Based on the results obtained from the two previous experiments, recycling of the biogas produced from the digester will now be discussed. The targets were to increase the mixing efficiency, stripping the biogas produced and to increase the amount of biogas concentrated in the digester. These aims were pursued by conducting two experiments:

1. Recycling the undiluted biogas in the digester.
2. Recycling the biogas after dilution by adding carbon dioxide.

## 7.4.1 Results and Discussion: Part III.

### 7.4.1.1 Recycling the Undiluted Biogas

As mentioned earlier, sparging in the gaslift digester using pure nitrogen leads to stripping of other gases that are required for certain bacteria to produce methane. To investigate this carbon dioxide was compensated for the second experiment.

The experiment in this part of the study was aimed at maintaining the concentration of biogas in the sludge by recirculation of biogas produced in the same digester. The study in this part depended on the setup of experiment that explained in parts 3.5.3 and 3.5.3.1 of chapter three. Figure 7.31 represents methane production from sparged and unsparged digestion. It can be clearly seen that more methane was produced from the sparged digester than from the unsparged digester. This behaviour was not evident in previous experiments when either nitrogen or nitrogen-carbon dioxide were used.

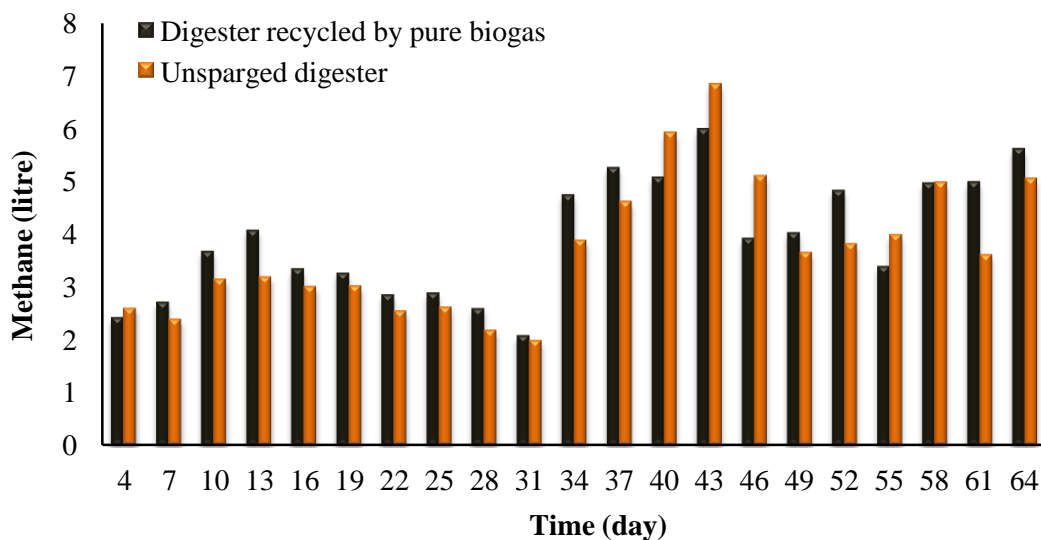


Figure 7.31: Methane produced from sparged and unsparged digester

In addition, the conventional digester produced less methane than the sparged digester for the first 37 days. Then, the pattern of behaviour changed, since the unsparged digester began to produce more methane than the other digesters, especially between 40 and 46 days. The reason for this reduction is that sedimentation of suspended solids occurred in the conventional digester, which made the sludge lighter than the sludge in the other digesters. This process contributed to a reduction in thermal resistance, thus the heat transfer flux to all areas of the reactor increased. As a result, during days 40-46

then unsparged (conventional) digester was operating closer towards thermophilic operation (i.e. temperature= 42 °C) and this gave temporarily increased methane production until this issue was rectified. The problem was addressed by changing the setting on the controller to ensure that all the digesters were operating at 35°C as shown in Table 7.1. After fixing the problem, methane production in the unsparged digester returned to normal.

Table 7.1: The temperature of the sludge before and after adjusting the setting of the controller

<b>Temperature of sludge</b>			
	Conventional digester	Sparged digester with pure biogas	Sparged digester with biogas and CO <sub>2</sub>
Before setting	42±1	35±1	35±1
After setting	35±1	35±1	35±1

#### **7.4.1.2 Recycling the Diluted Biogas**

In the second section, the methane concentration in biogas produced from sparged digestion was diluted by carbon dioxide as was described earlier.

The aim of the dilution was to strip more methane from the sludge, since the transfer of methane from the liquid phase to the gas phase increases when the concentration of methane in the bubbles is less than that in the sludge. The results in current study were obtained according to the materials and methodology that has been explained in parts 3.5.3 and 3.5.3.2 of chapter three. Figure 7.32 shows the cumulative methane production from the conventional digester and sparged digester after dilution of the biogas.

Whilst similar problems occurred to those experienced in the previous part, the cumulative methane production was higher than with conventional unsparged operation.

Recycling the biogas to the anaerobic digester in both cases led to an increase in methane production, maintaining the concentration of gases in the digestion, improving the efficiency of mixing and preventing the formation of thermal layers in the reactor.

More importantly, the work described here has furthered the development of a novel heating system for anaerobic digestion, which was adopted mainly on the basis of the

results of this experiment and subsequent experiments discussed in the latter part of this chapter. The proposed heating system for anaerobic digestion will be explained in chapter eight of this thesis.

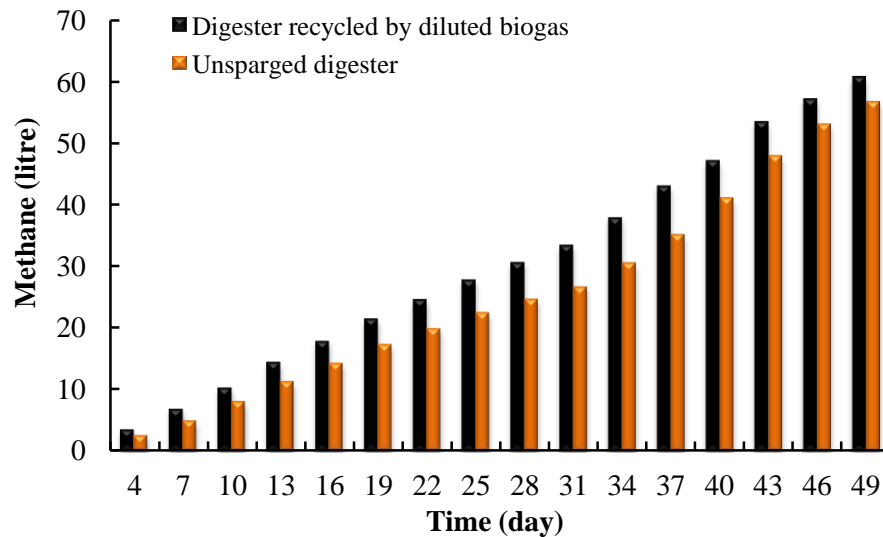


Figure 7.32: Cumulative methane production from sparged digester and unsparged digester.

The data obtained from the experiment illustrated that recirculation of biogas (either pure gas or biogas diluted with carbon dioxide) in anaerobic digestion did not, contrary to previous studies, reduce the performance of the digestion, although the proportion of methane in the gas phase reached as much as 60%. In fact, we observed an increase in the total methane produced by using sparging with both undiluted recycled biogas as well as recycled biogas that had been diluted by carbon dioxide. Thus the biodegradation steps continued without any negative effect on the production of methane. Low solubility of methane in the liquid and high carbon dioxide concentration in the biogas contributed to controlling the solubility of methane in the liquid phase.

On the other hand, the presence of methane gas and carbon dioxide together helped in controlling the environment of the whole process. Indeed, the methane acted as a determinant of the amount of carbon dioxide dissolved in the liquid phase. Therefore, it can be noted that the pH value remained within the required level as shown as in the Figure 7.33.

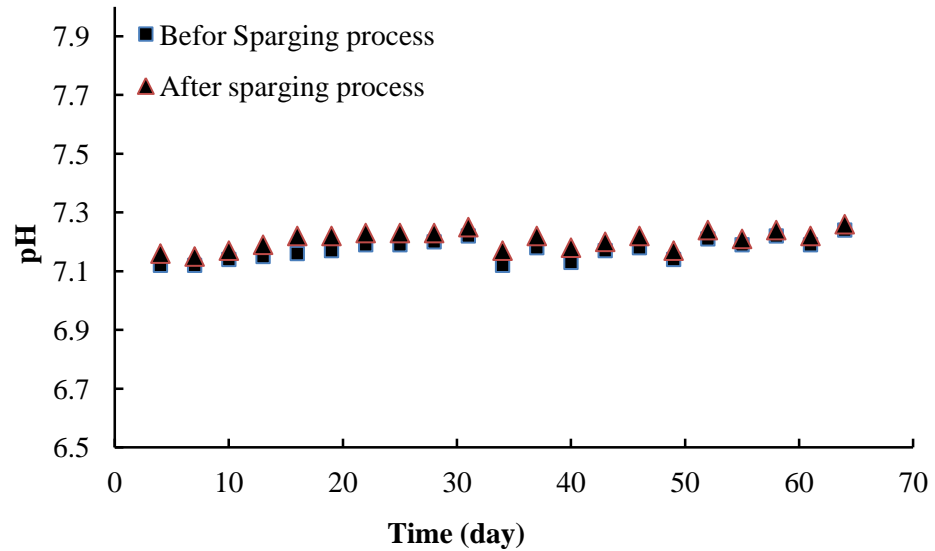


Figure 7.33: pH values in the sparged digester (before and after bubbling process)

In addition the recycling process causes stripping of hydrogen sulphide, the presence of which has a negative effect on the efficiency of methanogenic bacteria in the digester.

### 7.4.2 Conclusion: Part III

The effects of recycling biogas on the efficiency of anaerobic digestion were investigated in these experiments. Two experiments were carried out to explore the recirculation process. The first experiment involved recycling pure biogas, while the second experiment involved recycling diluted biogas (20 % methane and 80% carbon dioxide).

The results obtained from these experiments demonstrated that recycling the biogas does not reduce the efficiency of the process; in fact, the data show that the gaslift anaerobic digester produced more methane than the unsparged digester.

These results led to the development of the heating system for anaerobic digestion, which has been adopted mainly on the basis of results of this experiment. The heating system, which will be explained in chapter eight of this thesis, involves utilisation of recycled biogas for the purposes of improved flow dynamics, mass transfer and heat transfer when compared to conventional unsparged digesters.

## 7.5 Sparging Using Pure Carbon Dioxide: Part IV

The present study involves sparging pure carbon dioxide into an anaerobic digester where the organic matter is broken down by the microorganisms in the absence of oxygen. Carbon dioxide, which represents an electron acceptor, reacts with hydrogen to form one-third of the methane produced; while two-thirds are formed from acetate through acetoclastic methanogenesis.

The sparging process was carried out using microbubble generated by fluidic oscillation, of which the main principles were described in chapter two, while an investigation of the benefits of microbubble was conducted in chapter three and four.

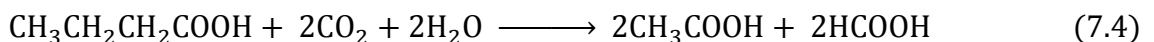
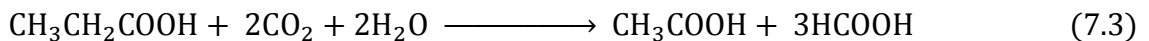
### 7.5.1 Results and Discussion: Part IV.

In anaerobic digestion, methane production by methanogenic bacteria is carried out via two routes: fermentation of acetate and the bio-reaction of carbon dioxide and hydrogen according to the following equations:



In spite of the absolute Gibbs free energy of acetate reduction being less than that of hydrogen reduction, the first reaction produces more methane than the second reaction (Metcalf and Eddy, 1991).

In addition, carbon dioxide is used for the formation of acetate, which represents an essential material in the production of methane from butyrate and propionate, as is shown in the following equation.



Therefore, sparging with carbon dioxide increases the production of methane from carbon dioxide with hydrogen also increase methane production for the fermentation of butyrate and propionate to produce acetate, which also converts to methane.

Materials and methodology used in the current study was explained in part 3.5.4 of chapter three. Figure 7.34 shows that the digester sparged by carbon dioxide produces more methane than the conventional digester.

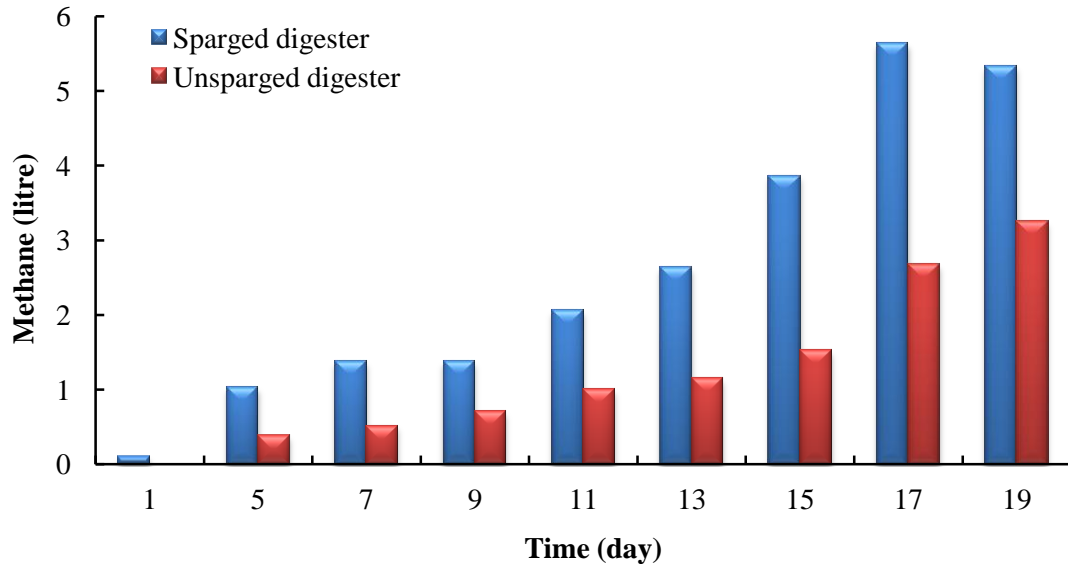


Figure 7.34: Methane produced from the gaslift digester and unsparged digestion over 19 days of operation

Sparging the carbon dioxide also helps in the removal of methane found in the headspace of the digester. After the sparging process is complete, the equilibrium partial pressure of the methane in the headspace is reduced from the value before sparging. The methane level increase as the methane found in the sludge or produced from the bacteria is transferred to the headspace without sparging.

High interfacial area, generated by the small microbubble size, and the low solubility of methane are parameters that play an important role in this process, since the use of the sparging system removes the largest amount of methane in a shorter time and has less effect on the value of the pH which is quickly compensated and controlled at the required level; thus the process did not require any further modification of pH value, as can be seen from Figure 7.35. The results show that production of methane in the digester with carbon dioxide exceeded the quantity produced by the other digester (unsparged digester) by 109% as shown in Figure 7.36.

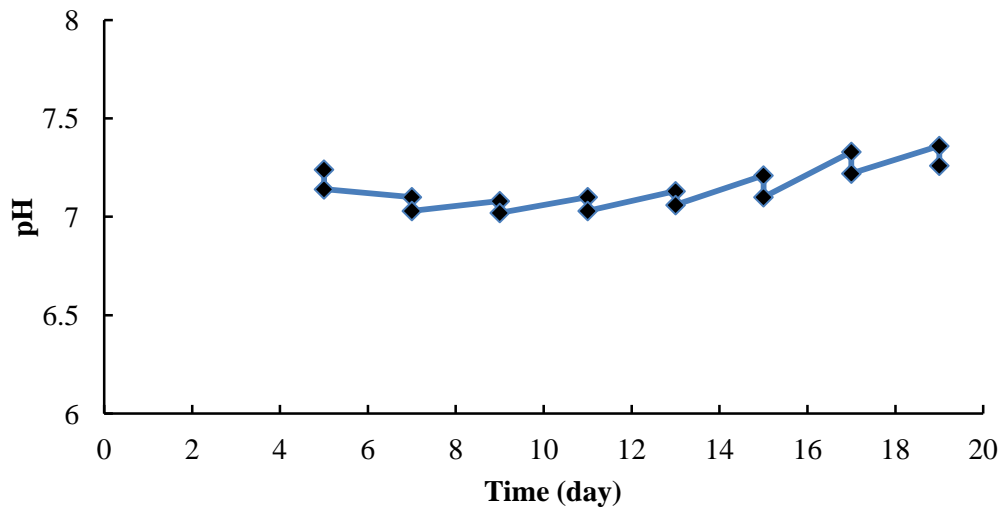


Figure 7.35: pH value in the gaslift digester sparged by pure carbon dioxide for 5 min

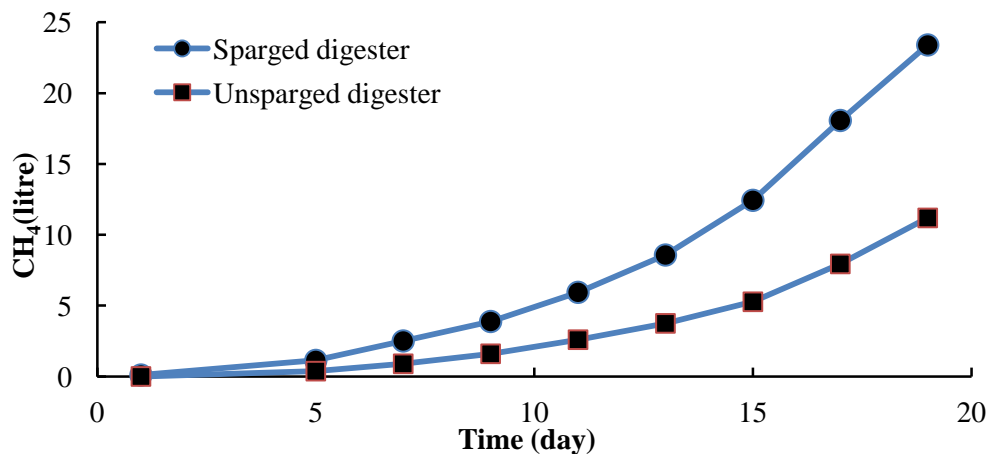


Figure 7.36: Cumulative methane production from the gaslift digester and unsparged digester when the pure carbon dioxide is sparged

## 7.5.2 Conclusion Part IV

This part of the study has investigated the effects of sparging with carbon dioxide in anaerobic fermentation. The results showed that the methane produced from the digester sparged with carbon dioxide and using microbubbles generated by a fluidic oscillator produced more methane than the unsparged digester. The data obtained from the current experiments indicate that the sparging system helps in stripping the methane produced by anaerobic bacteria. Removal of biogas from the headspace contributes to the transfer of biogas dissolved in the sludge to the headspace due to the difference in concentration between the two phases (sludge as a liquid and the remaining biogas in the headspace as gas).

## 7.6 Summary

This chapter discusses how a sparging system was applied in anaerobic digestion using an airlift bioreactor and different gas types (nitrogen, nitrogen and carbon dioxide, biogas (methane and carbon dioxide) and pure nitrogen under mesophilic conditions.

The results show that the application of the bubbling system with pure nitrogen in anaerobic digestion had a negative effect on the production of methane. This was because the sparging system stripped the carbon dioxide and hydrogen that are consumed by methanogenic bacteria in a route which normally accounts for 30% of total methane production. The results obtained from the experiments also showed that compensation with carbon dioxide after nitrogen bubbling does not lead to a sustained increase in daily methane production, regardless of the length of the period of sparging. This is despite the fact that sparging does initially increase methane production, but this is not sustained as was found for sparging with pure nitrogen. The results indicate that the daily sparging regime actually leads to a decrease in methane production, but this can be corrected by less frequent sparging to give the same production as can be achieved in a conventional digester. However, the results also indicated that recirculation of biogas in anaerobic digestion process can enhance production of methane (10-14%). The results can be utilised in development of heating system in the anaerobic digestion.

In final part of this chapter, anaerobic digester was sparged with pure carbon dioxide for short time using microbubbles technology. The results obtained from the experiments indicated that methane produced from sparged digester was more than that obtained from unsparged digester. According to results obtained from the above experiments in fourth parts, effect of sparging system on the methane production at different gases can be summarized in the Table 7.2.

Table 7.2: Effect the sparging system on methane produced from anaerobic digester

Part	Gas used in sparging system	Efficiency
Part I	Pure Nitrogen (9%)	Negative effect
Part II	Pure Nitrogen + pure carbon dioxide	Zero effect
Part III	Recycling the undiluted biogas	Positive effect (12-14%)
	Recycling the diluted biogas by carbon dioxide	Positive effect (10-12%)
Part IV	Pure carbon dioxide	Positive effect (100-110%)



CHEMICAL & BIOLOGICAL ENGINEERING

## **Chapter Eight**

# **Direct-Contact Evaporation to Direct-Contact Heating as a Step to Improve Heating in a Biological Application**

## Chapter Eight

### Direct-contact evaporation to direct-contact heating as a step to improve heating in a biological application

#### 8.1 Introduction

Combined Heat and Power engines produce electrical energy by internal combustion of biogas generated from anaerobic digestion. As mentioned earlier, CHP is an exothermic system thus the heat energy produced can be utilized for heating other endothermic bioprocesses such as anaerobic digestion. In wastewater treatment plants, the hot water produced from CHP is widely used for heating in anaerobic digestion. However, this system still faces several problems. Corrosion and poor heating are serious problems that face the development of heating system in anaerobic digestion as well as other operational difficulties.

The current chapter addresses the utilization of the hot exhaust gas produced from CHP to supply the heating in anaerobic digestion. The temperature of hot exhaust gas is about 200-300 °C depending on the type and size of CHP. Utilization of hot gas in anaerobic digestion can be achieved by direct contact evaporation process (DCE). It is a process consisting of a column of liquid through which a superheated gas is bubbled leading to increase in liquid temperature depending on the kinetics of mass and heat transfer as well as on residence time (GUY et al., 1992). DCE has been used in several applications for concentrating heat-sensitive solutions (Ribeiro and Lage, 2005, Zaida et al., 1987, Thierbanch and Hanssen, 2002, Ribeiro et al., 2004 and 2005).

In the present study, direct contact evaporation is converted to direct contact heating, since the evaporation of medium is undesirable in biological processes. The dewatering has negative effects on the bioprocess because it creates thermal layers with a poor pH distribution due to a reduction in the mixing efficiency. Schematic of the integration of

anaerobic digestion with CHP suggested in current study has been illustrated in Figure 8.1. The heat recovery from CHP is achieved by a heat exchanger with the biogas produced from the anaerobic digester. Previous chapter demonstrated that the biogas produced from anaerobic digestion can be used not only for generating the electricity from CHP, but can also be used for mixing the sludge in anaerobic digestion which helps prevent thermal layer and create a more uniform acidity in the sludge. It is also useful for stripping biogas produced from anaerobic bacteria. Furthermore, the Author has demonstrated that the recycle of biogas leads to an increase in methane production.

Mixing, mass transfer and heat transfer processes can be carried out simultaneously in a single bubble column in the anaerobic digestion process.

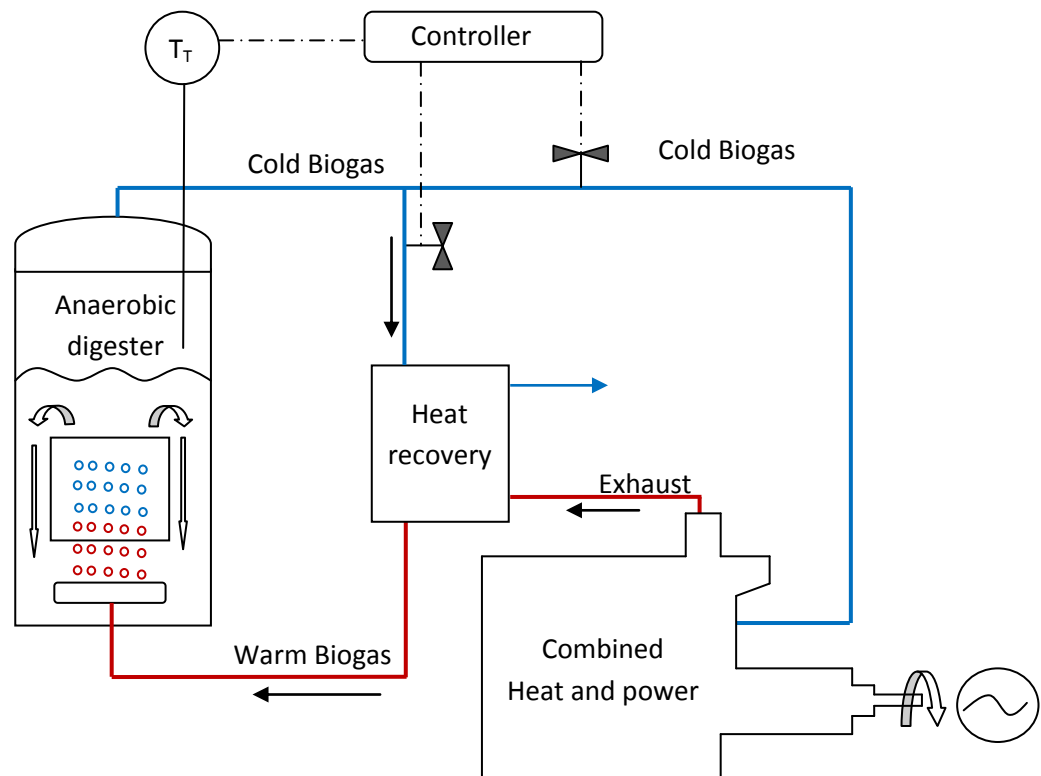


Figure 8.1: Integration between anaerobic digestion and combined heat and power

## 8.2 Objective of the Proposed Heating System

Application of the proposed heating system has the following advantages:

1. Heat recovery from the combined heat and power engine (CHP) can be used for heating other endothermic processes.

2. The CHP is separated completely from the anaerobic digester, thus, any potential leakage in heat exchanger would not affect the operation of CHP.
3. Reduction of the global warming caused by hot gas exhaust produced from CHP.
4. Maintenance and installation cost are lower compared to conventional heating system.
5. Heat energy provided by *hot water* produced from CHP could be advantageous used to heat other processes.
6. Lower thermal resistance between the hot bubbles and sludge leads to an increase the efficiency of heating system in anaerobic digestion.
7. Saves the electric power used for mixing system in the anaerobic digestion, since the proposed system will provide an efficient mixing system to prevent formation of thermal layers and more uniform pH value in all parts of anaerobic digestion.
8. The proposed heating system uses biogas produced from the same digester, therefore, the cost of operation is lower.

Volume of liquid, heating time, flow rate etc are important parameters that can affect the operation of heating system. The dominance of the sensible heat or latent heat can be identified by considering these parameters. In the present chapter, the effect of these parameters on the heating rate has been studied using a numerical model developed using *Central Composite Rotatable Design*. This numerical model can be used to analyse the behaviour of these variables in the process.

### 8.3 Results and Discussion

The key variables that affect the efficiency of evaporation and the water temperature are the flow rate of air, water level, and time required for heating. In order to study these variables, the temperature of air (in the inlet and outlet stream of the tank) and relative humidity were monitored and recorded during all experiments as mentioned in chapter three. The preparation of experiments that was explained in part 3.6 of chapter three has adopted in present study. The results show that the relative humidity was stable with a value of 100% for all the experiments as shown in the Figure 8.2. The inlet air temperature during the tests was nearly stable with a value of 135 °C, while the outlet air temperature was much lower than 135 °C. The results, also, showed that the outlet air temperature did not exceed 34 degrees during all experiments; however, this value

depends on the height of the water level in the tank. Figure 8.3 demonstrates that during 100 min of sparging process with the hot bubbles, the temperature of air decreased with increasing liquid level in the tank.

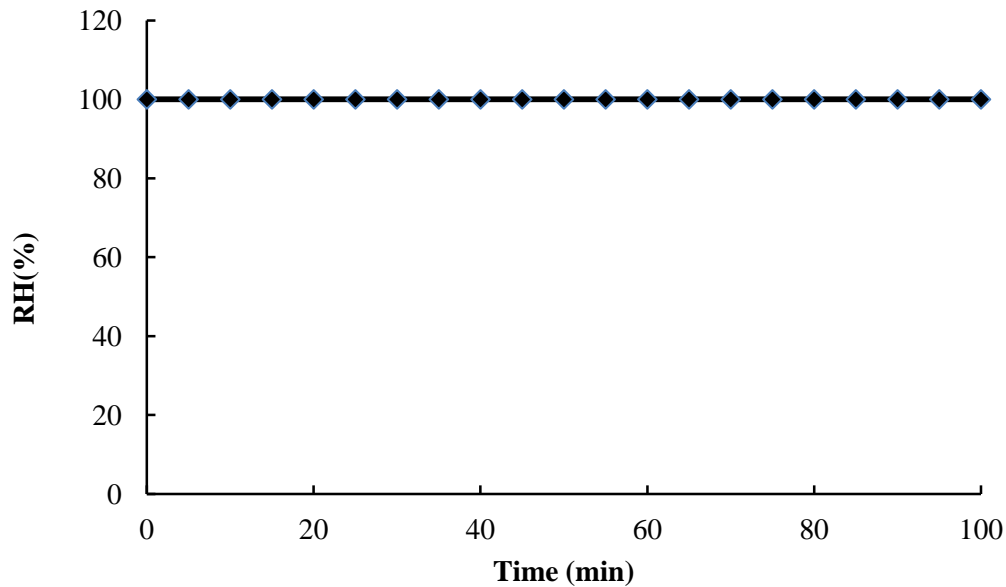


Figure 8.2: Relative humidity of outlet air

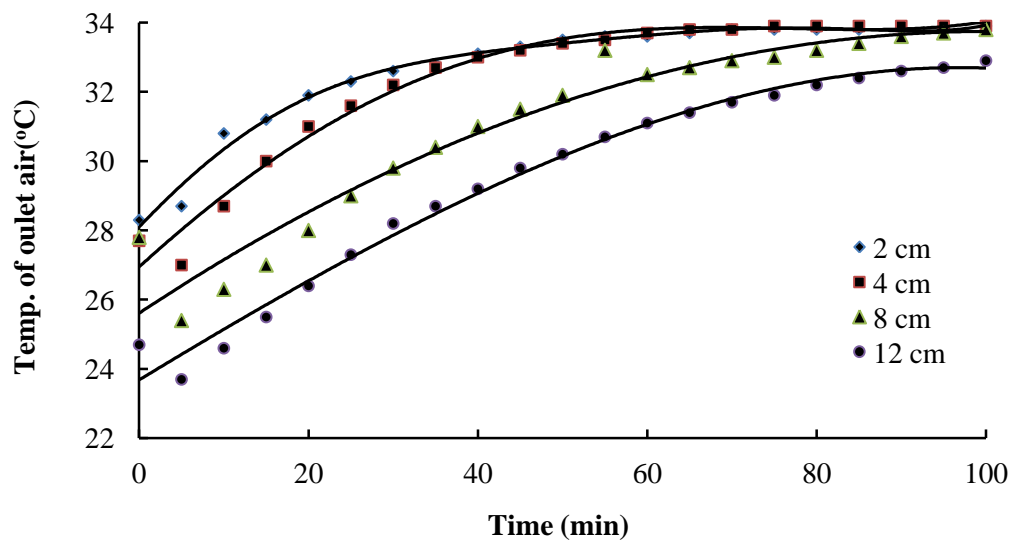


Figure 8.3: The variation of outlet air temperature at different heights of water above the ceramic diffuser (2, 4, 8, and 12 cm)

The outlet air temperature and relative humidity were used to determine the absolute humidity from psychrometric chart. Absolute humidity increases with air temperature,

because the relative humidity was constant at a value of 100%. Higher air temperature indicates higher absolute humidity as shown in Figure 8.4.

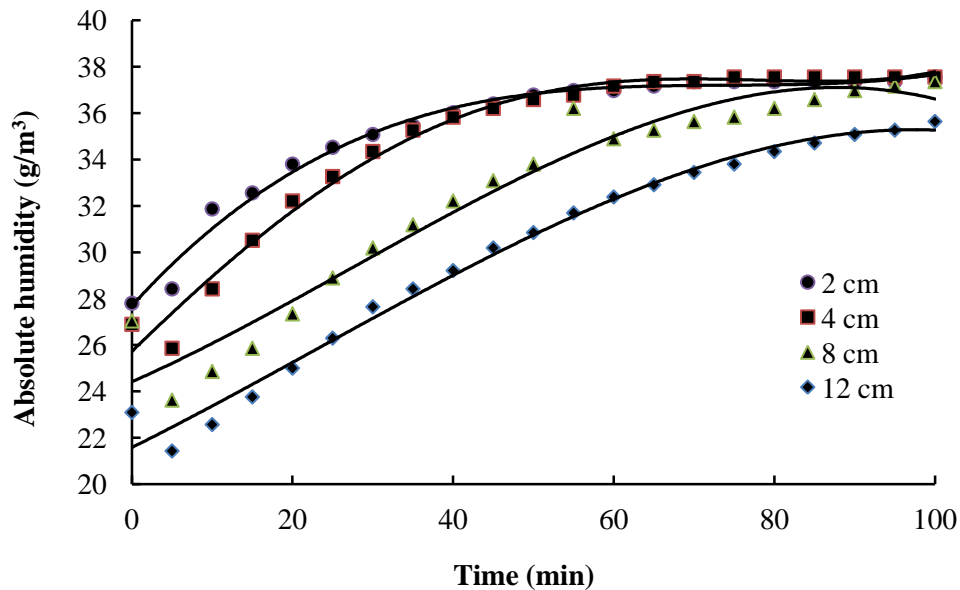


Figure 8.4: Plot of outlet air humidity versus time for different liquid levels

Energy of the water molecules is governed by the liquid temperature. Increasing the liquid temperature leads to increase this energy.

Therefore, molecules with energy higher than average energy will escape from liquid phase leading to an increase in the saturated vapour pressure. Liquid evaporation is an endothermic process, thus, it requires heat which is provided by the hot bubbles. Evaporation of the liquid is achieved by heating the water surrounding the bubbles without heating the temperature of the water that is at a significant distance from the direct-contact process. Therefore, the energy of water molecules in the contact region will increase rapidly to a level which allows them to escape from the liquid phase to vapour phase. The hot gas bubble, which was injected at the bottom of tank, carries a quantity of gained heat. Direct-contact of this bubbles with water leads to (1) transfer of heat to liquid phase as sensible heat and (2) evaporation of liquid due to transfer of heat as latent heat. Traditionally, the fraction of the original energy converted to latent heat is much greater than that transferred as sensible heat during direct contact heating. The water level plays an important role in determining which one will be more dominant: latent heat or sensible heat. The results show that the final steady state water temperature is nearly constant at different water level as illustrated in Figure 8.5. For example, the temperature of water rose to 34 °C when the level of liquid was 4 cm,

while with level at 8 cm, the temperature of liquid reached 33.8°C. Thus, the doubling liquid volume does not have much effect on the final temperature of water.

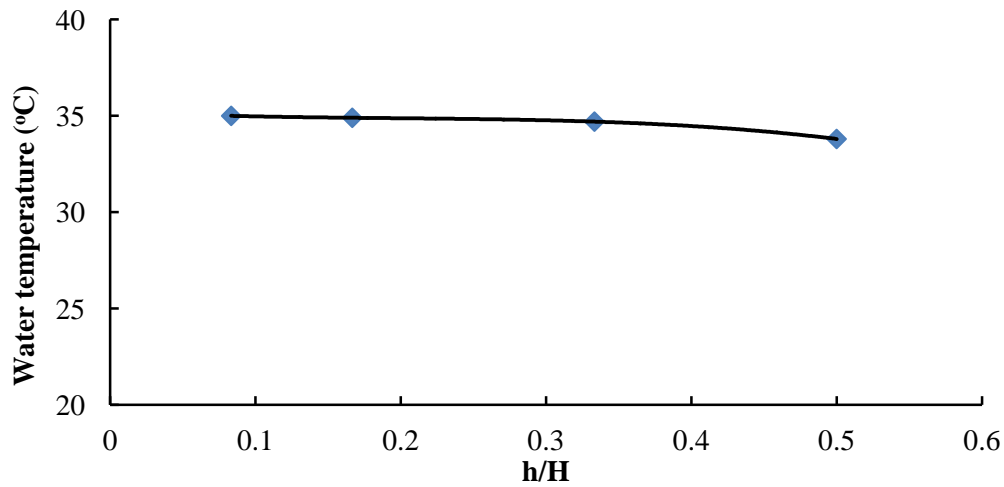


Figure 8.5: Water temperature at different water levels in tank

During direct contact evaporation, a fraction of water is evaporated to the vapour phase, and, most of the total energy is consumed in the evaporation process, but some portion of energy is used to increase the temperature of the water. As the bubbles rise to upper layers, they have an opportunity to contact with cooler liquid layers leading to vapour re-condensation to the liquid phase. This condensation will lead to the return of the heat that was consumed during evaporation, thus the water temperature will rise in the upper layers. Consequently the percentage of evaporation of water and humidity decreases when the water level is increased as shown in Figure 8.6.

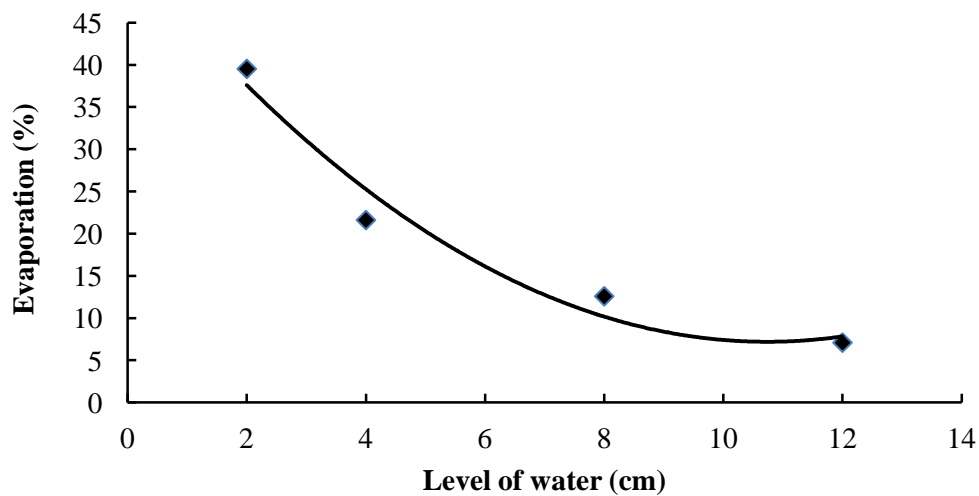


Figure 8.6: Percentage of evaporation at different water levels in tank

Figure 8.7 shows that the temperature of water can be increased by increasing the height of water. The upper cold layers are able to reduce the saturation vapour pressure of the rising gas bubbles so as to allow re-condensation of the initially vaporized liquid which in turn leads to an increase in the water temperature in a particular region. The efficiency of this process depends mainly on the height of the liquid, if other variables were constant, for instance the type of liquid, initial air temperature, etc

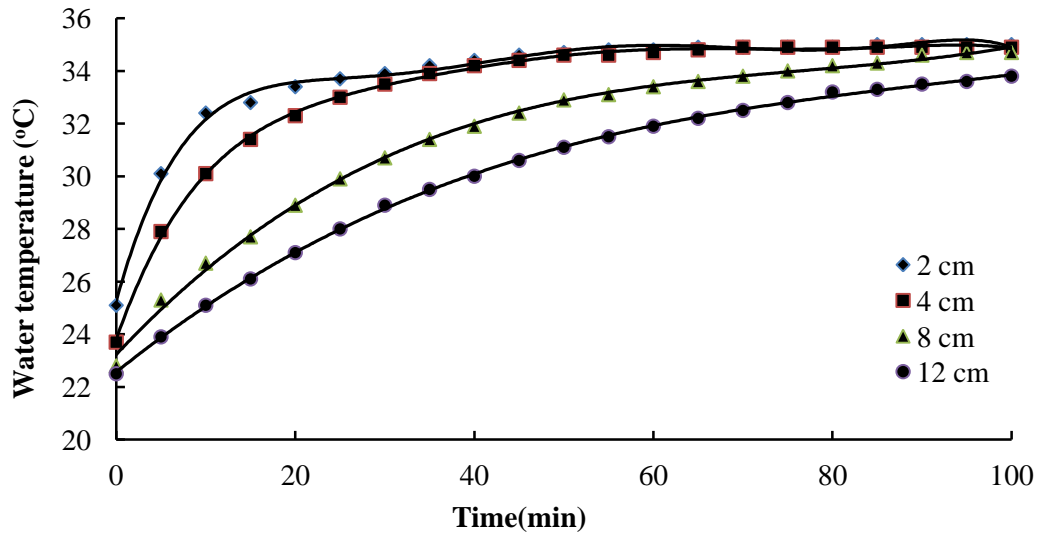


Figure 8.7: Liquid temperature at different liquid level

As the efficiency of evaporation increases, the efficiency of liquid heating will decrease since there will be less contact time between vapour and liquid phase to allow re-condensation as illustrated in Figure 8.8.

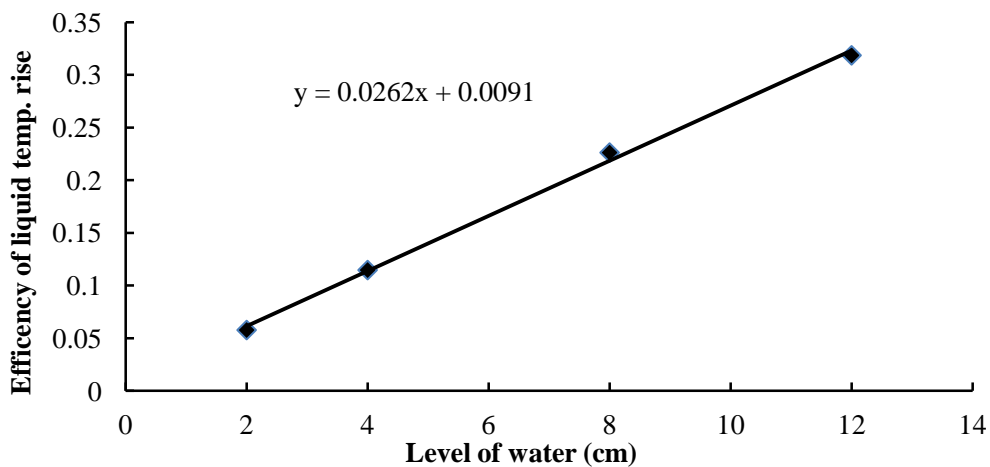


Figure 8.8: Efficiency of liquid temperature at different water levels in column

In applications where a liquid temperature rise is required, the liquid level should be chosen to optimise sensible heat transfer and minimize evaporation. This may involve using an intermediate liquid level.

## 8.4 Model Development and Analysis

### 8.4.1 Percentage of Evaporation

In the present study, a CCRD design was used to develop a second order equation with the response corresponding to percentage evaporation and the three x-variables corresponding to: air flow-rate, liquid level and evaporation time. In this study, the three x-variables and their coded levels are given in Table 8.1

Table 8.1: Real and coded levels of operating variables

Air-inlet flow rate (L/min)	Liquid Level (cm)	Evaporation time (min)	Code value
30	2	40	-1.682
35	4	70	-1
40	8	100	0
45	10	130	+1
50	12	160	+1.682

Ideally to allow rotatability, the value for  $\alpha$  should be  $2^{k/4}$ , which equates to 1.682 for a CCRD design of 3 x-variables (Cochran & Cox, 1992, p347; Aslan, 2008; Cukor *et al*, 2011).

Data for percentage evaporation were obtained from different experimental runs within the specified design region, after which the coefficients ( $\beta_0$ ,  $\beta_i$ ,  $\beta_{ii}$ ,  $\beta_{ij}$ ) of the second order response model will be estimated from the following standard relations. (Cochran & Cox, 1992, p350). Table 8.2 presents the coded and real levels of x-variables in a central composite design matrix format.

Table 8.2: Coded and real levels of x-variables used in present study

Exp. No.	Level of water		Flow Rate		Heating time	
	Real Value	Code (x1)	Real Value	Cod (x2)	Real Value	Cod (x3)
1	4	-1	35	-1	70	-1
2	10	1	35	-1	70	-1
3	4	-1	45	1	70	-1
4	10	1	45	1	70	-1
5	4	-1	35	-1	130	1
6	10	1	35	-1	130	1
7	4	-1	45	1	130	1
8	10	1	45	1	130	1
9	2	-1.682	40	0	100	0
10	12	1.682	40	0	100	0
11	8	0	30	-1.682	100	0
12	8	0	50	1.682	100	0
13	8	0	40	0	40	-1.682
14	8	0	40	0	160	1.682
15	8	0	40	0	100	0
16	8	0	40	0	100	0
17	8	0	40	0	100	0
18	8	0	40	0	100	0
19	8	0	40	0	100	0
20	8	0	40	0	100	0

As noted earlier, a total of 20 experiments were required in order to develop multiple linear regressions for 3x-variables. For 3 x-variables, the response function takes the following form:

$$Y_{\text{evap.}} = B_0 + B_1X_1 + B_2X_2 + B_3X_3 + B_{11}X_1^2 + B_{22}X_2^2 + B_{33}X_3^2 + B_{12}X_1 X_2 + B_{13}X_1 X_3 + B_{23}X_2 X_3 \quad (8.1)$$

The values of the regression coefficients have been calculated and are provided in the Table 8.3, Note that  $X_1 X_2, X_3$  are coded values (i.e. -1.682, -1, 0, +1, +1.682) which represent real values of the three operating variables of interest.

Table 8.3: Regression coefficients of model equation

B0	B1	B2	B3	B11	B22	B33	B12	B13	B23
11.3362	-7.6425	2.2570	4.7291	4.1436	-0.0109	-0.0764	-1.0153	-1.6996	0.9054

The values of regression coefficients gives the following relationship between percentage evaporation ( $Y_{\text{evap.}}$ ) and liquid level ( $X_1$ ), air flow rate( $X_2$ ) and evaporation time( $X_3$ ):

$$Y_{\text{evap.}} = 11.3362 - 7.6425X_1 + 2.2570X_2 + 4.7291X_3 + 4.1436X_1^2 - 0.0109X_2^2 - 0.0764X_3^2 - 1.0153X_1 X_2 - 1.6996X_1 X_3 + 0.9054X_3 \quad (8.2)$$

The percentage evaporation (Y response) at different liquid level, evaporation time and air inlet flow rate can be calculated from equation (8.2). It is useful to validate the developed equation by comparing predicted values for percentage evaporation to observed experimental values. Table 8.4 shows the predicted values that have been estimated from equation (8.2) and observed data obtained from our experiments. A good agreement between the predicted values and observed values can be observed from Figure 8.9 which has an  $R^2$  value of 97.5%.

Table 8.4: Predicted data and experimental data of percentage of evaporation (%)

Test No.	Variables			Percentage of evaporation (%)	
	Liquid level	Flow rate	Time	Observed	Predicted
1	4	35	70	12.84	14.24
2	10	35	70	4.82	4.38
3	4	45	70	16.89	18.97
4	10	45	70	6.33	5.06
5	4	35	130	23.24	25.28
6	10	35	130	9.94	8.63
7	4	45	130	32.43	33.64
8	10	45	130	13.55	12.93
9	2	40	100	39.53	35.92
10	12	40	100	7.66	10.21
11	8	30	100	8.15	7.51
12	8	50	100	15.56	15.10
13	8	40	40	3.85	3.17
14	8	40	160	19.48	19.08
15	8	40	100	11.48	11.40
16	8	40	100	11.85	11.40
17	8	40	100	11.11	11.40
18	8	40	100	11.26	11.40
19	8	40	100	11.26	11.40
20	8	40	100	11.26	11.40

Using the developed equation, the evaporation process has been investigated by studying the effect of each operating variable on the percentage of evaporation. This was achieved by utilizing the code value for each parameter. Figure 8.10 shows that the percentage of evaporation decreases rapidly with increasing liquid level, while it increases slightly with increasing air flow rate and time of evaporation.

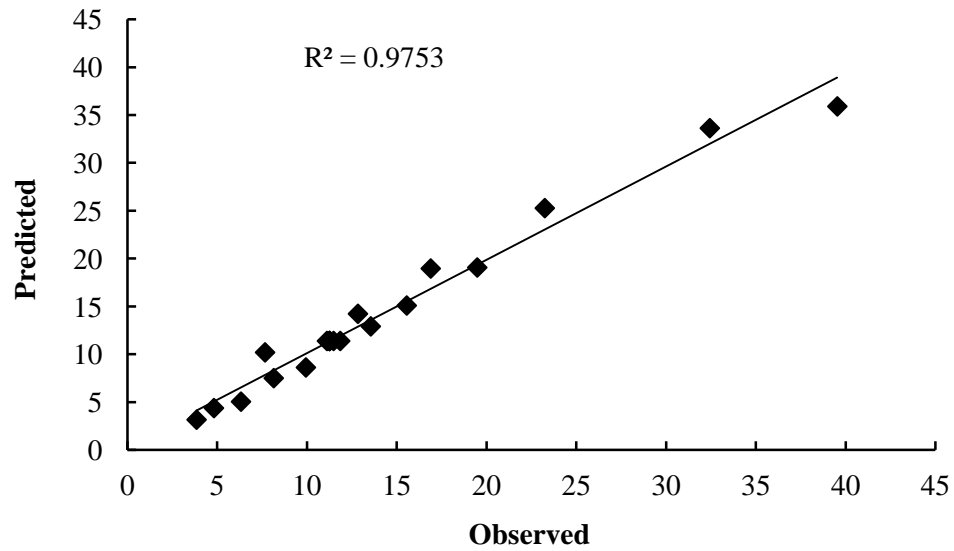


Figure 8.9: Observed values and predicted values resulted from developed equation.

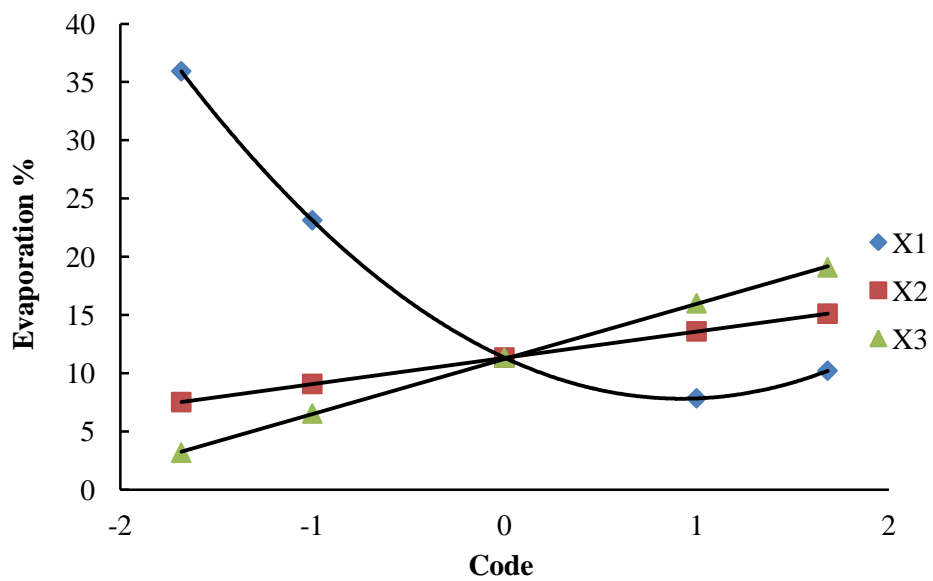


Figure 8.10: Variation of percentage of evaporation with different code levels

In order to compare the effect of each operating variable on percentage of evaporation, the codes values of liquid level ( $X_1$ ), air flow rate ( $X_2$ ), and evaporation time ( $X_3$ ) have been re-arranged as given in Table 8.5.

Table 8.5: Re-arrangement of percentage of evaporation with codes

X <sub>1</sub>	X <sub>2</sub>	X <sub>3</sub>	Evaporation rate	X <sub>1</sub>	X <sub>2</sub>	X <sub>3</sub>	Evaporation rate	X <sub>1</sub>	X <sub>2</sub>	X <sub>3</sub>	Evaporation rate
-1	-1	-1	12.84	-1	-1	-1	12.84	-1	-1	-1	12.84
-1	1	-1	16.89	1	-1	-1	4.82	1	-1	-1	4.82
-1	-1	1	23.24	-1	-1	1	23.24	-1	1	-1	16.89
-1	1	1	32.43	1	-1	1	9.94	1	1	-1	6.33
average			21.35	average			12.71	average			10.22
1	-1	-1	4.82	-1	1	-1	16.89	-1	-1	1	23.24
1	1	-1	6.33	1	1	-1	6.33	1	-1	1	9.94
1	-1	1	9.94	-1	1	1	32.43	-1	1	1	32.43
1	1	1	13.55	1	1	1	13.55	1	1	1	13.55
average			8.66	average			17.3	average			19.79

The average value of percentage evaporation was calculated based on the code values of each operating variable. For example, the average percentage evaporation was calculated to be 21.35 % when the code of liquid level (X<sub>1</sub>) was -1, while the average was 8.66 % when the code of liquid level (X<sub>1</sub>) was +1. This method was used to calculate the percentage evaporation for all variables and the results are provided in Table 8.6. Figure 8.11 shows straight line plots of each variable (liquid level, flow rate, and heating time) estimated between code values of -1 and +1.

Table 8.6: Re-arrangement of average of evaporation with codes

COD	Liquid level	Flow rate	Heating time
-1	21.35	12.71	10.22
1	8.66	17.30	19.79

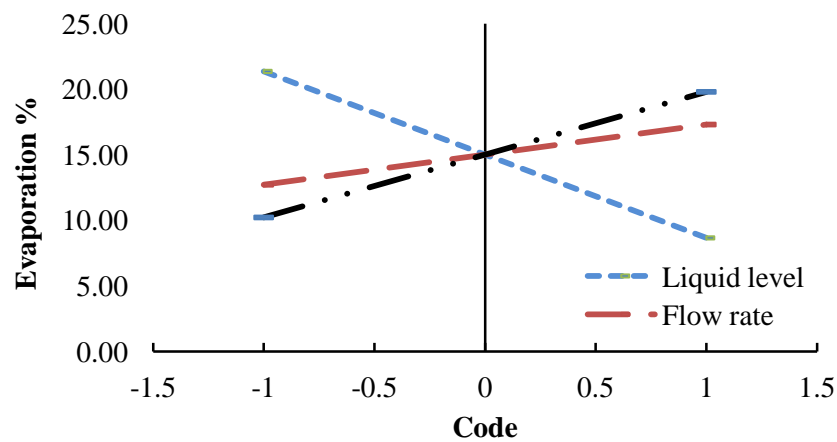


Figure 8.11: Effect of liquid level, flow rate and heating time on percentage of evaporation

It can be seen that the slope of the straight lines have been estimated to be 6 for liquid level, 4 for air flow rate and 2 for evaporation time. This means that changing liquid level has a stronger effect on percentage of evaporation when compared to other variables (i.e. flow rate and evaporation time). Therefore, percentage of evaporation can be controlled more effectively by changing liquid level instead of other variables.

#### **8.4.1.1 Effect of Liquid Level and Air Flow Rate on Percentage of Evaporation**

In previous sections, the effect of each operating variable on percentage of evaporation was studied when other variables are constant. For example, the effect of liquid level on percentage of evaporation was studied when air flow rate and evaporation time was kept constant. However, the interaction between liquid level, flow rate and time requires more clarity. Equation 8.2 can be used to analyze the interaction between the operating variables by changing two of these variables, while the third one is kept constant. MATLAB has been used to construct 3D response surface plots which will serve as an analysis aid.

Figure 8.12 is a 3D response surface plot showing the effect of liquid level and air flow rate on the percentage of evaporation when the evaporation time is at a constant value of 100 minutes. The figure indicates that higher evaporation rates (as percentage) can be achieved using lower liquid levels and high flow rates. According to our experimental design, reducing liquid level from 12cm to 2 cm while maintaining a flow rate of 30 L/min, leads to a 280% increase in evaporation efficiency, while, at the same liquid level (2 cm) increasing the flow rate from 30 to 50 L/min increases the percentage of evaporation by 45% only. This sort of behaviour applies to all ranges of liquid level and air flow rate.

The main reason for this behaviour is that increasing air flow rate creates bigger bubbles, hence decreases the bubble surface area even though it would have contributed to reducing the residence time of the bubble. Lower surface area means that the heat transferred is decreased and may not be sufficient to cause evaporation. Therefore increasing the flow rate causes higher sensible heat transfer, hence decreasing the fraction of heat used in evaporation. Our results suggest that there exist a competition between sensible heat transfer and evaporation. This behaviour can be explored in industrial processes that require an evaporation system such as food industries. High

efficiency of the evaporation can be achieved by reduction of liquid level which will also save energy and time. Whereas increasing the air flow rate, even if it leads to increased evaporation efficiency, would require more energy and time. Furthermore, if a high gas flow rate is to be employed, it may necessitate the use of larger equipment which will increase capital cost. The safety of the procedure will also be affected when using high gas flow rates especially because the gas flow is likely to be at a very high temperature and pressure. Therefore, it is highly favourable to improve percentage of evaporation by decreasing liquid level rather than increasing gas flow rate.

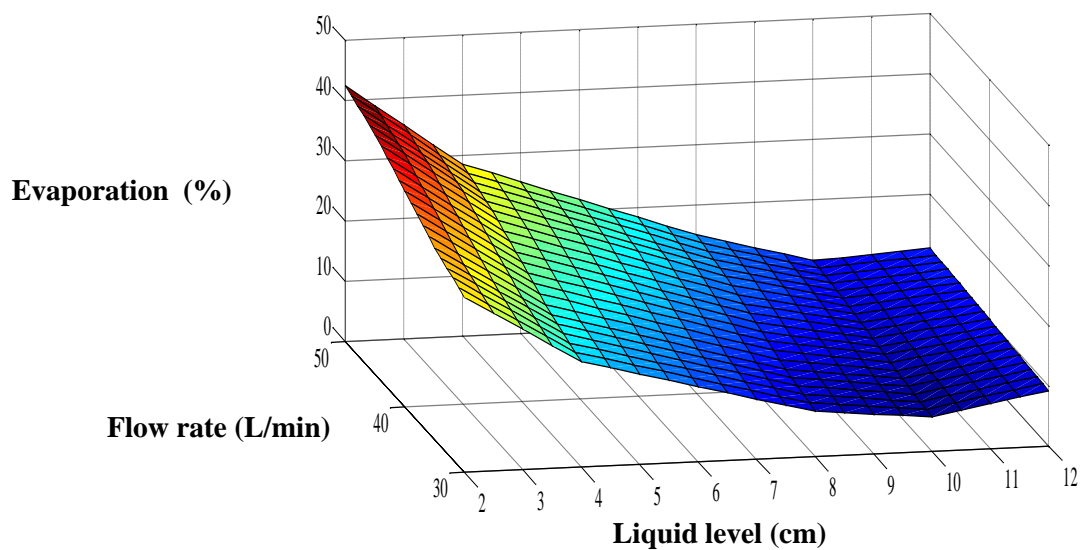


Figure 8.12: Response surface predicting percentage of evaporation from the model equation: effect of flow rate and liquid level

#### 8.4.1.2 Effect of Liquid Level and Evaporation Time on the Percentage of Evaporation

The combined effect of liquid level and evaporation time on percentage of evaporation has been represented by a 3D response surface plot as shown in Figure 8.13. From Figure 8.13, it is observed that an increase in evaporation time enhances the percentage of evaporation at all liquid levels. Increasing the evaporation time, raises the temperature of liquid (as we will see later) thereby increasing the kinetic energy of the liquid molecules. Higher kinetic energy means that molecules will more readily escape from liquid phase to vapour phase due to an increase in vapour pressure. At the beginning of the experiment, the percentage of evaporation is very low because more of the supplied energy is transferred from hot bubbles to liquid phase as a sensible heat.

This behaviour occurs because the temperature of the upper layers of the liquid is much less than the lower layers at the start of the experiments. Therefore as the bubbles rise upwards they are more likely to re-condense upon contact with the cool layers. As time passes, the temperature of upper layer increases to a certain level when re-condensation is minimal thus enhancing evaporation.

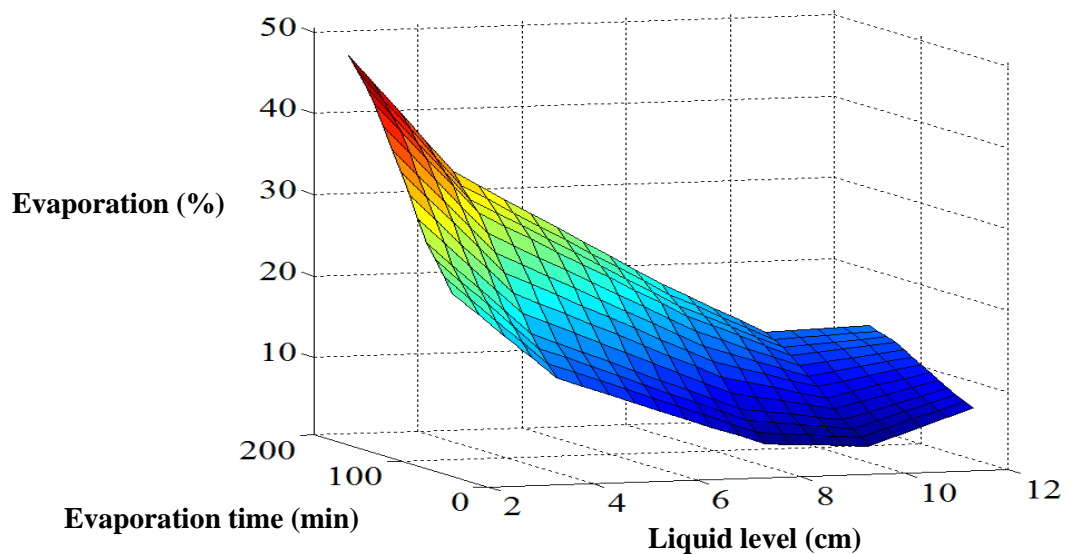


Figure 8.13: Response surface predicting percentage of evaporation from the model equation: effect of liquid level and evaporation time.

From Figure 8.14, the evaporation time required to evaporate 12% of liquid when the liquid level is 10 cm, is the same as that required to evaporate 48% of the same liquid if the liquid level was reduced to 2 cm. An evaporation time of 160 minutes enables a percentage evaporation of 48% using a liquid level of 2 cm. In order to achieve the same percentage evaporation using a liquid level of 10cm, the evaporation time needed is a lot more than 160minutes. Consequently, longer time, more energy and larger equipment size is required to improve percentage of evaporation at high liquid levels, not to mention added operational difficulties.

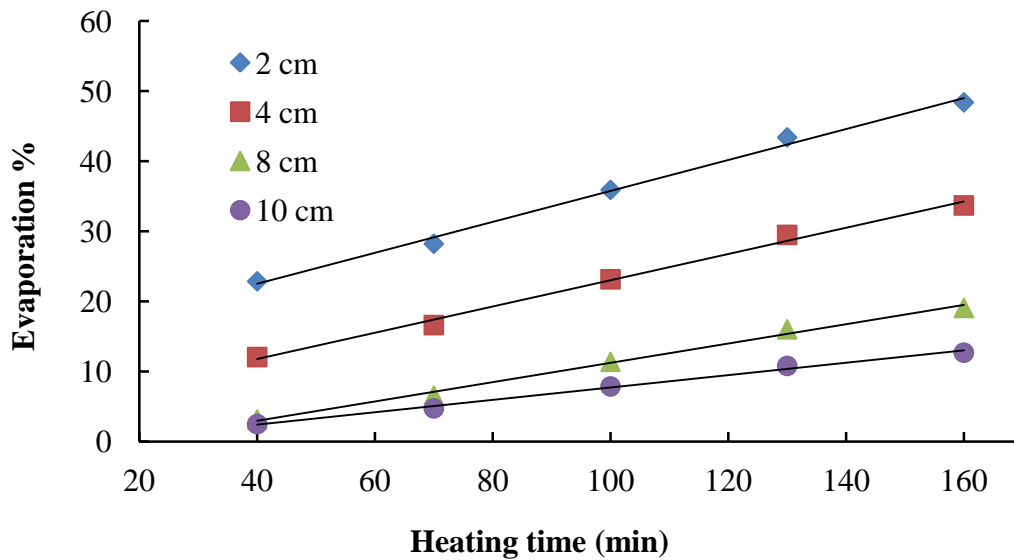


Figure 8.14: Effect of evaporation time (heating time) on the percentage of evaporation at different liquid level

### 8.4.1.3 Effect of Evaporation Time and Flow Rate on the Percentage of Evaporation

In this section, the effect of evaporation time and gas flow rate on percentage of evaporation is discussed. The liquid level was maintained at 2cm. From Figures 8.15 and 8.16, it can be observed that increasing either the time for evaporation or the flow rate increases the amount of evaporated liquid. According to our experimental design, 58% of water can be evaporated if the air flow rate is 50 L/min and the evaporation time is 160 min. Increasing the evaporation time leads to an increase in liquid temperature as well as kinetic energy thereby increasing the vapour pressure. In addition, increasing the flow rate leads to a decrease in bubble residence time. Both processes cause the enhancement of percentage of evaporation. It is also important to consider the economic aspects of the process. Higher energy consumption, larger equipment, and longer evaporation time are all economically unfavourable options that will be incurred if the flow rate and evaporation time are used as means of improving percentage of evaporation as opposed to changing liquid level.

Furthermore, high flow rates will also result in higher cost especially if the gas employed in the sparging system is expensive. There are also problems regarding compromising the safety of the procedure especially because the gas flow will be at a

high temperature. Therefore, in order to improve the rate of evaporation in evaporation systems, increasing the time for evaporation or air flow rate is not as attractive as reducing liquid level.

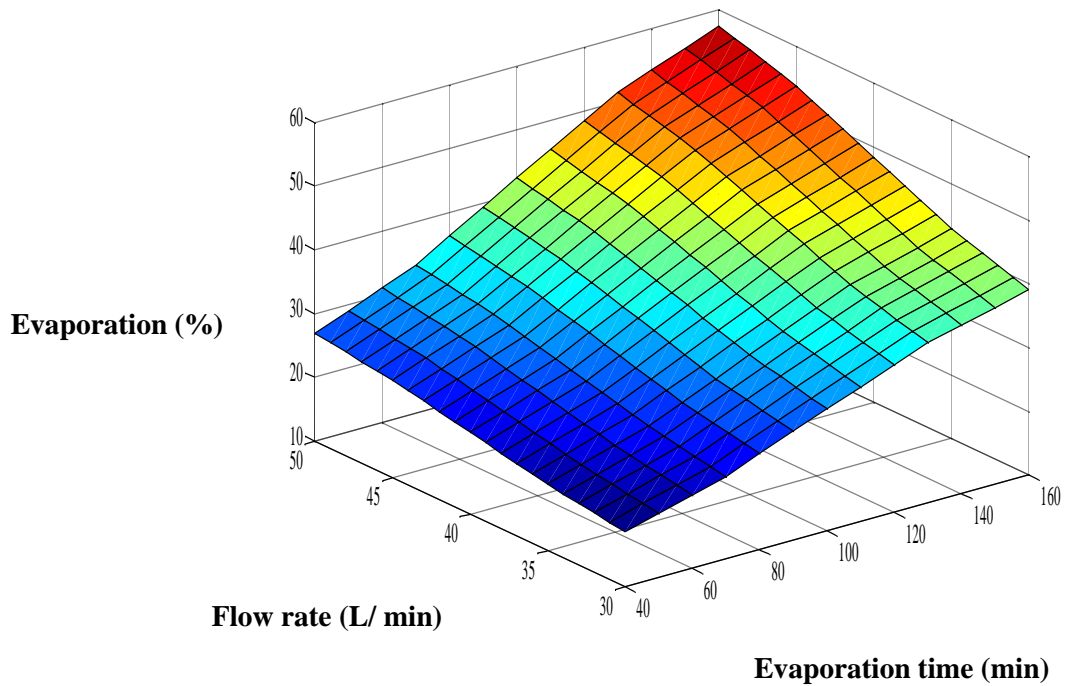


Figure 8.15: Response surface predicting percentage of evaporation from the model equation: effect of evaporation time and flow rate.

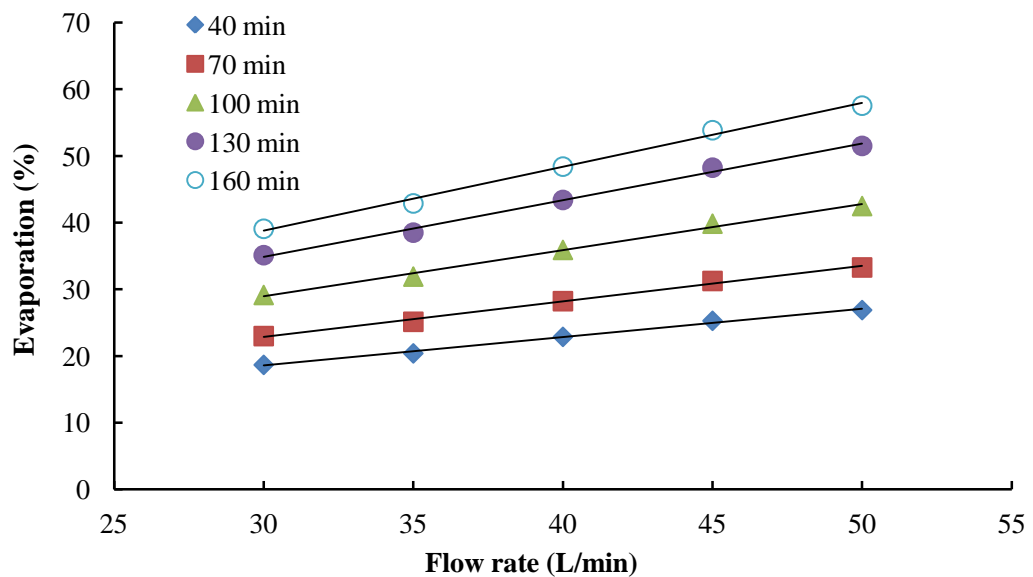


Figure 8.16: Effect of flow rate on the percentage of evaporation at different evaporation time

It can be concluded that higher evaporation rates (as percentage) can be achieved by increasing gas flow rate, decreasing liquid level and increasing evaporation time. Liquid level has a stronger effect on percentage of evaporation compared to gas flow rate and evaporation time. Although percentage of evaporation can be enhanced by increasing air flow rate and evaporation time, these variables significantly increase the temperature of the liquid which may be undesirable in some applications. Increasing air flow rate and evaporation time can also increase cost and compromise the safety of DCE, whereas decreasing liquid level will incur lower if any additional cost and does not affect safety of the procedure. Therefore it is more favourable to decrease liquid level as a means of enhancing percentage of evaporation.

### 8.4.2 Liquid Temperature

The effect of the inlet air flow rate, liquid level and time of heating on liquid temperature has been investigated by creating a model equation using *Central composite rotatable design*.

$$Y_{\text{Liq,temp.}} = B_0 + B_1X_1 + B_2X_2 + B_2X_2 + B_{11}X_1^2 + B_{22}X_2^2 + B_{33}X_3^2 + B_{12}X_1X_2 + B_{13}X_1X_3 + B_{23}X_2X_3 \quad (8.3)$$

Where  $B_0, B_1, B_2, B_3, B_{11}, B_{22}, B_{33}, B_{12}, B_{13},$  and  $B_{23}$  are regression coefficients with their values are represented in Table 8.7,  $X_1, X_2, X_3$  are code values (-1.682, -1, 0, +1, +1.682) equivalent to (2, 4, 8, 10, 10, 12 cm) for level of water, (30, 35, 40, 45, 50 L/min) for flow rate, and (40, 70, 100, 130, 160 min) for heating time.

Table 8.7: Regression coefficients of model equation

B0	B1	B2	B3	B11	B22	B33	B12	B13	B23
34.5501	-0.2576	0.5981	0.6943	-0.0002	0.0529	-0.3185	-0.0375	0.0875	-0.1375

$$Y_{\text{Liq,temp.}} = 34.5501 - 0.2576X_1 + 0.5981X_2 + 0.6943X_2 - 0.0002X_1^2 + 0.0529X_2^2 - 0.3185X_3^2 - 0.0375X_1X_2 + 0.0875X_1X_3 - 0.1375X_2X_3 \quad (8.4)$$

The response of liquid temperature at different liquid level, heating time and air inlet flow rate can be calculated from equation (8.4). Table 8.8 shows the predicted data that was estimated from equation (8.4) and observed data of liquid temperature obtained from our experiments.

Table 8.8: Predicted data and experimental data of liquid temperature

Test No.	Variables			Temperature (°C)	
	Liquid level (cm)	Flow rate (L/min)	Time (min)	Observed	Predicted
1	4	35	70	33.30	33.16
2	10	35	70	33.10	32.55
3	4	45	70	35.00	34.71
4	10	45	70	34.10	33.94
5	4	35	130	34.70	34.65
6	10	35	130	34.30	34.39
7	4	45	130	35.30	35.65
8	10	45	130	35.30	35.23
9	2	40	100	35.00	34.98
10	12	40	100	33.80	34.12
11	8	30	100	33.40	33.69
12	8	50	100	35.70	35.71
13	8	40	40	31.90	32.48
14	8	40	160	35.10	34.82
15	8	40	100	34.60	34.55
16	8	40	100	34.50	34.55
17	8	40	100	34.50	34.55
18	8	40	100	34.50	34.55
19	8	40	100	34.70	34.55
20	8	40	100	34.60	34.55

A good agreement does exist between the predicted values and observed values of percentage of evaporation and this has been illustrated through Figure 8.17 which has an  $R^2$  value of 92.15%.

Based on the model created in Equation 8.4, Figure 8.18 shows that the temperature of liquid decreases slightly with increasing liquid level. Whilst increasing flow rate and time of heating lead to an increase in the liquid temperature. However, only a slight change in liquid temperature was observed.

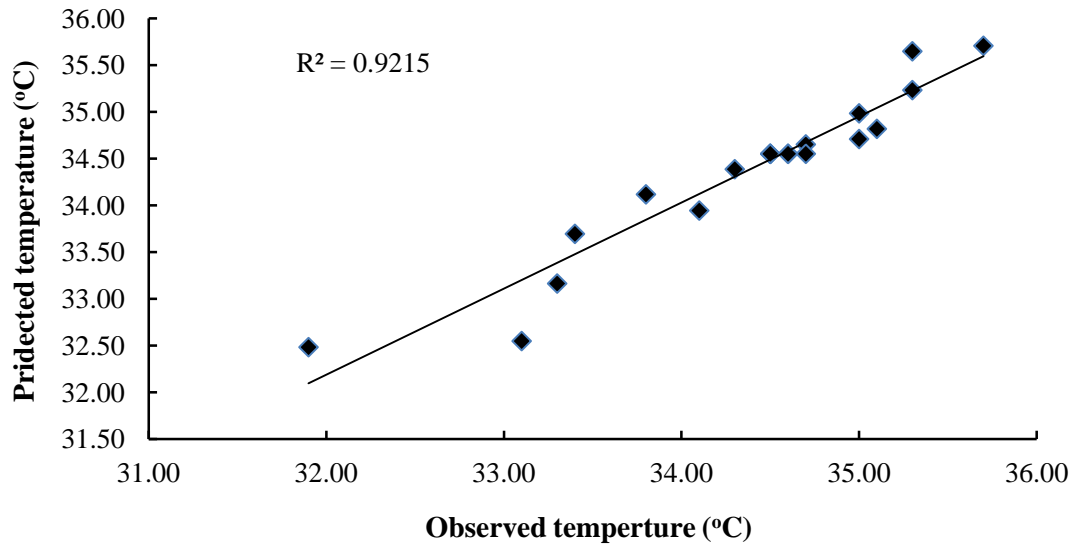


Figure 8.17: Observed values and predicted values resulted from developed equation

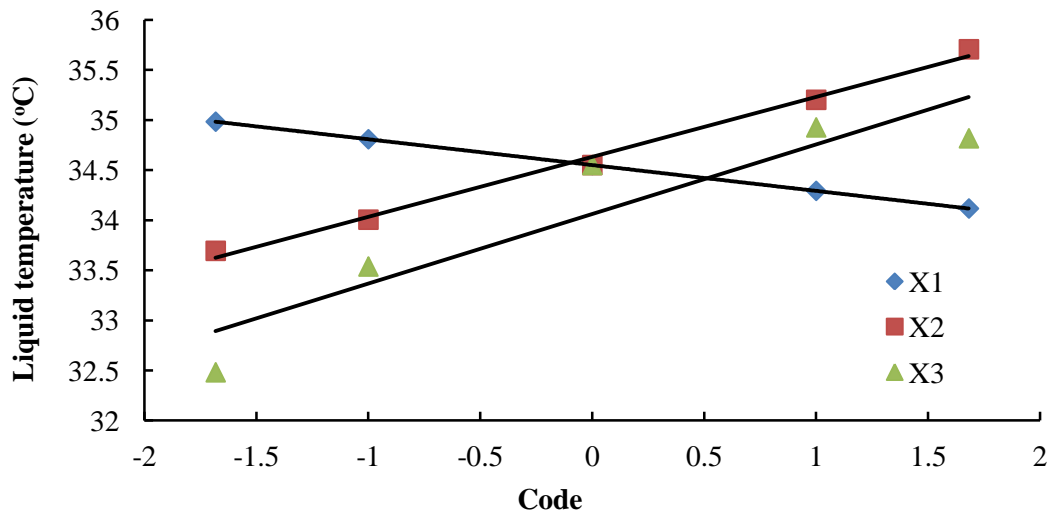


Figure 8.18: Variation of liquid temperature with different code levels

From obtained results, it can be inferred that direct contact evaporation is beneficial for liquid heating. Conversion of the evaporation process into a heating process can be carried out by choosing suitable liquid level, flow rate, and heating time. The effect of liquid level on heating system is more dominant than the effect of flow rate or heating time. In addition, there are other advantages that are associated with this process, for instance no moving part inside the bioreactor, low cost of installation and maintenance. Moreover, it contributes to reducing the partial pressure of the produced biogas, and hence; the bioreactions in the anaerobic digester become thermodynamically favourable and moves towards the formation of more products.

### 8.4.2.1 Effect of Liquid Level and Flow Rate on Liquid Temperature

Effect of the variables (liquid level, flow rate, and time) on liquid temperature is discussed in this section by making use of the created model Equation 8.4 and MATLAB software. Figure 8.19 shows 3D response surface plot which illustrates the effect of these variables on the percentage of evaporation assuming that the heating time is at a constant value of 100 min.

For the same amount of heat supply and heating time, the final liquid temperature at high liquid levels is expected to be significantly less than that at lower liquid levels. However, Figure 8.19 shows that increasing liquid level does not significantly reduce the final liquid temperature even though the amount of liquid became larger. The reason for this behaviour is that increasing liquid level leads to an increase in the residence time of the bubbles in liquid, thus part of the latent heat is converted into sensible heat which leads to an increase in liquid temperature due to vapour re-condensation. The figure also illustrates that increasing the flow rate of hot air increases temperature of the liquid. However, an increase in flow rate up to 40% did not achieve much improvement in temperature (only 6%), although the heat supply to the process was significantly increased. Since this increase in flow rate led to an increase in the bubble size which in turn results in a reduction of the residence time of bubbles in liquid phase, thus most of the energy provided by hot gas was lost as a latent heat of vaporisation.

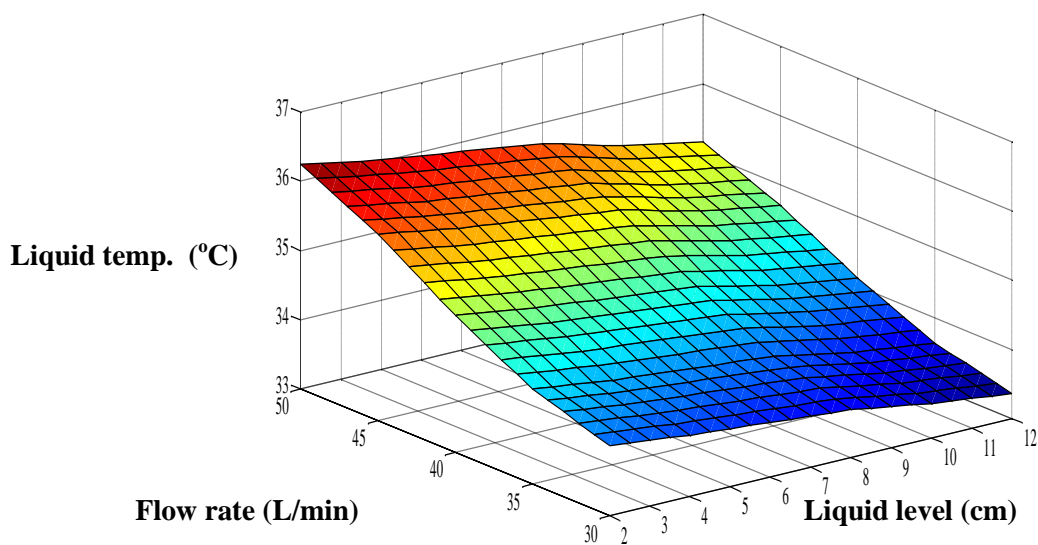


Figure 8.19: Response surface predicting liquid temperature from the model equation: effect of flow rate and liquid level

For evaporation process that deals with thermal sensitive liquid reducing the liquid level will maintain the liquid temperature at desired value. However, in the heating process, this behaviour can be made useful through increasing the liquid level. In this way, it may not be necessary to increase the air flow rate in order to achieve liquid heating.

#### 8.4.2.2 Effect of Heating Time and Flow Rate on Liquid Temperature

The effect variables (heating time and flow rate) on the temperature of liquid is represented in Figure 8.20. It can be observed that the liquid temperature increases with an increase in heating time and flow rate due to an increase in the amount of supplied heat and time.

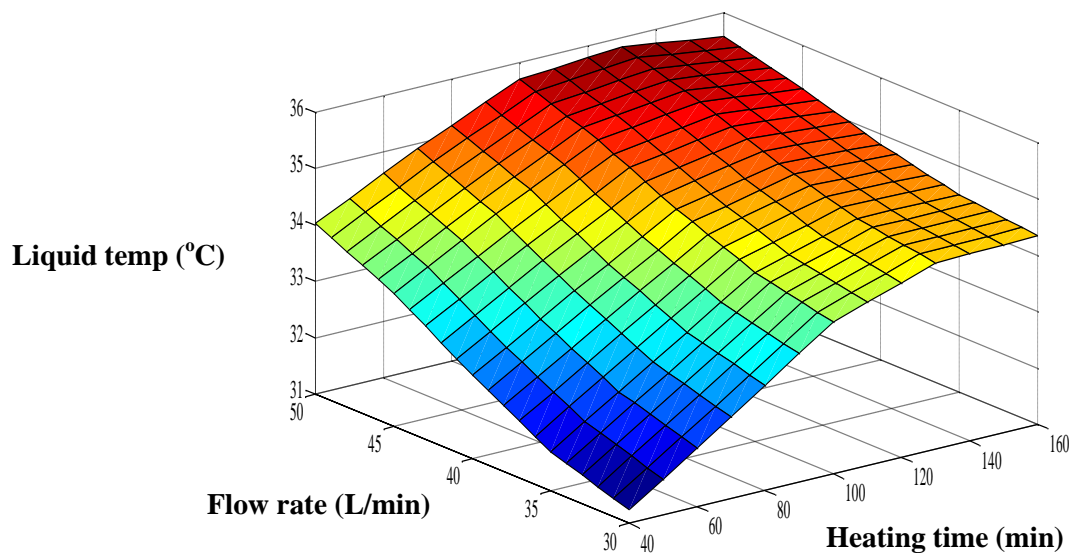


Figure 8.20: Response surface predicting liquid temperature from the model equation: effect of flow rate and heating time

Nevertheless the liquid temperature finally reaches a steady state value (i.e 35 °C) depending on operating condition.

The economic aspect is a very important factor that is considered in the present study. High consumption of energy, larger equipment, and loss of time as well as operational difficulties are major problems that are associated with the heating process, especially if the gas used for bubble formation is very costly.

### 8.4.2.3 Effect of Liquid Level and Heating Time on Liquid Temperature

Figure 8.21 shows the effect of liquid level and heating time on liquid temperature, when the flow rate was held constant at 40 L/min. From 3D surface plot, it can be observed that increasing the heating time and decreasing liquid level leads to an increase in the temperature of liquid. However, according to our experimental conditions, the final steady state temperature is stable within 35-36 °C after 60-80 min depending on the liquid level. Based on our observation, during this time, the percentage of evaporation was increased, because increasing the liquid temperature increases the kinetic energy and the vapour pressure. Furthermore, this increase in the liquid temperature helps in reducing vapour re-condensation. Consequently, a much higher fraction of the total heat provided by hot bubbles is converted to the latent heat when compared to sensible heat. The time required to achieve steady state temperature is inversely proportional to liquid level.

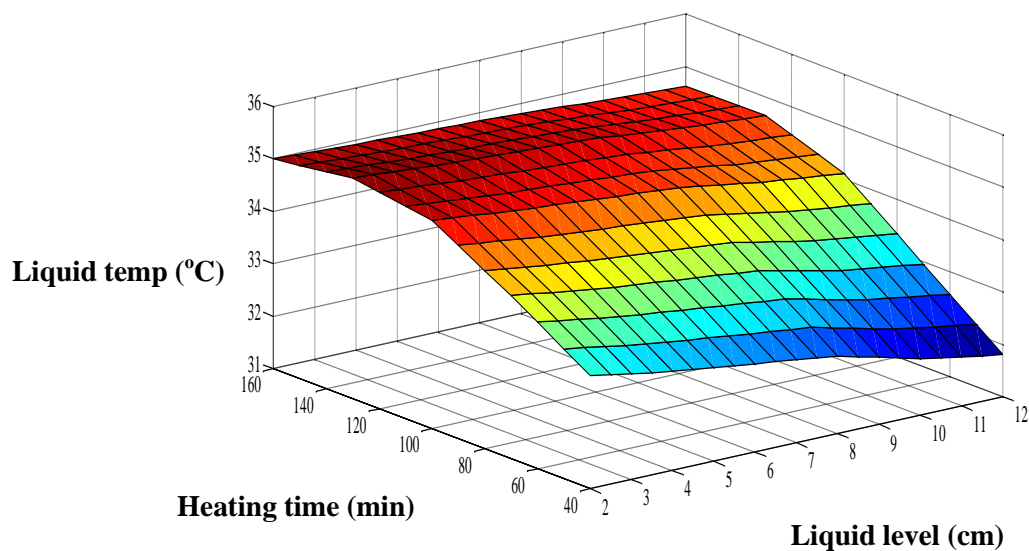


Figure 8.21: Response surface predicting liquid temperature from the model equation: effect of liquid level and heating time

According to above results, it can be concluded that the control on the sensible heat and latent heat in the direct contact evaporation process (or heating) can be utilised in development the heating system in bioprocess. Consequently, give many objectives as mentioned in the beginning of this chapter.

The direct-contact-heating suggested in present study can be used in various applications. Anaerobic digestion, which needs a heating system to increase activity of bacteria, is one of these bioprocesses that need such this technology. This unit has a noticeable height of the liquid phase that can be utilised to increase the sensible heat over the latent heat. Microbubble generated by fluidic oscillation, plays an important role in increasing efficiency of the heating system with lower percentage of evaporation by increasing the residence time of the gas bubbles in liquid phase and enhancement of mixing system in anaerobic digestion, thus, the cost of operational conditions decreases.

## 8.5 Summary

Previous studies have shown that a rise in reaction temperature increases bacteria growth rate in biochemical reactions. Although there has been a rapid development of heating systems and they are widely used in various bioprocess applications, there is still need for further technical developments in order to increase the efficiency of heat transfer rate in these processes. The low efficiency, high cost of installation, maintenance, and the potential operational problems are important challenges that have been faced the development of these systems. This chapter addresses the utilization of direct-contact evaporation (DCE) for process heating through the conversion of direct-contact evaporation into direct-contact heating (DCH).

This Chapter focused its study on three parameters; liquid volume, flow rate of hot gas and heating time. The desired percentage of evaporation and liquid temperature can be achieved by adjusting the liquid volume, flow rate, and heating time. Central composite rotatable design was used as an experimental design method in order to study the effect of these parameters on evaporation efficiency and liquid temperature. Five values were taken for the individual parameters in each experiment while the humidity, evaporation and water temperature was measured as objective variables. The data obtained from the experiments show that a competition exists between the latent heat transferred and the sensible heat. Based on the created equation, the liquid level has a significant effect on the fraction of heat that is used in heating the liquid (i.e. sensible heat). The fraction of the supplied heat transferred as sensible heat was observed to increase with increasing liquid level. In addition the percentage of evaporation increased with an increase in the flow rate of hot gas and time of heating while it decreased as the volume of liquid increased.



CHEMICAL AND BIOLOGICAL ENGINEERING

# **Chapter nine**

## **Conclusion and Future Work**

## Chapter nine

# Conclusions and Future Work

### 9.1 Conclusions

In this study, a sparging system was applied to anaerobic digestion. The sparging process was carried out using microbubbles generated by a fluidic oscillator and fine bubbles. The aims were to develop the mixing system for anaerobic digestion, enhance the production of methane as a renewable energy source, re-processing the digested sludge from the acid gases and develop the heating system.

The results obtained from the experiments in the present study led to the following conclusions:

#### **9.1.1 Anaerobic Digestion for Laboratory Purpose (Materials and Methods).**

The preceding section have discussed the use of prepared sludge for laboratory experiments in anaerobic digestion instead of normal sludge, which was collected from primary and secondary clarifiers at a wastewater treatment plant in Sheffield city. The experiments were conducted using a mixture of kitchen food waste and digested sludge, which poses less danger than that collected from treatment units. The suggested sludge was tested experimentally for 35 days. The results showed that there was a significant decrease only in the methane produced in the digester fed with digested sludge during the first days of operation, whilst in the anaerobic digester fed with simulated sludge; the methane production rate remained almost stable throughout the working operation (e.g. 35 days) with relatively low H<sub>2</sub>S production.

In addition, this study included improvement of the method of biogas collection. A new method for biogas collection was suggested here for laboratory purposes. The traditional methods usually cause pressure build-up in the headspace of the digester in addition to other problems, while the method in this part of study allows the anaerobic digestion to operate under atmospheric pressure (e.g. 1 atm) by utilisation of phenomena of communicating vessels to create vacuum pressure as a first stage. The second stage is to treat this vacuum pressure with hydrostatic pressure that has the same value but in different direction as action and reaction. This method was also applied to real anaerobic digesters.

**Objectives:**

1. Creation a new method to collect the biogas produced from bioprocess.
2. Reduction of operational problems due to use the sparging system in anaerobic digestion processes
3. Synthesis of the sludge for laboratory purposes, thus, minimizes the health and environmental problems.

### **9.1.2 Carbon Dioxide Mass Transfer Induced Through an Airlift Loop**

This study has investigated the dynamics of microbubble clouds that are possible with fluidic oscillation in enhancing Carbon dioxide gas transfer for either scrubbing or stripping operations in aqueous solution. Carbon dioxide scrubbing and stripping are essential elements of carbon capture and utilization systems, so the dynamics are topical. As Carbon dioxide has a reactive dissolution in aqueous solution, potentially controllable with pH, the analysis here for both measurement inference of the compositional state of the aqueous solution and for the assessment of mass transfer rates is useful for a number of operations. For instance, (bio)gas sweetening is important for sour natural gas (up to 15% acid gases), unconventional natural gases (over 20% acid gases), biogases (approximately 40% CO<sub>2</sub>), and liquefying natural gas for cryogenic storage. With microbubble mediation of both scrubbing and stripping (regeneration) operations in aqueous solution, it is clear that both operations can be sufficiently enhanced in rate to make aqueous solution a viable alternative to conventional CCS liquids such as methanolamine or ionic liquids.

The comparison of measured overall mass transfer rates between fine bubbles and microbubbles demonstrates the expected rate enhancement, but surprisingly no role is

played particularly by the dissociation of carbon dioxide into carbonate and bicarbonate ions. The strong solubility of carbon dioxide is fully responsible for the slower extraction rate of carbon dioxide by comparison to the rate of scrubbing carbon dioxide, but microbubbles are sufficiently good at enhancing stripping so as to make regeneration operations feasible. The CFD modeling using the laminar bubbly flow approach by adapting Tsuji's (Crowe 1998) two-fluid particle model captures the major features of the flow structure and the appropriate trends, achieving the same order of magnitude of overall mass transfer prediction, although under predicted. This suggests that CFD modelling is sufficient for design purposes. We speculate that the common gas-liquid interfacial boundary conditions for the two fluid model are the major idealizations responsible for the discrepancy. Observations both here and in other microbubble cloud studies (Zimmerman et al. 2011; 2009 and 2011(a)) show that the violent bursting of bubbles and the migration of bubbles along the liquid surface have a substantial momentum recoil and produce greater mixing effects than the smooth and regular effects predicted by the CFD model. This added feature of momentum and mass exchange is unexpected in traditional models and warrants greater exploration, particularly flow visualization and velocimetry along with bubble cloud mapping with either optical or acoustic imaging methods.

The objectives that can be achieved from this study can be summarised that use the microbubbles technology leads to:

1. Improve the biogas purification process.
2. Reduce the cost of carbon dioxide capture and regeneration cost of the carrier liquid.
3. Provide another source of pure carbon and free from impurities for other biological processes (Microalgae process).
4. Test the ability of computational modelling in study mass transfer in gas-liquid systems at different operational conditions.

### **9.1.3 Gaslift Bioreactor for Biological Applications with Microbubble Mediated Transport Processes (Design and Simulation)**

Understanding and optimising the efficiency of mixing and mass transfer is a key concern in many bioprocess applications including those that use airlift bioreactors. Aeration remains a key concern and cost factor in many processes and even anaerobic processes such as biogas production can be significantly enhanced by better gas-liquid

mass transfer. The design and simulation of an airlift bioreactor with aeration using microbubbles generated by fluidic oscillation has been addressed in the present study. This is the first simulation study to comprehensively analyse the effect of microbubbles on mixing and transport in airlift reactors. The results show that the use of microbubbles of 40  $\mu\text{m}$  diameter can dramatically increase the interfacial area available for mass transfer and also the residence time of the gas bubbles. This is due to much higher levels of gas recirculation for microbubbles when compared to larger bubbles. In addition, the results also show that, for the low gas flow rate studied (300 ml/min), microbubbles increase the liquid circulation velocity and hence potentially give better mixing. This is a somewhat counter intuitive result given the slower rise velocity of smaller bubbles, but it stems from the increased momentum transfer from gas to liquid for smaller bubbles. Finally, we used the simulations to investigate key design decisions on the geometry of the bioreactor: the vertical positioning of the diffuser and the draft tube diameter in order to avoid dead zones of poor mixing and mass transfer. Overall, the results obtained suggest enormous potential for microbubble aeration for improving the efficiency of mixing and mass transfer. They also demonstrate the power of computational modelling for the analysis and design of the next generation airlift bioreactors for bioprocess applications.

Microbubbles technology was used to design of reactor, which has the following specifications:

1. Low energy required to increase the efficiency of mixing system in biological processes
2. Increase of mass transfer and heat transfer between the gas and liquid can be achieved if this technology is used.
3. Lower dead zones inside the reactor.

#### **9.1.4 Removal of Acid-gases from Digested Sludge**

The benefits of the airlift bioreactor for enhancing methane production from digested sludge are demonstrated in this work. The results also show a high hold-up of methane in the digester which far exceeds the equilibrium solubility levels and may inhibit biogas production in the unsparged digester. Through 170 hours of processing we also measured much greater removal of the  $\text{CO}_2$  and  $\text{H}_2\text{S}$  compared to a conventional digester due to the sparging with 300ml/min of nitrogen for 1 hour each day.

Utilization of the fluidic oscillator in generating the microbubble was investigated in the current chapter. Throughout seven days of processing, the experimental data showed that the removal of carbon dioxide and hydrogen sulphide, in gaslift anaerobic digester with microbubble generated by fluidic oscillator were more than that for the conventional digester.

According to results obtained from experiments in chapter seven, the increase of time of sparging does not give a significant difference in efficiency of process, whether the digester operates with or without fluidic oscillator. Therefore, and in order to study of this technology, it is necessary to determine the sparging time to be suitable with size of digester.

Certainly, further investigation is required to uncover of the dissolved gases are responsible for limiting anaerobic digestion. Whatever the chemical or biological mechanisms at play, this appears to be a very fruitful area of research. It should also be noted that nitrogen sparging at the volumetric rate used in this study is not a realistic proposition since it drastically dilutes the energy density of the digester off-gas. Future work will therefore focus on sparging with recycled biogas, pure methane, or other mixes of CO<sub>2</sub> and CH<sub>4</sub>. This will shed further light on which gases are limiting and will be closer to a workable system for industrial scale enhanced biogas production. Airlift digesters can provide good mixing with lower energy consumption and enhanced of stripping of limiting gases. They could provide the basis for more productive and controllable anaerobic digestion in the future.

**Objectives:**

1. Processing the digested sludge from acid-gases
2. Protection pipeline and pumps from corrosion and damages.
3. Control of the odours emitted from digested sludge.

### **9.1.5 Investigation of the Effects of Sparging in Anaerobic Digestion Using Various Gases and Microbubbles Generated by Fluidic Oscillation**

The present study investigates sparging with microbubbles generated by a fluidic oscillator and fine bubbles in the anaerobic digestion process using different gases

(nitrogen, nitrogen with carbon dioxide, recycled the biogas and pure carbon dioxide). The results show that using nitrogen in airlift anaerobic digestion leads to a reduction in methane production. The reason for this situation is that the stripping of methane from the digestion process causes stripping of gases such as carbon dioxide and hydrogen that are required in order for methanogenic bacteria to methane.

Although, as is discussed in the second part of this chapter, the carbon dioxide is compensated, there is no significant increase in methane production except during the first days of the experiments.

The recycling of pure biogas to the digester, discussed in the third part of this chapter led to 10-14% enhancement of methane production. This system was utilized to develop the heating system in anaerobic digestion, as is discussed in the chapter eight. In order to strip amounts of methane from the digester during the recycling process, the dilution of the recycled biogas with carbon dioxide was required to give enhancement of methane production. In addition, the sparged digester using pure carbon dioxide was shown to produce double the amount of methane produced by the conventional digester.

Based all the results described here; therefore, sparging with pure carbon dioxide appears to be the best strategy for increased methane production. This finding should be tempered by the fact that the dilution causes the resulting off-gas to have lower specific energy content.

These results and previous studies, as is described in chapter six, concluded that the over-saturation of biogas produced in the sludge leads to decrease the mass transfer rate of these gases from the cells. Therefore; removal of the biogas, regardless of type method used, increases the concentration driving forces between the medium inside the cell (high concentration) and its outside, which becomes lower concentration after the removal process, and thus, leads to increase the mass transfer rate and to make the biogas production reactions thermodynamically more favourable.

**Objectives:**

1. Improvement of performance of the anaerobic digestion.
2. Enhancement of methane production by conversion portion of the carbon dioxide to methane.
3. Use this technology to create an integration between the anaerobic digestion and the CHP.

4. Reduction of greenhouse gases in the atmosphere.
5. Minimize the cost of biogas production.

### **9.1.6 Improvement Heating System in Anaerobic Digester**

Conversion of the latent heat into sensible heat in direct contact evaporation was investigated in the present thesis. Three parameters were studied in the present chapter; liquid level, flow rate of hot gas and heating time. In addition, the central composite rotatable design was used as an experimental design method in order to study the effect of these parameters on the evaporation efficiency and liquid temperature. Based on the created equation, the liquid level has a very strong effect on percentage of evaporation, while it has a slight effect on the liquid temperature. The present study has also concluded that the desired percentage of evaporation and temperature can be achieved by controlling the sensible heat and latent heat in gas-liquid system through the adjustment of liquid level, flow rate, and heating time. In addition, the data obtained from experiments show that the percentage of evaporation increases with increasing flow rate of hot gas and time of heating, while it decreases with increase in the liquid level. Although the percentage of evaporation is decreased with increasing level of liquid, the final temperature of water is only slightly affected. Therefore, conversion of the evaporation process into heating process can carry out by choosing suitable values for parameters (liquid level, flow rate, and heating time). The effect liquid level on heating system is more dominant than the effect of the flow rate or the heating time.

#### **Objectives:**

1. Heat recovery from the hot gas exhaust can be utilised to heat the anaerobic digestion process.
2. Low cost of operating, installation and maintenance.
3. Reduction in effect of hot gases on the global warming.
4. Minimize the problems that associated with traditional methods, for example corrosion of heat exchanger pipes and increasing the thermal resistance.

### **9.2. Integration of Biological Processes in a Wastewater Treatment Plant Using Microbubble Generated by Fluidic Oscillator.**

The present experiments used microbubbles generated by fluidic oscillator in anaerobic digestion. The results demonstrated that the recycling of pure biogas to the digester, as

is discussed above, led to enhancement of methane production, but did not affect the efficiency of the process. This advantage was utilised to develop the heating system in anaerobic digestion, as is discussed in another chapter of this thesis. In order to strip methane from the digester during the recycling process, the dilution of the recycled biogas with carbon dioxide was required. The results showed that enhancement of methane production occurred. In addition, the sparged digester that used pure carbon dioxide was shown to produce double the amount of methane produced by the conventional digester. Furthermore, the results obtained from the (*CO<sub>2</sub> Mass Transfer section*) suggest the possibility of using microbubble technology in the upgrading of biogas using water, which can be regenerated by using the same technology.

Depending on these results and conclusions, the study concluded that it is possible to integrate anaerobic digestion and other units to achieve the goal which forms the hypothesis this search.

The integration of biological processes in the wastewater treatment plant with biofuel production processes using microbubbles generated by fluidic oscillator is presented in the following figure (9.1).

The main input to this integration is wastewater, whilst the products can be listed as the following (see figure (9.2)):

1. Production of **extra Biogas** (methane) by using microbubble technology with carbon dioxide in anaerobic digestion.
2. The captured carbon dioxide can be used in other bioprocesses such as production of biofuel from microalgae with **lower production costs**.
3. Production of **extra electricity** through the use of microbubble technology to mix the medium, with lower energy requirements.
4. Production of **extra heat energy** due to the use of direct-contact-evaporation
5. Production of digested sludge for use as soil fertilizer
6. Production of treated water biologically
7. **NO Carbon dioxide** is released into the atmosphere.



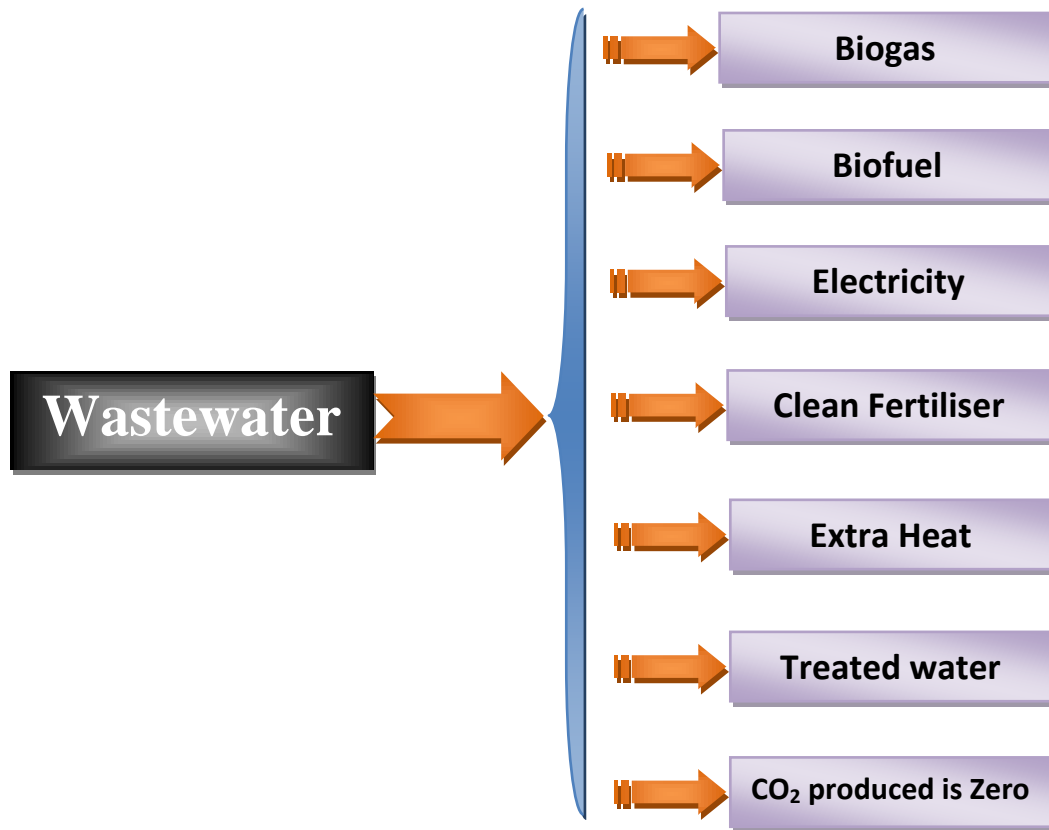


Figure 9.2: Benefits of the integration process

### 9.3 Future Work

The current study used a sparging system and micro technique in anaerobic digestion to achieve the desired goals. However the author suggests some recommendations for future work:

#### 9.3.1 Mass Transfer Study

1. The current research suggested the use of water with microbubble technology generated by fluidic oscillator in the upgrading of biogas; however, this process could potentially be optimized by testing the technology further with other solvents.
2. Study variables that affect the upgrading of biogas, with and without the use of microbubble technology.
3. The study used a batch reactor in the dissolution and stripping processes. Therefore it is necessary to scale-up from a batch process to a continuous process.

#### 9.3.2 Simulation Study

4. Development of the model by using a turbulent flow model and studying the same parameters, as were investigated in the present study.
5. Study other variables that affect the fluidic dynamic
6. Development of the model for a mass transfer study and heat transfer study after providing the required information and equations.

#### 9.3.3 Removal of Acid Gases

7. Repeat the experiment under thermophilic conditions to investigate the effects of microbubble technology on the removal efficiency of acid gases.
8. Study other parameters that affect the efficiency of the process.
9. Study the removal process with lower sparging time.

#### 9.3.4 Anaerobic Digestion

10. Use different concentrations of carbon dioxide for the sparging system of anaerobic digestion
11. Use the microbubbles generated by the fluidic oscillator in the recycling of undiluted and diluted biogas in anaerobic digestion.
12. Use carbon and hydrogen in anaerobic digestion

12. Because of importance of these experiments, the author recommends repeating the experiments with same conditions used in present study as well as with thermophilic conditions.

#### **9.3.5. Heating System**

13. Application of the suggested method for real anaerobic digestion to investigate its efficiency.

14. Study the effects of inlet air temperature and liquid temperature.



CHEMICAL & BIOLOGICAL ENGINEERING

# References

## References

- ABATZOGLOU, N. & BOIVIN, S. 2009. A review of biogas purification processes. *Biofuels, Bioproducts and Biorefining*, 3, 42-71.
- ABU-ZAHRA, M. R. M., NIEDERER, J. P. M., FERON, P. H. M. & VERSTEEG, G. F. 2007. CO<sub>2</sub> capture from power plants: Part II. A parametric study of the economical performance based on mono-ethanolamine. *International Journal of Greenhouse Gas Control*, 1, 135-142.
- AHRING, B. 2003. *perspectives for anaerobic digestion biomethanation i.springer berlin / heidelberg, book, 81:1-30.*
- AHRING, B. K. 1995. Methanogenesis in thermophilic biogas reactors. *Antonie Van Leeuwenhoek International Journal of General and Molecular Microbiology*, 67, 91-102.
- AHRING, B. K., IBRAHIM, A. A. and MLADENOVSKA, Z. 2001. Effect of temperature increase from 55 to 65 degrees C on performance and microbial population dynamics of an anaerobic reactor treating cattle manure. *Water Research*, 35, 2446-2452.
- AL-MASHHADANI, M. K. H., BANDULASENA, H. C. H. and ZIMMERMAN, W. B. 2011. CO<sub>2</sub> Mass Transfer Induced through an Airlift Loop by a Microbubble Cloud Generated by Fluidic Oscillation. *Industrial & Engineering Chemistry Research*, 51, 1864-1877.
- ALSHIYAB, H., KALIL, M. S., HAMID, A. A. & YUSOFF, W. M. W. 2008. Removal of headspace CO<sub>2</sub> increases biological hydrogen production by *C. acetobutylicum*. *Pakistan Journal of Biological Sciences*, 11, 2336-2340.
- AMARO, H. M., GUEDES, A. C. and MALCATA, F. X. 2011. Advances and perspectives in using microalgae to produce biodiesel. *Applied Energy*, 88, 3402-3410.
- ANGELIDAKI, I. and AHRING, B. K. 1994. Anaerobic thermophilic digestion of manure at different ammonia loads: Effect of temperature. *Water Research*, 28, 727-731.

- APPELS, L., BAEYENS, J., DEGRÈVE, J. & DEWIL, R. 2008. Principles and potential of the anaerobic digestion of waste-activated sludge. *Progress in Energy and Combustion Science*, 34, 755-781.
- ASLAN, N. 2007. Application of response surface methodology and central composite rotatable design for modeling the influence of some operating variables of a Multi-Gravity Separator for coal cleaning. *Fuel*, 86, 769-776.
- ASLAN, N. 2008. Application of response surface methodology and central composite rotatable design for modeling and optimization of a multi-gravity separator for chromite concentration. *Powder Technology*, 185, 80-86.
- ASTARITA, G., SAVAGE, D. W. & BISIO, A. 1983. Gas treating with chemical solvents, wiley-interscience: New York.
- B.R.E. 2012. Biogas composition[Online].[http://www.biogas-renewable-energy.info/biogas\\_composition.html](http://www.biogas-renewable-energy.info/biogas_composition.html).
- BAILEY, J. E. & OLLIS, D. F. 1986. *Biochemical Engineering Fundamentals*, McGraw-Hill Science: New York
- BANERJEE, A., SHARMA, R., CHISTI, Y. & BANERJEE, U. C. 2002. *Botryococcus braunii*: A renewable source of hydrocarbons and other chemicals. *Critical Reviews in Biotechnology*, 22, 245-279.
- BARBER, R. D. & FERRY, J. G. 2001. Methanogenesis, *Encyclopaedia of life sciences*, Nature Publishing Group.
- BARKER, D. J., TURNER, S. A., NAPIER-MOORE, P. A., CLARK, M. & DAVISON, J. E. 2009. CO<sub>2</sub> capture in the cement industry. *Greenhouse Gas Control Technologies* 9, 1, 87-94
- BARTLETT, R. E. 1971. *Public health Engineering-design in metric wastewater treatment*, Applied Science Publishers LTD.
- BATES, E. D., MAYTON, R. D., NTAI, I. and DAVIS, J. H. 2002. CO<sub>2</sub> Capture by a Task-Specific Ionic Liquid. *Journal of the American Chemical Society*, 124, 926-927.
- BAUDEZ, J. C., GINISTY, P., PEUCHOT, C. and SPINOSA, L. 2007. The preparation of synthetic sludge for lab testing, *Water Science Technology*, 56, 67-74.

- BECKER, S., SOKOLICHIN, A. & EIGENBERGER, G. 1994. Gas—liquid flow in bubble columns and loop reactors: Part II. Comparison of detailed experiments and flow simulations. *Chemical Engineering Science*, 49, 5747-5762.
- BELLO-MENDOZA, R. & SHARRATT, P. N. 1998. Modelling the effects of imperfect mixing on the performance of anaerobic reactors for sewage sludge treatment. *Journal of Chemical Technology and Biotechnology*, 71, 121-130.
- BENEMANN, J. R. 1997. CO<sub>2</sub> mitigation with microalgae systems. *Energy Conversion and Management*, 38, Supplement, S475-S479.
- BOROLE, A. P., KLASSON, K. T., RIDENOUR, W., HOLLAND, J., KARIM, K. & AL-DAHMAN, M. H. 2006. Methane production in a 100-L upflow bioreactor by anaerobic digestion of farm waste. *Applied Biochemistry and Biotechnology*, 131, 887-896.
- BOSOAGA, A., MASEK, O. & OAKLEY, J. E. 2009. CO<sub>2</sub> capture technologies for cement industry. *Greenhouse Gas Control Technologies* 9, 1, 133-140
- BOUALLAGUI, H., BEN CHEIKH, R., MAROUANI, L. & HAMDY, M. 2003. Mesophilic biogas production from fruit and vegetable waste in a tubular digester. *Bioresource Technology*, 86, 85-89.
- BRAGUGLIA, C. M., GIANICO, A. & MININNI, G. 2011. Laboratory-scale ultrasound pre-treated digestion of sludge: Heat and energy balance. *Bioresource Technology*, 102, 7567-7573.
- BREDWELL, M. & WORDEN, R. 1998. Mass-transfer properties of microbubbles. 1. Experimental studies. *Biotechnol Prog.*, 14, 31-38.
- BROWN, L. M. 1996. Uptake of carbon dioxide from flue gas by microalgae. *Energy Conversion and Management*, 37, 1363-1367.
- BUDZIANOWSKI, W. M. 2012. Sustainable biogas energy in Poland: Prospects and challenges. *Renewable and Sustainable Energy Reviews*, 16, 342-349.
- CALDEIRA, K. & RAU, G. H. 2000. Accelerating carbonate dissolution to sequester carbon dioxide in the ocean: Geochemical implications. *Geophys. Res. Lett.*, 27, 225-228.

- CALVO, E. G. & LETÓN, P. 1991. A fluid dynamic model for bubble columns and airlift reactors. *Chemical Engineering Science*, 46, 2947-2951.
- CALVO', E. G., LETDN, P. & ARRANZ, M. A. 1991. Prediction of gas hold up and liquid velocity in airlift loop reactors containing highly viscous Newtonian liquids. *Chemical Engineennq Science*, 46, 2951-2954.
- CAO, Y., LI, S. & PETZOLD, L. 2002. Adjoint sensitivity analysis for differential-algebraic equations: algorithms and software. *Journal of Computational and Applied Mathematics*, 149, 171-191.
- CHAMY, R. & RAMOS, C. 2011. Factors in the determination of methanogenic potential of manure. *Bioresource Technology*, 102, 7673-7677.
- CHATTERJEE, A., MAGEE, J. L. & DEY, S. K. 1983. The Role of homogeneous reactions in the radiolysis of water. *Radiation Research*, 96, 1-19.
- CHEREMISINOFF, N. P. 1996. *Biotechnology for industrial and municipal wastes*, Noyes publications.
- CHISTI, M. Y. 1989. *Airlift bioreactor*, Elsevier Applied Science.
- CHISTI, Y. 2007. Biodiesel from microalgae. *Biotechnology Advances*, 25, 294-306.
- CHISTI, Y. 2008. Biodiesel from microalgae beats bioethanol. *Trends in Biotechnology*, 26, 126-131.
- CLARKE, J. K. A. 1964. Kinetics of absorption of carbon dioxide in monoethanolamine solutions at short contact times. *Industrial & Engineering Chemistry Fundamentals*, 3, 239-245.
- COCHRAN, W. G. & COX, G. M. 1968. *Experimental designs*, John Wiley & Sons, Inc. Proprietor.
- CORTE, B., VERHAEGEN, K., BOSSIER, P. & VERSTRAETE, W. 1988. Effect on methane digestion of decreased H<sub>2</sub> partial pressure by means of phototrophic or sulfate-reducing bacteria grown in an auxiliary reactor. *Applied Microbiology and Biotechnology*, 27, 410-415.
- CROWE, C., SOMMERFIELD, M. & TSUJI, Y. 1998. *Multiphase flows with droplets and particles*, CRC Press: Boca Raton.

- CUKOR, G., JURKOVI, Z. & SEKULI, M. 2011. Rotatable central composite design of experiments versus taguchi method in the optimization of turning. *METABK*, 50, 17-20.
- DAVEY, K. R. 1994. Modelling the combined effect of temperature and pH on the rate coefficient for bacterial growth. *International Journal of Food Microbiology*, 23, 295-303.
- DE WIT, M., JUNGINGER, M., LENSINK, S., LONDO, M. & FAAIJ, A. 2010. Competition between biofuels: Modeling technological learning and cost reductions over time. *Biomass and Bioenergy*, 34, 203-217.
- DEGRÈVE, J., EVERAERT, K. and BAEYENS, J. 2001. The use of gas membranes for VOC-air separations. *Filtration and Separation*, 38, 48-54.
- DONOSO-BRAVO, A., RETAMAL, C., CARBALLA, M., RUIZ-FILIPPI, G. & CHAMY, R. 2009. Influence of temperature on the hydrolysis, acidogenesis and methanogenesis in mesophilic anaerobic digestion: parameter identification and modeling application. *Water Science and Technology*, 60, 9-17.
- DRYZEK, J. S., NORGAARD, R. B. and SCHLOSBERG, D. 2011. *The oxford handbook of climate change and society: approaches and responses* Oxford university Press Inc., New York. Chapter one.
- ERIKSEN, N. T. 2008. The technology of microalgal culturing. *Biotechnology Letters*, 30, 1525-1536.
- FAKHERI, F., MOGHADDAS, J., ZADGHAFARI, R. & MOGHADDAS, Y. 2012. Application of Central Composite Rotatable Design for Mixing Time Analysis in Mechanically Agitated Vessels. *Chemical Engineering & Technology*, 35, 353-361.
- FENG 2008. Microalgae cultivation in bioreactors for CO<sub>2</sub> mitigation from power plant flue gas and fuel production by supercritical CO<sub>2</sub> extraction. *AIChE Annual Meeting, Conference Proceedings*.
- FRANK, M. J. W., KUIPERS, J. A. M. & VAN SWAAIJ, W. P. M. 1996. Diffusion coefficients and viscosities of CO<sub>2</sub> + H<sub>2</sub>O, CO<sub>2</sub> + CH<sub>3</sub>OH, NH<sub>3</sub> + H<sub>2</sub>O, and NH<sub>3</sub> + CH<sub>3</sub>OH liquid mixtures. *Journal of Chemical and Engineering Data*, 41, 297-302.

- FRANCIS, M. J. & PASHLEY, R. M. 2009. Thermal desalination using a non-boiling bubble column. *Desalination and Water Treatment*, 12, 155–161.
- GARBER, W. F. & OHARA, G. T. 1972. Operation and Maintenance Experience in Screening Digested Sludge. *Journal (Water Pollution Control Federation)*, 44, 1518-1526.
- GARCIA CALVO, E. 1989. A fluid dynamic model for airlift loop reactors. *Chemical Engineering Science*, 44, 321-323.
- GARRETT, B. C., AL, E. & ET AL. 2005. Role of Water in Electron-Initiated Processes and Radical Chemistry: Issues and Scientific Advances. *ChemInform*, 36, no-no.
- GARY, R. K. 2004. The concentration dependence of the  $\Delta s$  term in the gibbs free energy function: Application to Reversible Reactions in Biochemistry. *Journal of Chemical Education*, 81, 1599-1604.
- GERARDI, M. H. 2003. *Microbiology of anaerobic digestion*, John Wiley interscience.
- GOUVEIA, L. & OLIVEIRA, A. C. 2009. Microalgae as a raw material for biofuels production. *Journal of Industrial Microbiology & Biotechnology*, 36, 269-274.
- GUJER W., Z. A. J. B. 1983. Conversion processes in anaerobic digestion. *Water Science & Technology*, 15, 127-167.
- GUNTER, W. D., PERKINS, E. H. & MCCANN, T. J. 1993. Aquifer disposal of CO<sub>2</sub>-rich gases: Reaction design for added capacity. *Energy Conversion and Management*, 34, 941-948.
- GUPTA, N., GATTRELL, M. & MACDOUGALL, B. 2006. Calculation for the cathode surface concentrations in the electrochemical reduction of CO<sub>2</sub> in KHCO<sub>3</sub> solutions. *Journal of Applied Electrochemistry*, 36, 161-172.
- HANSEN, K. H., ANGELIDAKI, I. & AHRING, B. K. 1998. Anaerobic digestion of swine manure: inhibition by ammonia. *Water Research*, 32, 5-12.
- HANSSON, G. 1979. Effects of carbon dioxide and methane on methanogenesis. *Applied Microbiology and Biotechnology*, 6, 351-359.

- HARASIMOWICZ, M., ORLUK, P., ZAKRZEWSKA-TRZNADEL, G. & CHMIELEWSKI, A. G. 2007. Application of polyimide membranes for biogas purification and enrichment. *Journal of Hazardous Materials*, 144, 698-702.
- HARTMAN, R. P. A., BRUNNER, D. J., CAMELOT, D. M. A., MARIJNISSEN, J. C. M. & SCARLETT, B. 2000. Jet Break-Up In Electrohydrodynamic Atomization In The Cone-Jet Mode. *Journal of Aerosol Science*, 31, 65-95.
- HETTINGA, W. G., JUNGINGER, H. M., DEKKER, S. C., HOOGWIJK, M., MCALOON, A. J. & HICKS, K. B. 2009. Understanding the reductions in US corn ethanol production costs: An experience curve approach. *Energy Policy*, 37, 190-203.
- HILTON, M. G. & ARCHER, D. B. 1988. Anaerobic digestion of a sulfate-rich molasses wastewater: Inhibition of hydrogen sulfide production. *Biotechnology and Bioengineering*, 31, 885-888.
- HORIKAWA, M. S., ROSSI, F., GIMENES, M. L., COSTA, C. M. M. & SILVA, D. M. G. C. D. 2004. Chemical absorption of H<sub>2</sub>S for biogas purification. *Brazilian Journal of Chemical Engineering*, 21, 415 - 422.
- HUANG, Q., YANG, C., YU, G. & MAO, Z. S. 2010. CFD simulation of hydrodynamics and mass transfer in an internal airlift loop reactor using a steady two-fluid model. *Chemical Engineering Science*, 65, 5527-5536.
- HUSSY, I., HAWKES, F. R., DINSDALE, R. & HAWKES, D. L. 2005. Continuous fermentative hydrogen production from sucrose and sugarbeet. *International Journal of Hydrogen Energy*, 30, 471-483.
- HWU, C. S., TSENG, S.-K., YUAN, C. Y., KULIK, Z. & LETTINGA, G. 1998. Biosorption of long-chain fatty acids in UASB treatment process. *Water Research*, 32, 1571-1579.
- JOU, F. Y., MATHER, A. E. & OTTO, F. D. 1995. The solubility of CO<sub>2</sub> in a 30 mass percent monoethanolamine solution. *Can. J. Chem. Eng.*, 73, 140-147.
- JUNGE A, P. and W. 1989. Proton diffusion along the membrane surface of thylakoids is not enhanced over that in bulk water. *Biophys J*, 56, 27-31.

- KADAM, K. L. 1997. Power plant flue gas as a source of CO<sub>2</sub> for microalgae cultivation: economic impact of different process options. *Energy Conversion and Management*, 38, 505-510.
- KARIM, K., THOMA, G. J. & AL-DAHMAN, M. H. 2007. Gas-lift digester configuration effects on mixing effectiveness. *Water Research*, 41, 3051-3060.
- KARIM, K., HOFFMANN, R., KLASSON, K. T. & AL-DAHMAN, M. H. 2005. Anaerobic digestion of animal waste: Effect of mode of mixing. *Water Research*, 39, 3597-3606.
- KARIM, K., KLASSON, K. T., HOFFMANN, R., DRESHER, S. R., DEPAOI, D. W. & AL-DAHMAN, H. 2003. Anaerobic digestion of animal waste: effect of mixing. *Energy and the Environment*, 7, 175-185
- KATEHIS, D., DIYAMANDOGLU, V. & FILLOS, J. 1998. Stripping and recovery of ammonia from centrate of anaerobically digested biosolids at elevated temperatures. *Water Environment Research*, 70, 231-240.
- KATO, M. T., FIELD, J. A. & LETTINGA, G. 1993. Methanogenesis in granular sludge exposed to oxygen. *FEMS Microbiology Letters*, 114, 317-323.
- KHALILITEHRANI, M. 2011. An investigation on modeling and simulation of chilled ammonia process using of method. Master, Chalmers University of Technology.
- KIM, D. H., HAN, S. K., KIM, S.-H. and SHIN, H. S. 2006. Effect of gas sparging on continuous fermentative hydrogen production. *International Journal of Hydrogen Energy*, 31, 2158-2169.
- KIM, H., NAM, J. and HS.SHIN 2011. A comparison study on the high-rate co-digestion of sewage sludge and food waste using a temperature-phased anaerobic sequencing batch reactor system. *Bioresour Technol.*, 102, 7272-9.
- KIM, J. N., CHUE, K. T., CHO, S. H. & KIM, J. D. 1995. Production of High-Purity Nitrogen from Air by Pressure Swing Adsorption on Zeolite-X. *Separation Science and Technology*, 30, 347-368.
- KRAEMER, J. T. and BAGLEY, D. M. 2006. Supersaturation of dissolved H<sub>2</sub> and CO<sub>2</sub> during fermentative hydrogen production with N-2 sparging. *Biotechnology Letters*, 28, 1485-1491.

- KRAEMER, J. T. and BAGLEY, D. M. 2008. Optimisation and design of nitrogen-sparged fermentative hydrogen production bioreactors. *International Journal of Hydrogen Energy*, 33, 6558-6565.
- KYAZZE, G., MARTINEZ-PEREZ, N., DINSDALE, R., PREMIER, G. C., HAWKES, F. R., GUWY, A. J. & HAWKES, D. L. 2006. Influence of substrate concentration on the stability and yield of continuous biohydrogen production. *Biotechnology and Bioengineering*, 93, 971-979.
- LASTELLA, G., TESTA, C., CORNACCHIA, G., NOTORNICOLA, M., VOLTASIO, F. & SHARMA, V. K. 2002. Anaerobic digestion of semi-solid organic waste: biogas production and its purification. *Energy Conversion and Management*, 43, 63-75.
- LAY, J.-J. 2000. Modeling and optimization of anaerobic digested sludge converting starch to hydrogen. *Biotechnology and Bioengineering*, 68, 269-278.
- LAY, J.-J. 2001. Biohydrogen generation by mesophilic anaerobic fermentation of microcrystalline cellulose. *Biotechnology and Bioengineering*, 74, 280-287.
- LEITÃO, R. C., VAN HAANDEL, A. C., ZEEMAN, G. & LETTINGA, G. 2006. The effects of operational and environmental variations on anaerobic wastewater treatment systems: A review. *Bioresource Technology*, 97, 1105-1118.
- LESTER, W. G. S. & M. A. D., P. 1970. Temperature and fluid property effects on cavitation in Aircraft fuel pumps. *Eng. Phys. Dept. Farnborough C. P. No. 1128*
- LI, K. & TEO, W. K. 1993. Use of an internally staged permeator in the enrichment of methane from biogas. *Journal of Membrane Science*, 78, 181-190.
- LI, Y., HORSMAN, M., WU, N., LAN, C. Q. and DUBOIS-CALERO, N. 2008. Biofuels from Microalgae. *Biotechnology Progress*, 24, 815-820.
- LIANG, T. M., CHENG, S.-S. & WU, K. L. 2002. Behavioral study on hydrogen fermentation reactor installed with silicone rubber membrane. *International Journal of Hydrogen Energy*, 27, 1157-1165.
- LIU, T. & SUNG, S. 2002. Ammonia inhibition on thermophilic aceticlastic methanogens. *Water Science and Technology*, 45, 113-120.

- LUOSTARINEN, S., LUSTE, S. & SILLANPÄÄ, M. 2009. Increased biogas production at wastewater treatment plants through co-digestion of sewage sludge with grease trap sludge from a meat processing plant. *Bioresource Technology*, 100, 79-85.
- LUSK, P. 1998. Methane recovery from animal manures the current opportunities casebook. National Renewable Energy Laboratory, NREL/SR-580-25145, 2-11.
- MACEIRAS, R., ÁLVAREZ, E. & CANCELA, M. A. 2010. Experimental interfacial area measurements in a bubble column. *Chemical Engineering Journal*, 163, 331-336.
- MAJIZAT, A., MITSUNORI, Y., MITSUNORI, W., MICHIMASA, N. & JUN'ICHIRO, M. 1997. Hydrogen gas production from glucose and its microbial kinetics in anaerobic systems. *Water Science and Technology*, 36, 279-286.
- MALÝ, J. & FADRUS, H. 1971. Influence of temperature on anaerobic digestion. *Journal Water Pollution Control Federation*, 43, 641-650.
- MCCARTY, P. L. & SMITH, D. P. 1986. Anaerobic waste-water treatment .4. *Environmental Science & Technology*, 20, 1200-1206.
- MCHEDLOV-PETROSSYAN, P. O., KHOMENKO, G. A. & ZIMMERMAN, W. B. 2003(a). Nearly irreversible, fast heterogeneous reactions in premixed flow. *Chemical Engineering Science*, 58, 3005-3023.
- MCHEDLOV-PETROSSYAN, P. O., ZIMMERMAN, W. B. & KHOMENKO, G. A. 2003(b). Fast binary reactions in a heterogeneous catalytic batch reactor. *Chemical Engineering Science*, 58, 2691-2703.
- MCMAHON, K. D., STROOT, P. G., MACKIE, R. I. & RASKIN, L. 2001. Anaerobic codigestion of municipal solid waste and biosolids under various mixing conditions - II: Microbial population dynamics. *Water Research*, 35, 1817-1827.
- MERCHUK, J. C. & SIEGEL, M. H. 1988. Air-lift reactors in chemical and biological technology. *Journal of Chemical Technology & Biotechnology*, 41, 105-120.
- MERONEY, R. N. & COLORADO, P. E. 2009. CFD simulation of mechanical draft tube mixing in anaerobic digester tanks. *Water Research*, 43, 1040-1050.

- METCALF and Eddy. 1991. Wastewater Engineering Treatment and reuse, McGraw Hill.
- METCALF and Eddy. 2003. Wastewater Engineering Treatment and reuse, McGraw Hill.
- MIRON, Y., ZEEMAN, G., VAN LIER, J. B. & LETTINGA, G. 2000. The role of sludge retention time in the hydrolysis and acidification of lipids, carbohydrates and proteins during digestion of primary sludge in CSTR systems. *Water Research*, 34, 1705-1713.
- MIZUNO, O., DINSDALE, R., HAWKES, F. R., HAWKES, D. L. & NOIKE, T. 2000. Enhancement of hydrogen production from glucose by nitrogen gas sparging. *Bioresource Technology*, 73, 59-65.
- MONTEITH, H. D. & STEPHENSON, J. P. 1981. Mixing efficiencies in full-scale anaerobic digesters by tracer methods. *Journal Water Pollution Control Federation*, 53, 78-84.
- MORAVEJI, M. K., SAJJADI, B., JAFARKHANI, M. & DAVARNEJAD, R. 2011. Experimental investigation and CFD simulation of turbulence effect on hydrodynamic and mass transfer in a packed bed airlift internal loop reactor. *International Communications in Heat and Mass Transfer*, 38, 518-524.
- MOSEY, F. E. & FERNANDES, X. A. 1989. Patterns of hydrogen in biogas from the anaerobic digestion of milk-sugars. *Waf. Sci. Tech.*, 21, 187-196.
- MUDDE F. R. & VAN DEN AKKER E. A. H. 2001. 2D and 3D simulations of an internal airlift loop reactor on the basis of a two-fluid model. *Chemical Engineering Science*, 56, 6351-6358.
- NATH, K. & DAS, D. 2004. Improvement of fermentative hydrogen production: various approaches. *Applied Microbiology and Biotechnology*, 65, 520-529.
- NEGORO, M., HAMASAKI, A., IKUTA, Y., MAKITA, T., HIRAYAMA, K. & SUZUKI, S. 1993. Carbon-Dioxide Fixation by Microalgae Photosynthesis Using Actual Flue-Gas Discharged from a Boiler. *Applied Biochemistry and Biotechnology*, 39, 643-653.

- NEGORO, M., SHIOJI, N., MIYAMOTO, K. & MIURA, Y. 1991. Growth of microalgae in high CO<sub>2</sub> gas and effects of sox and nox. *Applied Biochemistry and Biotechnology*, 28-9, 877-886.
- NESIC, S., POSTLETHWAITE, J. & OLSEN, S. 1996. An electrochemical model for prediction of corrosion of mild steel in aqueous carbon dioxide solutions. *Corrosion*, 52, 280–294.
- NGES, I. A., ESCOBAR, F., FU, X. & BJÖRNSSON, L. 2012. Benefits of supplementing an industrial waste anaerobic digester with energy crops for increased biogas production. *Waste Management*, 32, 53-59.
- OEY, R. S., MUDDE, R. F., PORTELA, L. M. & VAN DEN AKKER, H. E. A. 2001. Simulation of a slurry airlift using a two-fluid model. *Chemical Engineering Science*, 56, 673-681.
- OFORI-BOATENG, C. & KWOFIE, M. E. 2009. Water scrubbing: A better option for biogas purification for effective storage. *World Appl. Sci. J.*, 5, 122–125.
- PADFIELD, D. H. 1973. Control of odor from recovery units by direct-contact evaporative scrubbers with oxidized black liquor. *Tappi*, 56, 83-86.
- PANDE, D. R. & FABIANI, C. 1989. Feasibility studies on the use of a naturally occurring molecular sieve for methane enrichment from biogas. *Gas Separation & Purification*, 3, 143-147.
- PARK, W., HYUN, S. H., OH, S. E., LOGAN, B. E. & KIM, I. S. 2005. Removal of headspace CO<sub>2</sub> increases biological hydrogen production. *Environmental Science and Technology*, 39, 4416-4420.
- PARKINSON, L., SEDEV, R., FORNASIERO, D. L. & RALSTON, J. 2008. The terminal rise velocity of 10-100 microm diameter bubbles in water. *J. Colloid Interface Sci.*, 322, 168–172.
- PAUSS, A., ANDRE, G., PERRIER, M. & GUIOT, S. R. 1990. Liquid-to-gas mass transfer in anaerobic processes: inevitable transfer limitations of methane and hydrogen in the biomethanation process. *Appl Environ Microbiol.*, 56, 1636–1644.

- PÉREZ-ELVIRA, S. I., FDZ-POLANCO, M. & FDZ-POLANCO, F. 2011. Enhancement of the conventional anaerobic digestion of sludge: Comparison of four different strategies. *Water Science and Technology*, 64, 375-383.
- PEROT, C., SERGENT, M., RICHARD, P., PHAN, T. L. R. & MILLOT, N. 1988. The effects of pH, temperature and agitation speed on sludge anaerobic hydrolysis-acidification. *Environmental Technology Letters*, 9, 741-752.
- POESCHL, M., WARD, S. & OWENDE, P. 2010. Prospects for expanded utilization of biogas in Germany. *Renewable and Sustainable Energy Reviews*, 14, 1782-1797.
- PORRAS, J. P. & GEBRESENBET, G. 2003. Review of biogas development in Developing countries with special emphasis in india, Department of Agricultural Engineering.
- RATKOWSKY, D. A., LOWRY, R. K. & MCMEEKIN, T. A. 1983. Model for bacterial culture growth rate throughout the entire biokinetic temperature range. *Journal of Bacteriology*, 154, 1222-1226.
- RATKOWSKY, D. A., OLLEY, J., MCMEEKIN, T. A. & BALL, A. 1982. Relationship between temperature and growth rate of bacterial cultures. *Journal of Bacteriology*, 149, 1-5.
- RENGEL, A., ZOUGHAIB, A., DRON, D. & CLODIC, D. 2012. Hydrodynamic study of an internal airlift reactor for microalgae culture. *Applied Microbiology and Biotechnology*, 93, 117-129.
- RIBEIRO JR, C. P. & LAGE, P. L. C. 2004. Population balance modeling of bubble size distributions in a direct-contact evaporator using a sparger model. *Chemical Engineering Science*, 59, 2363-2377.
- RIBEIRO JR, C. P. & LAGE, P. L. C. 2004. Direct-contact evaporation in the homogeneous and heterogeneous bubbling regimes. Part I: experimental analysis. *International Journal of Heat and Mass Transfer*, 47, 3825-3840.
- RIBEIRO JR, C. P. & LAGE, P. L. C. 2004. Direct-contact evaporation in the homogeneous and heterogeneous bubbling regimes. Part II: dynamic simulation. *International Journal of Heat and Mass Transfer*, 47, 3841-3854.

- RIBEIRO JR, C. P., BORGES, C. P. & LAGE, P. L. C. 2007. Sparger effects during the concentration of synthetic fruit juices by direct-contact evaporation. *Journal of Food Engineering*, 79, 979-988.
- RIBEIRO, C. P. & LAGE, P. L. C. 2005. Gas-liquid direct-contact evaporation: A review. *Chemical Engineering & Technology*, 28, 1081-1107.
- ROLFE, R. D., HENTGES, D. J., BARRETT, J. T. & CAMPBELL, B. J. 1977. Oxygen tolerance of human intestinal anaerobes. *American Journal of Clinical Nutrition*, 30, 1762-1769.
- ROSGAARD, L., DE PORCELLINIS, A. J., JACOBSEN, J. H., FRIGAARD, N. U. & SAKURAGI, Y. 2012. Bioengineering of carbon fixation, biofuels, and biochemicals in cyanobacteria and plants. *Journal of Biotechnology*.
- SAHLSTRÖM, L. 2003. A review of survival of pathogenic bacteria in organic waste used in biogas plants. *Bioresource Technology*, 87, 161-166.
- SALOMONI, C. & PETAZZONI, E. 2006. CO<sub>2</sub> capture and use in organic mater digestion for methane production. Bologna patent application.
- SCHENK, P. M., THOMAS-HALL, S. R., STEPHENS, E., MARX, U. C., MUSSGNUM, J. H., POSTEN, C., KRUSE, O. & HANKAMER, B. 2008. Second generation biofuels: high-efficiency microalgae for biodiesel production. *Bioenergy Research*, 1, 20-43.
- SCHINK, B. 1997. Energetics of syntrophic cooperation in methanogenic degradation. *Microbiology and Molecular Biology Reviews*, 61, 262-280.
- SCHMIDT, J. E. & AHRING, B. K. 1993. Effects of hydrogen and formate on the degradation of propionate and butyrate in thermophilic granules from an upflow anaerobic sludge blanket reactor. *Applied and Environmental Microbiology*, 59, 2546-2551.
- SCOTT, R. I., WILLIAMS, T. N. & LLOYD, D. 1983. Oxygen sensitivity of methanogenesis in rumen and anaerobic digester populations using mass-spectrometry. *Biotechnology Letters*, 5, 375-380.
- SCOTT, S. A., DAVEY, M. P., DENNIS, J. S., HORST, I., HOWE, C. J., LEA-SMITH, D. J. & SMITH, A. G. 2010. Biodiesel from algae: challenges and prospects. *Current Opinion in Biotechnology*, 21, 277-286.

- SHAMPINE, L. & GEAR, C. 1979. A User's View of Solving Stiff Ordinary Differential Equations. *SIAM Review*, 21, 1-17.
- SIEGRIST, H., HUNZIKER, W. & HOFER, H. 2005. Anaerobic digestion of slaughterhouse waste with UF-membrane separation and recycling of permeate after free ammonia stripping. *Water Science Technology*, 52(1), 531-536.
- SIGGINS, A., ENRIGHT, A. M. & O'FLAHERTY, V. 2011. Temperature dependent (37-15°C) anaerobic digestion of a trichloroethylene-contaminated wastewater. *Bioresource Technology*, 102, 7645-7656.
- ŠIMČÍK, M., MOTA, A., RUZICKA, M. C., VICENTE, A. & TEIXEIRA, J. 2011. CFD simulation and experimental measurement of gas holdup and liquid interstitial velocity in internal loop airlift reactor. *Chemical Engineering Science*, 66, 3268-3279.
- SINGH, V. 2012. Effect of corn quality on bioethanol production. *Biocatalysis and Agricultural Biotechnology*, 1, 353-355.
- SOBCZUK, T. M., CAMACHO, F. G., RUBIO, F. C., FERNÁNDEZ, F. G. A. & GRIMA, E. M. 2000. Carbon dioxide uptake efficiency by outdoor microalgal cultures in tubular airlift photobioreactors. *Biotechnology and Bioengineering*, 67, 465-475.
- SOKOLICHIN, A., EIGENBERGER, G. & LAPIN, A. 2004. Simulation of buoyancy driven bubbly flow: Established simplifications and open questions. *AIChE Journal*, 50, 24-45.
- SPEECE, R. E. 1983. Anaerobic biotechnology for industrial wastewater treatment. *Environmental Science and Technology*, 17, 416A-427A.
- STAFFORD, D. A. 1982. The effects of mixing and volatile fatty acid concentrations on anaerobic digester performance. *Biomass*, 2, 43-55.
- STAMS, A. J. M., PLUGGE, C. M., DE BOK, F. A. M., VAN HOUTEN, B. H. G. W., LENS, P., DIJKMAN, H. & WEIJMA, J. 2005. Metabolic interactions in methanogenic and sulfate-reducing bioreactors.
- STANNARD, C. J., WILLIAMS, A. P. & GIBBS, P. A. 1985. Temperature/growth relationships for psychrotrophic food-spoilage bacteria. *Food Microbiology*, 2, 115-122.

- STERN, S. A., KRISHNAKUMAR, B., CHARATI, S. G., AMATO, W. S., FRIEDMAN, A. A. & FUESS, D. J. 1998. Performance of a bench-scale membrane pilot plant for the upgrading of biogas in a wastewater treatment plant. *Journal of Membrane Science*, 151, 63-74.
- STROOT, P. G., MCMAHON, K. D., MACKIE, R. I. & RASKIN, L. 2001. Anaerobic codigestion of municipal solid waste and biosolids under various mixing conditions-I. digester performance. *Water Research*, 35, 1804-1816.
- SUALI, E. & SARBATLY, R. 2012. Conversion of microalgae to biofuel. *Renewable and Sustainable Energy Reviews*, 16, 4316-4342.
- SUNG, S. & LIU, T. 2003. Ammonia inhibition on thermophilic anaerobic digestion. *Chemosphere*, 53, 43-52.
- TANISHO, S., KUROMOTO, M. & KADOKURA, N. 1998. Effect of CO<sub>2</sub> removal on hydrogen production by fermentation. *International Journal of Hydrogen Energy*, 23, 559-563.
- TERASHIMA, GOEL, R., KOMATSU, K., YASUI, H., TAKAHASHI, H., LI, Y. & NOIKE, T. 2009. CFD simulation of mixing in anaerobic digesters. *Bioresour Technol.*, 100, 2228-33.
- TESAŘ, V., HUNG, C.-H. & ZIMMERMAN, W. B. 2006. No-moving-part hybrid-synthetic jet actuator. *Sensors and Actuators A: Physical*, 125, 159-169.
- THIERBACH, R. D. & HANSEN, H. 2002. Utilisation of energy from digester gas and sludge incineration at Hamburg's Köhlbrandhöft WWTP.
- TIEHM, A., NICKEL, K., ZELLHORN, M. & NEIS, U. 2001. Ultrasonic waste activated sludge disintegration for improving anaerobic stabilization. *Water Research*, 35, 2003-2009.
- VAN LIER, J. B., REBAC, S. & LETTINGA, G. 1997. High-rate anaerobic wastewater treatment under psychrophilic and thermophilic conditions. *Water Science and Technology*, 35, 199-206.
- VANLIER, J. B., REBAC, S. & LETTINGA, G. 1997. High-rate anaerobic wastewater treatment under psychrophilic and thermophilic conditions. *Water Science and Technology*, 35, 199-206.

- VAREL, V. H., HASHIMOTO, A. G. & CHEN, Y. R. 1980. Effect of temperature and retention time on methane production from beef cattle waste. *Appl Environ Microbiol.*, 40, 217-222.
- VASUDEVAN P. T. , B., M. 2008. Biodiesel production—current state of the art and challenges. *J Ind Microbiol Biotechnol*, 35, 421–430.
- VAVILIN, V. A., FERNANDEZ, B., PALATSI, J. & FLOTATS, X. 2008. Hydrolysis kinetics in anaerobic degradation of particulate organic material: An overview. *Waste Management*, 28, 939-951.
- VESVIKAR, M. S. & AL-DAHAN, M. 2005. Flow pattern visualization in a mimic anaerobic digester using CFD. *Biotechnology and Bioengineering*, 89, 719-732.
- VINTON, W. B. 1944. Digester heating and mixing equipment. *Sewage Works Journal*, 16, 534-539.
- WANG, B., LI, Y., WU, N. & LAN, C. 2008. CO<sub>2</sub> bio-mitigation using microalgae. *Applied Microbiology and Biotechnology*, 79, 707-718.
- WANG, Q., KUNINOBU, M., KAKIMOTO, K., I-OGAWA, H. & KATO, Y. 1999. Upgrading of anaerobic digestion of waste activated sludge by ultrasonic pretreatment. *Bioresource Technology*, 68, 309-313.
- WEISS, R. F. 1974. Carbon dioxide in water and seawater: the solubility of a non-ideal gas. *Marine Chemistry*, 2, 203-215.
- WILLIAM, J. and BOHR, P. 2010. Conquering the cavitation conundrum [Online]. Blacker company ATK2102-025.
- WORDEN, R. M. & BREDWELL, M. D. 1998. Mass-transfer properties of microbubbles. 2. analysis using a dynamic model. *biotechnology progress*, 14, 39-46.
- WORRELL, E., PRICE, L., MARTIN, N., HENDRIKS, C. and MEIDA, L. O. 2001. Carbon dioxide emissions from the global cement industry. *Annual Review of Energy and the Environment*, 26, 303-329.
- WU, B. & CHEN, S. 2008. CFD simulation of non-Newtonian fluid flow in anaerobic digesters. *Biotechnology and Bioengineering*, 99, 700-711.

- WU, B. 2009. CFD analysis of mechanical mixing in anaerobic digesters. *Transactions of the ASABE*, 52, 1371-1382.
- WU, B. 2010. CFD simulation of mixing in egg-shaped anaerobic digesters. *Water Research*, 44, 1507-1519.
- XIONG, W., GAO, C., YAN, D., WU, C. & WU, Q. 2010. Double CO<sub>2</sub> fixation in photosynthesis–fermentation model enhances algal lipid synthesis for biodiesel production. *Bioresource Technology*, 101, 2287-2293.
- ZAIDA, A. H., SARMA, S. C., GROVER, P. D. & HELDMAN, D. R. 1986. Milk concentration by direct contact heat exchange. *Journal of Food Process Engineering*, 9, 63-79.
- ZEHNDER, A. J. B. & WUHRMANN, K. 1977. Physiology of a Methanobacterium strain AZ. *Archives of Microbiology*, 111, 199-205.
- ZEILER, K. G., HEACOX, D. A., TOON, S. T., KADAM, K. L. & BROWN, L. M. 1995. The use of microalgae for assimilation and utilization of carbon dioxide from fossil fuel-fired power plant flue gas. *Energy Conversion and Management*, 36, 707-712.
- ZHANG, X. and HOUK, K. N. 2005. Acid/base catalysis by pure water: the aldol reaction. *The Journal of Organic Chemistry*, 70, 9712-9716.
- ZHANG, Y. 2008. *Geochemical kinetics*, Princeton University press.
- ZIMMERMAN, W. B. 2011. Electrochemical microfluidics. *Chemical Engineering Science*, 66, 1412-1425.
- ZIMMERMAN, W. B., HEWAKANDAMBY, B. N., TESAR, V., BANDULASENA, H. C. H. and OMOTOWA, O. A. 2009. On the design and simulation of an airlift loop bioreactor with microbubble generation by fluidic oscillation. *Food and Bioproducts Processing*, 87, 215-227.
- ZIMMERMAN, W. B., MCHEDLOV-PETROSSYAN, P. O. & KHOMENKO, G. A. 2007. Effects of transport and phase equilibrium on fast, nearly irreversible reactive extraction. *Chemical Engineering Science*, 62, 1770-1782.
- ZIMMERMAN, W. B., TESAR, V. & BANDULASENA, H. C. H. 2011. Towards energy efficient nanobubble generation with fluidic oscillation. *Current Opinion in Colloid & Interface Science*, 16, 350-356.

- 
- ZIMMERMAN, W. B., TESAR, V., BUTLER, S. & BANDULASENA, H. C. H. 2008. Microbubble generation. *Recent Patents on Engineering*, 2, 1-8.
- ZUPANČIČ, G. D. & ROŠ, M. 2003. Heat and energy requirements in thermophilic anaerobic sludge digestion. *Renewable Energy*, 28, 2255-2267.
- ZWIETERING, M. H., DE KOOS, J. T., HASENACK, B. E., DE WIT, J. C. & VAN 'T RIET, K. 1991. Modeling of bacterial growth as a function of temperature. *Applied and Environmental Microbiology*, 57, 1094-1101.
- ZWIETERING, M. H., DE WIT, J. C., CUPPERS, H. G. A. M. & VAN'T RIET, K. 1994. Modeling of bacterial growth with shifts in temperature. *Applied and Environmental Microbiology*, 60, 204-213.



CHEMICAL & BIOLOGICAL ENGINEERING

# APPENDIX

### A.1 Chemical Oxygen Demand (COD):

It is a vital test commonly used for assessing the quality of water and measuring the amount of pollution in wastewater (organic compounds) indirectly as well as being an indicator for treatment plant efficiency.

Chemical oxygen demand (COD) can be evaluated by measuring the degree of green coloration of chromate ions those results from a reaction of sulphuric acid potassium solution with oxidizable substances that exist in a sample of the wastewater in the presence of a silver sulphate catalyst.

The COD of the sludge in the present study was evaluated by using reagent provided by HLFWQ company with range (5-60 g/l).

#### The procedure for measuring the organic acids is:

1. Invert the cuvette a few times to mix the suspension and sediment.
2. Place a pipette containing 0.2 ml of wastewater carefully inside the cuvette.
3. Close the cuvette and clean it and then invert again.
4. Heat the cuvette to 148 °C for 120 min.
5. Remove the hot cuvette and invert it twice, then leave it in a cool place to cool to 25 °C.
6. Clean the outside of the cuvette and evaluate the COD (g/L) using the device spectrometer (DR2800 (Model)).

### A.2 Volatile Acids:

The evaluation of volatile acids with mg/L existing in a wastewater sample can be achieved by esterification of the carboxylic acids using spectrometer (DR 2800).

The range of volatile acids used in present study was (27–2800 mg/l)

Table A.1: Reagents used in measuring the volatile acid

Name of reagents	Quantity for each test
1. Ethylene Glycol	1.5 ml
2. Sulfuric Acid Solution	0.2 ml
3. Hydroxylamine Hydrochloride Solution, 100-g/L	0.5 ml
4. Sodium Hydroxide Standard Solution, 4.5 N	2.0 ml
5. Ferric Chloride Sulfuric Acid Solution	10.0 ml
6. Water, deionized	10.5 ml

Table A.2 Equipments and tools required for measuring

Equipment	Model
1. Centrifuge	
2. Spectrometer	DR 2800
3. Centrifuge Tubes, 50-ml	
4. Sample Cells, 25 ml,	
5. Sample Cells, 10 ml,	
6. Heater for water bath	
7. Pipet, volumetric 10 ml	
8. Pipet, volumetric 50-1000 $\mu\text{m}$	

### Procedure for evolution of volatile acids:

1. Prepare a centrifuge sample of wastewater for 10 min at 2000 rpm using (Eppendorf centrifuge 5810). Then pipette 0.5 ml into the sample cell (25 ml)
2. Prepare a blank sample by pipetting 0.5 ml of deionized water into the second sample cell (25 ml) for calibration of the device
3. Put 1.5 ml of Ethylene Glycol solution into each sample cell and swirl them to mix the solutions.
4. Pipette 0.2 of Sulphuric Acid Solution into each sample cell and mix them.
5. Insert both sample cells in boiling water for 3 min.
6. Cool both sample cells to room temperature
7. Pipette 0.5 of Hydroxylamine Hydrochloride Solution into each sample cell and swirl them to mix the solutions.
8. Pipette 2.0 ml of Sodium Hydroxide Standard Solution (4.5 N) into each sample cell, then swirl them to mix the solutions.
9. Pipette 10 ml of Ferric Chloride Sulphuric Acid Solution into each sample cell, then swirl them to mix the solutions.
10. Pipette 10 of deionized water and invert them to mix the solution
11. Pipette 10 ml from the deionized sample cell into another dried sample cell (10-ml). Then pipette 10 ml from the wastewater sample cell into another dried sample cell (10-ml).
12. Turn-on the timer for three minutes and during this period, turn on the spectrometer device and select the 770 volatile acid software.
13. Measure the deionized sample cell used for calibration of the device and the wastewater sample cell to evaluate the Volatile acids.

